

ISSN 1881-7815    Online ISSN 1881-7823

# **BST**

## **BioScience Trends**

Volume 13, Number 6  
December, 2019



[www.biosciencetrends.com](http://www.biosciencetrends.com)



# BST

## BioScience Trends



ISSN: 1881-7815

Online ISSN: 1881-7823

CODEN: BTIRCZ

Issues/Year: 6

Language: English

Publisher: IACMHR Co., Ltd.

**BioScience Trends** is one of a series of peer-reviewed journals of the International Research and Cooperation Association for Bio & Socio-Sciences Advancement (IRCA-BSSA) Group and is published bimonthly by the International Advancement Center for Medicine & Health Research Co., Ltd. (IACMHR Co., Ltd.) and supported by the IRCA-BSSA and Shandong University China-Japan Cooperation Center for Drug Discovery & Screening (SDU-DDSC).

**BioScience Trends** devotes to publishing the latest and most exciting advances in scientific research. Articles cover fields of life science such as biochemistry, molecular biology, clinical research, public health, medical care system, and social science in order to encourage cooperation and exchange among scientists and clinical researchers.

**BioScience Trends** publishes Original Articles, Brief Reports, Reviews, Policy Forum articles, Case Reports, News, and Letters on all aspects of the field of life science. All contributions should seek to promote international collaboration.

## Editorial Board

### Editor-in-Chief:

Norihiro KOKUDO  
*National Center for Global Health and Medicine, Tokyo, Japan*

### Co-Editors-in-Chief:

Xue-Tao CAO  
*Nankai University, Tianjin, China*  
Rajendra PRASAD  
*University of Delhi, Delhi, India*  
Arthur D. RIGGS  
*Beckman Research Institute of the City of Hope, Duarte, CA, USA*

### Chief Director & Executive Editor:

Wei TANG  
*National Center for Global Health and Medicine, Tokyo, Japan*

### Senior Editors:

Xunjia CHENG  
*Fudan University, Shanghai, China*  
Yoko FUJITA-YAMAGUCHI  
*Beckman Research Institute of the City of Hope, Duarte, CA, USA*  
Na HE  
*Fudan University, Shanghai, China*  
Kiyoshi KITAMURA  
*The University of Tokyo, Tokyo, Japan*  
Misao MATSUSHITA  
*Tokai University, Hiratsuka, Japan*  
Munehiro NAKATA  
*Tokai University, Hiratsuka, Japan*  
Takashi SEKINE

*Toho University, Tokyo, Japan*  
Fanghua QI  
*Shandong Provincial Hospital, Ji'nan, China*  
Ri SHO  
*Yamagata University, Yamagata, Japan*  
Yasuhiko SUGAWARA  
*Kumamoto University, Kumamoto, Japan*  
Ling WANG  
*Fudan University, Shanghai, China*

### Managing Editor:

Jianjun GAO  
*Qingdao University, Qingdao, China*

### Web Editor:

Yu CHEN  
*The University of Tokyo, Tokyo, Japan*

### Proofreaders:

Curtis BENTLEY  
*Roswell, GA, USA*  
Thomas R. LEBON  
*Los Angeles, CA, USA*

### Editorial Office

Pearl City Koishikawa 603,  
2-4-5 Kasuga, Bunkyo-ku, Tokyo 112-0003, Japan  
Tel: +81-3-5840-8764 Fax: +81-3-5840-8765  
E-mail: office@biosciencetrends.com

# BioScience Trends

## Editorial and Head Office

Pearl City Koishikawa 603, 2-4-5 Kasuga, Bunkyo-ku,  
Tokyo 112-0003, Japan

Tel: +81-3-5840-8764, Fax: +81-3-5840-8765  
E-mail: office@biosciencetrends.com  
URL: www.biosciencetrends.com

## Editorial Board Members

Girdhar G. AGARWAL <i>(Lucknow, India)</i>	De-Fei HONG <i>(Hangzhou, China)</i>	Yutaka MATSUYAMA <i>(Tokyo, Japan)</i>	Puay Hoon TAN <i>(Singapore, Singapore)</i>
Hirotsugu AIGA <i>(Geneva, Switzerland)</i>	De-Xing HOU <i>(Kagoshima, Japan)</i>	Qingyue MENG <i>(Beijing, China)</i>	Koji TANAKA <i>(Tsu, Japan)</i>
Hidechika AKASHI <i>(Tokyo, Japan)</i>	Sheng-Tao HOU <i>(Ottawa, Canada)</i>	Mark MEUTH <i>(Sheffi eld, UK)</i>	John TERMINI <i>(Duarte, CA, USA)</i>
Moazzam ALI <i>(Geneva, Switzerland)</i>	Yong HUANG <i>(Ji'ning, China)</i>	Satoko NAGATA <i>(Tokyo, Japan)</i>	Usa C. THISYAKORN <i>(Bangkok, Thailand)</i>
Ping AO <i>(Shanghai, China)</i>	Hirofumi INAGAKI <i>(Tokyo, Japan)</i>	Miho OBA <i>(Odawara, Japan)</i>	Toshifumi TSUKAHARA <i>(Nomi, Japan)</i>
Hisao ASAMURA <i>(Tokyo, Japan)</i>	Masamine JIMBA <i>(Tokyo, Japan)</i>	Xianjun QU <i>(Beijing, China)</i>	Kohjiro UEKI <i>(Tokyo, Japan)</i>
Michael E. BARISH <i>(Duarte, CA, USA)</i>	Chunlin JIN <i>(Shanghai, China)</i>	John J. ROSSI <i>(Duarte, CA, USA)</i>	Masahiro UMEZAKI <i>(Tokyo, Japan)</i>
Boon-Huat BAY <i>(Singapore, Singapore)</i>	Kimitaka KAGA <i>(Tokyo, Japan)</i>	Carlos SAINZ-FERNANDEZ <i>(Santander, Spain)</i>	Junming WANG <i>(Jackson, MS, USA)</i>
Yasumasa BESSHO <i>(Nara, Japan)</i>	Ichiro KAI <i>(Tokyo, Japan)</i>	Yoshihiro SAKAMOTO <i>(Tokyo, Japan)</i>	Xiang-Dong Wang <i>(Boston, MA, USA)</i>
Generoso BEVILACQUA <i>(Pisa, Italy)</i>	Kazuhiro KAKIMOTO <i>(Osaka, Japan)</i>	Erin SATO <i>(Shizuoka, Japan)</i>	Hisashi WATANABE <i>(Tokyo, Japan)</i>
Shiuan CHEN <i>(Duarte, CA, USA)</i>	Kiyoko KAMIBEPPU <i>(Tokyo, Japan)</i>	Takehito SATO <i>(Isehara, Japan)</i>	Jufeng XIA <i>(Tokyo, Japan)</i>
Yuan CHEN <i>(Duarte, CA, USA)</i>	Haidong KAN <i>(Shanghai, China)</i>	Akihito SHIMAZU <i>(Tokyo, Japan)</i>	Lingzhong XU <i>(Ji'nan, China)</i>
Naoshi DOHMAE <i>(Wako, Japan)</i>	Bok-Luel LEE <i>(Busan, Korea)</i>	Zhifeng SHAO <i>(Shanghai, China)</i>	Masatake YAMAUCHI <i>(Chiba, Japan)</i>
Zhen FAN <i>(Houston, TX, USA)</i>	Mingjie LI <i>(St. Louis, MO, USA)</i>	Judith SINGER-SAM <i>(Duarte, CA, USA)</i>	Aitian YIN <i>(Ji'nan, China)</i>
Ding-Zhi FANG <i>(Chengdu, China)</i>	Shixue LI <i>(Ji'nan, China)</i>	Raj K. SINGH <i>(Dehradun, India)</i>	George W-C. YIP <i>(Singapore, Singapore)</i>
Xiaobin FENG <i>(Beijing, China)</i>	Ren-Jang LIN <i>(Duarte, CA, USA)</i>	Peipei SONG <i>(Tokyo, Japan)</i>	Xue-Jie YU <i>(Galveston, TX, USA)</i>
Yoshiharu FUKUDA <i>(Ube, Japan)</i>	Lianxin LIU <i>(Hefei, China)</i>	Junko SUGAMA <i>(Kanazawa, Japan)</i>	Rongfa YUAN <i>(Nanchang, China)</i>
Rajiv GARG <i>(Lucknow, India)</i>	Xinqi LIU <i>(Tianjin, China)</i>	Zhipeng SUN <i>(Beijing, China)</i>	Benny C-Y ZEE <i>(Hong Kong, China)</i>
Ravindra K. GARG <i>(Lucknow, India)</i>	Daru LU <i>(Shanghai, China)</i>	Hiroshi TACHIBANA <i>(Isehara, Japan)</i>	Yong ZENG <i>(Chengdu, China)</i>
Makoto GOTO <i>(Tokyo, Japan)</i>	Hongzhou LU <i>(Shanghai, China)</i>	Tomoko TAKAMURA <i>(Tokyo, Japan)</i>	Chengchao ZHOU <i>(Ji'nan, China)</i>
Demin HAN <i>(Beijing, China)</i>	Duan MA <i>(Shanghai, China)</i>	Tadatoshi TAKAYAMA <i>(Tokyo, Japan)</i>	Xiaomei ZHU <i>(Seattle, WA, USA)</i>
David M. HELFMAN <i>(Daejeon, Korea)</i>	Masatoshi MAKUUCHI <i>(Tokyo, Japan)</i>	Shin'ichi TAKEDA <i>(Tokyo, Japan)</i>	<i>(as of October, 2019)</i>
Takahiro HIGASHI <i>(Tokyo, Japan)</i>	Francesco MAROTTA <i>(Milano, Italy)</i>	Sumihito TAMURA <i>(Tokyo, Japan)</i>	

---

**Policy Forum**

---

- 464 - 469 **Progress on drug pricing negotiations in China.**  
*Mi Tang, Peipei Song, Jiangjiang He*

---

**Review**

---

- 469 - 475 **The pro-tumor effect and the anti-tumor effect of neutrophils extracellular traps.**  
*Yufeng Liu, Lianxin Liu*
- 476 - 487 **A review of traditional Chinese medicine for treatment of glioblastoma.**  
*Jinjing Wang, Fanghua Qi, Zhixue Wang, Zhikun Zhang, Ni Pan, Lei Huai, Shuyu Qu, Lin Zhao*
- 488 - 501 **The state of minimally invasive pancreaticoduodenectomy in Chinese mainland: A systematic literature review.**  
*Jianyi Ding, Chengwu Zhang, Dongsheng Huang, Yuhua Zhang*

---

**Original Article**

---

- 502 - 509 **Human cytomegalovirus IE2 protein regulates macrophage-mediated immune escape by upregulating GRB2 expression in UL122 genetically modified mice.**  
*Yanan Yang, Guohua Ren, Zhifei Wang, Bin Wang*
- 510 - 515 **A multiplex loop-mediated isothermal amplification assay for rapid detection of *Bacillus cereus* and *Staphylococcus aureus*.**  
*Yanglong Deng, Yanquan Liu, Zubin Jiang, Jingxin Wang, Qing Zhang, Yeqian Qian, Yuan Yuan, Xiangyu Zhou, Guiling Fan, Yufeng Li*
- 516 - 522 **IL16 deficiency enhances Th1 and cytotoxic T lymphocyte response against influenza A virus infection.**  
*Ran Jia, Shuai Liu, Jin Xu, Xiaozhen Liang*
- 523 - 529 **IFITM3 upregulates c-myc expression to promote hepatocellular carcinoma proliferation via the ERK1/2 signalling pathway.**  
*Jiaqi Min, Junwen Hu, Chen Luo, Jinfeng Zhu, Jiefeng Zhao, Zhengming Zhu, Linqun Wu, Rongfa Yuan*
- 530 - 538 **Shufengjiedu capsules protect against neuronal loss in olfactory epithelium and lung injury by enhancing autophagy in rats with allergic rhinitis.**  
*Jinyu Mei, Hua Kong, Zhentao Zhao, Ziyu Chen, Yatang Wang, Jianming Yang*
- 539 - 545 **The impact of apurinic-apyrimidinic endonuclease I on hepatocyte immunoinflammatory factors and cell apoptosis.**  
*Tatsuo Sawakami, Zhipeng Sun, Yoshinori Inagaki, Kiyoshi Hasegawa, Wei Tang, Guangzhong Xu, Nengwei Zhang*

## CONTENTS

(Continued)

---

- 546 - 555**      **Male rats exhibit higher pro-BDNF, c-Fos and dendritic tree changes after chronic acoustic stress.**  
*David Fernandez-Quezada, Alejandra García-Zamudio, Yaveth Ruvalcaba-Delgadillo, Sonia Luquín, Joaquín García-Estrada, Fernando Jáuregui Huerta*

### Brief Report

---

- 556 - 561**      **PRKCH polymorphism is associated with rheumatoid arthritis in a Chinese population.**  
*Yue Zhuang, Yanan Di, Lulin Huang, Jing Zhu*

### Guide for Authors

---

### Copyright

---

## Progress on drug pricing negotiations in China

Mi Tang<sup>1</sup>, Peipei Song<sup>2</sup>, Jiangjiang He<sup>1,3,\*</sup>

<sup>1</sup>Department of Health Policy Research, Shanghai Health Development Research Center (Shanghai Medical Information Center), Shanghai, China;

<sup>2</sup>Institute for Global Health Policy Research, Bureau of International Health Cooperation, National Center for Global Health and Medicine, Tokyo, Japan;

<sup>3</sup>School of Public Health, Fudan University, Shanghai, China.

### Summary

On November 28<sup>th</sup>, 2019, the National Healthcare Security Administration (NHSA) and the Ministry of Human Resources and Social Security (MOHRSS) of China announced the results of drug pricing negotiations. Seventy first-negotiated drugs with 60.7% average price decrease and twenty-seven re-negotiated medicines with 26.4% average price fall, involving 11 disease categories, were successfully incorporated into National Reimbursement Drug List (NRDL). Medicines that successfully get accessed to NRDL are mostly new listings with high clinical value, and more than half of them are manufactured by Chinese enterprises. Compared to the negotiated drug list of 2017, the biggest increase in western medicines is the alimentary tract and metabolism (10 drugs added), and the traditional Chinese medicine is internal medicine (17 drugs added). The negotiation follows the process including preparation, examination, negotiation, and announcement. There are several innovations in the procedure, such as the parallel calculation of the floor price, the introduction of competitive negotiations, allowing companies to apply for price confidentiality, and increasing government-enterprise communication before negotiations. Incorporating patented drugs into NRDL by negotiation not only helps patients reduce the economic burden, but also encourages pharmaceutical companies to innovate.

**Keywords:** National Reimbursement Drug List, pricing negotiation, negotiation process

### 1. Introduction

On November 28<sup>th</sup>, 2019, the National Healthcare Security Administration (NHSA) and the Ministry of Human Resources and Social Security (MOHRSS) of China officially issued the results of the drug pricing negotiations. Seventy first-negotiated and twenty-seven re-negotiated medicines, involving 11 disease categories, were successfully incorporated in National Reimbursement Drug List (NRDL). The average price decrease of the first-negotiated and re-negotiated drugs are 60.7% and 26.4%, and the price of drugs for

hepatitis C that has received much attention fell by an average of more than 85% (1). Incorporating drugs into NRDL through negotiation, which is a major innovation in China's reimbursement drugs list adjustment in recent years, can significantly improve the availability and affordability of patent drugs for patients, and can make the NRDL structure more optimal (2).

This article intends to analyze China's drugs pricing negotiations in 2019 from the aspects of the policy background, progress, similarities and differences with conventional access, and potential impact.

### 2. Policy background for drug pricing negotiations

Patented drugs, as an inadequately competitive commodity in the pharmaceutical market, have both clinical value and high price (3). In order to introduce patented drugs into the Chinese market at a price acceptable to all three parties who are pharmaceutical companies, medicare payers, and patients, in February

Released online in J-STAGE as advance publication December 26, 2019.

\*Address correspondence to:

Jiangjiang He, Shanghai Health Development Research Center (Shanghai Medical Information Center), No.1477 Beijing (W) Road, Jing'an District, Shanghai 200040, China.  
E-mail: hejiangjiang@shdrc.org

2015, the State Council of China issued *the Guidelines on Improving the Centralized Procurement of Drugs for Public Hospital*, and proposed establishing an open and transparent price negotiation mechanism for some patented and exclusively manufactured drugs (4). In the same year, the former National Health and Family Planning Commission (NHFPC), National Development and Reform Commission (NDRC) and the MOHRSS initiated the first round of national-level drug pricing negotiations and announced the results on May 20<sup>th</sup>, 2016. The price of three drugs, Iressa, Kemena and Werder's, have dropped significantly after negotiations, with an average reduction of 58.6% (5). In 2017, the MOHRSS introduced pharmacoeconomic evaluation as a negotiation tool for the first time, and successfully incorporated 36 drugs, with an average reduction of 44% (6), which are used to cure cancer or major diseases. In 2018, The NHSA included another 17 anti-cancer drugs, and proposed that medical institutions whose actual cost exceeded controlled index of total amount due to policy reasons (e.g. negotiated drugs were incorporated in list) should be appropriately reimbursed when it was time for year-end clearing, thereby guaranteeing the initiative of supplying and using negotiated drugs (7).

Apart from national level drug negotiations, in some areas such as Qingdao, Jiangsu, Jiangxi, Zhejiang, etc. also actively explored the mechanism of drug pricing negotiations (8). Drug pricing negotiations at the local level mainly included some drugs, with accurate and effective effects but are expensive, which are essential for the treatment of severe and catastrophic diseases. Local level negotiations are preceded by the national negotiation, which offered referential experience and lessons for the national negotiation. Nevertheless, with the release of 2019 NRDL, provincial governments do not have authorization to adjust Type B NRDL.

Explorations at the national and local levels have actively promoted construction of the drug pricing negotiations access mechanism in China. However, since China's drug pricing negotiations started late, there are deficiencies in actual work, such as fewer drugs were negotiated resulting in less patient benefit, and the negotiation mechanism is still incomplete leading to misjudgment of relevant information by enterprises. In this context, taking the opportunity of the overall adjustment of the NRDL in 2019, China has launched the fourth drugs pricing negotiation.

### 3. Progress on Drug Pricing Negotiations in China

#### 3.1. Basic situation and characteristics of negotiated drugs

The drugs to be negotiated in 2019 are for exclusive drugs that entered the Chinese market before December 31, 2018 (9). Among all the exclusive medicines, 119 medicines were selected for negotiation after expert

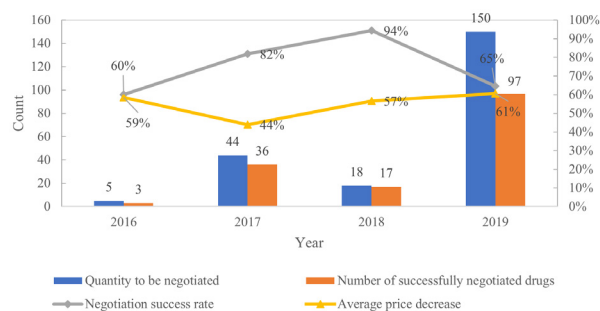


**Figure 1. Status of medicines negotiated in China NRDL from 2016 to 2019.** Data source: The information of drug price negotiations is collected from the NHSA, MOHRSS and the former NHFPC of China from 2016 to 2019 (4-6). MOHRSS, Ministry of Human Resources and Social Security; NHFPC, National Health and Family Planning Commission; NHSA, National Healthcare Security Administration.

review and voting, and enterprises confirming. In addition, there are 31 medicines that were negotiated in 2017 that need to be re-negotiated to determine whether the contract can be renewed. The two parts add up to a total of 150 (1). Compared with previous years, the number of successfully negotiated drugs has reached a record. Although the negotiation success rate has declined, the price decline of successfully negotiated drugs is still steady (Figure 1).

Most drugs successfully negotiated in 2019 are new to the Chinese market in recent years and have high clinical value. These drugs cover 11 clinical treatment categories including cancer, rare diseases, hepatitis, diabetes, multi-drug resistant tuberculosis, rheumatic immunity, cardiovascular and cerebrovascular diseases, and digestion, etc. of which respiratory medicine is a new treatment category. Compared with the number of negotiated medicines in 2017, the number in all categories has increased. The largest increase in western medicine is for digestive and metabolic drugs (10 drugs added), and Chinese medicine is for internal medicine (17 drugs added), which reflects China's focus on proprietary Chinese medicines (Table 1).

In the context of the innovation capabilities of foreign companies far exceeding those of domestic companies, more than half of the drugs successfully negotiated at this time were those produced by Chinese companies (Figure 2). It is estimated that prices of drugs produced by Chinese companies have fallen less than those of foreign companies, which is conducive to improving the innovation capabilities of Chinese pharmaceutical companies.

#### 3.2. The procedure of drug pricing negotiations

The negotiation follows the processes including preparation, evaluation, negotiation, and announcement (Figure 3) (10,11).

*i) Preparation.* A total of three tasks are performed during the preparation phase. First, drawing up a work

**Table 1. Distribution of treatment categories of drugs negotiated successfully from 2016 to 2019 in China NRDL**

Categories	2019		2018		2017		2016		Total	
	N	%	N	%	N	%	N	%	N	%
Total	97	100.00	17	100.00	36	100.00	3	100.00	153	100.00
Western medicine	74	76.29	17	100.00	31	86.11	3	100.00	125	81.70
Antineoplastic agent	22	22.68	16	94.12	16	44.44	2	66.67	56	36.60
Antiinfectives for systemic use	11	11.34	0	0.00	2	5.56	1	33.33	14	9.15
Alimentary tract and metabolism	11	11.34	0	0.00	1	2.77	0	0.00	12	7.85
Blood and blood forming organs	8	8.25	0	0.00	3	8.33	0	0.00	11	7.19
Cardiovascular system	6	6.19	0	0.00	3	8.33	0	0.00	9	5.88
Sensory organs	5	5.16	0	0.00	2	5.56	0	0.00	7	4.57
Nervous system	4	4.12	0	0.00	2	5.56	0	0.00	6	3.92
Various	4	4.12	0	0.00	2	5.56	0	0.00	6	3.92
Respiratory system	3	3.09	0	0.00	0	0.00	0	0.00	3	1.96
Systemic hormone preparations, excl. sex hormones and insulins	0	0.00	1	5.88	0	0.00	0	0.00	1	0.66
Chinese patent medicine	23	23.71	0	0.00	5	13.89	0	0.00	28	18.30
Internal medicine	19	19.59	0	0.00	2	5.56	0	0.00	21	13.73
Antitumor medicine	4	4.12	0	0.00	3	8.33	0	0.00	7	4.57

*Data source:* The data comes from the negotiating materials published by the former NHFPC, the MOHRSS, the NHSA and other related departments of China from 2016 to 2019 (11). MOHRSS, Ministry of Human Resources and Social Security; NHFPC, National Health and Family Planning Commission; NHSA, National Healthcare Security Administration; NRDL, National Reimbursement Drug List.

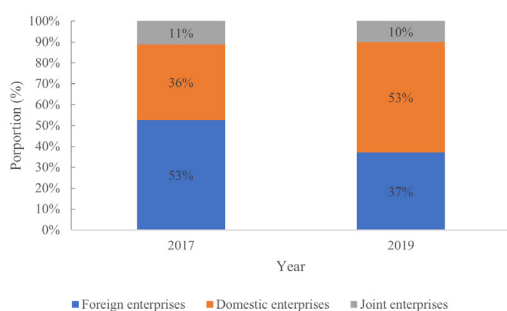


**Figure 2. Category change of drug company negotiated successfully in China NRDL.** *Data resource:* According to the negotiation information published by the NHSA of China (9). NHSA, National Healthcare Security Administration; NRDL, National Reimbursement Drug List.

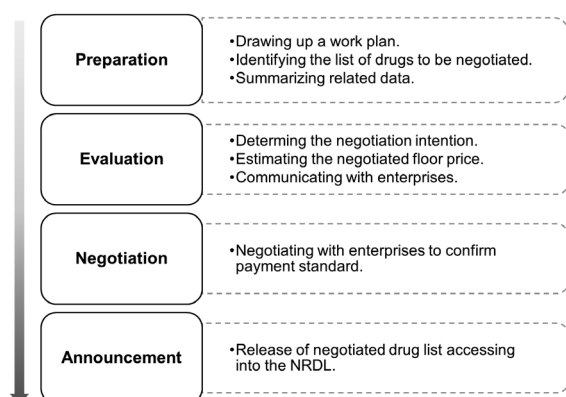


**Figure 3. Drug pricing negotiation process of China NRDL.** NRDL, National Reimbursement Drug List.

plan. The NHSA works with relevant departments to formulate the *2019 Work Plan for Drugs Pricing Negotiation to the NRDL*. Second, identifying the list of

drugs to be negotiated. NHSA with related departments organize consultants (around 300, recommended by academic associations and industry associations) and experts (around 25,000, most of them are experts in clinical medicine or medical insurance management, recommended by local academic and industry associations in various provinces) to determine the list of drugs to be negotiated by evaluating and bidding. Third, summarizing related data. The relevant data of the drugs, which laid a solid foundation for the negotiation, are collected through multiple stakeholders, such as local medical insurance departments, enterprises, and drug recruitment platforms.

*ii) Evaluation.* The evaluation stage consists of three parts. The first is to determine the negotiation intention. The NHSA confirms the negotiation intentions of relevant companies, and organizes the companies that have willingness to negotiate to provide materials on the basis of prescribed format and time limit. The second is to estimate the negotiated floor price. Authoritative experts on pharmacoeconomics and medical insurance management are selected nationwide, and the pharmacoeconomics measurement group and fund measurement group are established respectively. Two groups make parallel calculations according to the technical points, and finally generate the floor price. The third is to communicate with enterprises. The NHSA organizes a centralized communication meeting to introduce the negotiation work arrangements, price calculation considerations, and negotiation rules to the companies to lead them to form reasonable expectations. In addition, NHSA also listens to the opinions of enterprises, and responds in time, and organizes experts to demonstrate to them if necessary.

*iii) Negotiation.* First, according to the negotiation

rules and procedures, the NHSA unified the caliber and standard of negotiations. Then the negotiators, composed of representatives from the national or local medical insurance agency, conduct on-site negotiations with the enterprises based on the evaluation opinions. After the negotiation, the negotiators announce the results on the spot and sign a confirmation contract with the enterprises. Finally, NHSA signs formal agreements with the enterprises one by one based on the results of the negotiations.

*iv) Announcement.* Release of negotiated drug list accessing into the NRDL.

### 3.3. Highlights of the negotiation mechanism

Compared with previous years' drugs pricing negotiations, there are several following highlights in this negotiations. First, calculating the floor price parallelly. In this negotiation, the pharmacoeconomics measurement team and the fund measurement team calculate the floor price separately according to the technical points, and convert the measured price of the two groups into the final price according to the prescribed method, which guarantee fairness and confidentiality of the measurement results. Second, introducing competitive negotiations. Because the six hepatitis C medications are generally effective and the cost of each treatment is more than 50,000 yuan, it is difficult to guide companies to reduce the price into a reasonable range based on pharmacoeconomic calculations and conventional access negotiations. Therefore, the method of competitive negotiation was creatively introduced, only two drugs with the lowest full-course cost could be allowed to enter the catalogue within 2 years, to guide enterprises to fully compete. Third, enabling companies to apply for price confidentiality. The rule of pricing negotiation allows companies to ask for confidentiality of the transaction price, in order to induce companies to reduce prices significantly. Fourth, strengthening communication between government and enterprises. This negotiation has added a communication meeting with the enterprise in the evaluation stage. The purpose of communication is to reach a consensus with the enterprise on basic information and materials, to prevent the failure of negotiations due to misunderstanding of information.

### 4. Similarities and differences with conventional admission

Due to the limited time and manpower of the management department, the adjustment of the NRDL was divided into conventional admission and negotiation admission based on the characteristics of new drugs. Conventional admission is a quick way for most new drugs to be incorporated into NRDL. First, the management department delineates the scope of

candidate drugs based on registration information from the China Food and Drug Administration (CFDA) to ensure legality. Second, clinical medicine and pharmacy experts conduct secondary selection to ensure the candidate medicines meet clinical need. Among these candidate drugs, if the price is not higher than similar products in the NRDL, they can be directly accepted.

Negotiation admission is a process for a few highly innovative but expensive medicines. As with conventional access, these new drugs also need to be legally compliant, safe, effective, and meet clinical need. However, different from conventional admission, the management department will refer to the multi-dimensional price information, which plays a decisive role in the negotiations, including the international price, self-pay price, gift items, medical insurance budget impact, cost-effectiveness, *etc.* and invite experts to screen and evaluate this information. Based on this information, the final negotiated floor price is formed (12,13).

## 5. Potential impact

### 5.1. Reduce patient's financial burden

In this negotiation, the price of the newly added 70 drugs has decreased by 60.7%. If the actual reimbursement ratio is 50%, the patient's out-of-pocket ratio will be reduced to less than 20%, and even some drugs will be reduced to 5%. It is foreseeable that with the substantial decline in personal out-of-pocket costs, patients' affordability and availability of patented drugs will increase simultaneously.

### 5.2. Encourage pharmaceutical companies to innovate

Adjusting NRDL by negotiating will promote innovation in pharmaceutical companies. Most of the successfully negotiated drugs are new listings in recent years and are quickly included in the catalog, which releases a clear signal to support innovation. At the same time, drastic price reductions of drugs also put forward higher requirements for the company's R & D and pricing. It is required that companies could not simply consider costs and benefits of the company or price elasticity of the market when pricing the products, but also need to think about how to benefit multiple parties at the same time, such as meeting patients' medication needs and maintaining medical insurance funds sustainability (14).

## Acknowledgements

This paper was supported by grants from the China Medical Board Collaborating Project "Establishing Health Policy Transformation Network of China (Project number: CMB-CP 14-190)".

## References

1. National Healthcare Security Administration of China. Notice on the inclusion of drugs negotiated in 2019 in the scope of Class B of the "National Basic Medical Insurance, Work Injury Insurance and Maternity Insurance Drug Catalogue". [http://www.nhsa.gov.cn/art/2019/11/28/art\\_37\\_2050.html](http://www.nhsa.gov.cn/art/2019/11/28/art_37_2050.html) (accessed December 5, 2019) (in Chinese)
2. National Healthcare Security Administration of China. Interpretation of the "2019 National Medical Insurance Drug Catalog Adjustment Work Plan". [http://www.nhsa.gov.cn/art/2019/4/17/art\\_38\\_1212.html](http://www.nhsa.gov.cn/art/2019/4/17/art_38_1212.html) (accessed December 5, 2019) (in Chinese)
3. Gandjour A. Reference pricing and price negotiations for innovative new drugs: Viable policies in the long term? *Pharmacoeconomics*. 2013; 31:11-14.
4. The State Council. Guiding Opinions on Improving Centralized Drug Procurement in Public Hospitals. [http://www.gov.cn/zhengce/content/2015-02/28/content\\_9502.htm](http://www.gov.cn/zhengce/content/2015-02/28/content_9502.htm) (accessed December 5, 2019) (in Chinese)
5. The former National Health and Family Planning Commission. Notice on announcing the results of national drug price negotiations. <http://www.nhc.gov.cn/yaozs/s7655/201605/58c5bc1ed0f14c75b8f15f1c149b35f4.shtml> (accessed December 5 2019) (in Chinese)
6. Ministry of Human Resources and Social Security of China. Notice on involving 36 drugs into Type B Medicine List for National Basic Medical Insurance, Employment Injury Insurance and Maternity Insurance. [http://www.mohrss.gov.cn/SYrlzyhshbzb/shehuibaozhang/zcwj/yiliao/201707/t20170718\\_274153.html](http://www.mohrss.gov.cn/SYrlzyhshbzb/shehuibaozhang/zcwj/yiliao/201707/t20170718_274153.html) (accessed August 25, 2019) (in Chinese)
7. National Healthcare Security Administration. Notice on involving 17 drugs into Type B Medicine List for National Basic Medical Insurance, Employment Injury Insurance and Maternity Insurance. [http://www.nhsa.gov.cn/art/2018/10/10/art\\_19\\_397.html](http://www.nhsa.gov.cn/art/2018/10/10/art_19_397.html) (accessed December 5, 2019) (in Chinese)
8. Chang F. A study on negotiation mechanism and manage innovation of China's Medical Insurance Price. Price: Theory & Practice. 2017; 5:18-22 (in Chinese)
9. National Healthcare Security Administration of China. Policy interpretation of the adjustment scheme for 2019 national healthcare insurance drug list. [http://www.nhsa.gov.cn/art/2019/4/17/art\\_38\\_1212.html](http://www.nhsa.gov.cn/art/2019/4/17/art_38_1212.html) (accessed December 5, 2019) (in Chinese)
10. National Healthcare Security Administration of China. Announcement on publishing the adjustment scheme for 2019 national healthcare insurance drug list. [http://www.nhsa.gov.cn/art/2019/4/17/art\\_37\\_1214.html](http://www.nhsa.gov.cn/art/2019/4/17/art_37_1214.html) (accessed December 5, 2019) (in Chinese)
11. National Healthcare Security Administration of China. Policy Interpretation of the "Notice regarding the inclusion of the negotiated drugs in 2019 in the <National Basic Medical Insurance, Work Injury Insurance and Maternity Insurance Drug Catalog> Class B scope". [http://www.nhsa.gov.cn/art/2019/11/28/art\\_38\\_2056.html](http://www.nhsa.gov.cn/art/2019/11/28/art_38_2056.html) (accessed December 5, 2019) (in Chinese)
12. Hu SL. Five highlights of the pharmacoeconomic calculation process in drug pricing negotiations. [https://mp.weixin.qq.com/s?\\_\\_biz=MjM5ODQ4MjU4MQ==&mid=2651240278&idx=2&sn=fad303cd3aac00086dd840efd71c7b76&chksm=bd3810ac8a4f99bab8deed8df7985dbd0b343d90850a56e8cf937355ba429cd0fb1881900c52&mpshare=1&scene=1&srcid=&sharer\\_sharetime=1575339292015&sharer\\_shareid=18308ae37d50cd6d2b57beb0959cfd9c#rd](https://mp.weixin.qq.com/s?__biz=MjM5ODQ4MjU4MQ==&mid=2651240278&idx=2&sn=fad303cd3aac00086dd840efd71c7b76&chksm=bd3810ac8a4f99bab8deed8df7985dbd0b343d90850a56e8cf937355ba429cd0fb1881900c52&mpshare=1&scene=1&srcid=&sharer_sharetime=1575339292015&sharer_shareid=18308ae37d50cd6d2b57beb0959cfd9c#rd) (accessed August 25, 2019) (in Chinese)
13. Li H, Liu GG, Wu J, Wu JH, Dong CH, Hu SL. Recent pricing negotiations on innovative medicines pilot in China: Experiences, implications, and suggestions. *Value in Health*. 2018; 15:133-137.
14. Sina Medical news. 2019 healthcare insurance list confirms 128 drugs to be negotiated How to negotiate? The key is value! [https://med.sina.com/article\\_detail\\_103\\_2\\_70500.html](https://med.sina.com/article_detail_103_2_70500.html) (accessed August 25, 2019) (in Chinese)

(Received December 8, 2019; Revised December 16, 2019; Accepted December 20, 2019)

# The pro-tumor effect and the anti-tumor effect of neutrophils extracellular traps

Yufeng Liu, Lianxin Liu\*

Department of General Surgery, the First Affiliated Hospital of Harbin Medical University, Harbin, China.

## Summary

Significant advances in our understanding of neutrophil biology were made in the past several years. A newly discovered mechanism was discovered, the formation of neutrophils extracellular traps (NETs). The structure of NETs is composed of the DNA strand and neutrophil granule proteins. NETs were found to have an association with tumor progression. This review highlights the latest knowledge about the controversial effect on tumors of NETs. Pro-tumor and anti-tumor effects are described respectively. The probable mechanisms of the anti-tumor effect are related to its direct killing of cancer cells or stimulation of the immune system to fight against the tumor. The pro-tumor effect has a correlation with matrix metalloproteinase 9 (MMP-9), cathepsin G, and neutrophil elastase (NE). Moreover, the structure of the NETs makes it able to catch the circulating tumor cells, which could lead to metastasis. This review summarizes our knowledge about the proven roles of NETs in the progression of cancer with particular focus on the components of the NETs, and considers NETs as a potential target for cancer therapy.

**Keywords:** Neutrophils extracellular traps; tumor; cancer metastasis

## 1. Introduction

For decades, neutrophils were considered to be a significant infection defender for both innate and acquired immune systems. It was understood that neutrophils act in two ways: either by releasing antimicrobial proteins through degranulation into extracellular space or by phagocytosis of pathogenic microbes. However, a series of recent findings suggest that neutrophils could play their roles in another way: neutrophils extracellular traps (NETs) (1).

NETs were first found in 2004 (2). When neutrophils are activated, they can form extracellular fibrous structures composed of DNA and some proteins from azurophilic, specific and tertiary granules derived from activated neutrophils. Among these components, histones comprise the highest proportion of NETs

(3). The remainder of proteins that exist on the DNA scaffold include granular protein, cytoplasmic proteins, cytoskeletal proteins, and some other enzymes. Most of these molecules have been shown to participate in both direct and indirect pathogen-killing mechanisms. With such a number of proteins, as a result, NETs can influence the internal environment in different ways (4).

Although NETs play an important role in killing pathogenic microbes like bacteria or fungi, in some conditions when it is excessively generated, NETs can do harm to the human body (5). For instance, evidence showed that it can promote vasculitis and thrombosis. Moreover, NETs have been implicated in sterile inflammation diseases such as rheumatoid arthritis and systematic lupus erythematosus (6).

Recently, some studies have found that NETs are also involved with tumors. Nevertheless, these results go in two different directions: one is NETs can promote tumor proliferation, invasion, and metastasis, while the other suggests that NETs can inhibit cancer cell proliferation and invasion. Since this research was performed under different experimental conditions and the diseases being studied were different, there is not a clear conclusion on how NETs affect tumors or whether it is a pro-tumor factor or an anti-tumor factor.

Released online in J-STAGE as advance publication December 21, 2019.

\*Address correspondence to:

Dr. Lianxin Liu, Department of General Surgery, the First Affiliated Hospital of Harbin Medical University, Harbin, Heilongjiang, 150001, China.

E-mail: liulianxin@ems.hrbmu.edu.cn

Therefore, in this review, we aimed to elaborate on these findings and explore how NETs affect tumors and which mechanism could be a potential therapeutic target.

## 2. Formation of NETs in tumor progression

The formation of NETs also referred to as "NETosis" is a complicated process. It is related to the regulation of peptidyl arginine deiminase 4 (PAD4) and reactive oxygen species (ROS). PAD4 could convert histone methylarginine residues to citrulline by a novel reaction termed demethyliminium (7). The mouse with PAD4 knocked out can't generate NETs (8). However, NETs added with wild neutrophils can be generated again. Taken together, these findings suggest that PAD4 is an important factor that could regulate the formation of NETs. Another researcher found that when phorbol myristate acetate (PMA) adds to neutrophils, it could oxidize nicotinamide adenine dinucleotide phosphate (NADPH). NADPH-oxidase activation generates the superoxide anion (9). A series of down enzymes convert the superoxide to a series of other reactive oxygen species (ROS). After that, neutrophils release the DNA and relevant protein to form NETs.

Currently recognized stimuli for NETs formation and release include Nitric oxide (10), cytokines (11), microbes and their products (12), antimicrobial peptides (13) and some medicine like statins (14). The recently discovered anti-bacterial mechanism of NETs indicated their positive role in infections. There is an abundance of data suggesting that the processes between inflammation and neoplasia are kind of similar. The mediators and effector cells were found to be critical in the promotion and progression of the neoplastic process. Thus, people hypothesized NETs could be crucial in tumor development progress.

High expression of NETs is found in some malignant cancers. For example, researchers found that in the specimens of 8 patients with Ewing sarcoma there is a high expression of NETs and tumor-associated neutrophils. And in 2 of 8 patients, they observed NETs deposition in the tumor focus (15). Moreover, another study found that in a 9-day-old tumor of lewis lung carcinoma, a large number of neutrophils and extracellular chromatin were observed (16). Also, in other malignant tumors such as breast cancer and lymphoma, NETs are found with immunofluorescence or laser scanning confocal microscopy (17,18).

As NETs are observed in tumor tissues, people wonder whether cancer cells can stimulate the formation of NETs. Therefore, some researchers co-cultured cancer cells with vital neutrophils. As expected, when co-cultured with vital neutrophils, breast cancer cells (19), diffuse large B cell lymphoma and (20) non-small-cell lung cancer cells can stimulate neutrophils to form and release NETs. Cancer cells themselves can

be an antigen to initiate NETosis and it can also release cytokines or make normal tissue damaged to generate nitric oxide to do the same. A study has proved that tumor-derived cytokine, IL-8 or murine homologue, can induce the formation of NETs. Besides, with the tumor's growth, it can lead to tissue damage and intravascular tumor thrombosis which can cause ischemic necrosis (21). Taken together, those factors can all stimulate the formation of NETs.

## 3. Controversial effect of NETs in tumor disease

Some researchers investigated whether NETs have correlations with tumor patients' prognosis. Interestingly, the prognosis depends on the tumor type. In breast cancer (19) and lung cancer (22), a larger amount of NETs are observed at an advanced stage than in the primary stage. And NETs levels could be an independent prognostic factor in pancreatic ductal adenocarcinoma (PDAC) (23). Tumor-infiltrating NETs predicted poor postsurgical survival of patients with PDAC. NETs were an independent prognostic factor in PDAC and incorporation of NETs along with the standard TNM staging system refined risk-stratification and predicted survival in PDAC with improved accuracy.

Those studies above all suggest that NETs indicate poor prognosis. Nevertheless, there are studies that suggest NETs deposition in tumor tissue has a cytotoxic effect. In malignant melanoma, NETs play an antineoplastic role (24). In the ulcerated area, the researchers detected more NETs, and NETs can come into contact with tumor cells. Then, surprisingly, they found that contacting NETs can inhibit melanoma cell migration and viability.

## 4. Anti-tumor effect of NETs

There is speculation that NETs play an anti-cancer role because of its direct killing of cancer cells or stimulation of the immune system to fight against the tumor.

Myeloperoxidase (MPO) is a component of NETs. MPO is present at 71.3 mg per gram of NET DNA, or a 1.01 molar amount (25). MPO could kill melanoma cells and inhibit their growth after implementation. The study found that patients with chronic granulomatous disease fail to make NETs because of the mutations that disrupt the ability of the nicotinamide adenine dinucleotide phosphate (NADPH) oxidase to generate superoxide, which dismutates to hydrogen peroxide, the substrate of MPO. These patients are susceptible to infection and have a higher incidence of cancer than healthy people (26). Therefore, MPO is a representative component of NETs that makes NETs an anti-tumor factor.

The components that comprise the highest proportion of neutrophil extracellular trap proteins are histones. Especially, H2A, H2B, and H3 are present

in amounts of 379, 299 and 199 mg per gram of NET DNA. Histones, another important element of the NETs, are able to do damage to epithelial cells and consequently do damage to the blood vessels feeding the tumor. Also, it represents a potential attachment site for pathogens and carries antibacterial activity. Studies have shown that integrin mediates cancer cell adhesion by binding to fibronectin, which co-localize with histone H3 and the web-like structure of NETs (25).

Not only histones provide a site for the pathogen to bind, but the DNA structure also plays an important role in capturing cancer cells. The study we mentioned above (24) found that when melanoma cell line A375 was co-cultured with NETs, their ability to metastasize and proliferate declined. *In vivo* experiment showed the same result. However, when co-cultured with neutrophils' DNA *in vitro* or with DNase treatment *in vivo*, cancer cells' ability to proliferate and metastasize can't be inhibited. These findings suggest that it is the web-like structure but not the DNA that causes this anti-effect. The web-like structure promotes the adhesion of melanoma cells similar to the mechanism for capturing microbes (2).

### 5. Pro-tumor effect of NETs

As we all know, NETs could improve immune capacity to eliminate microbes or cancer cells. However, the special structure and proteases may degrade extracellular matrix and promote metastasis of neoplastic cells. What's more, the tumor's microenvironment can predispose neutrophils to release NETs. Some studies hypothesized that the scaffold structure of NETs can stimulate platelet adhesion and contribute to formation of blood clots in progression of cancer (27,28).

These findings suggest that NETs could promote tumor progression and metastasis within the tumor. However, there is no study to explain clearly the mechanism. Some published literature reports NETs-derived components anti-tumor effects. As previously said, neutrophils extracellular traps component include neutrophil-derived chromatin, enzymes, antimicrobial proteins, and peptides. Some of these components have been proved to promote cancer proliferation and metastasis. These include matrix metalloproteinase 9(MMP-9), cathepsin G, and neutrophil elastase (NE). It is known that NETs could adhere to cancer cells. As a result, the adhesion may provide a microenvironment for tumor cells and those functional molecules to contact with each other where the biologically active proteins have a high local concentration. These events can act to promote proliferation, inhibit apoptosis and induce metastasis.

Neutrophil elastase is a kind of serine protease that is stored in azurophilic granules of neutrophils. During the process of "NETosis", activated neutrophils can

release the neutrophil elastase into the extracellular matrix. The main physiological function of NE is to clear pathogens during infection. However, NE can also degrade extracellular matrix, which leads to tissue damage. Both *in vivo* and *in vitro*, neutrophil elastase has demonstrated a number of pro-tumorigenic roles. In some global NE deletion mouse models, tumor burden is significantly reduced, which proves that NE plays an important role in tumor development.

Using the model of lung adenocarcinoma, mice lacking NE showed a longer survival time than the control group mice with NE. *In vitro*, NE could also enhance proliferation and migration of the tumor cells. When the A549 cell is co-cultured with polymorphonuclear leukocytes, cell proliferation is increased. Interestingly, it is inhibited while A549 is co-cultured with NE<sup>-/-</sup> polymorphonuclear leukocytes. What's more, adding NE inhibitors into culture media, proliferation of the tumor cell is attenuated (29). The pro-tumor effects of NE were proved to be mediated by the phosphatidylinositol-4, 5-bisphosphate 3-kinase (PI3K) pathway. Moreover, this NE-mediated proliferation of A549 cells is attenuated by specific PI3K inhibitors. Therefore, researchers wonder what is activated downstream. To that end, it was found that the degradation of insulin receptor substrate-1 leads to PI3k activation and increases proliferation (30). Other studies proved that NE could also increase the concentration of transforming growth factor  $\alpha$ , vascular endothelial growth factor(VEGF) and platelet-derived growth factor (PDGF) in the tumor cell culture in the media (31). These findings suggest that NE may promote release of these pro-tumor factors into the extracellular environment, promoting interactions with their cognate receptors (32). Taken together, these mechanisms implicate the direct and indirect roles for NE in promoting tumor progression.

Matrix metalloproteinase 9(MMP-9) is another crucial component of NETs that could promote tumor metastasis *via* the degradation of the extracellular matrix. In a study, a researcher found a decreased frequency of invasive tumors in a mice group with MMP-9 inhibitor. Furthermore, this finding was supported by immunohistochemical analysis of squamous cell carcinoma, which proved that MMP-9 existed mostly in invading granulocytes. Thus, the authors indicated that MMP-9 is associated with increased proliferation of neoplastic cells. Besides, MMP-9 could also facilitate tumor cells by inhibiting apoptosis in tumor cells (33). In the study above, the authors demonstrated an 81% increase in metastatic foci after tail vein injection of LLC cells compared to MMP-9<sup>-/-</sup> mice. Moreover, it proved that MMP-9 in metastatic tumor foci is derived from infiltrated neutrophils and NETs (34). NETs-derived MMP-9 could also improve tumor angiogenesis, which could maintain both primary and metastatic tumor growth.

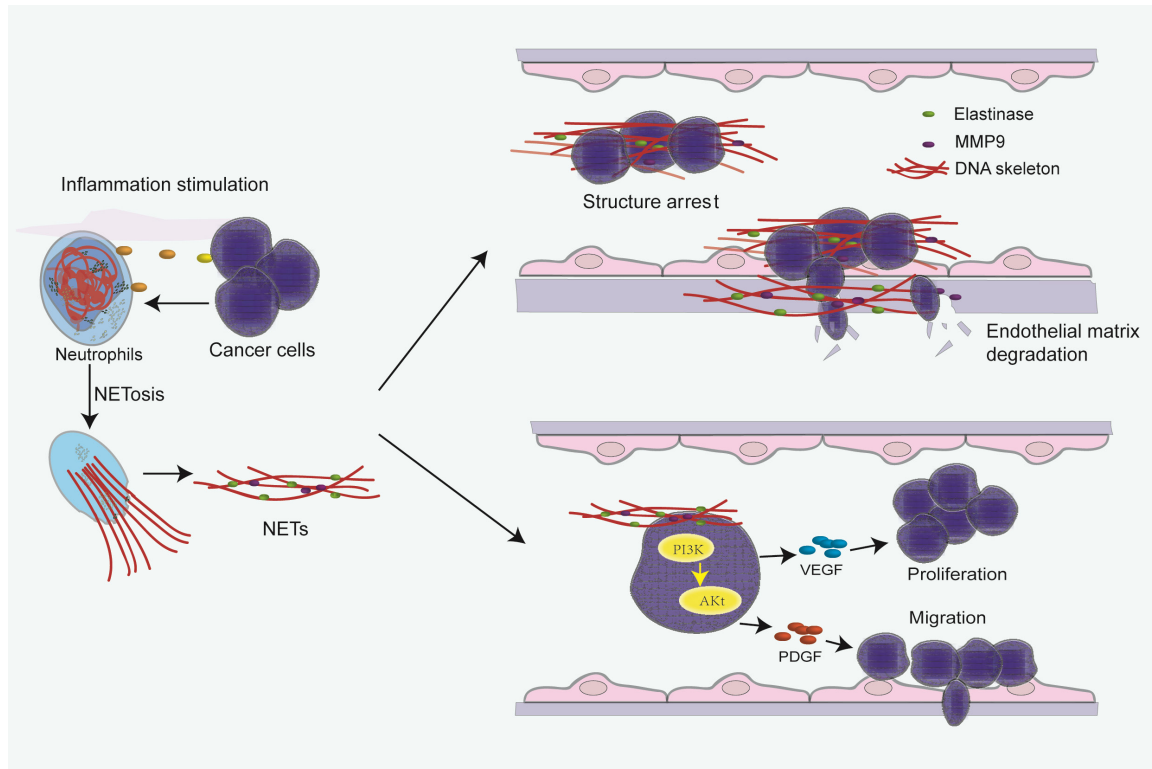


**Figure 1. The pro-tumor mechanism of NETs.** Cancer cells could promote neutrophils to release NETs. The net structure of NETs makes it able to catch the circulating tumor cell and carry them to other organs. The MMP-9 could degrade the extracellular matrix. NE and elastase on the NETs could promote tumor proliferation and migration via VEGF and PDGF signal pathways.

Some studies hypothesized MMP-9 takes part in liberating VEGF from the ECM. Inhibition of MMP-9 with the small molecule inhibitor R94138 can cause a decrease of angiogenic and an 80% reduction in the number of tumors (35). Taken together, these findings suggest that NETs-derived MMP-9 is a mediator of angiogenesis in this animal model. Moreover, this effect can be inhibited by anti-VEGF antibodies. With the addition of heparanase, this effect can be replicated. These all indicate that MMP-9 promotes tumor progression by liberating VEGF from the extracellular matrix *via* degradation activity.

Besides NE and MMP-9, there is another representative peptidase in NETs that promote tumor progression, cathepsin G. It is a peptidase inside the azurophilic granules (35,36). Cathepsin G could degrade bacteria during phagocytosis and remodel ECM (37). It has been proved that cathepsin G could also facilitate angiogenesis and tumor cell migration. People know that tumor cells could aggregate in the vasculature and form tumor emboli at a distant location. Cathepsin G showed the ability to facilitate formation of tumor aggregates in a mouse model of breast cancer (38). This aggregation was mediated by intracellular adhesion *via* E-cadherin. It also proved that inhibition of cathepsin G reduced aggregation of tumor cells. Tumor cells aggregation progress is mediated by binding of cathepsin G to their cell surface, benefited by its enzymatic activity.

Except for the components of NETs, the special structure also contributes to its tumorigenicity. First, it is well known that circulating tumor cells (CTC) contribute a lot to cancer metastasis. Due to the web-like structure and the stickiness of it, NETs are able to arrest intravascular bacteria. Thus, it may be able to capture CTC and cause adhesion to it in the same way. There is a researcher who tested whether NETs could augment tumor metastasis. In a septic mouse model, which has a larger amount of NETs, after injection with LLC cells, enhanced tumor cells arrested by NETs could be directly visualized compared to healthy controls (39). Moreover, deletion of neutrophils abrogates this effect and decreases the amount of CTC adhesion within the liver. When neutrophils with DNase contact tumor cells, the effect was abrogated. This proved that it is NETs but not neutrophils that promotes tumors (40). Furthermore, another researcher used PMA to induce a mouse model to induce NETs. In the PMA treatment group, the adhesion ability of lung carcinoma cells was increased fivefold when compared to the control group. This phenomenon was abrogated when using DNase or NETs formation inhibitor (18). This mechanism may be correlated by the  $\beta 1$ -integrin that expressed both NETs and a cancer cell surface. Taken together, as NETs could carry tumor cells just like they carry other pathogenic microbes to an adjacent area where there are more antibacterial proteins or peptides, this function of

it could promote tumor cell metastasis. Besides, NETs may promote a more malignant phenotype in cancer cells because of the interaction of NETs and tumor cells (Figure 1).

## 6. NETs as potential therapeutic targets

Some studies measured extracellular DNA and extracellular DNase levels in some patients' samples. It showed that mean DNase I levels were lower than the healthy control samples. Moreover, extracellular DNA levels were higher than the healthy control samples. For many years, researchers believed that cell-free DNA comes from mostly tumor cells. By now, it is known that NETs play a part in extracellular DNA and contribute to tumor progression and metastasis.

Therefore, people hypothesized that using DNase I to degrade the cell-free DNA could inhibit tumor progression. Salganik *et al.* used spontaneous lymphatic leukemia in the mouse as an animal model to detect the effect of injection of DNase I. The study found that the injection results in a decrease in lymph node size and prolonged survival time by 12 weeks (41). Other studies found that pre-treatment of DNase I led to an inhibition of cancer cell metastasis (42).

In many tumor models, we have already seen that DNase I treatment can reverse some pro-tumor effects of some factors. Thus, DNase I treatment may be a treatment target for cancer. Administration of human DNase I on adults and children with other diseases did not lead to severe adverse effects (43). With that, using DNase I alone or combining DNase I with other means seems available to treat some cancers. Recently, a number of clinical trials using DNase I treatment are in progress. However, there is no such treatment that can significantly reduce tumor size or metastasis in humans.

As the above said, peptidyl arginine deiminase 4 is a critical protein to regulate the formation of NETs. Using the PAD4 inhibitor can lead to a similar result inhibiting NETs formation. Nowadays, by using the mouse model with the PAD4 gene knocked out, researchers could explore various kinds of factors in a NETs-free microenvironment (44).

Lastly, NETs could capture microbes threatening people's life. Patients with such treatment are susceptible to other diseases such as sepsis, and other life-threatening conditions. Although the treatments above cannot inhibit all formation of NETs, it is still a challenge for people to overcome.

## 7. Concluding remarks

Despite that there are a number of studies about NETs, it is difficult to prove whether NETs have a pro-tumor effect or an anti-tumor effect. However, in the data that present the anti-tumor effect of NETs, like in Fiona Schedel's study (24), the researcher added NETs other

than with neutrophils into the cell culture media. It may be the components of NETs that play an anti-tumor role. These factors may have some binding sites with specific tumor cell surfaces. But the formation process of NETs and the migration of NETs can do harm to the peripheral tissue. Prolonged damage may lead to gene mutation or cause the normal cell to acquire tumorigenicity.

Whatever the mechanisms of NETs are, they show important value in clinical diagnosis and treatment. The circulating NETs may be a diagnostic marker or a prognostic indicator. DNase I is a potential treatment, as well as other NETs inhibitors. Moreover, a single component of NETs could be a therapeutic target for a kind of disease. Taken together, the recent development and safe utilization of NETs are promising and NETs are warranted for further investigation in the cancer field.

## References

1. Branzk N, Papayannopoulos V. Molecular mechanisms regulating NETosis in infection and disease. *Semin Immunopathol.* 2013; 35:513-530.
2. Brinkmann V, Reichard U, Goosmann C, Fauler B, Uhlemann Y, Weiss DS, Weinrauch Y, Zychlinsky A. Neutrophil extracellular traps kill bacteria. *Science.* 2004; 303:1532-1535.
3. Jaillon S, Peri G, Delneste Y, Fremaux I, Doni A, Moalli F, Garlanda C, Romani L, Gascan H, Bellocchio S, Bozza S, Cassatella MA, Jeannin P, Mantovani A. The humoral pattern recognition receptor PTX3 is stored in neutrophil granules and localizes in extracellular traps. *J Exp Med.* 2007; 204:793-804.
4. Jorch SK, Kubes P. An emerging role for neutrophil extracellular traps in noninfectious disease. *Nat Med.* 2017; 23:279-287.
5. Gregory AD, Houghton AM. Tumor-associated neutrophils: new targets for cancer therapy. *Cancer Res.* 2011; 71:2411-2416.
6. Erpenbeck L, Schon MP. Neutrophil extracellular traps: protagonists of cancer progression? *Oncogene.* 2017; 36:2483-2490.
7. Wang Y, Li M, Stadler S, Correll S, Li P, Wang D, Hayama R, Leonelli L, Han H, Grigoryev SA, Allis CD, Coonrod SA. Histone hyperacetylation mediates chromatin decondensation and neutrophil extracellular trap formation. *J Cell Biol.* 2009; 184:205-213.
8. Li P, Li M, Lindberg MR, Kennett MJ, Xiong N, Wang Y. PAD4 is essential for antibacterial innate immunity mediated by neutrophil extracellular traps. *J Exp Med.* 2010; 207:1853-1862.
9. Karlsson A, Dahlgren C. Assembly and activation of the neutrophil NADPH oxidase in granule membranes. *Antioxid Redox Signal.* 2002; 4:49-60.
10. Keshari RS, Jyoti A, Kumar S, Dubey M, Verma A, Srinag BS, Krishnamurthy H, Barthwal MK, Dikshit M. Neutrophil extracellular traps contain mitochondrial as well as nuclear DNA and exhibit inflammatory potential. *Cytometry A.* 2012; 81:238-247.
11. Gonzalez-Aparicio M, Alfaro C. Influence of Interleukin-8 and Neutrophil Extracellular Trap (NET)

- Formation in the Tumor Microenvironment: Is There a Pathogenic Role? *J Immunol Res.* 2019; 2019:6252138.
12. Fuchs TA, Abed U, Goosmann C, Hurwitz R, Schulze I, Wahn V, Weinrauch Y, Brinkmann V, Zychlinsky A. Novel cell death program leads to neutrophil extracellular traps. *J Cell Biol.* 2007; 176:231-241.
  13. Kraemer BF, Campbell RA, Schwertz H, Cody MJ, Franks Z, Tolley ND, Kahr WH, Lindemann S, Seizer P, Yost CC, Zimmerman GA, Weyrich AS. Novel anti-bacterial activities of beta-defensin 1 in human platelets: suppression of pathogen growth and signaling of neutrophil extracellular trap formation. *PLoS Pathog.* 2011; 7:e1002355.
  14. Chow OA, von Kockritz-Blickwede M, Bright AT, Hensler ME, Zinkernagel AS, Cogen AL, Gallo RL, Monestier M, Wang Y, Glass CK, Nizet V. Statins enhance formation of phagocyte extracellular traps. *Cell Host Microbe.* 2010; 8:445-454.
  15. Berger-Achituv S, Brinkmann V, Abed UA, Kuhn LI, Ben-Ezra J, Elhasid R, Zychlinsky A. A proposed role for neutrophil extracellular traps in cancer immunoediting. *Front Immunol.* 2013; 4:48.
  16. Ho-Tin-Noe B, Carbo C, Demers M, Cifuni SM, Goerge T, Wagner DD. Innate immune cells induce hemorrhage in tumors during thrombocytopenia. *Am J Pathol.* 2009; 175:1699-1708.
  17. Demers M, Krause DS, Schatzberg D, Martinod K, Voorhees JR, Fuchs TA, Scadden DT, Wagner DD. Cancers predispose neutrophils to release extracellular DNA traps that contribute to cancer-associated thrombosis. *Proc Natl Acad Sci U S A.* 2012; 109:13076-13081.
  18. Najmeh S, Cools-Lartigue J, Rayes RF, Gowing S, Vourtzoumis P, Bourdeau F, Giannias B, Berube J, Rousseau S, Ferri LE, Spicer JD. Neutrophil extracellular traps sequester circulating tumor cells *via* beta1-integrin mediated interactions. *Int J Cancer.* 2017; 140:2321-2330.
  19. Park J, Wysocki RW, Amoozgar Z, *et al.* Cancer cells induce metastasis-supporting neutrophil extracellular DNA traps. *Sci Transl Med.* 2016; 8:361ra138.
  20. An Z, Li J, Yu J, Wang X, Gao H, Zhang W, Wei Z, Zhang J, Zhang Y, Zhao J, Liang X. Neutrophil extracellular traps induced by IL-8 aggravate atherosclerosis *via* activation of NF-kappaB signaling in macrophages. *Cell Cycle.* 2019; 18:2928-2938.
  21. Yang C, Sun W, Cui W, Li X, Yao J, Jia X, Li C, Wu H, Hu Z, Zou X. Procoagulant role of neutrophil extracellular traps in patients with gastric cancer. *Int J Clin Exp Pathol.* 2015; 8:14075-14086.
  22. Rayes RF, Mouhanna JG, Nicolau I, Bourdeau F, Giannias B, Rousseau S, Quail D, Walsh L, Sangwan V, Bertos N, Cools-Lartigue J, Ferri LE, Spicer JD. Primary tumors induce neutrophil extracellular traps with targetable metastasis promoting effects. *JCI Insight.* 2019; 5.
  23. Jin W, Xu HX, Zhang SR, Li H, Wang WQ, Gao HL, Wu CT, Xu JZ, Qi ZH, Li S, Ni QX, Liu L, Yu XJ. Tumor-Infiltrating NETs Predict Postsurgical Survival in Patients with Pancreatic Ductal Adenocarcinoma. *Ann Surg Oncol.* 2019; 26:635-643.
  24. Schedel F, Mayer-Hain S, Pappelbaum KI, Metze D, Stock M, Goerge T, Loser K, Sunderkotter C, Luger TA, Weishaupt C. Evidence and impact of neutrophil extracellular traps in malignant melanoma. *Pigment cell & melanoma research.* 2019.
  25. Urban CF, Ermert D, Schmid M, Abu-Abed U, Goosmann C, Nacken W, Brinkmann V, Jungblut PR, Zychlinsky A. Neutrophil extracellular traps contain calprotectin, a cytosolic protein complex involved in host defense against *Candida albicans*. *PLoS Pathog.* 2009; 5:e1000639.
  26. Metzler KD, Fuchs TA, Nauseef WM, Reumaux D, Roesler J, Schulze I, Wahn V, Papayannopoulos V, Zychlinsky A. Myeloperoxidase is required for neutrophil extracellular trap formation: implications for innate immunity. *Blood.* 2011; 117:953-959.
  27. Demers M, Wagner DD. Neutrophil extracellular traps: A new link to cancer-associated thrombosis and potential implications for tumor progression. *Oncoimmunology.* 2013; 2:e22946.
  28. Fuchs TA, Brill A, Duerschmied D, Schatzberg D, Monestier M, Myers DD, Jr., Wroblewski SK, Wakefield TW, Hartwig JH, Wagner DD. Extracellular DNA traps promote thrombosis. *Proc Natl Acad Sci U S A.* 2010; 107:15880-15885.
  29. Houghton AM, Rzymkiewicz DM, Ji H, *et al.* Neutrophil elastase-mediated degradation of IRS-1 accelerates lung tumor growth. *Nat Med.* 2010; 16:219-223.
  30. Gregory AD, Hale P, Perlmutter DH, Houghton AM. Clathrin pit-mediated endocytosis of neutrophil elastase and cathepsin G by cancer cells. *J Biol Chem.* 2012; 287:35341-35350.
  31. Wada Y, Yoshida K, Tsutani Y, Shigematsu H, Oeda M, Sanada Y, Suzuki T, Mizuiri H, Hamai Y, Tanabe K, Ukon K, Hihara J. Neutrophil elastase induces cell proliferation and migration by the release of TGF-alpha, PDGF and VEGF in esophageal cell lines. *Oncol Rep.* 2007; 17:161-167.
  32. Wada Y, Yoshida K, Hihara J, Konishi K, Tanabe K, Ukon K, Taomoto J, Suzuki T, Mizuiri H. Sivelestat, a specific neutrophil elastase inhibitor, suppresses the growth of gastric carcinoma cells by preventing the release of transforming growth factor-alpha. *Cancer Sci.* 2006; 97:1037-1043.
  33. Acuff HB, Carter KJ, Fingleton B, Gorden DL, Matrisian LM. Matrix metalloproteinase-9 from bone marrow-derived cells contributes to survival but not growth of tumor cells in the lung microenvironment. *Cancer Res.* 2006; 66:259-266.
  34. Coussens LM, Tinkle CL, Hanahan D, Werb Z. MMP-9 supplied by bone marrow-derived cells contributes to skin carcinogenesis. *Cell.* 2000; 103:481-490.
  35. Nozawa H, Chiu C, Hanahan D. Infiltrating neutrophils mediate the initial angiogenic switch in a mouse model of multistage carcinogenesis. *Proc Natl Acad Sci U S A.* 2006; 103:12493-12498.
  36. Segal AW. How neutrophils kill microbes. *Annu Rev Immunol.* 2005; 23:197-223.
  37. Campanelli D, Detmers PA, Nathan CF, Gabay JE. Azurocidin and a homologous serine protease from neutrophils. Differential antimicrobial and proteolytic properties. *J Clin Invest.* 1990; 85:904-915.
  38. Gabay JE, Almeida RP. Antibiotic peptides and serine protease homologs in human polymorphonuclear leukocytes: defensins and azurocidin. *Curr Opin Immunol.* 1993; 5:97-102.
  39. McDonald B, Spicer J, Giannias B, Fallavollita L, Brodt P, Ferri LE. Systemic inflammation increases cancer cell adhesion to hepatic sinusoids by neutrophil mediated

- mechanisms. *Int J Cancer*. 2009; 125:1298-1305.
40. Spicer JD, McDonald B, Cools-Lartigue JJ, Chow SC, Giannias B, Kubes P, Ferri LE. Neutrophils promote liver metastasis *via* Mac-1-mediated interactions with circulating tumor cells. *Cancer Res*. 2012; 72:3919-3927.
  41. Salganik RI, Martynova RP, Matienko NA, Ronichevskaya GM. Effect of deoxyribonuclease on the course of lymphatic leukaemia in AKR mice. *Nature*. 1967; 214:100-102.
  42. Hawes MC, Wen F, Elquza E. Extracellular DNA: A Bridge to Cancer. *Cancer Res*. 2015; 75:4260-4264.
  43. Guichard MJ, Patil HP, Koussoroplis SJ, Wattiez R, Leal T, Vanbever R. Production and characterization of a PEGylated derivative of recombinant human deoxyribonuclease I for cystic fibrosis therapy. *Int J Pharm*. 2017; 524:159-167.
  44. van der Windt DJ, Sud V, Zhang H, Varley PR, Goswami J, Yazdani HO, Tohme S, Loughran P, O'Doherty RM, Minervini MI, Huang H, Simmons RL, Tsung A. Neutrophil extracellular traps promote inflammation and development of hepatocellular carcinoma in nonalcoholic steatohepatitis. *Hepatology*. 2018; 68:1347-1360.

(Received December 4, 2019; Revised December 12, 2019; Accepted December 15, 2019)

# A review of traditional Chinese medicine for treatment of glioblastoma

Jinjing Wang<sup>1</sup>, Fanghua Qi<sup>2</sup>, Zhixue Wang<sup>2</sup>, Zhikun Zhang<sup>1</sup>, Ni Pan<sup>1</sup>, Lei Huai<sup>1</sup>, Shuyu Qu<sup>1</sup>, Lin Zhao<sup>2,\*</sup>

<sup>1</sup>Shandong University of Traditional Chinese Medicine, Ji'nan, China;

<sup>2</sup>Department of Traditional Chinese Medicine, Shandong Provincial Hospital affiliated to Shandong University, Ji'nan, China.

## Summary

Glioblastoma (GBM) is the most common primary malignant intracranial tumor. Due to its high morbidity, high mortality, high recurrence rate, and low cure rate, it has brought great difficulty for treatment. Although the current treatment is multimodal, including surgical resection, radiotherapy, and chemotherapy, it does not significantly improve survival time. The dismal prognosis and inevitable recurrence as well as resistance to chemoradiotherapy may be related to its highly cellular heterogeneity and multiple subclonal populations. Traditional Chinese medicine has its own unique advantages in the prevention and treatment of it. A comprehensive literature search of anti-glioblastoma active ingredients and derivatives from traditional Chinese medicine was carried out in literature published in PubMed, Scopus, Web of Science Cochrane library, CNKI, Wanfang, and VIP database. Hence, this article systematically reviews experimental research progress of some traditional Chinese medicine in treatment of glioblastoma from two aspects: strengthening vital *qi* and eliminating pathogenic *qi*. Among, strengthening vital *qi* medicine includes panax ginseng, licorice, lycium barbarum, angelica sinensis; eliminating pathogenic medicine includes salvia miltiorrhiza bunge, scutellaria baicalensis, coptis rhizoma, thunder god vine, and sophora flavescens. We found that the same active ingredient can act on different signaling pathways, such as ginsenoside Rg3 inhibited proliferation and induced apoptosis via the AKT, MEK signal pathway. Hence, this multi-target, multi-level pathway may bring on a new dawn for the treatment of glioblastoma.

**Keywords:** Glioblastoma (GBM), traditional Chinese medicines (TCMs), active ingredients, migration and invasion, autophagy, signal pathway

## 1. Introduction

Gliomas, which arise from glial or precursor cells, are the most common primary intracranial tumors. Gliomas includes diffuse astrocytic, oligodendroglial tumor, glioblastoma, ependymal tumor and so on (1,2). According to the World Health Organization (WHO) classification system, gliomas are classified into WHO grade I-IV.

Among these, WHO grade I and WHO grade II belong to low grade gliomas, WHO grade III and WHO grade IV belong to high grade gliomas. The higher the level, the higher the degree of malignancy, and the worse the prognosis. Clearly, glioblastoma (GBM), belonging to WHO grade IV, is the most frequent as well as malignant glioma in astrocytoma. In 2016, WHO according to histology combined with molecular features reclassified central nervous system (CNS) tumors, and glioblastomas were divided into glioblastoma, *IDH*-wildtype, glioblastoma, *IDH*-mutant, as well as glioblastoma, not otherwise specified (NOS) (2). Among glioblastomas, *IDH*-wildtype is mostly known as primary or de novo glioblastoma, accounting for about 90% of patients, and it is more common in elderly people over 60 years old, with poor prognosis. However, glioblastoma, *IDH*-

Released online in J-STAGE as advance publication December 23, 2019.

\*Address correspondence to:

Dr. Lin Zhao, Department of Traditional Chinese Medicine, Shandong Provincial Hospital affiliated to Shandong University, No. 324, Jingwuweiqi Road, Ji'nan 250021, Shandong, China.

E-mail: zhaolin5757@126.com

mutant, known as secondary glioblastoma, is mostly evolved from low grade astrocytoma and it is more common in young people, with better prognosis, only accounting for about 10% of patients in clinic (3).

Glioblastoma has characteristics of three high and one low, namely high morbidity, high mortality, high recurrence rate, low cure rate, so the prognosis of it is very poor. According to CBTRUS statistical report in the United States in 2007-2011, it accounts for 15.4% of the primary brain tumors and 45.6% of the primary malignant brain tumors (1). The morbidity of glioblastoma is about 3.19 per 100,000 population in malignant tumors and increases with age mostly focused on 75 to 84 years, and the 5-year survival rate of patients is about 5% (1). The conventional treatment of glioblastoma is surgical resection as far as possible, followed by radiotherapy and adjuvant chemotherapy, however, its median survival is only 15 months without significant improvement (4,5). As tumor cells of glioblastoma can infiltrate into normal brain tissue, the majority of glioblastomas invariably recur despite initial treatment (6). The most advanced multimodal treatment can effectively prolong survival, however, the operation can easily cause side effects such as cerebral hemorrhage and cerebral edema, radiotherapy can cause radiation brain damage and chemotherapy can cause severe bone marrow suppression, nausea, vomiting and so on, which seriously affects patients' quality of life. The dismal prognosis and inevitable recurrence as well as resistance to chemoradiotherapy in glioblastoma may be attributed to its cellular heterogeneity and multiple subclonal populations (4). In addition, according to genomic profiling, the four glioblastoma subtypes have been defined, namely classical, mesenchymal, neural, and pro-neural and different subtypes may require different treatments (7). Hence, in order to improve the survival rate of GBM patients, it is necessary to adopt novel personalized treatment programs such as targeted therapy, immunotherapy, traditional Chinese medicine therapy and other ways. Although there are three signaling pathways (RTK/RAS/PI-3K, P53 and RB signaling) in GBM, the efficacy of related inhibitors is limited in targeted therapy of clinical trials (8). Similarly, a part of the tumor vaccines have been terminated in clinical trials of GBM immunotherapy because the effect is not obvious (9). PD-1/PD-L1 inhibitors and CTLA-4 inhibitors have been proved to effectively inhibit other tumors such as melanoma, but the role of anti-GBM is still clearly illustrated (9). Therefore, immunotherapy and targeted therapy have broad prospects in the clinical application of glioblastoma. Of course, so is traditional Chinese medicine therapy.

Traditional Chinese Medicine (TCM) has a unique and integrative theoretical system. It is a summary of the Chinese people's experience in their struggle against diseases, with a history of thousands of years. The holistic concept and syndrome differentiation are the dominant idea in clinical practice. TCM, as an important part

of complementary and alternative medicine, plays an important role in various diseases, whether used alone or in combination with western therapy. As we all known, in October 2015, Chinese scientist Tu Youyou was honored with the Nobel Prize in Physiology or Medicine because she discovered artemisinin, an extract derived from *Artemisia annua*, which can significantly and effectively treat malaria results while saving millions of lives (10). Of course, TCM has its own unique advantages in the prevention and treatment of tumors. Overall, TCM can prevent the formation of tumors, increase efficiency and reduce toxicity, reduce tumor recurrence and metastasis, prolong survival time and improve patients' quality of life (11). Without doubt, no matter a single or formulations of traditional Chinese herbs, TCM has also made great achievements in cancer. Such as, PHY906 (YIV-906), a mixture of four herbs (Astragalus, Licorice, Peony, Jujube), which was developed by Yale university professor Yungchi Cheng, and combined with chemotherapy and radiotherapy has significant effects on clinical trials of colorectal cancer, liver cancer and pancreatic cancer. In addition, Vincristine is a naturally alkaloid extracted from the leaves of *Catharanthus roseus* and it is remarkably effective in treatment of acute lymphoblastic leukemia, Hodgkin's disease and non-Hodgkin's disease, which was approved for marketing by the US FDA in 1960 (12). There are many natural anti-tumor active ingredients like this, such as paclitaxel, brucea oil, *etc.* However, at present, there are relatively few studies on traditional Chinese medicine for GBM. Therefore, this paper mainly reviews the experimental study of some traditional Chinese medicines in glioblastoma, and provides reference for its future treatment or adjuvant therapy.

## 2. The general principle of TCM in the treatment of GBM

As stated in Huangdi's Canon of Medicine, if the body owns sufficient vital *qi* inside, the pathogenic *qi* can't invade. The so-called "vital *qi*" is the body's resistance to the pathogenic microorganisms and the body's ability to adjust and adapt. However, "pathogenic *qi*" refers to various pathogenic factors, including wind, cold, summer-heat, dampness, dryness, heat (fire). Surely, whether the disease occurs is determined by the result of the struggle between the vital *qi* and the pathogenic *qi* in the body. If the vital *qi* is victorious, then it will not happen; however, if the pathogenic *qi* is successful, then the disease will occur, according to the theory of TCM. Therefore, strengthening vital *qi* with eliminating pathogenic *qi* is the general principle of treating diseases.

### 2.1. The traditional Chinese medicines against glioblastoma with strengthening vital *qi*

The most traditional Chinese medicines with the function

of strengthening vital *qi* in the body have the effect of invigorating *qi* and nourishing blood, nourishing *yin* and strengthening *yang*, in order to improve the body's immunity and resistance, expel the pathogen, and achieve the purpose of overcoming diseases and restoring health, as shown in Table 1

### 2.1.1. *Panax Ginseng*

*Panax Ginseng* has the effect of reinforcing vital energy and is known as the king of the herbs in the Orient, which originates in the dried root of the Araliaceous plant *Panax ginseng* C.A.Mey (Figure 1A) (13,14). It has gained popularity as a tonic, prophylactic and restorative agent for at least 2000 years (13). Red ginseng is a cooked product of ginseng. Its medicinal properties are warmer and better at nourishing (Figure 1B). It is reported that ginseng is contained in many active constituents such as ginsenosides, polysaccharides, alkaloids, glucosides, phenolic acid, and so on (15). Studies on ginseng have focused on ginsenosides, followed by polysaccharides. According to the positioning of sugar moieties at carbon -3 and -6, ginsenosides can be divided into protopanaxadiol (ginsenoside Rb1, Rb2, Rg3, Rc, and Rd) and pro-topanaxatriol (ginsenoside Re, Rg1, Rg2, and Rh1) groups; since carbon C-20 position substituted poorly with isobutyl, and it is further divided into 20 (S) and 20 (R) (Figures 1C-1F) (15). Modern pharmacological studies have shown that ginseng has many biological activities including anti-adhesive, anti-tumor, anti-diabetic, anti-age, neuroregulation, immunomodulation, etc (15). Studies revealed that chronic treatment with 20(s)-Rg3 induced senescence-like growth arrest in U87 glioma cells *via* AKT activation and p53/p21 signal pathway to induce reactive oxygen species (ROS) generation (16). Also, ginsenoside Rg3 inhibited growth and induced apoptosis in the U87MG cell lines, the mechanisms were related to the MEK signaling pathway and ROS (17). Additionally, ginsenoside Rd (Gs-Rd) induced apoptosis and inhibited proliferation of human glioma U251 cells by up-regulating the expression of caspase-3 and down-regulating the expression of Bcl-2 and hTERT in a dose-time-dependent manner, which may be attributed to inhibition of telomerase activity (18). The combined ginsenoside Rg3 with low-dose metronomic temozolomide displayed additive antiangiogenic effects through arresting the cell cycle and inducing apoptosis in rat C6 and human umbilical vein endothelial cells (19). Some research demonstrated that ginsenoside Rh2 exerted an anti-tumor effect on human A172 glioma cells *via* induced cell cycle arrest at G1 phase, which was related to modulating the expression of CDK4/CyclinD complex and Akt (20). Compound K, a particular ginsenoside metabolite, inhibits SDF-1-induced cells migration by down-regulating PKC $\alpha$  and ERK1/2 activation and changes downstream signal transduction

of the CXCR4/CXCR12 pathway (21). A new style administration has been paid more and more attention by people because of its inherent advantages, such as crossing the blood-brain barrier and sustained release. Angiopep-2 functionalized ginsenoside-Rg3 loaded nanoparticles (ANG-Rg3-NP) inhibited the proliferation of C6 glioma cells in a concentration-dependent manner and easily crossed the blood-brain barrier (22). What's more, the synergistic effect of ginsenoside-Rh2 lipid nanoparticles and borneol inhibited the proliferation of C6 glioma cells more effectively (23).

### 2.1.2. *Licorice*

Licorice (gancào in Chinese), is the dried root and rhizome of the *Glycyrrhiza uralensis* Fich, or *Glycyrrhiza Bat*, or *Glycyrrhiza glabra* L (Figures 1G and 1H). It was first recorded in Shennong's Herbal Classic (Shennong Bencao Jing), the oldest Chinese pharmacopoeia, with functions of tonifying the spleen, invigorating *qi*, dispelling phlegm, relieving coughing, clearing heat, detoxifying, and mediating various medicines. Licorice is widely used in clinical prescriptions of traditional Chinese medicine, even "nine out of ten prescriptions contain licorice, which is called "national elder" in China. Up to now, more than 300 flavonoids, more than 20 triterpenoids, polysaccharides, and alkaloids have been isolated from it (24). Modern pharmacological studies have shown that licorice possesses multiple biological activities such as antitumor, antiviral, anti-inflammatory, antioxidative immunoregulatory, hepatoprotective, nerve protective and other activities (25). Licochalcone A (LA) is a natural chalcone derived from licorices and its chemical structure is shown in Figure 1(I). It induced mitochondrial dysfunction in glioma stem cells to further activate mitochondrial apoptosis signaling pathways, which led to cell death *in vitro* (26). Besides, a recent study indicated that LA inhibited U87 gliomas cell growth by concurrently arresting cell cycle in the G0/G1 and G2/M phases (27). Isoliquiritigenin (ISL), a member of the flavonoids (Figure 1J) has been found to inhibit proliferation and induce differentiation of glioma stem cells *through* the Notch1 signaling pathway (28). ISL attenuated cell proliferation of U87 cells in a time and concentration dependent manner and arrested cell cycle in the S and G2/M phase. Meanwhile, ISL upregulated expression of p21 and p27 proteins, indicating that caspase mediated apoptosis was an important mechanism of ISL against glioma U87 (29). Moreover, ISL attenuated migration and invasion of SHG44 human glioma stem cells by down-regulating expression of MMP-2 and MMP-9 (30).

### 2.1.3. *Lycium barbarum*

*Lycium barbarum*, the mature fruit of *Lycium barbarum* L., is also known as wolfberry, gogi berry, and gouqizi

Table 1. Experiments and corresponding mechanisms of some TCM with strengthening vital qi acting on anti-GBM

TCM name	Tilt the Latin name	Main active compounds	Cell lines	Stages of action	Related pathway	Effects and related mechanisms	Ref.
Panax Ginseng	Ginseng Ra-dix et Rhi-zoma	20(s)-Rg3	U87	Induced senescence	AKT and p53/p21	↑p-Akt; ↑p53; ↑p21; ↑ROS;	16
		ginsenoside Rg3	U87MG	Induced apoptosis	MEK	Inhibited growth; ↑Bax; ↓Bcl-2; ↑ROS	17
		ginsenoside Rg3	C6; HUVEC	antiangiogenesis	-	arrested cycle at S phase; suppressed proliferation; ↓VEGFA; ↓Bcl-2;	19
Licorice	Glycyrrhizae Radix et Rhizoma	ginsenoside Rh2	U87MG; A172	Inhibits proliferation; induces cell cycle arrest;	Akt	arrested cycle at G1 phase; ↓CDK4; ↓CyclinD; ↓Akt; ↓p-Akt	20
		Licochalcone A	glioma stem cells	induced mitochondrial dysfunction	mitochondrial apoptotic	induced caspase-dependent cell death; Induced mitochondrial fragmentation; reduced the membrane potential; ↓ATP production	26
		Isoliquiritigenin	glioma stem cells	inhibited proliferation and induced differentiation	Notch1	↓Hes1; ↓Notch1;	28
Lycium barbarum	Lycii Fruc-tus	LBPs	SHG44 human glioma stem cells	inhibit migration and invasion	-	↓MMP-2; ↓MMP-9	30
		LBPS +TMZ	rat C6 glioma	Inhibit growth, regulate immunity	-	↑CD3 <sup>+</sup> T; ↑CD8 <sup>+</sup> T; ↑TNF- $\alpha$ ;	34-35
		AS-C BP	rat C6 gliomas	Inhibit proliferation, arrested cell cycle in the G0-G1 phase, induced apoptosis	-	↑CD4 + CD25 + Tr ↓ANXA1; ↓IL-10	36
Angelica sinensis	Angelicae Sinensis Radix	PCH4	DBTRG-05MG; GBM8401; GBM8901;	Inhibited growth, induced apoptosis; reduced migrate;	JNK signaling pathway	↑IL-17; ↓Foxp3mRNA; ↓Treg; ↓Th17/Treg	42
		APs	U251	inhibited growth; inhibited proliferation; induce apoptosis	(TGF)- $\beta$	Inhibited proliferation; arrested cell cycle in the G0-G1 phase; induced apoptosis; ↑p21; ↑P16; ↓p-Rb; ↑p-P53; ↑P53; ↑Bax; ↓Bcl-2; ↑caspase9; ↑caspas3; ↑Fax; ↑caspase 8	40-41
		AS-C BP	DBTRG-05MG; GBM8401	Inhibited growth; induced apoptosis; reduced migrate;	JNK signaling pathway	↑p-JNK; ↑p-ERK; ↑Nur77;	42

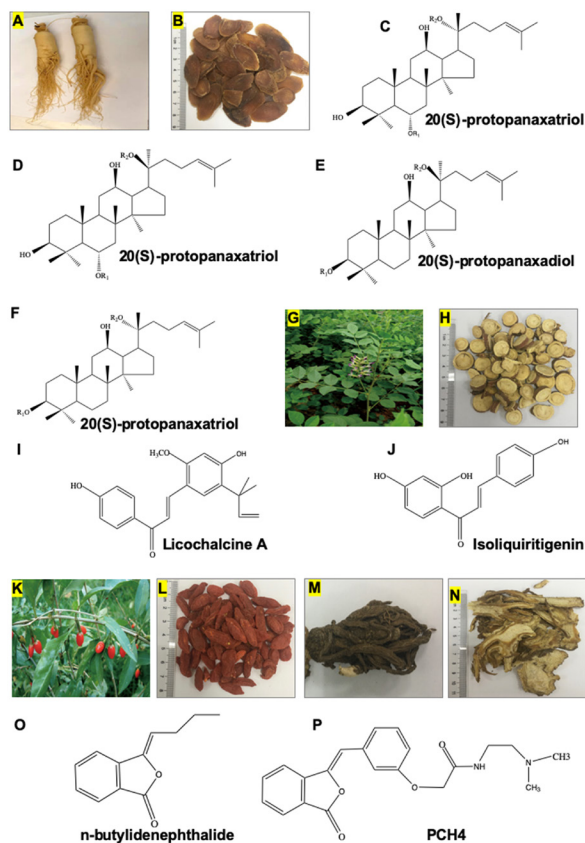


**Figure 1. Some anti-GBM TCMs with activities of strengthening vital qi, including ginseng, lico-riceLycium barbarum, and Angelica sinensis, and their major active ingredients.** (A) The roots of panax ginseng. (B) Chinese herbal pieces of red ginseng. (C) 20(R)-protopanaxatriol, (D) 20(S)-protopanaxatriol, (E) 20(S)-protopanaxadiol, and (F) 20(S)-protopanaxatriol, are the major active ingredients of panax ginseng. (G) The plants of licorice (91). (H) Chinese herbal pieces of licorice. (I) Licochalcine A and (J) Isoliquiritigenin are the major active ingredients of licorice. (K) The fruits of Lycium barbarum (91). (L) Chinese herbal pieces of Lycium barbarum. (M) The roots of Angelica sinensis. (N) Chinese herbal pieces of Angelica sinensis. (O) n-butylidenephthalide and (P) PCH4 are the major active ingredients of Angelica sinensis.

in Chinese (Figures 1K and 1L). It has been used in traditional homology of medicine and food for thousands of years in China. Lycium barbarum is mainly distributed in Northwest China, however lycium barbarum of the Ningxia region in China is famous for its highest quality, with an effect of nourishing liver, kidneys and eyes, and is listed in Pharmacopoeia of the People's Republic of China 2010 version (31,32). Various active compounds have been isolated from lycium barbarum, including polysaccharides, betaine, phenylpropanoids, coumarin, lignans, carotenoids, zeaxanthin dipalmitate, alkaloids, sterols, peptides, *et al* (32,33). However, Lycium barbarum polysaccharides (LBPs) accounted for 5.42-8.23% of total dried fruit and were considered the most major ingredients, while measuring the quality and pharmacological activities of lycium barbarum (31,32). It was reported that LBPs have many

biological activities, such as antiaging, neuroprotection, immunoregulatory, antioxidant, hepatoprotective, renalprotective, antidiabetic, antitoxic, and antitumor. Recent research demonstrated that LBPs inhibited the growth of tumors and prolonged the survival of rats C6 gliomas *in vivo*, which mechanism may be related to the regulation of immunity and the blood-brain barrier accompanying CD8+ Tcells entering the brain, exerting antitumor effects (34). This was consistent with the findings of Shan *et al.* in 2015 (35). In addition, the combination LBPs and temozolomide (TMZ) can better inhibit tumor growth compared to TMZ alone on brain glioma in rats, and this may be connected with regulation and distribution of Th17 and Treg cells (36). In short, the anti-GBM effect of LBPs may be related to immune regulation, but the specific mechanism remains unclear. In addition, there are few studies published in the English literature, and further research is needed.

#### 2.1.4. *Angelica sinensis*

*Angelica sinensis*, called danggui in Chinese, is the root of *Angelica sinensis* (Oliv) Diels (Figures 1M and 1N). It is a Chinese herbal medicine with a history of more than 2000 years and a good medicine for tonifying blood (37). It can be cultivated in many provinces in China, especially in Minxian County, Gansu Province (38). According to ancient Chinese medicine records *Angelica sinensis* has the functions of tonifying blood and regulating menstruation, promoting blood circulation and relieving pain, moistening intestine and relaxing bowel. It is mainly used to treat various gynecological diseases, including dysmenorrhea, amenorrhea, irregular menstruation, menopause and postpartum blood deficiency (37,38). More than 50 constituents have been isolated from the roots of *Angelica sinensis*. However, more than 165 constituents have been isolated from the whole plant since the 1970s (38). The chemical constituents of it include volatile oil, organic acids, polysaccharides and flavonoids. According to the current Chinese Pharmacopoeia (2010 edition), *Z*-ligustilide and ferulic acid have been officially used as marker compounds to characterize the quality of *Angelica sinensis* (38). In addition, polysaccharides have also attracted widespread attention as one of its main components (39). A series of studies have confirmed that *Angelica sinensis* and its derivatives have anti-glioma effects. AS-C, a chloroform extract from it, treated with glioma cells, showed that it not only inhibited cell proliferation, arrested cell cycle in the G0-G1 phase, induced apoptosis through P53-dependent and independent pathways, but had less toxic side effects compared with the current chemotherapy drugs such as Carmustine (BCNU), Taxol, and Temozolomide (40). Moreover, further studies confirmed that n-butylidenephthalide (BP), a major component of *Angelica sinensis* chloroform extract

(Figure 1O), has the same mechanism of action against glioma as described above (41). In order to study the gene expression of BP-induced glioma cell apoptosis, studies have shown that BP increased the expression of Orphan nuclear receptor Nur77-gene, releasing Nur77 from the nucleus to the cytoplasm, releasing cytochrome C from mitochondria, and activating mitochondria-associated apoptotic pathway (42). In addition, PCH4 is one of the derivatives of BP (Figure 1P), which has four times the anti-tumor effect of BP and induces Nur77-mediated apoptosis *via* the JNK signaling pathway (43). Z-ligustilide (LIG), an essential oil extract of *Angelica siensis*, significantly reduces the migration of Human Glioblastoma T98G Cells (44). *Angelica polysaccharides* (APs) could inhibit U251 glioma cells proliferation, arrest cell cycle in G0/G1 phase, and promote apoptosis by up-regulating Bax and cleaved-caspase-3 and down-regulating Bcl-2 expression *in vitro* and *in vivo* (45).

## 2.2. The traditional Chinese medicines against glioblastoma with eliminating pathogenic qi

The most traditional Chinese medicines with the function of eliminating pathogenic *qi* in the body have the effect of clearing heat and removing toxins, activating blood and removing stasis, in order to directly expel the pathogen, promote blood circulation, and achieve the purpose of overcoming diseases and restoring health, as shown in Table 2.

### 2.2.1. *Salvia miltiorrhiza* Bunge

*Salvia miltiorrhiza* Bunge, also known as danshen in Chinese, derived from the dried roots and rhizomes of a *salvia* species of Lamiaceae family (Figures 2A and 2B). It was first cited in Shen Nong Ben Cao Jing and was classified as top grade goods, with the effect of promoting blood circulation to regulate menstruation, dispelling blood stasis to relieve pain, cooling blood to eliminate carbuncles, and tranquilizing mind (46). So far, there has been broad studies on the chemical constituents and pharmacological activities of it. It was found that Danshen contains more than 200 chemical constituents, which have been isolated and identified (46-48). These chemical constituents were classified into three groups according to their structures, such as lipophilic diterpenoids, hydrophilic phenolic acids and others, and the first two were considered to be the main bioactive constituents of Danshen (47,48). The lipophilic diterpenoids are mainly composed of tanshinones, including tanshinone I, tanshinone IIA, tanshinone IIB, cryptotanshinone, dihydrotanshinone *etc.* However, hydrophilic phenolic acids mainly included salvianolic acid A-E, rosmarinic acid and so on (49). Numerous studies have demonstrated its bioactivities such as anti-oxidative, anti-inflammation,

anti-atherogenesis, anti-thrombosis, anti-hypertension, anti-fibrotic, immunoregulatory, neuroprotective, anti-tumor, *etc.* Relevant literature has shown that many extracts of Danshen possess antiglioma properties. Dihydrotanshinone (Figure 2C) could effectively inhibit the proliferation of human glioma SHG-44 cells in a dose and time dependent manner and induce apoptosis *via* activation of caspase-3 and caspase-9 and promoting the release of cytochrome C, which further leads to nuclear condensation and DNA fragmentation (50). Moreover, *in vitro* Glioblastoma model experiment, dihydrotanshinone could increase the efficacy of temozolomide and reduce side effects (51). In addition, cryptotanshinone (Figure 2D) has been reported to inhibit U87 cells and T78G cells proliferation and arrest in G1/G0 phase *via* downregulating cell cycle-related proteins cyclinD1 and survivin regulated by the STAT3 signaling pathway (52). Wang *et al.* demonstrated that tanshinone IIA (Figure 2E) suppressed proliferation, induced apoptosis and differentiation in human glioma U87 cells (53). Additionally, Tang *etc.* also showed that tanshinone IIA inhibited growth and induced apoptosis in rat C6 glioma cells, which was related to the STAT3 signaling pathway (54).

### 2.2.2. *Scutellaria baicalensis*

*Scutellaria baicalensis* (*huangqin* in Chinese), is the dried root of the perennial herb Lamiaceae family *Scutellaria baicalensis* Georgi (Figures 2F and 2G). The earliest description of it was recorded in the *Shijing* of the Western Zhou Dynasty, however, *Shennong Herbal Classic*, written in the Han Dynasty, first recorded its medicinal application (55). In Chinese herbology, it exhibits functions of clearing heat, drying dampness, purging fire and detoxifying, hemostasis, and preventing miscarriage. It has been mainly used in the treatment of jaundice, dysentery, pyrexia, diarrhea, carbuncles, and infections of the respiratory and gastrointestinal tracts (56,57). So far, more than 295 compounds have been isolated from it (58). Among them, flavonoids and their glycosides including baicalein, baicalin, wogonin, wogonosides, oroxylin A, are the major compounds with anti-tumor, anti-oxidant, anti-inflammatory, anti-microbial, neuroprotective and other pharmacological activities (58,59). Some studies have shown that *Scutellaria baicalensis* and its extracts have an anti-glioma effect, which brings hope for the treatment of glioma in the future. Research by Zhang Li *et al.* showed that Wogonoside (Figure 2H) induced autophagy and promoted apoptosis on different glioma cell lines, the mechanisms of apoptosis were attributed to activation of the p38 MAPK signaling pathway, inhibition of the PI3K/AKT/mTOR/p70S6K signaling pathway and production of ROS (60). Wogonin (Figure 2I) effectively inhibited cell growth, induced cell cycle arrest at the G0/G1 phase and induced cell differentiation into mature

**Table 2. Experiments and corresponding mechanisms of some TCM with eliminating pathogenic qi acting on anti-GBM**

TCM name	Tilt the Latin name	Main active compounds	Cell lines	Stages of action	Related pathway	Effects and related mechanisms	Ref.
Salvia miltiorrhiza Bunge	Salviae Miltiorrhizae Radix et Rhizoma	Dihydratanshinone cryptotanshinone	SHG-44; U87MG; T98G U87; T78G	Inhibited proliferation; induced apoptosis; augment TMZ efficacy Suppress proliferation	- STAT3	↓proliferation; Induced DNA fragmentation; ↑nuclear condensation; ↑Caspase3; ↑caspase9; ↑cytochrome c; ↓proliferation; Arrested cell cycle in G1/G0 phase; ↓cyclin D1; ↓survivin; ↓p-STAT3 Tyr705; attenuated STAT3 nuclear translocation	50, 51 52
Scutellaria baicalensis	Scutellariae Radix	Tanshinone IIA Wogonoside	U87 U251MG; SHG44; A172; U87MG	Inhibited proliferation; induced apoptosis; induced differentiation Induced autophagy; promoted apoptosis	- P38 MAPK; PI3K/AKT/mTOR/p70S6K;	↓proliferation; Arrested cell cycle in G1/G0 phase; ↑ADPRTL1mRNA; ↑CYP1A1; ↑GFAP; ↓nestin; Inhibited viability; induced mitochondrial apoptosis; ↓Bcl-2; ↑Bax; ↑cytochrome c; induced autophagy; ↑Beclin 1; ↑LC3-II; ↓p-p38; ↓p-AKT; ↓p-mTOR; ↓p-p70S6K; ↓p-JNK; ↑ROS	53 60
Coptis Rhizoma	Coptidis Rhizoma	wogonin baicalin	C6; U251 U87; U251	Inhibited proliferation; induced apoptosis; induced differentiation Inhibited migration and invasion	GSK-3β/catenin P38	↓proliferation; Arrested cell cycle in G1/G0 phase; ↓Cyclin D1; ↓CDK4; ↓CDK2; ↑P27; ↑GFAP; ↑GSK-3β; ↓β-catenin ↓proliferation; ↓migration; ↓invasion; ↓MMP-2; ↓MMP-9; ↑TIMP-1; ↑TIMP-2; ↓p-p38;	61 64
Coptis Rhizoma	Coptidis Rhizoma	Coptis chinensis granules berberine	U87; U251 U87; U251	Changed morphology; inhibited proliferation; intervated migration inhibits angiogenesis	STAT3 VEGF2/ERK	↓proliferation; changed morphology; ↓migration; induced G2/M arrest; induced apoptosis; ↓Total caspase3; ↑cleaved caspase 3; ↓HDAC3; ↓p-STAT3; ↓viability; ↓proliferation; ↓migration; ↑angiogenesis; ↓CD31; ↓p-VEGFR2; ↓p-ERK; ↓p-P38;	68 70
Thunder god vine	Radix et Rhizoma Tripterygii	berberine celastrol	T98G; U87; U251; SHG-44; U118; P53 U251; U87; C6	Induced autophagy; induced apoptosis; inhibited migration and invasion Inhibited proliferation; Induced autophagy; induced apoptosis	EGFR-MEK-ERK AMPK/mTOR/ULK1 ROS/JNK; AKT/mTOR	↓proliferation; ↑ROS; ↑Ca2+; ↑ER stress; mitochondrial dysfunction; ↓migration; ↓invasion; ↑p-PERK; ↑p-eIF2α; ↑GRP78/Bip; ↑CHOP/GADD135; ↓procaspase 3; ↑Bax; ↑cleaved PARP; ↑Cytochrome C; ↓Bcl-2; ↓EGFR; ↓p-RAF; ↓p-MEK; ↓p-ERK; ↑p-AMPK; ↓p-ULK1; ↑p-Becclin-1; ↓p-mTOR cell cycle arrest in G2/M phase; ↑Chk2; ↑p-Chk2; ↑cyclin B1; p-Cdc25C; ↑p-cdc2; ↑P21; ↓Cdc25c; change morphology; ↑cleaved PARP; ↑caspase3; ↑caspase9; ↑caspase 8; ↑autophagosomes; ↑LC3B; ↑Beclin-1; ↑P62; ↑ROS; ↑p-p38; ↑p-JNK; ↓p-Akt; ↓p-mTOR;	72-74 78
Sophora flavescens	Sophorae Flavescents Radix	triptolide matrine	U251; U87; C6; T98 U251; U87	induced apoptosis; inhibited migration and invasion induced apoptosis; inhibited migration and invasion	P53-independent P38 MAPK and AKT	↓proliferation; ↓Bcl-2; ↑Bax; cell cycle arrest in G0/G1 phase; ↓cyclin D1; ↓CDK6; ↓CDK4; ↓RB; change morphology; ↓migration; ↓invasion; ↓proliferation; ↓migration; ↓invasion; ↓N-cadherin; ↓EMT; ↑E-cadherin; ↓p-p38; ↓p-AKT;	79-80 86
		matrine	U251	Induced apoptosis; induced autophagy	PI3K/AKT; Wnt-β-catenin	↓Cyclin D1; ↑p53; ↑caspase3; ↑caspase9; ↓Bcl-2; ↓P62; ↑Beclin-1; ↑LC3III/LC3I; ↓circRNA-104075; ↓Wnt3a; ↓β-catenin; ↓p/t-PI3K; ↓p/t-AKT; ↓Bcl-9	87
		oxymatrine	U251	Inhibited proliferation; induced apoptosis	E G F R / P I 3 K / A K T / m T O R and STAT3	↓proliferation; arrested the cell cycle at the G0/G1 phase; ↓cyclin D1; ↓CDK6; ↓CDK4; ↓invasion; ↑caspase3; ↑Bax; ↓Bcl-2; ↓p-EGFR; ↓p-Akt; ↓p-mTOR; ↓p-STAT3	89

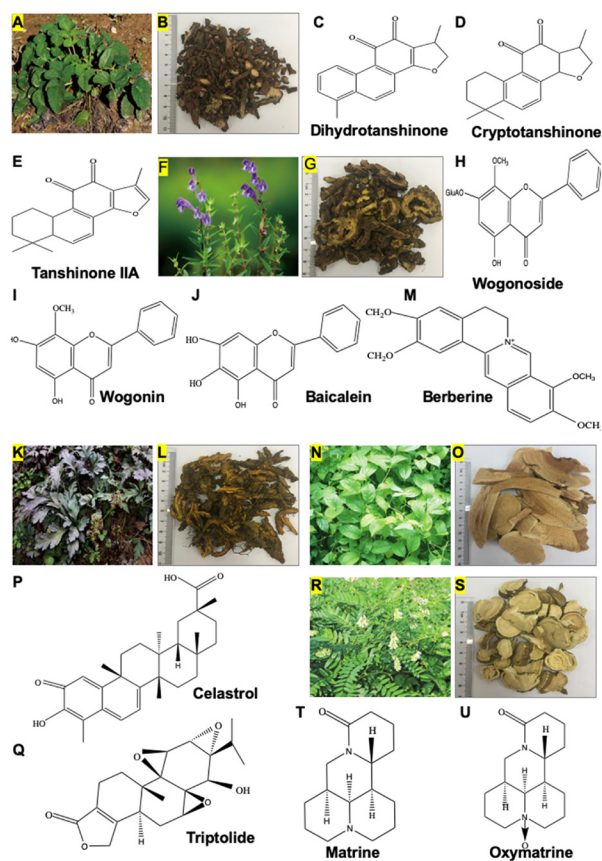


**Figure 2.** Some anti-GBM TCMs with activities of eliminating pathogenic qi, including *Salvia miltiorrhiza* Bunge, *Scutellaria baicalensis*, *Coptis Rhizoma*, thunder god vine, and *Sophora flavescens*, and their major active ingredients. (A) The plants of *Salvia miltiorrhiza* Bunge. (B) Chinese herbal pieces of *Salvia miltiorrhiza* Bunge. (C) Dihydrotanshinone, (D) Cryptotanshinone, and (E) Tanshinone IIA are the major active ingredients of *Salvia miltiorrhiza* Bunge. (F) The plants of *Scutellaria baicalensis*. (G) Chinese herbal pieces of *Scutellaria baicalensis*, (H) Wogonoside, (I) Wogonin, and (J) Baicalein are the major active ingredients of *Scutellaria baicalensis*. (K) The plants of *Coptis Rhizoma*. (L) Chinese herbal pieces of *Coptis Rhizoma*. (M) Berberine is one of the major active ingredients of *Coptis Rhizoma*. (N) The plants of thunder god vine plants. (O) Chinese herbal pieces of thunder god vine, (P) Celastrol and (Q) Triptolide are the major active ingredients of thunder god vine. (R) The plants of *Sophora flavescens*. (S) Chinese herbal pieces of *Sophora flavescens*. (T) Matrine and (U) Oxymatrine are the major active ingredients of *Sophora flavescens*.

astrocytes, which may be related to the inhibition of the GSK-3 $\beta$ / $\beta$ -catenin signaling pathway in C6 and U251 cells (61). In addition, wogonin induced growth arrest at the G1 phase, suppressed protein synthesis by activating AMPK to inhibit the mTOR pathway, induced apoptosis by activating the AMPK and p53 signaling pathways in human glioblastoma cells (62). Furthermore, it has also been reported that wogonin induced apoptosis *via* ROS generation and ER stress activation in U251 and U87 Human Glioma Cells (63). Baicalein (Figure 2J) reduced cell mobility, inhibited invasion and metastasis of U87MG and U251MG cell lines *in vitro* *via* downregulating MMP-2 and MMP-9 expression and

upregulating TIMP-1 and TIMP-2 expression through directly inhibiting the p38 signaling pathway (64).

### 2.2.3. *Coptis Rhizoma*

*Coptis Rhizoma* (CR), known as huanglian in China, is the dried rhizome of the family Ranunculaceae, which included *Coptis chinensis* Franch. (Weilian in Chinese), *Coptis deltoidea* C.Y. Cheng et Hsiao (Yalian in Chinese), or *Coptis teeta* Wall. (Yunlian in Chinese) (Figures 2K and 2L) (65,66). CR was also first mentioned in the Shen Nong Ben Cao Jing and was recorded with the effect of clearing heat, eliminating dampness, purging fire and detoxification (65,67). It is usually used to treat diarrhea, vomiting, abdominal distention, jaundice, high fever and coma, toothache, diabetes and eczema (66). Modern studies have confirmed that CR has multiple pharmacological spectrums, such as antibacterial, antiviral, anti-inflammatory, antihepatic steatosis, anti-atherosclerosis, antimyocardial ischaemia/reperfusion injury, antidiabetic, antihypertention, antihyperlipidemia, antiarrhythmia, antioxidation and antitumour effects (66). These pharmacological actions are closely related to its structure and active ingredients. So far, more than 100 components have been identified and separated from it. Among these, alkaloids are considered as the main bioactive ingredients, including berberine, palmatine, coptisine, epiberberine, jatrorrhizine and columamine (66,67). Many studies have shown that *Coptis Rhizoma* and its extract have obvious anti-glioma effects. *In vivo* and *in vitro* experiments have shown that *coptis chinensis* granules inhibited the proliferation of glioma cells, arrested cell cycle in G2/M phase and induced apoptosis *via* the down-regulation of photosynthesis of STAT3 by reducing HDAC3 (68). Berberine (Figure 2M) not only significantly inhibited inflammatory cytokine Caspase-1 activation *via* ERK1/2 signaling and subsequently decreased production of IL-1 $\beta$  and IL-18 in U251 and U87 cells, but inhibited the process of EMT through upregulating the protein expression of  $\beta$ -catenin,  $\alpha$ -catenin, and downregulating the protein expression of vimentin,  $\alpha$ -SMA, so, it could effectively inhibit glioma cell proliferation, invasion and metastasis (69). Jin reported that berberine exerted the function of anti-angiogenesis in glioblastoma *via* targeting the VEGFR2/EPK pathway (70). Sun reported that berberine could inhibit mitochondrial aerobic respiration and induce oncosis-like cell death (71). Besides, berberine also was reported to induce autophagy by inhibiting the AMPK/mTOR/ULK1 pathway and induce senescence by the EGFR-MEK-ERK signaling pathway, and induce apoptosis *via* ER stress, ROS and mitochondrial-dependent pathway in glioblastoma cells (72-74).

### 2.2.4. Thunder God Vine

Thunder god vine (Leigongteng in Chinese) is the dried root or xylem of the root of the *Tripterygium wilfordii* hook.f. the family Celastraceae (Figures 2N and 2O). According to the records, *Tripterygium wilfordii* has the functions of dispelling wind dampness, activating blood circulation, removing swelling and pain, killing insects and detoxifying. So, it has been widely used to treat rheumatoid arthritis, nephrotic syndrome, systemic lupus erythematosus, dermatitis, eczema and so on (75). Recently, people are paying more attention to its role as an anti-tumor agent. More than 300 compounds have been identified from it, and celastrol and triptolide are the most effective bioactive components, its chemical structures are shown in Figures 2P and 2Q (75,76). Previous research has shown that Celastrol inhibits tumor growth and reduces the density of microvessels and inhibits the expression and transcription of VEGF receptors (VEGFR-1 and VEGFR-2) in nude mice human glioma xenografts (77). Recent research confirmed that celastrol inhibited proliferation, arrested cell cycle in G2/M phase, induced apoptosis and triggered autophagy in glioma cells, which was closely related to the activation of ROS/JNK signaling and the blockade of the Akt/mTOR signaling pathway (78). Of course, triptolide, another major natural compound of *Tripterygium wilfordii*, also has anti-glioma effects. Triptolide had been reported to inhibit the proliferation and invasion, and induce apoptosis of glioma cells, and enhance temozolomide-induced apoptosis and potentiate inhibition of NF- $\kappa$ B signaling in glioma initiating cells (79-81).

#### 2.2.5. *Sophora flavescens*

*Sophora flavescens* (kushen in Chinese) is the dried root of the Fabaceae family *Sophora flavescens* Ait., which also was first recorded in Shen Nong Ben Cao Jing (Figures 2R and 2S). It has the effect of clearing heat and dampness, killing insects and diuresis, according to the theory of traditional Chinese medicine. It is mainly used to treat dysentery, jaundice, hematochezia, eczema and other skin diseases as well as gynecopathy such as pruritus and swelling of vulva (82). It is also popular in Japan, Korea, Hawaii and other countries (83). More than 200 compounds were isolated and identified from it, among which alkaloids and flavonoids are its main active ingredients (83). Among these, matrine and oxymatrine chemical structures are as shown in Figure 2T and 2U. They are also the main biologically active ingredients and have a wide range of pharmacological effects such as antiinflammatory, antiviral, antifibrotic, antiallergic, immunoregulatory, antitumor and so on (84,85). A great amount of research has revealed that matrine and oxymatrine have anticancer activity such as lung cancer, breast cancer, liver cancer, gastric cancer, pancreatic cancer and other cancers (84). Assuredly, it also has an anti-glioma effect. Matrine could inhibit invasion and metastasis in human glioma cells *via*

regulating epithelial-to-mesenchymal transition, which may be related to the inhibition of p38 MAPK and AKT signaling (86). Matrine could induce apoptosis and autophagy in U251 cells through down-regulating circRAN-104075 and Bcl-9 expression, which is attributed to regulate the PI3K/AKT and Wnt- $\beta$ -catenin pathways (87). Oxymatrine also inhibited proliferation and migration, as well as promoted apoptosis in Human Glioblastoma Cells (88). In addition, Wang *et al* further proved that Oxymatrine inhibited proliferation, arrested the cell cycle at the G0/G1 phase, induced apoptosis *via* the EGFR/PI3K/Akt/mTOR signaling pathway and STAT3 in U251MG human malignant glioma cells (89).

### 3. Conclusion

Glioblastoma, as a WHO grade IV glioma, is the most common primary malignant intracranial tumor. At present, conventional treatment (surgery, chemoradiotherapy) can't significantly improve the survival of patients. Hence, it is time to adopt novel personalized treatment programs such as targeted therapy, immunotherapy, gene therapy, traditional Chinese medicine therapy and other ways. Traditional Chinese medicine, as an important part of complementary and alternative medicine, the toxicity and safety of it have received increasing attention, but rational treatment and optimal application may avoid this problem (90). Traditional Chinese medicine play an important role in various diseases, whether used alone or in combination with Western therapy. Its active ingredients and derivatives have made great achievements in the treatment of diseases, such as artemisinin, vincristine, and paclitaxel, PHY906 and so on. This article studied the effects of active ingredients and derivatives about a part of traditional Chinese medicine on anti-glioblastoma, from the two aspects of strengthening vital *qi* and eliminating pathogenic *qi*. We find that the active components and derivatives of traditional Chinese medicine have functions of inhibiting proliferation, inducing cell cycle arrest, inhibiting invasion and migration, inducing apoptosis, anti-angiogenesis and improving immunity. However, since the current study is still relatively small, it is necessary to have large samples, and multicenter randomized double-blind controlled trials in the future. In addition, we also found that the same active ingredient can act on different signaling pathways. Hence, this multitarget, multi-level pathway would likely bring new directions for the treatment or adjuvant therapy of glioblastoma in the near future.

### Acknowledgements

This study was funded by National Natural Science Foundation of China (No.81503613) and National Natural Science Foundation of China (No. 81603449).

## References

- Ostrom QT, Gittleman H, Liao P, Rouse C, Chen Y, Dowling J, Wolinsky Y, Kruchko C, Barnholtz-Sloan J. CBTRUS statistical report: primary brain and central nervous system tumors diagnosed in the United States in 2007-2011. *Neuro Oncol.* 2014; 16 Suppl 4:iv1-63.
- Louis DN, Perry A, Reifenberger G, von Deimling A, Figarella-Branger D, Cavenee WK, Ohgaki H, Wiestler OD, Kleihues P, Ellison DW. The 2016 World Health Organization Classification of Tumors of the Central Nervous System: a summary. *Acta Neuropathol.* 2016; 1316:803-820.
- Ohgaki H, Kleihues P. The definition of primary and secondary glioblastoma. *Clin Cancer Res.* 2013; 194:764-772.
- Qazi MA, Vora P, Venugopal C, Sidhu SS, Moffat J, Swanton C, Singh SK. Intratumoral heterogeneity: pathways to treatment resistance and relapse in human glioblastoma. *Ann Oncol.* 2017; 287:1448-1456.
- Lim M, Xia Y, Bettgowda C, Weller M. Current state of immunotherapy for glioblastoma. *Nat Rev Clin Oncol.* 2018; 157:422-442.
- Wang Q, Hu B, Hu X, *et al.* Tumor Evolution of Glioma-Intrinsic Gene Expression Subtypes Associates with Immunological Changes in the Microenvironment. *Cancer Cell.* 2017; 321:42-56.e46.
- Verhaak RG, Hoadley KA, Purdom E, *et al.* Integrated genomic analysis identifies clinically relevant subtypes of glioblastoma characterized by abnormalities in PDGFRA, IDH1, EGFR, and NF1. *Cancer Cell.* 2010; 171:98-110.
- Taylor OG, Brzozowski JS, Skelding KA. Glioblastoma Multiforme: An Overview of Emerging Therapeutic Targets. *Front Oncol.* 2019; 9:963.
- Davis ME. Glioblastoma: Overview of Disease and Treatment. *Clin J Oncol Nurs.* 2016; 205 Suppl:S2-8.
- The Lancet O. Rethinking traditional Chinese medicines for cancer. *Lancet Oncol.* 2015; 1615:1439.
- Ling CQ, Yue XQ, Ling C. Three advantages of using traditional Chinese medicine to prevent and treat tumor. *J Integr Med.* 2014; 124:331-335.
- Silverman JA, Deitcher SR. Marqibo® (vincristine sulfate liposome injection) improves the pharmacokinetics and pharmacodynamics of vincristine. *Cancer Chemother Pharmacol.* 2013; 713:555-564.
- Xiang YZ, Shang HC, Gao XM, Zhang BL. A comparison of the ancient use of ginseng in traditional Chinese medicine with modern pharmacological experiments and clinical trials. *Phytother Res.* 2008; 227:851-858.
- Qi F, Zhao L, Zhou A, Zhang B, Li A, Wang Z, Han J. The advantages of using traditional Chinese medicine as an adjunctive therapy in the whole course of cancer treatment instead of only terminal stage of cancer. *Biosci Trends.* 2015; 91:16-34.
- Ru W, Wang D, Xu Y, He X, Sun YE, Qian L, Zhou X, Qin Y. Chemical constituents and bioactivities of *Panax ginseng* (C. A. Mey.). *Drug Discov Ther.* 2015; 91:23-32.
- Sin S, Kim SY, Kim SS. Chronic treatment with ginsenoside Rg3 induces Akt-dependent senescence in human glioma cells. *Int J Oncol.* 2012; 415:1669-1674.
- Choi YJ, Lee HJ, Kang DW, Han IH, Choi BK, Cho WH. Ginsenoside Rg3 induces apoptosis in the U87MG human glioblastoma cell line through the MEK signaling pathway and reactive oxygen species. *Oncol Rep.* 2013; 303:1362-1370.
- Gu B, Wang J, Song Y, Wang Q, Wu Q. The inhibitory effects of ginsenoside Rd on the human glioma U251 cells and its underlying mechanisms. *J Cell Biochem.* 2019; 1203:4444-4450.
- Sun C, Yu Y, Wang L, Wu B, Xia L, Feng F, Ling Z, Wang S. Additive antiangiogenesis effect of ginsenoside Rg3 with low-dose metronomic temozolomide on rat glioma cells both *in vivo* and *in vitro*. *J Exp Clin Cancer Res.* 2016; 35:32.
- Li KF, Kang CM, Yin XF, Li HX, Chen ZY, Li Y, Zhang Q, Qiu YR. Ginsenoside Rh2 inhibits human A172 glioma cell proliferation and induces cell cycle arrest status *via* modulating Akt signaling pathway. *Mol Med Rep.* 2018; 172:3062-3068.
- Kim H, Roh HS, Kim JE, Park SD, Park WH, Moon JY. Compound K attenuates stromal cell-derived growth factor 1 (SDF-1)-induced migration of C6 glioma cells. *Nutr Res Pract.* 2016; 103:259-264.
- Su X, Zhang D, Zhang H, Zhao K, Hou W. Preparation and Characterization of Angiopep-2 Functionalized Ginsenoside-Rg3 Loaded Nanoparticles and the Effect on C6 Glioma Cells. *Pharm Dev Technol.* 2019:1-37.
- L Z, J F, W L, T Y, XH G, L Y. Preparation and characterization of ginsenoside-Rh2 lipid nanoparticles and synergistic effect with borneol in resisting tumor activity. *Zhongguo Zhong Yao Za Zhi.* 2016; 4107:1235-1240 (in Chinese).
- Wang L, Yang R, Yuan B, Liu Y, Liu C. The antiviral and antimicrobial activities of licorice, a widely-used Chinese herb. *Acta Pharm Sin B.* 2015; 54:310-315.
- Asl MN, Hosseinzadeh H. Review of pharmacological effects of *Glycyrrhiza* sp. and its bioactive compounds. *Phytother Res.* 2008; 226:709-724.
- Kuramoto K, Suzuki S, Sakaki H, Takeda H, Sanomachi T, Seino S, Narita Y, Kayama T, Kitanaka C, Okada M. Licochalcone A specifically induces cell death in glioma stem cells *via* mitochondrial dysfunction. *FEBS Open Bio.* 2017; 76:835-844.
- Lu WJ, Wu GJ, Chen RJ, Chang CC, Lien LM, Chiu CC, Tseng MF, Huang LT, Lin KH. Licochalcone A attenuates glioma cell growth *in vitro* and *in vivo* through cell cycle arrest. *Food Funct.* 2018; 98:4500-4507.
- Lin Y, Sun H, Dang Y, Li Z. Isoliquiritigenin inhibits the proliferation and induces the differentiation of human glioma stem cells. *Oncol Rep.* 2018; 392:687-694.
- Zhou GS, Song LJ, Yang B. Isoliquiritigenin inhibits proliferation and induces apoptosis of U87 human glioma cells *in vitro*. *Mol Med Rep.* 2013; 72:531-536.
- Y D, YL L, HJ S, JJ S, CD L, ZY L. Isoliquiritigenin can inhibit migration and invasion of human glioma stem cells by down-regulating matrix metalloproteinases. *Zhejiang Da Xue Xue Bao Yi Xue Ban.* 2018; 4702:181-186. (in Chinese).
- Masci A, Carradori S, Casadei MA, Paolicelli P, Petralito S, Ragno R, Cesa S. *Lycium barbarum* polysaccharides: Extraction, purification, structural characterisation and evidence about hypoglycaemic and hypolipidaemic effects. A review. *Food Chem.* 2018; 254:377-389.
- Qian D, Zhao Y, Yang G, Huang L. Systematic Review of Chemical Constituents in the Genus *Lycium* (Solanaceae). *Molecules.* 2017; 226.
- Xiao X, Ren W, Zhang N, Bing T, Liu X, Zhao Z, Shangguan D. Comparative Study of the Chemical Constituents and Bioactivities of the Extracts from Fruits, Leaves and Root Barks of *Lycium barbarum*. *Molecules.*

- 2019; 248.
34. JC W, YR Z, Y L, Q W, B Z, HB L, W Z, B S. Lycium barbarum polysaccharide inhibits the growth of rat glioma by regulating the blood-brain barrier. *Toumor*. 2018; 3802:102-110+151 (in Chinese).
  35. TY S, XL P, J D, SH Z, MF W, DZ H, FL L, Z Y, HP Z, GY L. Effect and Its Mechanism of Lycium Barbarum Polysaccharide Combined with Temozolomide on Rat Glioma. *Guangdong Medical Journal* 2015; 3623:3601-3603 (in Chinese).
  36. XF L, JR L, XY L, DC W, MS Z. The effect and mechanisms of combined lycium bararum polysaccharides with temozolomide on brain glioma in rats . *Journal of Guangxi Medical University* 2017; 3403:350-354.(in Chinese).
  37. Hook IL. Danggui to Angelica sinensis root: are potential benefits to European women lost in translation? A review. *J Ethnopharmacol*. 2014; 1521:1-13.
  38. Wei WL, Zeng R, Gu CM, Qu Y, Huang LF. Angelica sinensis in China-A review of botanical profile, ethnopharmacology, phytochemistry and chemical analysis. *J Ethnopharmacol*. 2016; 190:116-141.
  39. Jin M, Zhao K, Huang Q, Xu C, Shang P. Isolation, structure and bioactivities of the polysaccharides from Angelica sinensis (Oliv.) Diels: a review. *Carbohydr Polym*. 2012; 893:713-722.
  40. Tsai NM, Lin SZ, Lee CC, Chen SP, Su HC, Chang WL, Harn HJ. The antitumor effects of Angelica sinensis on malignant brain tumors *in vitro* and *in vivo*. *Clin Cancer Res*. 2005; 119:3475-3484.
  41. Tsai NM, Chen YL, Lee CC, Lin PC, Cheng YL, Chang WL, Lin SZ, Harn HJ. The natural compound n-butylidenephthalide derived from Angelica sinensis inhibits malignant brain tumor growth *in vitro* and *in vivo*. *J Neurochem*. 2006; 994:1251-1262.
  42. Lin PC, Chen YL, Chiu SC, Yu YL, Chen SP, Chien MH, Chen KY, Chang WL, Lin SZ, Chiou TW, Harn HJ. Orphan nuclear receptor, Nurr-77 was a possible target gene of butylidenephthalide chemotherapy on glioblastoma multiform brain tumor. *J Neurochem*. 2008; 1063:1017-1026.
  43. Chang LF, Lin PC, Ho LI, Liu PY, Wu WC, Chiang IP, Chang HW, Lin SZ, Harn YC, Harn HJ, Chiou TW. Overexpression of the orphan receptor Nur77 and its translocation induced by PCH4 may inhibit malignant glioma cell growth and induce cell apoptosis. *J Surg Oncol*. 2011; 1035:442-450.
  44. Yin J, Wang C, Mody A, Bao L, Hung SH, Svoronos SA, Tseng Y. The Effect of Z-Ligustilide on the Mobility of Human Glioblastoma T98G Cells. *PLoS One*. 2013; 86:e66598.
  45. Zhang WF, Yang Y, Li X, Xu DY, Yan YL, Gao Q, Jia AL, Duan MH. Angelica polysaccharides inhibit the growth and promote the apoptosis of U251 glioma cells *in vitro* and *in vivo*. *Phytomedicine*. 2017; 33:21-27.
  46. Xu J, Wei K, Zhang G, Lei L, Yang D, Wang W, Han Q, Xia Y, Bi Y, Yang M, Li M. Ethnopharmacology, phytochemistry, and pharmacology of Chinese Salvia species: A review. *J Ethnopharmacol*. 2018; 225:18-30.
  47. Pang H, Wu L, Tang Y, Zhou G, Qu C, Duan JA. Chemical analysis of the herbal medicine salviae miltiorrhizae Radix et Rhizoma (Danshen). *Molecules*. 2016; 211:51.
  48. XD ME, Cao YF, Che YY, Li J, Shang ZP, Zhao WJ, Qiao YJ, Zhang JY. Danshen: a phytochemical and pharmacological overview. *Chin J Nat Med*. 2019; 171:59-80.
  49. Shi M, Huang F, Deng C, Wang Y, Kai G. Bioactivities, biosynthesis and biotechnological production of phenolic acids in Salvia miltiorrhiza. *Crit Rev Food Sci Nutr*. 2019; 596:953-964.
  50. Cao Y, Huang B, Gao C. Salvia miltiorrhiza extract dihydrotanshinone induces apoptosis and inhibits proliferation of glioma cells. *Bosn J Basic Med Sci*. 2017; 173:235-240.
  51. Kumar V, Radin D, Leonardi D. Probing the oncolytic and chemosensitizing effects of dihydrotanshinone in an *in vitro* Glioblastoma Model. *Anticancer Res*. 2017; 3711:6025-6030.
  52. Lu L, Li C, Li D, Wang Y, Zhou C, Shao W, Peng J, You Y, Zhang X, Shen X. Cryptotanshinone inhibits human glioma cell proliferation by suppressing STAT3 signaling. *Mol Cell Biochem*. 2013; 3811-2:273-282.
  53. Wang J, Wang X, Jiang S, Yuan S, Lin P, Zhang J, Lu Y, Wang Q, Xiong Z, Wu Y, Ren J, Yang H. Growth inhibition and induction of apoptosis and differentiation of tanshinone IIA in human glioma cells. *J Neurooncol*. 2007; 821:11-21.
  54. Tang C, Xue HL, Huang HB, Wang XG. Tanshinone IIA inhibits constitutive STAT3 activation, suppresses proliferation, and induces apoptosis in rat C6 glioma cells. *Neurosci Lett*. 2010; 4702:126-129.
  55. Zhao T, Tang H, Xie L, Zheng Y, Ma Z, Sun Q, Li X. Scutellaria baicalensis Georgi. (Lamiaceae): a review of its traditional uses, botany, phytochemistry, pharmacology and toxicology. *J Pharm Pharmacol*. 2019; 719:1353-1369.
  56. Cheng CS, Chen J, Tan HY, Wang N, Chen Z, Feng Y. Scutellaria baicalensis and Cancer Treatment: Recent Progress and Perspectives in Biomedical and Clinical Studies. *Am J Chin Med*. 2018; 461:25-54.
  57. Li X, Lee YJ, Kim HY, Tan R, Park MC, Kang DG, Lee HS. Beneficial Effects of Scutellaria baicalensis on Penile Erection in Streptozotocin-Induced Diabetic Rats. *Am J Chin Med*. 2016; 442:305-320.
  58. Shang X, He X, He X, Li M, Zhang R, Fan P, Zhang Q, Jia Z. The genus Scutellaria an ethnopharmacological and phytochemical review. *J Ethnopharmacol*. 2010; 1282:279-313.
  59. Wang ZL, Wang S, Kuang Y, Hu ZM, Qiao X, Ye M. A comprehensive review on phytochemistry, pharmacology, and flavonoid biosynthesis of Scutellaria baicalensis. *Pharm Biol*. 2018; 561:465-484.
  60. Zhang L, Wang H, Cong Z, Xu J, Zhu J, Ji X, Ding K. Wogonoside induces autophagy-related apoptosis in human glioblastoma cells. *Oncol Rep*. 2014; 323:1179-1187.
  61. Wang Y, Zhang Y, Qian C, Cai M, Li Y, Li Z, You Q, Wang Q, Hu R, Guo Q. GSK3beta/beta-catenin signaling is correlated with the differentiation of glioma cells induced by wogonin. *Toxicol Lett*. 2013; 2222:212-223.
  62. Lee DH, Lee TH, Jung CH, Kim YH. Wogonin induces apoptosis by activating the AMPK and p53 signaling pathways in human glioblastoma cells. *Cell Signal*. 2012; 2411:2216-2225.
  63. Tsai CF, Yeh WL, Huang SM, Tan TW, Lu DY. Wogonin induces reactive oxygen species production and cell apoptosis in human glioma cancer cells. *Int J Mol Sci*. 2012; 138:9877-9892.
  64. Zhang Z, Lv J, Lei X, Li S, Zhang Y, Meng L, Xue R,

- Li Z. Baicalein reduces the invasion of glioma cells *via* reducing the activity of p38 signaling pathway. *PLoS One*. 2014; 92:e90318.
65. Tan HL, Chan KG, Pusparajah P, Duangjai A, Saokaew S, Mehmood Khan T, Lee LH, Goh BH. Rhizoma Coptidis: A Potential Cardiovascular Protective Agent. *Front Pharmacol*. 2016; 7:362.
  66. Wang J, Wang L, Lou GH, Zeng HR, Hu J, Huang QW, Peng W, Yang XB. Coptidis Rhizoma: a comprehensive review of its traditional uses, botany, phytochemistry, pharmacology and toxicology. *Pharm Biol*. 2019; 571:193-225.
  67. Meng FC, Wu ZF, Yin ZQ, Lin LG, Wang R, Zhang QW. Coptidis rhizoma and its main bioactive components: recent advances in chemical investigation, quality evaluation and pharmacological activity. *Chin Med*. 2018; 13:13.
  68. Li J, Ni L, Li B, Wang M, Ding Z, Xiong C, Lu X. Coptis Chinensis affects the function of glioma cells through the down-regulation of phosphorylation of STAT3 by reducing HDAC3. *BMC Complement Altern Med*. 2017; 171:524.
  69. Tong L, Xie C, Wei Y, Qu Y, Liang H, Zhang Y, Xu T, Qian X, Qiu H, Deng H. Antitumor Effects of Berberine on Gliomas *via* Inactivation of Caspase-1-Mediated IL-1beta and IL-18 Release. *Front Oncol*. 2019; 9:364.
  70. Jin F, Xie T, Huang X, Zhao X. Berberine inhibits angiogenesis in glioblastoma xenografts by targeting the VEGFR2/ERK pathway. *Pharm Biol*. 2018; 561:665-671.
  71. Sun Y, Yu J, Liu X, Zhang C, Cao J, Li G, Liu X, Chen Y, Huang H. Oncosis-like cell death is induced by berberine through ERK1/2-mediated impairment of mitochondrial aerobic respiration in gliomas. *Biomed Pharmacother*. 2018; 102:699-710.
  72. Eom KS, Kim HJ, So HS, Park R, Kim TY. Berberine-induced apoptosis in human glioblastoma T98G cells is mediated by endoplasmic reticulum stress accompanying reactive oxygen species and mitochondrial dysfunction. *Biol Pharm Bull*. 2010; 3310:1644-1649.
  73. Liu Q, Xu X, Zhao M, Wei Z, Li X, Zhang X, Liu Z, Gong Y, Shao C. Berberine induces senescence of human glioblastoma cells by downregulating the EGFR-MEK-ERK signaling pathway. *Mol Cancer Ther*. 2015; 142:355-363.
  74. Wang J, Qi Q, Feng Z, Zhang X, Huang B, Chen A, Prestegarden L, Li X, Wang J. Berberine induces autophagy in glioblastoma by targeting the AMPK/mTOR/ULK1-pathway. *Oncotarget*. 2016; 741:66944-66958.
  75. Brinker AM, Ma J, Lipsky PE, Raskin I. Medicinal chemistry and pharmacology of genus Tripterygium (Celastraceae). *Phytochemistry*. 2007; 686:732-766.
  76. Liu Z, Ma L, Zhou GB. The main anticancer bullets of the Chinese medicinal herb, thunder god vine. *Molecules*. 2011; 166:5283-5297.
  77. Huang Y, Zhou Y, Fan Y, Zhou D. Celastrol inhibits the growth of human glioma xenografts in nude mice through suppressing VEGFR expression. *Cancer Lett*. 2008; 2641:101-106.
  78. Liu X, Zhao P, Wang X, Wang L, Zhu Y, Song Y, Gao W. Celastrol mediates autophagy and apoptosis *via* the ROS/JNK and Akt/mTOR signaling pathways in glioma cells. *J Exp Clin Cancer Res*. 2019; 381:184.
  79. Lin J, Chen LY, Lin ZX, Zhao ML. The effect of triptolide on apoptosis of glioblastoma multiforme (GBM) cells. *J Int Med Res*. 2007; 355:637-643.
  80. Zhang H, Zhu W, Su X, Wu S, Lin Y, Li J, Wang Y, Chen J, Zhou Y, Qiu P, Yan G, Zhao S, Hu J, Zhang J. Triptolide inhibits proliferation and invasion of malignant glioma cells. *J Neurooncol*. 2012; 1091:53-62.
  81. Sai K, Li WY, Chen YS, Wang J, Guan S, Yang QY, Guo CC, Mou YG, Li WP, Chen ZP. Triptolide synergistically enhances temozolomide-induced apoptosis and potentiates inhibition of NF-kappaB signaling in glioma initiating cells. *Am J Chin Med*. 2014; 422:485-503.
  82. Zheng K, Li C, Shan X, Liu H, Fan W, Wang Z. A study on isolation of chemical constituents from *Sophora flavescens* Ait. and their anti-glioma effects. *Afr J Tradit Complement Altern Med*. 2014; 111:156-160.
  83. He X, Fang J, Huang L, Wang J, Huang X. *Sophora flavescens* Ait.: Traditional usage, phytochemistry and pharmacology of an important traditional Chinese medicine. *J Ethnopharmacol*. 2015; 172:10-29.
  84. Rashid HU, Xu Y, Muhammad Y, Wang L, Jiang J. Research advances on anticancer activities of matrine and its derivatives: An updated overview. *Eur J Med Chem*. 2019; 161:205-238.
  85. Yong J, Wu X, Lu C. Anticancer Advances of Matrine and Its Derivatives. *Curr Pharm Des*. 2015; 2125:3673-3680.
  86. Wang Z, Wu Y, Wang Y, Jin Y, Ma X, Zhang Y, Ren H. Matrine inhibits the invasive properties of human glioma cells by regulating epithelial to mesenchymal transition. *Mol Med Rep*. 2015; 115:3682-3686.
  87. Chi G, Xu D, Zhang B, Yang F. Matrine induces apoptosis and autophagy of glioma cell line U251 by regulation of circRNA-104075/BCL-9. *Chem Biol Interact*. 2019; 308:198-205.
  88. Liu F, Wang B, Wang J, Ling X, Li Q, Meng W, Ma J. Oxymatrine Inhibits Proliferation and Migration While Inducing Apoptosis in Human Glioblastoma Cells. *Biomed Res Int*. 2016; 2016:1784161.
  89. Dai Z, Wang L, Wang X, Zhao B, Zhao W, Bhardwaj SS, Ye J, Yin Z, Zhang J, Zhao S. Oxymatrine induces cell cycle arrest and apoptosis and suppresses the invasion of human glioblastoma cells through the EGFR/PI3K/Akt/mTOR signaling pathway and STAT3. *Oncol Rep*. 2018; 402:867-876.
  90. Cai P, Qiu H, Qi F, Zhang X. The toxicity and safety of traditional Chinese medicines: Please treat with rationality. *Biosci Trends*. 2019; 135:367-373.
  91. Zhu YL, Li B, Zhou B. *New Atlas of Chinese Herbal Medicine*. China Beijing, Chemical Industry Press, 2016; pp. 64-65, p. 454, p. 574, p. 622 (in Chinese).
  92. Qu TB. *New Chinese herbal medicine illustrated book*. China Jiangxi, Jiangxi Science and Technology Press, 2018; p. 108, p. 140 (in Chinese).

(Received November 12, 2019; Revised December 2, 2019; Accepted December 18, 2019)

# The state of minimally invasive pancreaticoduodenectomy in Chinese mainland: A systematic literature review

Jianyi Ding<sup>1,2</sup>, Chengwu Zhang<sup>2</sup>, Dongsheng Huang<sup>2</sup>, Yuhua Zhang<sup>2,\*</sup>

<sup>1</sup>Zhejiang Chinese Medical University, Hangzhou, Zhejiang, China;

<sup>2</sup>Division of Hepatobiliary and Pancreatic Surgery and Minimally Invasive Surgery, Zhejiang Provincial People's Hospital, People's Hospital of Hangzhou Medical College, Hangzhou, Zhejiang, China.

## Summary

The development of Minimally invasive pancreaticoduodenectomy (MIPD) in Chinese mainland has been extremely quick. However, the safety and oncologic outcomes remain controversial. This review evaluates the current status of MIPD in Chinese mainland. A systematic literature search was performed using: Pubmed, Web of Sci, CNKI, Wanfang Data and Sinomed databases to filter all studies published up to and including June 2019 using key words "pancreaticoduodenectomy," or "Whipple operation" combined with "laparoscopy," or "laparoscopic," or "robotic," or "da Vinci," or "minimally invasive," or "hand-assisted". This systematic review included 39 articles that documented 2,653 MIPDs in Chinese mainland. The weighted average operative time was 370.6 min, and the weighted average blood loss was 278.0 mL. The overall morbidity was 31.9%, which Clavien-Dindo  $\geq 3$  complications accounted for 13.4%. Pancreatic fistula, delayed gastric emptying, bile leak and postoperative hemorrhage were reported in 20.9%, 5.5%, 3.5% and 6.0% of patients respectively. The average length of hospital stay was 16.1 days. The overall surgical mortality was 1.7%. The mean number of harvested lymph nodes was 13.5, and the rate of positive margin was 5.3%. Based on Chinese national condition, the operative volume of MIPD in Chinese mainland is the leading position in the world, and compared with some large international meta-analysis, no inferior perioperative and short-term oncological outcomes were observed in MIPD of Chinese mainland. However, research on survival analysis and phased learning curve outcomes is needed urgently before the innovative techniques are widely accepted.

**Keywords:** Minimally invasive surgery, pancreaticoduodenectomy, Chinese mainland, laparoscopy, robot

## 1. Introduction

Pancreaticoduodenectomy (PD), as the only potentially curative option in patients with periampullary malignancy, has been recognized as one of the most complicated and risky procedures in general surgery for the past 100 years (1). With the development of

surgery technology, the first case of minimally invasive pancreaticoduodenectomy (MIPD) was described in 1994 by Gagner (2). However, its challenging anatomical and anastomotic techniques and inferior short-term outcomes slowed the acceptance of this operation.

After the first report of MIPD in Chinese mainland in 2003 (3), more challenge-pursing and innovative Chinese surgeons have contributed to explore better approaches and procedures with the introduction of advanced technologies.

Previous literature listed advantages of minimally invasive surgery in other fields of general surgery including lower blood loss, faster post operation recovery and comparable oncology outcomes (4). Unlike previous years, more and more small-sample studies have been documented in recent years, which marks attempts from

Released online in J-STAGE as advance publication December 24, 2019.

\*Address correspondence to:

Dr. Yuhua Zhang, Division of Hepatobiliary and Pancreatic Surgery and Minimally Invasive Surgery, Zhejiang Provincial People's Hospital, People's Hospital of Hangzhou Medical College, No. 158 of Shangtang Road, Hangzhou 310014, China.

E-mail: zhangyuhua1013@126.com

non-specialized centers.

In this paper, we reviewed the literature describing MIPD in Chinese mainland to provide a comprehensive evaluation of the current status, focusing on technical details and short-term outcomes of minimally invasive approaches.

## 2. Materials and Methods

### 2.1. Definitions and surgical techniques

MIPD included two main methods: laparoscopic pancreaticoduodenectomy (LPD) and robotic pancreaticoduodenectomy (RPD). Moreover, it could be further classified based on techniques used in resection and reconstruction:

- 1) Pure LPD, where the entire operation is completed with the assistance of laparoscopic technique;
- 2) Hand-assisted LPD, where a mini hand port is added to facilitate the procedure;
- 3) Laparoscopy-assisted LPD, where resection is carried out laparoscopically and reconstruction is completed using a small mini-laparotomy incision;
- 4) Robotic-assisted PD, where the entire operation or some parts of dissection and reconstruction are performed with the assistance of the da Vinci surgical system.

### 2.2. Literature review

A systematic literature search was performed using: Pubmed, Web of Sci, CNKI, Wanfang Data and Sinomed databases to filter all studies published up to and including June 2019 using key words "pancreaticoduodenectomy," or "Whipple operation" combined with "laparoscopy," or "laparoscopic," or "robotic," or "da Vinci," or "minimally invasive," or "hand-assisted." Relevant articles identified by cross-referencing were also retrieved and reviewed.

### 2.3. Inclusion criteria

Articles describing MIPD in Chinese mainland containing more than 10 cases were included. If patient data was documented more than once from the same institution, the most informative or recent article was considered to prevent data overlap.

### 2.4. Exclusion criteria

Articles lacking original data or missing lots of outcomes, studies referring to animals and cadavers, technique articles, multimedia literature, Chinese articles without English abstracts and academic degree articles were excluded.

### 2.5. Data extraction

All the retrieved studies that met the inclusion and

exclusion criteria were independently reviewed by two authors (Ding JY and Zhang YH). Discrepancies between the two reviewers were resolved by discussion.

The variables extracted from the included studies were as follows:

- 1) Basic information (first author, publication year, study period, number of cases);
- 2) Technical details (surgical procedures, management of pancreatic stump, management of gastroduodenal artery, specimen extraction site, anastomotic technique in gastroenterostomy, suture technique in choledochojunostomy, vascular resection and reconstruction);
- 3) Intraoperative outcomes (operative time, intraoperative blood loss, conversion rate, transfusion rate);
- 4) Short-term outcomes (overall morbidity, pancreatic fistula, usage of International Surgical Group of Pancreatic Fistula or not, delayed gastric emptying, bile leak, postoperative hemorrhage, length of postoperative hospital stay, Clavien-Dindo  $\geq 3$  complications, reoperation, surgical mortality);
- 5) Oncologic outcomes (malignancy rate, usage of tumor-node-metastasis stage or not, number of harvested lymph nodes, rate of margin negative resection).

### 2.6. Statistical analysis

A weighted average (WA) was used to express the statistical weighted mean of different variables:

$$WA = (w_1x_1 + w_2x_2 + \dots + w_nx_n) / (w_1 + w_2 + \dots + w_n)$$

where  $w$  is the number of cases in a publication and  $x$  is the mean of a specific variable. The  $x$  and its corresponding  $w$  are excluded if the variables in some studies are absent or not able to calculate.

The chi-square test was used to compare categorical variables between groups. The Student's unpaired  $t$  test or Mann-Whitney  $U$  test was used to compare continuous variables, as appropriate. Although this statistical method is not entirely rigorous, the results could be presented through a more intuitive way and some authors including Gumbs (5) and Boggi (6) have already applied this statistical method. Statistical analyses were finished by SPSS statistical software package (version 25.0, SPSS Inc., Chicago, IL, USA). A  $p$  value  $< 0.05$  was considered statistically significant.

## 3. Results

This systematic review included 39 articles that documented a total of 2,653 MIPDs (Table 1) (7-45). Seventeen articles were published between 2010 and 2017, documenting 540 cases (20.4%), whereas twenty-two were published in the next two years, reporting on 2,113 cases (79.6%) (Figure 1).

**Table 1. Summary of current articles on minimally invasive pancreaticoduodenectomy in more than 10 cases**

First author (Ref.)	Publication year	Study period	Methods	Cases
Chao Lu (32)	2018	2012-2017	PL	320
Xueqing Liu (30)	2018	2013-2017	PL	300
Yunqiang Cai (9)	2018	2015-2018	PL	238
Hang Zhang (43)	2018	2014-2016	PL	202
Wei Chai (10)	2019	2015-2017	PL/LA	102/86
Qingchun Li (27)	2019	2014-2017	PL	134
Xiaohui Duan (17)	2017	2014-2017	PL	101
Guolin Li (25)	2018	2016-2017	PL	100
Tao Zhang (45)	2018	2012-2016	RA	100
Yong An (7)	2019	2017-2018	PL	90
Yun Liang (28)	2019	2015-2018	PL	82
Defei Hong (19)	2016	2013-2016	PL,RA	80
Yusheng Du (16)	2019	2016-2017	PL	67
Shi Chen (14)	2015	2010-2013	RA	60
Fangkuan Li (24)	2017	2012-2016	PL	50
Peng Chen (13)	2018	2015-2018	PL, RA	40
Ronggui Lin (29)	2018	2017-2017	PL, RA, HA	35
Jianjun Li (26)	2013	2002-2012	PL, LA	34
Menghua Dai (15)	2018	2016-2018	PL	34
Zhigang Wei (37)	2018	2015-2018	PL	33
Fan Yang (JL) (41)	2018	2017-2017	PL	30
Rong Tang (34)	2017	2010-2013	LA	29
Fan Yang (CQ) (42)	2019	2016-2018	PL	29
Jianhui Chen (12)	2016	2012-2014	LA	25
Zuguang Wu (39)	2017	2014-2016	PL	22
Lei Zhang (44)	2019	2015-2018	PL	21
Jiacheng Wu (38)	2018	2017-2017	PL	21
Zhao Liu (31)	2015	2011-2012	LA	21
Qiang Huang (22)	2017	2016-2016	PL	20
Qiuya Wei (36)	2016	2013-2015	PL	19
Wentao Gao (18)	2017	2016-2016	PL	18
Hai Hu (20)	2019	2015-2018	RA	18
Qinzheng Bai (8)	2016	2015-2016	LA	16
Jinmeng Hu (21)	2018	2015-2017	PL	16
Huanwei Chen (11)	2019	2015-2018	PL/LA	10/5
Mingsheng Sun (33)	2015	2010-2015	LA	12
Jun Xu (40)	2010	2005-2008	LA, HA	12
Hongbo Wei (35)	2014	2012-2013	PL	11
Wu Ji (23)	2014	2010-2012	RA	10

PL, pure laparoscopic pancreaticoduodenectomy. LA, laparoscopy-assisted pancreaticoduodenectomy. RA, robotic-assisted pancreaticoduodenectomy. HA, hand-assisted pancreaticoduodenectomy. JL, Jilin Province. CQ, Chongqing City.

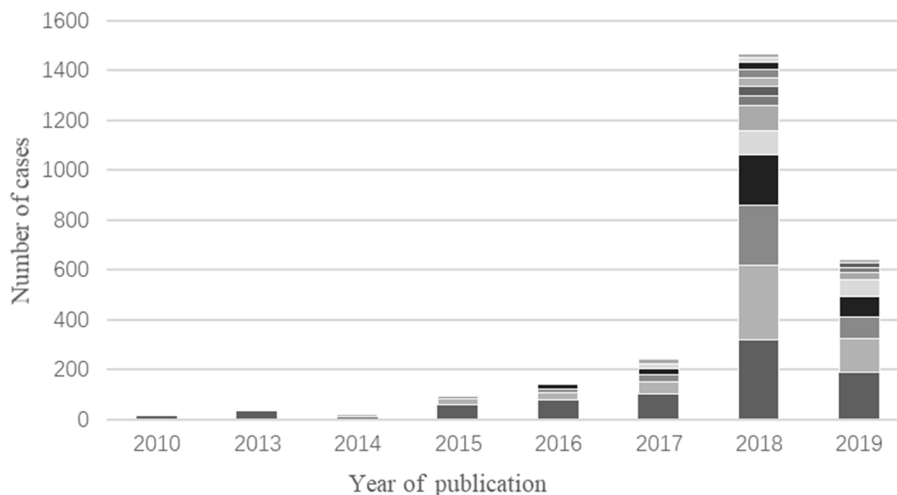


**Figure 1. Number of cases documented yearly.** The different depth of gray color in each bar represent different studies in that year and their heights mean the sample size of the corresponding study.

**Table 2. Management of pancreatic stump in minimally invasive pancreaticoduodenectomy**

First author (Ref.)	Management of pancreatic stump			
	PJ	PG	Technique	Stent
Chao Lu (32)	320	0	[E-to-S and D-to-M]	Selectively
Xueqing Liu (30)	295 <sup>a</sup>	0	30[E-to-E and Invaginating], 265[E-to-S and D-to-M]	Selectively
Yunqiang Cai (9)	238	0	[E-to-S and D-to-M]	Yes
Hang Zhang (43)	202	0	[E-to-S and D-to-M]	Yes
Wei Chai (10)	102(PL), 86(LA)	0	102[E-to-S and D-to-M], 86[E-to-S and Invaginating]	Yes
Qingchun Li (27)	134	0	[E-to-S and D-to-M]	Yes
Xiaohui Duan (17)	101	0	[E-to-S and D-to-M]	Yes
Guolin Li (25)	100	0	[E-to-S and D-to-M]	Selectively
Tao Zhang (45)	100	0	[E-to-S and D-to-M]	Yes
Yong An (7)	90	0	[E-to-S and D-to-M]	NA
Yun Liang (28)	82	0	[E-to-S and D-to-M]	NA
Dfei Hong <sup>b</sup> (19)	70	7	70[E-to-S and D-to-M], 7[E-to-S and Invaginating]	Yes
Yusheng Du (16)	67	0	67[E-to-S and D-to-M]	Yes
Shi Chen (14)	59	1 <sup>c</sup>	59[E-to-S and D-to-M]	Yes
Fangkuan Li (24)	50	0	[E-to-S and D-to-M]	NA
Peng Chen (13)	40	0	[E-to-S and D-to-M]	Yes
Ronggui Lin (29)	35	0	NA	NA
Jianjun Li (26)	34	0	[E-to-S and D-to-M]	Yes
Menghua Dai (15)	NA	NA	NA	NA
Zhigang Wei (37)	NA	NA	NA	NA
Fan Yang (JL) (41)	30	0	[E-to-S and D-to-M]	Yes
Rong Tang (34)	NA	NA	NA	NA
Fan Yang (CQ) (42)	29	0	[E-to-S and D-to-M]	Yes
Jianhui Chen (12)	NA	NA	NA	NA
Zuguang Wu (39)	22	0	[E-to-S and D-to-M]	NA
Lei Zhang (44)	21	0	[E-to-S and M-to-M]	Selectively
Jiacheng Wu (38)	21	0	[E-to-S and D-to-M]	Yes
Zhao Liu (31)	21	0	[E-to-S and D-to-M]	Yes
Qiang Huang (22)	20	0	[E-to-S and D-to-M]	Yes
Qiuya Wei (36)	19	0	[E-to-S and D-to-M]	Yes
Wentao Gao (18)	18	0	[E-to-S and D-to-M]	NA
Hai Hu (20)	18	0	NA	NA
Qinzheng Bai (8)	16	0	[E-to-S and D-to-M]	Yes
Jinmeng Hu (21)	16	0	[E-to-S and D-to-M]	Yes
Huanwei Chen (11)	5(PL), 10(LA)	0	[E-to-S and D-to-M], [E-to-S and D-to-M]	NA, Yes
Mingsheng Sun (33)	NA	NA	NA	NA
Jun Xu (40)	12	0	[E-to-E and Invaginating]	Selectively
Hongbo Wei (35)	11	0	[E-to-E and Invaginating] or [E-to-S and D-to-M]	NA
Wu Ji (23)	10	0	[E-to-S and D-to-M]	Yes

<sup>a</sup>Another 5 cases underwent total pancreatectomy. <sup>b</sup>Another 3 cases were not described due to conversion to laparotomy. <sup>c</sup>Pancreaticogastrostomy was not described in detail. PL, pure laparoscopic pancreaticoduodenectomy. LA, laparoscopy-assisted pancreaticoduodenectomy. PJ, pancreatojejunostomy. PG, pancreatogastrostomy. NA, not applicable. D-to-M, duct-to-mucosa. E-to-E, end-to-end. E-to-S, end-to-side. JL, Jilin Province. CQ, Chongqing City.

Pure laparoscopic pancreaticoduodenectomy (PL) have held a dominant position in MIPD according to the literature of recent years. 2070 PL (78.0%) were documented in our review. And 7 authors (8,10-12,31,33,34) describing 194 cases (7.3%) laparoscopy-assisted pancreaticoduodenectomy (LA).

Robotic-assisted pancreaticoduodenectomy (RA) was gradually put into application for pancreatic surgery in the recent few years. 188 cases (7.1%) RA were included in our analysis, while only 5 cases (0.2%) hand-assisted pancreaticoduodenectomy (HA) of two articles (29,40) are mentioned in our review.

In addition, seven authors applied more than one technique (10,11,13,19,26,29,40), and three of them (13,19,29) simultaneous applied LPD and RPD without data separation. Therefore, the three articles were excluded either in comparison of LPD and RPD or in

classification of technique.

### 3.1. Technical details

Technical details of MIPD are listed in Table 2 and Table 3, including management of pancreatic stump, closure of gastroduodenal artery, specimen extraction site, anastomotic technique in gastroenterostomy, suture technique in choledochojejunostomy and vascular resection and reconstruction.

Details on management of pancreatic stump were provided in 34 articles (87.2%). Pancreatojejunostomy (PJ) was the major selection to manage pancreatic stump while pancreatogastrostomy(PG) was only mentioned in 8 cases of 2 articles (14,19) and no duct occlusion was reported. Details about anastomosis methods were described in 32 articles (82.1%), including end-to-end

**Table 3. Technical details of minimally invasive pancreaticoduodenectomy**

First author (Ref.)	Management of GDA	Extraction site	Anastomotic technique in gastroenterostomy	Suture technique in choledochojejunostomy	Vascular resection and reconstruction
Chao Lu (32)	Clips	NA	Stapled	Selectively	NA
Xueqing Liu (30)	Clips or Ligature	Subxiphoid	Stapled (68.7%), Hand-sewn (31.3%)	RS	10
Yunqiang Cai (9)	NA	NA	NA	NA	0
Hang Zhang (43)	Clips	Infra-umbilical	Stapled	Selectively	2
Wei Chai (10)	NA	Subxiphoid	NA	NA	NA
Qingchun Li (27)	NA	Umbilical	NA	NA	NA
Xiaohui Duan (17)	Ligature and Clips	Infra-umbilical	Stapled	Selectively	NA
Guolin Li (25)	Ligature	NA	Stapled	RS	NA
Tao Zhang (45)	NA	Umbilical	NA	NA	0
Yong An (7)	NA	NA	Stapled	RS	3
Yun Liang (28)	NA	NA	NA	NA	NA
Defei Hong (19)	NA	NA	NA	NA	5
Yusheng Du (16)	NA	NA	NA	RS	NA
Shi Chen (14)	Ligature	NA	NA	Selectively	3
Fangkuan Li (24)	Clips	NA	Stapled	RS	NA
Peng Chen (13)	Ligature	NA	Stapled	NA	NA
Ronggui Lin (29)	Clips	NA	NA	NA	NA
Jianjun Li (26)	Ligature	Subxiphoid	NA	NA	NA
Menghua Dai (15)	NA	NA	NA	NA	2
Zhigang Wei (37)	Clips	NA	NA	NA	NA
Fan Yang (JL) (41)	NA	NA	Hand-sewn	NA	1
Rong Tang (34)	NA	Subxiphoid	NA	NA	NA
Fan Yang (CQ) (42)	Clips	NA	NA	RS	NA
Jianhui Chen (12)	NA	Subxiphoid	NA	NA	0
Zuguang Wu (39)	NA	Infra-umbilical	Stapled	NA	0
Lei Zhang (44)	NA	Subxiphoid	NA	NA	NA
Jiacheng Wu (38)	NA	Infra-umbilical	Stapled	RS	0
Zhao Liu (31)	Clips	Subxiphoid	NA	IS	0
Qiang Huang (22)	NA	NA	NA	NA	0
Qiuya Wei (36)	NA	NA	Stapled	RS	0
Wentao Gao (18)	NA	NA	Hand-sewn	RS	0
Hai Hu (20)	Ligature	Subxiphoid	NA	NA	0
Qinzheng Bai (8)	Clips	Subxiphoid	NA	NA	NA
Jinmeng Hu (21)	NA	NA	NA	NA	0
Huanwei Chen (11)	Ligature and Clips	Subxiphoidv (LA), Suprapubicv (PL)	Stapled	RS	0
Mingsheng Sun (33)	Clips	Subxiphoid	NA	NA	0
Jun Xu (40)	NA	Subxiphoid	NA	NA	0
Hongbo Wei (35)	NA	NA	NA	NA	NA
Wu Ji (23)	NAhi	Subxiphoid	NA	NA	NA

GDA, gastroduodenal artery. RS, running suture. IS, interrupted suture. NA, not applicable. JL, Jilin Province. CQ, Chongqing City.

and invaginating PJ, end-to-side and invaginating PJ, end-to-side and duct-to-mucosa PJ, end-to-side and invaginating PG according to Barreto's classification (46). Among the above methods, the end-to-side and duct-to-mucosa PJ was the most popular one. Undoubtedly, duct-to-mucosa anastomosis is the most difficult point in PJ. Hence, some modified or innovative methods such as purse-string, Bing's anastomosis (9) or Hong's single-stitch method (47) were applied for further reinforcing the junction between pancreatic duct and intestinal wall (9,10,16,19,21,41). Nevertheless, various modified methods haven't been marked in the tables so as to simplify our classification. As for stent for pancreatic duct, 25 authors (64.1%) implied entirely or selectively in their studies.

Seventeen authors (43.6%) described the closure of gastroduodenal artery (GDA). The methods contain clips

(9 articles) or ligature (5 articles). In addition, Duan *et al.* (17) and Chen *et al.* (11) applied clips plus ligature while Liu *et al.* (30) used clips or ligature. Specimen extraction site was described in 19 articles (48.7%). Chen *et al.* (11) applied two different incisions to extract specimens in different surgical procedures. 13 authors (68.4%) used a subxiphoid incision to extract specimens. In 4 articles (21.1%), the specimen was delivered through an infra-umbilical incision or enlarged port, in 2 articles (10.5%) through an umbilical incision or enlarged port. Besides, suprapubic incision was used by Chen *et al.* as the second method. Seven authors described the jejunal loop used for duodenal or gastric anastomosis (17.9%), and all patients in their studies followed an antecolic route. The retromesenteric and retrocolic routes were hardly employed according to the data we pooled. Anastomotic technique in gastroenterostomy and suture technique

**Table 4. Intraoperative outcomes of minimally invasive pancreaticoduodenectomy**

First author (Ref.)	Operative time (min)	Blood loss (mL)	Conversion <i>n</i> (%)	Transfusion <i>n</i> (%)
Chao Lu (32)	352.3 ± 53.2	198.8 ± 127.6	NA	59 (18.4%)
Xueqing Liu (30)	6.7 (2.5-12.0) <sup>e</sup> h	500 (100-3000) <sup>e</sup>	NA	NA
Yunqiang Cai (9)	358 (220-495) <sup>a</sup>	112 (50-800) <sup>a</sup>	1 (0.4%)	11 (4.6%)
Hang Zhang (43)	301 ± 175	194 ± 107	3 (1.5%)	19 (9.4%)
Wei Chai (10)	419.7 <sup>b</sup>	288.1 <sup>b</sup>	NA	NA
Qingchun Li (27)	275.7 <sup>b</sup>	114.5 <sup>b</sup>	0 (0%)	9 (6.7%)
Xiaohui Duan (17)	325.7 (220-575) <sup>c</sup>	175.9 (100-550) <sup>c</sup>	NA	2 (2.0%)
Guolin Li (25)	277.5 <sup>b</sup>	151.7 <sup>b</sup>	NA	NA
Tao Zhang (45)	357.87 ± 93.28	171.13 ± 144.46	5 (5.0%)	NA
Yong An (7)	377 <sup>b</sup>	296 <sup>b</sup>	NA	18(20.0%)
Yun Liang (28)	364.6 <sup>b</sup>	NA	7 (8.5%)	NA
Defei Hong (19)	351.2 ± 84.1	204.7 ± 165.9	3 (3.8%)	NA
Yusheng Du (16)	343.5 <sup>b</sup>	213.2 <sup>b</sup>	0 (0%)	5 (7.5%)
Shi Chen (14)	410 <sup>b</sup>	NA	NA	8 (13.3%)
Fangkuan Li (24)	396.4 ± 81.9	282.0 ± 192.4	4 (7.4%)	NA
Peng Chen (13)	487.73 ± 113.13	360.00 ± 407.49	NA	NA
Ronggui Lin (29)	NA	150.0 ± 34.6	0 (0%)	NA
Jianjun Li (26)	440.0 (382-510) <sup>c</sup>	NA	0 (0%)	NA
Menghua Dai (15)	427.16 ± 78.05	597.06 ± 327.74	4 (11.8%)	NA
Zhigang Wei (37)	414.5 (340-498) <sup>c</sup>	420 (150-800) <sup>c</sup>	0 (0%)	NA
Fan Yang (JL) (41)	4.3 ± 1.5 h	300 ± 75	0 (0%)	NA
Rong Tang (34)	7.5 ± 0.8 h	326.4 ± 86.5	0 (0%)	NA
Fan Yang (CQ) (42)	482 ± 86	400.0 (300-800) <sup>a</sup>	NA	10 (34.5%)
Jianhui Chen (12)	474.6 ± 54.2	265.5 ± 72.6	NA	2 (8.0%)
Zuguang Wu (39)	414.0 ± 31.0	176.0 ± 50.4	NA	NA
Lei Zhang (44)	317.14 ± 44.06	523.91 ± 261.54	0(0%)	NA
Jiacheng Wu (38)	352 ± 25	168 ± 34	0(0%)	0 (0%)
Zhao Liu (31)	316 (260-410) <sup>c</sup>	240 (30-1000) <sup>c</sup>	1 (4.8%)	NA
Qiang Huang (22)	645.0 ± 139.9	750.0 ± 417.6	0 (0%)	NA
Qiuya Wei (36)	407.8 ± 146.5	309.7 ± 151.2	NA	NA
Wentao Gao (18)	476 ± 50	439 ± 228	NA	NA
Hai Hu (20)	450 ± 30	525 ± 125	1 (5.6%)	0 (0%)
Qinzheng Bai (8)	470.31 ± 61.09	568.75 ± 298.26	0 (0%)	NA
Jinmeng Hu (21)	459.8 ± 121.6	178.1 ± 118.3	NA	NA
Huanwei Chen (11)	528.7 <sup>b</sup>	NA	0 (0%)	0 (0%)
Mingsheng Sun (33)	280 (240-340) <sup>c</sup>	300 (150-1200) <sup>c</sup>	2 (16.7%)	NA
Jun Xu (40)	6.5 (5-10) <sup>e</sup> h	435 (200-800) <sup>c</sup>	3 (25.0%)	NA
Hongbo Wei (35)	410.2 ± 85.0	168.2 ± 87.4	0 (0%)	NA
Wu Ji (23)	7.3 ± 3.6 h	320.0 ± 123.5	1 (10.0%)	0 (0%)
Total/mean	370.6	278.0	35 (2.6%)	143 (10.8%)

<sup>a</sup>Data are expressed as median and interquartile range. <sup>b</sup>Data are integration from multi-group data. <sup>c</sup>Data are expressed as mean and range. JL, Jilin Province. CQ, Chongqing City. NA, not applicable.

in choledochojejunostomy were mentioned in 14 and 15 articles respectively. The staple technique occupied the majority in gastroenterostomy (85.7%) and running suture was most common in choledochojejunostomy (66.7%). Besides, 4 authors (14,17,32,43) applied running or interrupted suture selectively depending on diameter of bile duct (26.7%). The information of vascular resection and reconstruction was mentioned by 7 authors while 14 studies regarded cases with vascular invasion as contraindications. Overall, 26 cases of vascular involvement were performed with vascular resection and reconstruction.

### 3.2. Intraoperative outcomes

Intraoperative outcomes of MIPD are documented in Table 4, containing operation time, blood loss, conversion rate to laparotomy and intraoperative

transfusion rate.

The mean operation time was provided in 37 articles (94.9%) and ranged from 258 to 645 min, with a WA of 370.6 min. The median operative time was only mentioned in Cai's study (9) with a result of 358 min. The mean blood loss was provided in 33 articles (84.6%) ranged from 114.5 to 750 mL, with a WA of 278.0 mL. The median blood loss was mentioned in 2 articles (9,42) with a result of 112 mL and 400 mL.

The information of conversion rate to laparotomy was available in 25 studies (64.1%). A total of 35 MIPDs were converted to laparotomy (2.6%). The reasons were as follows: uncontrolled vascular bleeding (*n* = 9, 25.7%), severe adhesions (*n* = 5, 14.3%), limited working space (*n* = 1, 2.9%), and unspecified reasons (*n* = 20, 57.1%). The data of intraoperative transfusion rate was available in 14 articles (35.9%). A total of 143 MIPDs performed intraoperative transfusion (10.8%).

**Table 5. Morbidity of minimally invasive pancreaticoduodenectomy**

First author (Ref.)	Morbidity <i>n</i> (%)	Pancreatic fistula <i>n</i> (%)	Usage of ISGPF	Delayed gastric emptying <i>n</i> (%)	Bile leak <i>n</i> (%)	Postoperative hemorrhage <i>n</i> (%)
Chao Lu (32)	103 (32.2%)	56 (17.5%)	+	3 (0.9%)	12 (3.8%)	29 (9.1%)
Xueqing Liu (30)	95 (31.7%)	NA	+	12 (4.0%)	12 (4.0%)	28 (9.3%)
Yunqiang Cai (9)	NA	51 (21.4%)	+	17 (7.1%)	6 (2.5%)	3 (1.3%)
Hang Zhang (43)	61 (30.2%)	29 (14.4%)	+	23 (11.4%)	3 (1.5%)	5 (2.5%)
Wei Chai (10)	67 (35.6%)	40 (21.3%)	+	12 (6.4%)	2 (1.1%)	3 (1.6%)
Qingchun Li (27)	18 (13.4%)	16 (11.9%)	+	2 (1.5%)	4 (3.0%)	3 (2.2%)
Xiaohui Duan (17)	NA	23 (22.8%)	+	4 (4.0%)	2 (2.0%)	7 (6.9%)
Guolin Li (25)	NA	63 (63.0%)	+	5 (5.0%)	4 (4.0%)	4 (4.0%)
Tao Zhang (45)	58 (58.0%)	24 (24.0%)	+	15 (15.0%)	11 (11.0%)	22 (22.0%)
Yong An (7)	19 (21.1%)	NA	+	5 (5.6%)	1 (1.1%)	1 (1.1%)
Yun Liang (28)	22 (26.8%)	NA	+	1 (1.2%)	NA	7 (8.5%)
Defei Hong (19)	NA	11 (13.8%)	+	5 (6.3%)	6 (7.5%)	6 (7.5%)
Yusheng Du (16)	20 (29.9%)	14 (20.9%)	+	2 (3.0%)	4 (6.0%)	1 (1.5%)
Shi Chen (14)	21 (35.0%)	8 (13.3%)	+	5 (8.3%)	5 (8.3%)	4 (6.7%)
Fangkuan Li (24)	12 (24.0%)	8 (16.0%)	+	2 (4.0%)	2 (4.0%)	0 (0%)
Peng Chen (13)	NA	10 (25.0%)	-	5 (12.5%)	NA	8 (20.0%)
Ronggui Lin (29)	NA	5 (14.3%)	+	1 (2.9%)	1 (2.9%)	1 (2.9%)
Jianjun Li (26)	10 (29.4%)	2 (5.9%)	+	0 (0%)	0 (0%)	5 (14.7%)
Menghua Dai (15)	15 (44.1%)	NA	+	0 (0%)	NA	1 (2.9%)
Zhigang Wei (37)	NA	3 (9.1%)	+	6 (18.2%)	1 (3.0%)	NA
Fan Yang (JL) (41)	NA	10 (33.3%)	+	NA	NA	0 (0%)
Rong Tang (34)	14 (48.3%)	6 (20.7%)	-	2 (6.9%)	3 (10.3%)	1 (3.4%)
Fan Yang (CQ) (42)	16 (55.2%)	8 (27.6%)	-	1 (3.4%)	1 (3.4%)	5 (17.2%)
Jianhui Chen (12)	7 (28.0%)	2 (8.0%)	-	0 (0%)	1 (4.0%)	2 (8.0%)
Zuguang Wu (39)	8 (36.4%)	4 (18.2%)	-	0 (0%)	0 (0%)	1 (4.5%)
Lei Zhang (44)	4 (19.0%)	1 (4.8%)	-	2 (9.5%)	0 (0%)	1 (4.8%)
Jiacheng Wu (38)	NA	15 (71.4%)	+	0 (0%)	0 (0%)	0 (0%)
Zhao Liu (31)	5 (23.8%)	1 (4.8%)	+	2 (9.5%)	0 (0%)	0 (0%)
Qiang Huang (22)	6 (30.0%)	6 (30.0%)	+	5 (25.0%)	1 (5.0%)	2 (10.0%)
Qiuya Wei (36)	NA	1 (5.3%)	-	0 (0%)	1 (5.3%)	2 (10.5%)
Wentao Gao (18)	10 (55.6%)	7 (38.9%)	+	4 (22.2%)	0 (0%)	1 (5.6%)
Hai Hu (20)	7 (38.9%)	4 (22.2%)	+	0 (0%)	1 (5.6%)	3 (16.7%)
Qinzheng Bai (8)	NA	6 (37.5%)	+	NA	NA	NA
Jinmeng Hu (21)	8 (50.0%)	5 (31.3%)	+	2 (12.5%)	0 (0%)	0 (0%)
Huanwei Chen (11)	NA	4 (26.7%)	+	1 (6.7%)	0 (0%)	0 (0%)
Mingsheng Sun (33)	3 (25.0%)	2 (16.7%)	+	0 (0%)	1 (8.3%)	0 (0%)
Jun Xu (40)	1 (8.3%)	0 (0%)	-	0 (0%)	1 (8.3%)	0 (0%)
Hongbo Wei (35)	4 (36.4%)	NA	-	NA	NA	NA
Wu Ji (23)	1 (10.0%)	1 (10.0%)	-	0 (0%)	0 (0%)	0 (0%)
Total/mean	615 (31.9%)	446 (20.9%)		144 (5.5%)	86 (3.5%)	156 (6.0%)

IGSPF, international surgical group definition of pancreatic fistula. JL, Jilin Province. CQ, Chongqing City. NA, not applicable.

### 3.3. Short-term outcomes

Short-term outcomes of MIPD are reported in Table 5 and Table 6, including morbidity, pancreatic fistula (PF) rate, delayed gastric emptying (DGE) rate, bile leak rate, postoperative hemorrhage rate, length of postoperative hospital stay (LOS), Clavien-Dindo  $\geq 3$  complication rate, reoperation rate and rate of mortality.

The data of morbidity was included in 27 articles (69.2%). The morbidity ranged from 8.3 to 58.0%. Overall, 615 cases of postoperative complications occurred (31.9%). Particularly, the incidence of pancreatic fistula was mentioned in 38 articles (97.4%). The usage of International Surgical Group of Pancreatic Fistula (ISGPF) was employed in 29 articles (76.3%). In this analysis, we excluded the articles which only presented the data of clinical relevant PF (grade B/C). Incidence of overall PF ranged from 0 to 71.4%. Overall,

446 cases developed PF, giving a total PF rate of 20.9%. The data of DGE was available in 36 articles (92.3%), and ranged from 0 to 25.0%. In a total of 144 cases DGE occurred (5.5%). 33 studies (84.6%) mentioned bile leak, and ranged from 0 to 11.0%. Overall, 86 cases suffered from bile leak (3.5%). 36 articles (92.3%) recorded postoperative hemorrhage rate, and ranged from 0 to 22.0%, which included intraperitoneal and gastrointestinal hemorrhage. In a total of 156 cases postoperative hemorrhage occurred (6.0%).

The mean LOS was reported in 30 articles (76.9%), and ranged from 8.8 to 27.41 days, with a WA of 16.1 days. As for Clavien-Dindo  $\geq 3$  complications, only 12 studies listed the results (30.8%), which ranged from 0 to 32.5% and in 116 cases patients developed Clavien-Dindo  $\geq 3$  complications, with an overall rate of 13.4%. The information of reoperation was described in 20 articles (51.3%), and ranged from 0 to 17.2%. A total of

**Table 6. Short-term outcomes of minimally invasive pancreaticoduodenectomy**

First author (Ref.)	LOS (days)	Clavien-Dindo $\geq 3$ complications <i>n</i> (%)	Reoperation <i>n</i> (%)	Mortality <i>n</i> (%)
Chao Lu (32)	18.3 $\pm$ 11.7	35 (10.9%)	17 (5.3%)	2 (0.6%)
Xueqing Liu (30)	17 (6-89)	NA	NA	13 (4.3%)
Yunqiang Cai (9)	10.2 (5-19) <sup>a</sup>	NA	2 (0.8%)	1 (0.4%)
Hang Zhang (43)	12.97 $\pm$ 7.21	NA	2 (1.0%)	1 (0.5%)
Wei Chai (10)	12.3 <sup>b</sup>	NA	3 (1.6%)	3 (1.6%)
Qingchun Li (27)	18.9 <sup>b</sup>	NA	NA	2 (1.5%)
Xiaohui Duan (17)	14.8 (8-29) <sup>c</sup>	9 (8.9%)	3 (3.0%)	1 (1.0%)
Guolin Li (25)	12.9 <sup>b</sup>	NA	NA	NA
Tao Zhang (45)	18 $\pm$ 13.46	22 (22.0%)	6 (6.0%)	3 (3.0%)
Yong An (7)	13.3 <sup>b</sup>	NA	1 (1.1%)	NA
Yun Liang (28)	NA	22 (26.8%)	5 (6.1%)	3 (3.7%)
Defei Hong (19)	16.6 $\pm$ 10.1	NA	8 (10.0%)	NA
Yusheng Du (16)	15.4 <sup>b</sup>	2 (3.0%)	1 (1.5%)	0 (0%)
Shi Chen (14)	20.0 $\pm$ 7.4	7 (11.7%)	2 (3.3%)	1 (1.7%)
Fangkuan Li (24)	17.17 $\pm$ 6.628	NA	NA	NA
Peng Chen (13)	25.86 $\pm$ 12.22	13 (32.5%)	NA	3 (7.5%)
Ronggui Lin (29)	12.9 $\pm$ 3.2	NA	NA	NA
Jianjun Li (26)	NA	3 (8.8%)	3 (8.8%)	1 (2.9%)
Menghua Dai (15)	NA	NA	1 (2.9%)	NA
Zhigang Wei (37)	NA	NA	NA	NA
Fan Yang (JL) (41)	16.3 $\pm$ 7.2	NA	NA	0 (0%)
Rong Tang (34)	9.0 $\pm$ 2.1	NA	NA	NA
Fan Yang (CQ) (42)	17 (15-20) <sup>a</sup>	NA	5 (17.2%)	2 (6.9%)
Jianhui Chen (12)	15.5 $\pm$ 4.2	NA	1 (4.0%)	0 (0%)
Zuguang Wu (39)	17.3 $\pm$ 2.0	NA	NA	NA
Lei Zhang (44)	27.41 $\pm$ 5.82	1 (4.8%)	1 (4.8%)	NA
Jiacheng Wu (38)	11.3 $\pm$ 2.0	NA	NA	0 (0%)
Zhao Liu (31)	NA	NA	NA	NA
Qiang Huang (22)	25.0 $\pm$ 9.3	0 (0%)	0 (0%)	0 (0%)
Qiuya Wei (36)	8.8 $\pm$ 2.1	NA	NA	0 (0%)
Wentao Gao (18)	15.5 $\pm$ 6.8	NA	NA	0 (0%)
Hai Hu (20)	16 $\pm$ 4	NA	0 (0%)	1 (5.6%)
Qinzheng Bai (8)	NA	NA	NA	0 (0%)
Jinmeng Hu (21)	19.1 $\pm$ 6.0	NA	NA	NA
Huanwei Chen (11)	14 <sup>b</sup>	NA	NA	0 (0%)
Mingsheng Sun (33)	NA	2 (16.7%)	2 (16.7%)	0 (0%)
Jun Xu (40)	15.0	NA	NA	0 (0%)
Hongbo Wei (35)	17.0 $\pm$ 2.2	NA	NA	0 (0%)
Wu Ji (23)	9.6 $\pm$ 4.3	0 (0%)	0 (0%)	0 (0%)
Total/mean	16.1	116 (13.4%)	63 (3.6%)	37 (1.7%)

<sup>a</sup>Data are expressed as median and interquartile range. <sup>b</sup>Date are integration from multi-group data. LOS, length of hospital stay. JL, Jilin Province. CQ, Chongqing City. NA, not applicable.

63 cases demanded reoperation (3.6%). Unfortunately, only 27 studies (69.2%) recorded the rate of mortality, which ranged from 0 to 7.5%, and in 37 cases patients died, with an overall postoperative mortality rate of 1.7%.

### 3.4. Oncologic outcomes

The pathology results are shown in Table 7, comprising the rate of malignancy, the number of harvested lymph nodes and the rate of negative tumor margin (R0).

The etiology was described in 35 articles (89.7%). We regarded ampullary adenocarcinoma, pancreatic ductal adenocarcinoma, distal cholangiocarcinoma, duodenal adenocarcinoma and other malignant tumors clearly identified by the authors as malignancy in our review because of the different attitudes to borderline tumors from different authors. Overall, 2084 cases (80.7%) were diagnosed with malignancy. Furthermore,

only 7 authors (17.9%) described the etiology using tumor-node-metastasis (TNM) stage. The mean number of harvested lymph nodes was provided in 20 articles (51.3%), and ranged from 7.02 to 23.1, with a WA of 13.5 lymph nodes. Margin status was documented in 25 articles (64.1%). In 9 articles, the R0 rate was 100%, whereas it ranged from 10 to 99.2% in the other 16 studies. A total of 79 cases were diagnosed with positive margins out of 1,492 malignancy cases (5.3%)

### 3.5. Comparison of the results of different surgical techniques

Comparisons of the outcomes between LPD, RPD and open pancreaticoduodenectomy (OPD) are summarized in Table 8. Excluding cumulative data of multiple techniques from three studies, a total of 2,310 LPD, 188 RPD and 779 OPD were accepted for comparison.

**Table 7. Oncologic outcomes of minimally invasive pancreaticoduodenectomy**

First author (Ref.)	Malignancy <sup>a</sup> n (%)	TNM stage	Harvested lymph node	R0 (%)
Chao Lu (32)	221 (69.1%)	-	NA	NA
Xueqing Liu (30)	258 (86.0%)	-	12 (2-60)	99.3%
Yunqiang Cai (9)	161 (67.6%)	-	NA	NA
Hang Zhang (43)	147 (72.8%)	+	9.81 ± 5.19	99.0%
Wei Chai (10)	188 (100.0%)	-	14.9 <sup>b</sup>	93.6%
Qingchun Li (27)	134 (100.0%)	+	23.1 <sup>b</sup>	92.5%
Xiaohui Duan (17)	101 (100.0%)	-	16.7 ± 4.2	95.0%
Guolin Li (25)	45 (45.0%)	-	NA	NA
Tao Zhang (45)	78 (78.0%)	-	7.02 ± 4.30	100.0%
Yong An (7)	71 (78.9%)	-	17.2 <sup>b</sup>	100.0%
Yun Liang (28)	60 (73.2%)	-	12.5 <sup>b</sup>	95.0%
Defei Hong (19)	71 (88.8%)	-	NA	100.0%
Yusheng Du (16)	60 (90.0%)	-	NA	NA
Shi Chen (14)	38 (63.3%)	+	13.6 ± 6.0	97.4%
Fangkuan Li (24)	46 (92.0%)	-	11.56 ± 6.174	97.8%
Peng Chen (13)	3 (75.0%)	-	NA	10.0%
Ronggui Lin (29)	24 (68.6%)	-	10.6 ± 4.0	100.0%
Jianjun Li (26)	34 (100.0%)	-	NA	NA
Menghua Dai (15)	31 (91.2%)	-	NA	93.5%
Zhigang Wei (37)	33 (100.0%)	-	NA	100.0%
Fan Yang (JL) (41)	26 (86.7%)	-	NA	92.3%
Rong Tang (34)	29 (100.0%)	+	NA	NA
Fan Yang (CQ) (42)	20 (69.0%)	+	NA	90.0%
Jianhui Chen (12)	25 (100.0%)	-	12.6 ± 3.3	100.0%
Zuguang Wu (39)	NA	-	9.3 ± 3.0	NA
Lei Zhang (44)	NA	-	7.24 ± 4.81	100.0%
Jiacheng Wu (38)	21 (100.0%)	-	NA	100.0%
Zhao Liu (31)	18 (85.7%)	-	14 (8-26)	94.4%
Qiang Huang (22)	18 (90.0%)	-	NA	NA
Qiuya Wei (36)	17 (89.5%)	-	17.7 ± 6.5	76.5%
Wentao Gao (18)	13 (72.2%)	-	NA	69.2%
Hai Hu (20)	9 (50.0%)	+	16 ± 4	88.9%
Qinzheng Bai (8)	12 (75.0%)	-	NA	NA
Jinmeng Hu (21)	NA	-	17.1 ± 9.7	100.0%
Huanwei Chen (11)	13 (86.7%)	-	NA	NA
Mingsheng Sun (33)	12 (100.0%)	+	10	100.0%
Jun Xu (40)	11 (91.7%)	-	NA	NA
Hongbo Wei (35)	NA	-	9.2 ± 4.0	100.0%
Wu Ji (23)	9 (90.0%)	-	NA	NA
Total/mean	2,084 (80.7%)		13.5	1,413 (94.7%)

<sup>a</sup>Malignancies include Ampullary adenocarcinoma, Pancreatic ductal adenocarcinoma, Distal cholangiocarcinoma, Duodenal adenocarcinoma and other malignant tumors clearly identified by the authors. <sup>b</sup>Date are integration from multi-group data. TNM, tumor-node-metastasis. JL, Jilin Province. CQ, Chongqing City. NA, not applicable

The operative time was significantly longer in LPD and RPD groups than in OPD groups. Compared with OPD, LPD shortened LOS significantly. As for morbidity, LPD, RPD and OPD had a result of 30.4%, 46.3% and 37.9% respectively. Interestingly, every two of them had a significant difference, and the three techniques had similar results in blood loss, pancreatic fistulas and mortality rates.

### 3.6. Comparison of the results of large and small series

Twenty-one articles documented on 30 or more MIPD ( $n = 2,318$ ), whereas eighteen studies on 29 or fewer MIPD ( $n = 335$ ). (Table 9)

In aspects of operative time and morbidity, the large series had more significant advantages than the small one. No significance, however, was mentioned in blood

loss, LOS, PF and mortality rate.

## 4. Discussion

Early in 1994, Gagner described the first case of laparoscopic pylorus-preserving pancreatoduodenectomy for chronic pancreatitis, which marked the beginning of a new era. However, the multiple technical complications covered the benefit of a laparoscopic approach (2). Furthermore, inherent technical limitations of laparoscopy and a long learning curve made this advanced technique develop slowly. Nine years later, Lu reported the first LPD for duodenal papillary cancer in Chinese mainland and achieved comparable outcomes to OPD in perioperative blood loss and short-term recovery (3). Afterwards, an increasing number of reports describing the attempt at MIPD were published.

**Table 8. Comparison of surgical techniques**

Items	LPD (n = 2,310)	RPD (n = 188)	OPD (n = 779)	p		
				LPD vs RPD	LPD vs OPD	RPD vs OPD
WA of operative time (min.)	367.5 (n = 2,072)	387.6 (n = 188)	327.7 (n = 779)	NS*	0.014*	0.007*
WA of blood loss (mL)	284.7 (n = 1912)	232.5 (n = 128)	374.6 (n = 613)	NS^	NS^	NS*
WA of LOS (days)	15.7 (n = 1811)	18.0 (n = 188)	20.9 (n = 733)	NS*	0.006*	NS*
Morbidity (%)	528 (30.4%) (n = 1737)	87 (46.3%) (n = 188)	267 (37.9%) (n = 704)	< 0.001°	< 0.001°	0.038°
Pancreatic fistula (%)	383 (21.4%) (n = 1793)	37 (19.7%) (n = 188)	150 (20.5%) (n = 731)	NS°	NS°	NS°
Mortality (%)	29 (1.5%) (n = 1894)	5 (2.7%) (n = 188)	14 (2.6%) (n = 537)	NS°	NS°	NS°

\*t test unpaired. ^Mann-Whitney U test. °Chi squared. LPD, laparoscopic pancreaticoduodenectomy. RPD, robotic pancreaticoduodenectomy. OPD, open pancreaticoduodenectomy. WA, weighted average. NS, no significant difference. LOS, length of hospital stay.

**Table 9. Comparison of large vs smaller series**

Items	Large series (n = 2,318)	Smaller series (n = 335)	p
WA of operative time (min.)	360.0 (n = 2045)	435.1 (n = 335)	0.013*
WA of blood loss (mL)	266.1 (n = 1904)	356.0 (n = 291)	NS^
WA of LOS (days)	16.1 (n = 1897)	15.8 (n = 257)	NS*
Morbidity (%)	466 (28.1%) (n = 1661)	94 (35.6%) (n = 264)	0.012°
Pancreatic fistula (%)	373 (20.6%) (n = 1812)	73 (22.5%) (n = 324)	NS°
Mortality (%)	34 (1.8%) (n = 1896)	3 (1.3%) (n = 226)	NS°

\*t test unpaired. ^Mann-Whitney U test. °Chi squared. WA, weighted average. NS, no significant difference. LOS, length of hospital stay.

As listed in this systematic review, the maturation of MIPD in Chinese mainland has been extremely quick. The present review is the largest study to evaluate current status of MIPD in both high-volume and low-volume hospitals of Chinese mainland. A total of 2,653 cases were reported in the recent ten years excluding articles of less than 10 cases and initial experience from some high-volume centers. The number of cases reported in the recent two years (from January 2018 to June 2019) was four times than that in the previous years. Although it can't represent the annual cases of MIPD, it demonstrated that MIPD is a research highlight in the Chinese mainland in recent years. In order to highlight distinctive characteristics of MIPD in China mainland and further analyze the difference between Chinese mainland and the world, we present several recent systematic reviews describing the development of MIPD in the world (Table 10).

As shown in this table, we have a more favorable outcome in operation time than Nickel (mean: 370.6 min vs 417.0 min). Probably, this is largely associated with the learning curve and operation mastery. Wang *et al* were of the view that the minimum number of cases needed to reach technical competency for LPD was 40 cases (48), while Boone *et al* were first able to reach proficiency after 80 cases in robotic-assisted PD (49). Based on Chinese national conditions, a large number of patients have had a tremendous advantage accumulating

surgeon's experience and accelerating surgeon's learning curve, especially in high-volume centers. While similar results of estimated blood loss were obtained by Nickel's study and this review, Jiang's research offered a worse outcome due to an initial study, which accounted for a large proportion of results.

In terms of morbidity, we found some complications related to MIPD in our review, such as PF, bile leak and postoperative hemorrhage, which were equivalent to those of MIPD as reported in the international reviews. Strangely, more cases suffering DGE were reported in Nickel's study (21.9% vs 5.5%). The reason that contributed to the significant difference maybe was a large number of authors in our review only selectively reported clinically related DGE (grade B/C) (50). Meanwhile, Nickel only selectively analyzed the clinically related PF because not all trials reported biochemical leaks. Therefore, it's not hard to conclude that we have a slightly better result in overall PF than Nickel, which largely benefited from modified or innovative methods to further reinforce the junction such as purse-string, Bing's anastomosis (9) or Hong's single-stitch method (47). Nonetheless, PF was still the most common postoperative complication no matter in Chinese or international studies. Also, the corrosiveness of pancreatic juice may increase the risk of late postoperative hemorrhage (51). Whatever, more effective and safer anastomosis methods are urgently needed to

**Table 10. Comparison of perioperative and oncological outcomes in previous systematic reviews and this review**

Variables	Nickel (52)	Jiang (54)	Wang (55)	This review
<b>Intraoperative outcomes</b>				
Operation time (min)	417.0			370.6
Blood loss (mL)	280.5	378.1		278.0
Conversion to laparotomy			61 (5.9%)	35 (2.6%)
Transfusion				143 (10.8%)
<b>Short-term outcomes</b>				
<b>Morbidity</b>				
Pancreatic fistula	20 (17.5%)	43 (15.1%)	338 (32.9%)	446 (20.9%)
Delayed gastric emptying	25 (21.9%)		172 (16.7%)	144 (5.5%)
Bile leak	10 (8.8%)		50 (4.9%)	86 (3.5%)
Postoperative hemorrhage	10 (8.8%)	24 (9.3%)	128 (12.4%)	156 (6.0%)
length of hospital stay(days)	10.6	10.0	13.5	16.1
Clavien-Dindo $\geq 3$ complications	33 (28.9%)		218 (21.2%)	116 (13.4%)
Reoperation	8 (7.0%)		88 (8.6%)	63 (3.6%)
Mortality	8 (7.0%)		25 (2.4%)	37 (1.7%)
<b>Oncologic outcomes</b>				
Harvested lymph node	14.3	19.4	10.5	13.5
R0 rate	91 (82.0%)	695 (79.9%)	1,004 (97.6%)	1,413 (94.7%)

decrease this formidable complication.

Regarding length of postoperative hospital stay, no significant difference existed between Nickel's and Jiang's studies. Surprisingly, the outcome we pooled was considerably longer than the former two. This difference could, in part, be caused by the different regulations and culture in different countries (6,52). Statistical analysis had been submitted at this point by Boggi with the result of 21.9 days in Europe, 13.0 days in Asia and 9.4 days in North America (6).

The first and the only patient-blinded, randomized clinical trial (LEOPARD-2) was stopped due to a higher mortality rate (14% vs 2%) in the LPD group when compared to the OPD group. However, the four centers included in this trial with a median of 11 LPD (range 6-15) annually. What's more, we couldn't get any information from the original article about how many LPD cases were performed by the surgeons before they participated in the trial and whether they had already finished the learning curve or not.

As for oncologic outcomes, we had a similar result as Nickel in harvested lymph nodes (13.5 vs 14.3), but both were less than Jiang's outcome of 19.4. However, in R0 resection, we had a significantly better result than the other two. Actually, certainty of evidence in margin status was low. Pathology information has not always been collected according to standardized methodology. Especially for borderline tumors, few authors described their classification criteria.

Wang's study is the Chinese largest multicenter study to date which pooled the data from 1,029 consecutive MIPD patients in 16 high-volume pancreatic centers in China. As shown in the table, we had slight advantages in many factors including conversion to laparotomy, overall and differing morbidity, Clavien-Dindo  $\geq 3$  complications, reoperation and mortality. The reasons are not unique. On the one hand, Wang *et al* pooled the

data from January 2010 to August 2016. With more advanced and innovative technologies introduced and the number of surgeons completing the learning curve increasing gradually, it is reasonable to assume that we can acquire better results in either intraoperation or short-term outcomes. On the other hand, reporting bias in low-volume hospitals cannot be ignored.

Major venous resection and reconstruction in MIPD has been regarded as a surgical forbidden zone for a long time. In this study, a total of 26 cases of MIPD combined with major venous resection and reconstruction were performed in 7 high-volume pancreatic centers. Besides, in 2018, Cai *et al* (53) reported an innovative approach to perform the above-mentioned challenging surgical procedures in 18 patients. No 30-day mortality was documented while only one case was converted to laparotomy due to uncontrolled bleeding from the splenic vein. Therefore, it is reasonable to believe that MIPD with major venous resection and reconstruction is technically feasible in selected patients, and with continuous accumulation of surgeons' experience and technological innovations, patients with vascular involvement will no longer be an absolute contraindication for MIPD.

This review is also subject to limitations. First, some technique details including pylorus preservation PD, section of pancreatic neck and long-term oncological outcomes such as overall survival and recurrence-free survival were not described in this study due to a lack of enough original data. Second, the study has not further compared and analyzed the outcomes of MIPD in different periods. Therefore, we can hardly observe the improvement and progress of results from recent years. Third, the quality of evidence is generally limited to cohort studies and case series.

In conclusion, although the developmental stage of MIPD in Chinese mainland was nearly a decade late,

its development was extremely quick, especially in the recent two years. The operative volume of MIPD in Chinese mainland is in the leading position in the world. Compared with some large international meta-analysis, non-inferior perioperative and short-term oncological outcomes were observed in MIPD of Chinese mainland. What's more, nearly 50 cases were documented in the condition of major vascular resection and reconstruction in Chinese mainland, which represented the operative quality to a certain degree. However, research on survival analysis and phased learning curve outcomes is urgently needed before the innovative surgical techniques are widely accepted.

## References

- Cameron JL, He J. Two thousand consecutive pancreaticoduodenectomies. *J Am Coll Surg.* 2015; 220:530-536.
- Gagner M, Pomp A. Laparoscopic pylorus-preserving pancreaticoduodenectomy. *Surg Endosc.* 1994; 8:408-410.
- Lu BY, Lu WQ, Cai XY, Wei YX, Jiang HX. Laparoscopic pancreaticoduodenectomy for duodenal papillary carcinoma: A case report. *Chinese Journal of Minimally Invasive Surgery.* 2003; 3:197-198. (in Chinese)
- Croome KP, Farnell MB, Que FG, Reid-Lombardo KM, Truty MJ, Nagorney DM, Kendrick ML. Total laparoscopic pancreaticoduodenectomy for pancreatic ductal adenocarcinoma: Oncologic advantages over open approaches? *Ann Surg.* 2014; 260:633-638; discussion 638-640.
- Gumbs AA, Rodriguez Rivera AM, Milone L, Hoffman JP. Laparoscopic pancreaticoduodenectomy: A review of 285 published cases. *Ann Surg Oncol.* 2011; 18:1335-1341.
- Boggi U, Amorese G, Vistoli F, Caniglia F, De Lio N, Perrone V, Barbarello L, Belluomini M, Signori S, Mosca F. Laparoscopic pancreaticoduodenectomy: A systematic literature review. *Surg Endosc.* 2015; 29:9-23.
- An Y, Zhang Y, Liu SY, Cai HH, Chen WB, Wu D, Sun DL, Chen XM. Comparison of the clinical application of three-dimensional and two-dimensional laparoscopic pancreaticoduodenectomy. *Zhonghua Wai Ke Za Zhi.* 2019; 57:353-357. (in Chinese)
- Bai QZ, Xu JW, Li F, Liu H, Wang L. The technique of laparoscopic pancreaticoduodenectomy surrounding the portal vein-superior mesenteric vein axis: a report of 16 cases. *Journal of Laparoscopic Surgery.* 2016; 21:776-779. (in Chinese)
- Cai YQ, Luo H, Li YB, Gao P, Peng B. A novel technique of pancreaticojejunostomy for laparoscopic pancreaticoduodenectomy. *Surg Endosc.* 2018; 33:1572-1577.
- Chai W, Lei B, Meng Y, Zhao XL, Zhang L, Kong DS, Liu RH. Choice of surgical methods and short-term therapeutic efficacy analysis of laparoscopic pancreaticoduodenectomy. *Chinese Journal of Pancreatology.* 2019; 19:98-102. (in Chinese)
- Chen HW, Wang FJ, Deng FW, Li JY, Hu JY. Preliminary experience of laparoscopic pancreaticoduodenectomy. *Chinese Journal of Hepatic Surgery.* 2019; 8:212-216.
- Chen JH, Lin SB, Li F, Shen Y, Zhou EC, Zhang RL. Comparison of short-term efficacy of laparoscopy-assisted and open pancreaticoduodenectomy. *Chinese Journal of General Surgery.* 2016; 25:401-406. (in Chinese)
- Chen P, Zhou B, Sun CD, Qiu FB, Zhang BY, Guo WD, Xu YZ. Preliminary comparison of perioperative outcomes between minimally invasive and open pancreaticoduodenectomy. *Journal of Laparoscopic Surgery.* 2018; 23:700-704. (in Chinese)
- Chen S, Chen JZ, Zhan Q, Deng XX, Shen BY, Peng CH, Li HW. Robot-assisted laparoscopic versus open pancreaticoduodenectomy: A prospective, matched, mid-term follow-up study. *Surg Endosc.* 2015; 29:3698-3711.
- Dai MH. Clinical significance of semi-Derotation artery first approach in laparoscopic pancreaticoduodenectomy. *Chinese Journal of Operative Procedures of General Surgery (Electronic Version).* 2018; 12:275-278. (in Chinese)
- Du YS, Wang J, Li Y, Ma HQ, Liu L, Zhu YX, Zhao WX. Clinical application of a modified pancreatojejunostomy technique for laparoscopic pancreaticoduodenectomy. *HPB (Oxford).* 2019; 21:1336-1343.
- Duan XH, Zhou LX, Tian BZ, Yang JH, Li X, Zeng YH, Jiang B, Mao XH. Three-dimensional laparoscopic pancreaticoduodenectomy for periampullary carcinoma: A single surgical team's experience. *Chinese Journal of General Surgery.* 2017; 26:1127-1132. (in Chinese)
- Gao WT, Xi CH, Tu M, DaI XL, Guo F, Chen JM, Wei JS, Lu ZP, Wu JL, Jiang KR, Miao Y. Laparoscopic pancreaticoduodenectomy with a novel artery first and uncinate process first approach through Treitz ligament. *Zhonghua Wai Ke Za Zhi.* 2017; 55:359-363. (in Chinese)
- Hong DF, Liu YH, Zhang YH, Zhang CW, Wang YC, Sun XD, Zhang W, Wu WD, Wang ZF, Shen GL, Cheng J, Zhang JG, Lu Y. Laparoscopic and hybrid laparoscopic robotic pancreaticoduodenectomy: A report of 80 cases. *Chinese Journal of Practical Surgery.* 2016; 36:885-888,893. (in Chinese)
- Hu H, Yu X, Hu G, Sun JC, Wang CF, Huang H. Performance experiences in robotic-assisted pancreaticoduodenectomy: A report of 18 cases. *Chinese Journal of General Surgery.* 2019; 28:260-266. (in Chinese)
- Hu JM, Dong JX, Qin J, Gao S, Zhao KL, Bai WW, Wang J. Pancreaticoduodenectomy: A single center experience of 118 patients. *Chinese Journal of Hepatobiliary Surgery.* 2018; 24:542-544. (in Chinese)
- Huang Q, Yang J, Shao CS, Lin XS, Xie F, Liu CH, Wang H, Lv XW. Totally laparoscopic pancreaticoduodenectomy: Analysis of 20 patients. *Journal of Abdominal Surgery.* 2017; 30:302-306. (in Chinese)
- Ji W, Ding K, Kao XM, He CS, Li N, Li JS. Robotic and laparoscopic hybrid pancreaticoduodenectomy: Surgical techniques and early outcomes. *Chin Med J (Engl).* 2014; 127:3027-3029.
- Li FK, Wang XM, Sun WD, Hu MH, Wu Q, Hu KT, Ji YH. Comparison of the short-term clinical efficacies of laparoscopic and open pancreaticoduodenectomy. *Acta Academiae Medicinae Wannan.* 2017; 36:535-538. (in Chinese)
- Li GL, Lin Q, Zheng SY, Zhou QB, Chen RF. The evaluation of laparoscopic pancreaticoduodenectomy with programmed process. *Chinese Journal of Laparoscopic*

- Surgery ( Electronic Edition). 2018; 11:85-89. (in Chinese)
26. Li JJ, Lu BY, Huang YB. Application of wrapping pancreatic duct-jejunum anastomosis in laparoscopic pancreaticoduodenectomy. *Chinese Journal of Digestive Surgery*. 2013; 12:116-119. (in Chinese)
  27. Li QC, Xue JH, Li WG. Clinical value of arterial first approach in laparoscopic pancreaticoduodenectomy for periampullary tumor. *Chinese Journal of Postgraduates of Medicine*. 2019; 42:14-18. (in Chinese)
  28. Liang Y, Zhao LT, Jiang CY, Hu PF, Wang HW, Cai ZW, Wang W. Laparoscopic pancreaticoduodenectomy in elderly patients. *Surg Endosc*. 2019. doi: 10.1007/s00464-019-06982-w.
  29. Lin RG, Huang HG, Chen YC, Lu FC, Lin XC, Yang HH, Fang HZ, Wang CF. Uncinate process resection *via* anterior "vein-first" combined with right posterior "artery-first" approach in laparoscopic pancreaticoduodenectomy: An analysis of 35 cases. *Chinese Journal of Practical Surgery*. 2018; 38:560-563. (in Chinese)
  30. Liu XQ, Xing ZQ, Qin JZ, Duan JY, Feng F, Wang WB, Yan CQ, Liu JH. Results of 300 consecutive laparoscopic pancreaticoduodenectomies: Experience of single institution. *Chinese Journal of Practical Surgery*. 2018; 38:306-311. (in Chinese)
  31. Liu Z, Yu MC, Zhao R, Liu YF, Zeng JP, Wang XQ, Tan JW. Laparoscopic pancreaticoduodenectomy *via* a reverse-"V" approach with four ports: Initial experience and perioperative outcomes. *World J Gastroenterol*. 2015; 21:1588-1594.
  32. Lu C, Jin WW, Mou YP, Zhou YC, Zhu QC, Shao HL, Chen K, Li SD. Experience on postoperative complications of laparoscopic pancreaticoduodenectomy. *Zhonghua Wai Ke Za Zhi*. 2018; 56:822-827. (in Chinese)
  33. Sun MS. Laparoscopic pancreaticoduodenectomy with uncinate process approach: A report of 12 cases. *Chinese Journal of General Surgery*. 2015; 24:1227-1231. (in Chinese)
  34. Tang R, Zheng H, Chen J, Ding YJ. Analysis of postoperative complications and prognosis of patients with pancreatic head cancer treated by laparoscopic pancreaticoduodenectomy. *Chinese Journal of the Frontiers of Medical Science (Electronic Version)*. 2017; 9:84-87. (in Chinese)
  35. Wei HB, Wei B, Zheng ZH, Huang Y, Huang JL, Fang JF. Comparative study of outcomes after laparoscopic versus open pancreaticoduodenectomy. *Chinese Journal of Gastrointestinal Surgery*. 2014; 17:465-468. (in Chinese)
  36. Wei QY, Liu YY, Yan WF, Fan Y, Wang C. A case matched study on laparoscopic versus open pancreaticoduodenectomy. *Chinese Journal of Hepatobiliary Surgery*. 2016; 22(332-335). (in Chinese)
  37. Wei ZG, Wei YX, Huo TY, Liu Y, Yu J, Yan H, Wang GM. Laparoscopic pancreaticoduodenectomy *via* a "G"-shaped approach: Experience of 33 cases. *Chinese Journal of General Surgery*. 2018; 33:575-577. (in Chinese)
  38. Wu JC, Zhang XW, Yang YS, Wang Y, Fang H, Lin RX. Application value of pancreaticojejunostomy with double-layer continuous suture in total laparoscopic pancreaticoduodenectomy. *Chinese Journal of Digestive Surgery*. 2018; 17:746-751. (in Chinese)
  39. Wu ZG, Deng GM, Zhang YM, Liu HT, Li ZW. An analysis between laparoscopic and open pancreaticoduodenectomy. *Lingnan Modern Clinics in Surgery*. 2017; 17:678-680. (in Chinese)
  40. Xu J, Liu C, Ji YC, Zhai B, Wang D. Report of 12 cases laparoscopic pancreaticoduodenectomy. *Journal of Laparoscopic Surgery*. 2010; 15:659-661. (in Chinese)
  41. Yang F, Liu YH, Liu SY, Zhang W, Jia BX, Wang YC. Clinical application of total laparoscopic pancreaticoduodenectomy with inferior-posterior uncinate process and artery first approach. *Chinese Journal of Minimally Invasive Surgery*. 2018; 18:908-910. (in Chinese)
  42. Yang F, Zhong GC, You K, Liu ZJ. Short-term clinical outcomes of laparoscopic pancreaticoduodenectomy versus open pancreaticoduodenectomy: A retrospective analysis. *Chinese Journal of Bases and Clinics in General Surgery*. 2019; 26:685-690. (in Chinese)
  43. Zhang H, Guo XJ, Xia J, Zhu F, Shen M, Wang X, Wang M, Qin RY. Comparison of Totally 3-Dimensional Laparoscopic Pancreaticoduodenectomy and Open Pancreaticoduodenectomy. *Pancreas*. 2018; 47:592-600.
  44. Zhang L, Zhang XJ. A Single-center Retrospective Study of Clinical Efficacy of Laparoscopic and Open Pancreaticoduodenectomy. *Medical Information*. 2019; 32:118-120. (in Chinese)
  45. Zhang T, Zhao ZM, Gao YX, Lau WY, Liu R. The learning curve for a surgeon in robot-assisted laparoscopic pancreaticoduodenectomy: A retrospective study in a high-volume pancreatic center. *Surg Endosc*. 2018; 33:2927-2933.
  46. Barreto SG, Shukla PJ. Different types of pancreaticoenteric anastomosis. *Transl Gastroenterol Hepatol*. 2017; 2:89.
  47. Hong DF, Liu YH, Zhang YH, Wang YC, Wang ZM, Wu WD, Shen GL, Zhang JG, Zhang W, Cheng J, Peng SY. The role of Hong's single-stitch duct to mucosa pancreaticojejunostomy in laparoscopic pancreaticoduodenectomy. *Zhonghua Wai Ke Za Zhi*. 2017; 55:136-140. (in Chinese)
  48. Wang M, Meng L, Cai Y, Li Y, Wang X, Zhang Z, Peng B. Learning curve for laparoscopic pancreaticoduodenectomy: A CUSUM analysis. *J Gastrointest Surg*. 2016; 20:924-935.
  49. Boone BA, Zenati M, Hogg ME, Steve J, Moser AJ, Bartlett DL, Zeh HJ, Zureikat AH. Assessment of quality outcomes for robotic pancreaticoduodenectomy: Identification of the learning curve. *JAMA Surg*. 2015; 150:416-422.
  50. Wente MN, Bassi C, Dervenis C, Fingerhut A, Gouma DJ, Izbicki JR, Neoptolemos JP, Padbury RT, Sarr MG, Traverso LW, Yeo CJ, Buchler MW. Delayed gastric emptying (DGE) after pancreatic surgery: A suggested definition by the International Study Group of Pancreatic Surgery (ISGPS). *Surgery*. 2007; 142:761-768.
  51. Wente MN, Veit JA, Bassi C, Dervenis C, Fingerhut A, Gouma DJ, Izbicki JR, Neoptolemos JP, Padbury RT, Sarr MG, Yeo CJ, Buchler MW. Postpancreatectomy hemorrhage (PPH): An International Study Group of Pancreatic Surgery (ISGPS) definition. *Surgery*. 2007; 142:20-25.
  52. Nickel F, Haney CM, Kowalewski KF, Probst P, Limen EF, Kalkum E, Diener MK, Strobel O, Muller-Stich BP, Hackert T. Laparoscopic Versus Open Pancreaticoduodenectomy: A Systematic Review and Meta-analysis of Randomized Controlled Trials. *Ann Surg*. 2019. doi: 10.1097/SLA.0000000000003309.
  53. Cai Y, Gao P, Li Y, Wang X, Peng B. Laparoscopic pancreaticoduodenectomy with major venous resection

- and reconstruction: Anterior superior mesenteric artery first approach. *Surg Endosc.* 2018; 32:4209-4215.
54. Jiang YL, Zhang RC, Zhou YC. Comparison of overall survival and perioperative outcomes of laparoscopic pancreaticoduodenectomy and open pancreaticoduodenectomy for pancreatic ductal adenocarcinoma: A systematic review and meta-analysis. *BMC Cancer.* 2019; 19:781.
55. Wang M, Peng B, Liu J, *et al.* Practice Patterns and Perioperative Outcomes of Laparoscopic Pancreaticoduodenectomy in China: A Retrospective Multicenter Analysis of 1029 Patients. *Ann Surg.* 2019. doi: 10.1097/SLA.0000000000003190.

*(Received October 11, 2019; Revised December 12, 2019; Accepted December 20, 2019)*

# Human cytomegalovirus IE2 protein regulates macrophage-mediated immune escape by upregulating GRB2 expression in UL122 genetically modified mice

Yanan Yang<sup>1</sup>, Guohua Ren<sup>2</sup>, Zhifei Wang<sup>3</sup>, Bin Wang<sup>1,\*</sup>

<sup>1</sup> Department of Special Medicine, Qingdao University College of Medicine, Qingdao, China;

<sup>2</sup> Dermatology, Heze Municipal Hospital, Heze, China;

<sup>3</sup> Department of Pathogen Biology, Qingdao University College of Medicine, Qingdao, China.

## Summary

Although cytomegalovirus (HCMV) infection is asymptomatic in healthy individuals, the virus can remain latent for many years due to its ability to evade host immune surveillance. However, reactivation of HCMV can lead to life-threatening disease. Recent studies have shown that HCMV infection mediates immune escape by regulating macrophage activity, although the role of the HCMV-encoded IE2 protein is unclear. A ul122 transgenic mouse model was created to stably express the IE2 protein, and the proportion of M1 and M2 macrophage populations in their spleen and bone marrow was compared to that in wild-type controls. In addition, the phagocytic function of the macrophages was evaluated in terms of neutral red dye uptake. Spleen and bone marrow macrophages in IE2-expressing mice were mainly of the M2 phenotype and displayed enhanced phagocytic function compared to that in control mice. The relative levels of expression of macrophage-related GRB2 and of IL-4, IFN- $\gamma$ , IL-13, and TNF- $\alpha$  were also analyzed in the spleen and bone marrow of the two groups. The IE2-expressing mice had increased expression of GRB2 and increased expression of the M2-related cytokines IL-4 and IL-13. Taken together, the current results suggest that HCMV IE2 polarizes the host macrophages to the M2 type via a GRB2/IL-4-related pathway, which enables long-term survival of the virus in the host.

**Keywords:** IE2, GRB2, macrophage polarization, immune escape

## 1. Introduction

Human cytomegalovirus (HCMV), also known as human herpes virus 5 (HHV5), belongs to the beta herpesvirus subfamily of the Herpesviridae subfamily and has a double-stranded DNA genome of ~240 kb that encodes more than 200 proteins (1,2). A large portion of the global population is infected with HCMV, with serum infection rates of 40-60% in developed countries and nearly 100% in developing countries (3). Although HCMV triggers a host immune

response that inhibits viral replication and lowers the viral load below the threshold of clinical detection, it cannot completely eliminate the virus (4). HCMV has evolved multiple strategies to evade the host immune surveillance and survive, resulting in lifelong latent infection (5). Although infection in healthy adults is usually asymptomatic or mild, it is often associated with the development of chronic inflammatory diseases and even cancer (6). There are even reports of HCMV proteins and nucleic acids in breast (7), colon (8) prostate (9), and mucoepidermoid salivary gland (10) cancers, as well as glioblastoma (11) tissues. In addition, reactivation of the virus during an immunodeficient state can result in severe clinical disease or even death (12,13).

The pathological changes associated with HCMV infection are largely mediated by infected monocytes. Due to diverse surface receptors and the high level of phagocytic activity, monocytes are often used

Released online in J-STAGE as advance publication December 23, 2019.

\*Address correspondence to:

Dr. Bin Wang, Department of Special Medicine, Qingdao University College of Medicine, 308 Ningxia Road, Qingdao, Shandong, China.

E-mail: 2017021555@qdu.edu.cn

by the virus as a conduit to enter other cells (14). In order to circumvent its short life cycle and inability to support its own replication, HCMV induces monocyte differentiation into long-lived macrophages that allow viral gene expression and replication (15,16). Macrophages are classified as the pro-inflammatory M1 type and anti-inflammatory M2 type that are induced by different cytokines (17). HCMV can replicate, survive for long durations in the host cell, and spread by regulating the polarization of macrophages. M1 macrophages facilitate establishment of HCMV infection and transmission, which induce acute inflammation and immune cell recruitment (18). M2 type macrophages, in contrast, promote chronic infection by producing anti-inflammatory mediators that facilitate long-term tissue distribution of the virus and that are activated under specific conditions (16). In addition, phagocytosis by macrophages is a common strategy used by viruses to evade host immune cells (19). Recent transcriptome studies have shown that both M1- and M2-related genes are expressed after HCMV infection of monocytes/macrophages, although the former is more significantly upregulated, resulting in M1 polarization (20).

Growth factor receptor-bound protein 2 (GRB2) is an adaptor protein associated with activated epidermal growth factor receptors (EGFRs), and GRB2 recruits accessory proteins in various receptor-mediated signaling pathways (21). It is up-regulated after HCMV infection, and it promotes viral replication and spread (22) and also affects the polarization, phagocytic function, proliferation, and migration of macrophages (23-25). HCMV genes are expressed in a temporal sequence and are accordingly divided into immediate early (IE), early (E), and late (L) genes (26). The two key regulators in HCMV replication are UL123 (IE1) and UL122 (IE2), which are encoded by the IE gene. They are expressed at high levels within hours after viral entry, and their re-expression is vital to HCMV reactivation (27). IE2 is essential for efficient viral replication, but since HCMV mutants defective in IE1 expression display a severe growth defect, IE2 is considered to be the main promoter of the E and L transcripts (28).

The aims of this study were to determine the effects of HCMV IE2 on macrophage polarization and function and to explore the role of GRB2. Due to the strict species-specificity of HCMV infection, previous studies were conducted using *in vitro* models. A ul122 transgenic mouse model was created to stably express IE2 in order to elucidate the mechanism of IE2 action *in vivo*.

## 2. Materials and Methods

### 2.1. Animals

The eukaryotic expression vector pAV.ExBi-CMV-IE2-IRES-eGFP initiated by the CMV promoter was

constructed and then microinjected into a fertilized egg to ultimately obtain an F0 generation ul122 transgenic mouse model. Four ul122 mice (2 males and 2 females) stably expressing IE2 were obtained from the Laboratory of Pathogen Biology of Qingdao University and mated with four randomly selected C57BL/6 wild-type breeding mice under SPF conditions. The progeny were genotyped with PCR, and 20-24 week-old male ul122-positive and wild-type mice (15 per group) were selected for study. All animal experiments were approved by the Animal Experiments Committee of Qingdao University.

### 2.2. Isolation of spleen cells

Spleen immune cells were isolated as previously described (29), with some minor modifications. Briefly, the spleen was washed twice with PBS, minced with surgical scissors and then homogenized with a sterile 20-mL syringe plunger against a 75- $\mu$ m stainless steel mesh in 2 mL of RPMI-1640 medium (HyClone, Logan, UT, USA) supplemented with 10% fetal bovine serum (FBS, HyClone, Logan, UT, USA). The homogenate was then filtered through another 75- $\mu$ m mesh to obtain a single cell suspension, which was centrifuged at  $60 \times g$  for 1 min to remove any remaining debris. The cells were pelleted at  $480 \times g$  for 8 min and then suspended in red blood cell lysis buffer (Solarbio, Beijing, China) and incubated at room temperature for 5 min to lyse red blood cells. After addition of 1 mL of FBS, the cell pellets were centrifuged at  $480 \times g$  for 8 min at 8°C and washed twice with PBS.

### 2.3. Isolation of bone marrow cells

Bone marrow cells were isolated as previously described (30), with minor modifications. The mice were sacrificed by cervical dislocation and soaked in 75% alcohol for about 5 min. The femur and tibia were disarticulated, and the muscles and fascia were removed in a Petri dish containing PBS. The bones were washed with PBS and immersed in RPMI-1640 medium (HyClone, Logan, UT, USA) on ice. The ends of the bones were cut with scissors, and the medullary cavity was flushed with 5 mL of RPMI 1640 using a 25-gauge needle into a fresh Petri dish. The marrow was fragmented and filtered through a 75- $\mu$ m stainless steel mesh to obtain a single cell suspension.

### 2.4. DNA extraction and PCR

DNA was extracted from the tails of mice using the CWBIO Universal Genomic DNA Kit (lot: 50223) according to the manufacturer's instructions. The primers used for amplifying the HCMV IE2 gene are listed in Table 1. The reaction conditions were as follows: pre-denaturation at 95°C for 5 min followed by

**Table 1. The primers used for PCR and qPCR**

Gene	Forward (5'-3')	Reverse (5'-3')
PCR		
IE2	CCGCAAGAAGAAGAGCAAACG	CACCTGGTGCATACTGGGAAT
qPCR		
GRB2	CGGGACATAGAACAGATGCCAC	TGAAGTCTCCTCTGCGAAAGCC
IL-4	GGTCTCAACCCCAAGCTAGT	GCCGATGATCTCTCAAGTGAT
IFN- $\gamma$	GCCACGGCACAGTCATTGA	TGCTGATGGCCTGATTGTCTT
IL-13	TGAGCAACATCACACAAGACC	GGCCTTGGCGTTACAGAGG
TNF- $\alpha$	CAGGCGGTGCCTATGTCTC	CGATCACCCCGAAGTTCAGTAG
GAPDH	CATCACTGCCACCCAGAAGACTG	ATGCCAGTGAGCTTCCCGTTCAG
IE2	CCGCAAGAAGAAGAGCAAACG	CACCTGGTGCATACTGGGAAT

34 cycles of 95°C for 30 sec, 60°C for 35 sec, and 72°C for 35 sec, and final extension at 72°C for 10 min. The PCR products were identified using restriction enzyme digestion and sequence analysis.

### 2.5. Real-time PCR assay

Total RNA was extracted from the spleen and bone marrow using an RNA isolation kit (TIANGEN, Shanghai, China) and reverse transcribed using a reverse transcription kit (Roche, Indianapolis, IN, USA) according to the manufacturer's instructions. The cDNA transcripts (5  $\mu$ L) were mixed with 15  $\mu$ L of a PCR mixture (FastStart Essential DNA Green Master) and run for 40 cycles in a BIO-Rad iQ<sup>TM</sup>5 Instrument. The primers are listed in Table 1. The mRNA levels were normalized to GAPDH using the 2<sup>- $\Delta\Delta$ Ct</sup> method.

### 2.6. Western blotting

Proteins were extracted from the spleen and quantified using the BCA method. Equal amounts of protein per sample were resolved with 10% SDS-PAGE and transferred to a 0.45-mm nitrocellulose membrane (EMD Millipore, Billerica, MA, USA) for 1 h. The membranes were blocked with 5% skim milk for 2 h at room temperature and then incubated overnight with the specific primary antibodies [diluted 1:1,000 in 5% skim milk in TBST (10 mM Tris-HCl, pH 8.0, 150 mM NaCl, 0.15% Tween-20)] against GRB2 (ab32037; Abcam),  $\beta$ -Actin (bsm-33036M; Bioss Bioscience), and IE2 (MAB8131; Millipore). The membranes were washed and separately placed in secondary antibodies. The membranes of GRB2 and  $\beta$ -actin were placed in anti-mouse IgG-HRP (abs20001; Absin Bioscience), and the membrane of IE2 was placed in anti-rabbit IgG-HRP (abs20002; Absin Bioscience) (both diluted 1:2,000 in 5% skim milk in TBST) for 2 h at room temperature. After membranes were washed three times with TBST at room temperature, positive bands were developed using the SuperSignal West Pico Trial kit (Thermo Fisher Scientific, Inc.) and detected with the VilberLourmat imaging system (VilberLourmat, Marne-la-Vallée, France).

### 2.7. Phagocytosis assay

Neutral red uptake by macrophages was measured using the method described by Long *et al.* (31) with some modifications. Briefly, the macrophages were seeded on 96-well plates at a density of 1  $\times$  10<sup>6</sup> cells/well and incubated for 4 h at 37°C in a 5% CO<sub>2</sub> atmosphere. The medium was discarded, and then cells were washed with PBS, and 100  $\mu$ L of 0.1% filtered neutral red dye was added to each well. The cells were incubated with the dye for 2 h. The un-phagocytized neutral red was rinsed off with PBS, and then 200  $\mu$ L of cell lysis buffer (acetic acid/ethanol = 1:1, mL/mL) was added to each well. The cells were incubated overnight with the lysis buffer at 4°C, and the OD at 570 nm was measured.

### 2.8. Flow cytometry analysis

All antibodies and buffers were from Biolegend (San Diego, CA). The cells were suspended in the staining buffer at a density of 1  $\times$  10<sup>7</sup> cells/mL and incubated with TruStainfcX<sup>TM</sup> (anti-mouse cd16/32) to block non-specific Fc staining. One-hundred-microliter aliquots were dispensed in different tubes and incubated with FITC anti-mouse/human CD11b, PerCP/Cyanine5.5 anti-mouse F4/80, APC anti-mouse CD80, PE anti-mouse CD206 (MMR), APC Armenian Hamster IgG isotype control, PE Rat IgG2a, and  $\kappa$  isotype control as appropriate at room temperature for 30 min. The reaction was stopped by adding 2 mL of staining buffer per tube, and the cells were pelleted at 350 g for 5 min. After fixation with 0.5 mL of fixation buffer at room temperature for 20 min, the cells were again pelleted and re-suspended in 2 mL of intracellular staining perm wash buffer. After centrifugation at 350 g for 5 min, the previous step was repeated twice. The cells were then re-suspended in 0.1 mL of intracellular staining perm wash buffer, and the appropriate amount of anti-CD206 antibody or the corresponding control was added. The cells were incubated at room temperature for 30 min, diluted with 2 mL of intracellular staining perm wash buffer, and pelleted. The supernatant was discarded, 0.1 mL of cell staining buffer was added, and the stained cells were analyzed in the Cyto-FLex flow cytometer

(Beckman Coulter). The results were analyzed with the software FlowJo Version 10 (TreeStar).

### 2.9. Statistical analysis

All images were formatted for optimal presentation using Adobe Illustrator CS4 (Adobe Systems, Inc., San Jose, CA, USA). The Student's *t*-test was used to compare two groups, and one-way analysis of variance (ANOVA) followed by the Newman-Keuls post hoc test was used to compare multiple groups. All statistical analyses were performed using GraphPad Prism 7 (GraphPad Software, Inc., La Jolla, CA, USA).

## 3. Results

### 3.1. Verification of *UL122* genetically modified mice

The progeny of the transgenic and wild-type mice were genotyped with PCR. The genotyping results are shown in Figure 1 and in the supplementary results (supplementary Figure S1. <http://www.biosciencetrends.com/action/getSupplementalData.php?ID=50>). Based on the presence or absence of the *UL122* gene, the mice were divided into a control group and an experimental group.

### 3.2. Effect of *IE2* on macrophage count and phagocytic function

Macrophages play a key role in the antiviral immune response (32). To determine the effect of *IE2* on the relative proportion and phagocytic function of macrophages, macrophages from the experimental group and control group were compared. There were no significant differences in the total number of bone marrow macrophages (BMs) and spleen macrophages (SPMs) in the two groups (Figures 2A-2C). The production of macrophages is related to the production of single cells per mouse. Neutral red absorption was used to detect the phagocytic activity of the macrophages, and significantly higher phagocytic activity was noted in both spleen (Figure 2D,  $p < 0.01$ ) and bone marrow (Figure 2E,  $p < 0.05$ ) macrophages in *IE2*-expressing mice compared to that in the controls. Taken together, these findings indicate that *IE2* enhances the phagocytic function of macrophages.

### 3.3. *IE2* induces *M2* polarization

Immuno-typing of the SPMs and BMs revealed a significant increase in the proportion of *M2*-type SPMs in *IE2*-expressing mice compared to that in the controls, with a concomitant decrease in *M1*-type macrophages (Figures 3A and 3B). Thus, *IE2* induces the polarization of macrophages to the anti-inflammatory *M2* phenotype (Figures 3C-3E).

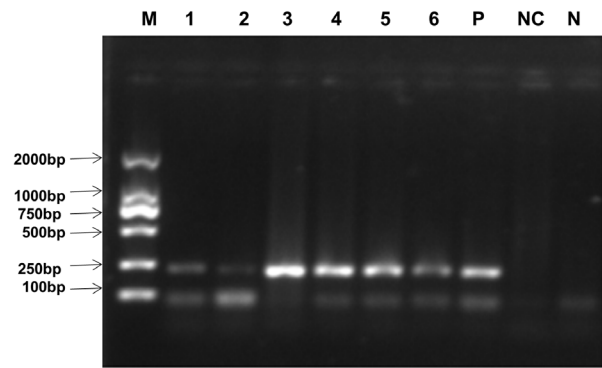


**Figure 1. Identification of *UL122*-positive and -negative mice with PCR.** Lanes 3-6 are positive and Lanes 1 and 2 negative for *UL122*. Lanes P, NC, and N are the positive control, water, and negative control, respectively. PCR product size = 229 bp.

### 3.4. *IE2* upregulates *GRB2* protein in *UL122* genetically modified mice

HCMV infection is known to upregulate *GRB2* in human cells (22). Consistent with this, levels of *GRB2* mRNA (Figures 4A and 4B) and protein (Figure 4C and 4D) were significantly up-regulated in the spleen and bone marrow of the transgenic mice compared to that in the wild-type control group.

### 3.5. Expression of mRNA of the polarization-related cytokines *IL-4*, *IFN- $\gamma$* , *IL-13*, and *TNF- $\alpha$*

To further confirm the polarizing effect of *IE2*, the levels of expression of *IL-4*, *IFN- $\gamma$* , *IL-13*, and *TNF- $\alpha$*  mRNA were evaluated in the spleen and bone marrow of the mice. While *IFN- $\gamma$*  and *TNF- $\alpha$*  activate *M1* macrophages, *IL-4* and *IL-13* are associated with *M2* polarization (33). As shown in Figure 5, *IL-4* and *IL-13* were both up-regulated in the *IE2*-expressing mice compared to the control group, with a significant increase in the level of *IL-4*.

## 4. Discussion

HCMV has developed several ways to evade the immune system, such as being phagocytosed by macrophages. As the first target of HCMV infection, they are essential for viral persistence and spread (34-37). *M1* and *M2* macrophages exhibit distinct phenotypes and functions. *M1* is the classic activated type, which functions in immune surveillance by secreting pro-inflammatory cytokines and chemokines and by presenting antigens to T cells. *M2* is an alternately activated type with weak antigen-presenting ability, and it plays an important role in immune tolerance by secreting inhibitory cytokines (38). HCMV infection polarizes a macrophage subpopulation to the *M1* type, which enables their migration from the blood into the tissues, thereby

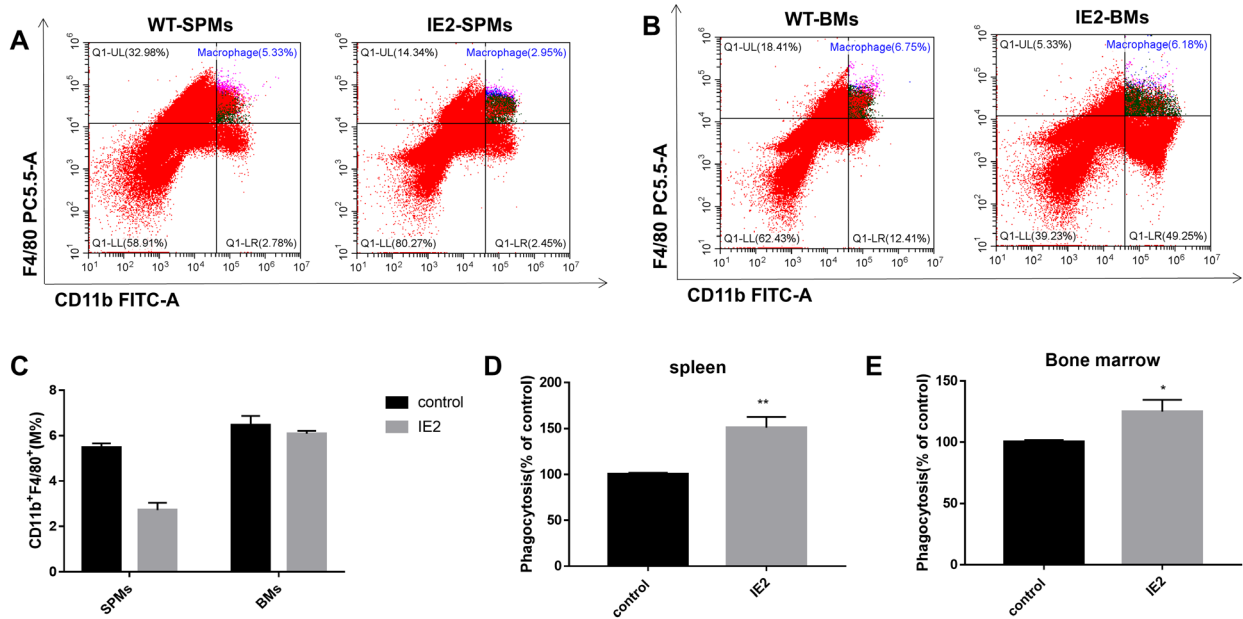


**Figure 2. Effect of IE2 on macrophage count and phagocytic function.** Representative FACS plots of total (A) SPMs and (B) BMs in the control group and IE2 mice. Bar graphs showing the number of macrophages (C) in the spleen and bone marrow. The phagocytic activity of (D) SPMs and (E) BMs in IE2 mice was higher than that in the control group. Data are expressed as the mean  $\pm$  SEM,  $n = 15$ . \* $p < 0.05$ , \*\* $p < 0.01$  vs. NC.

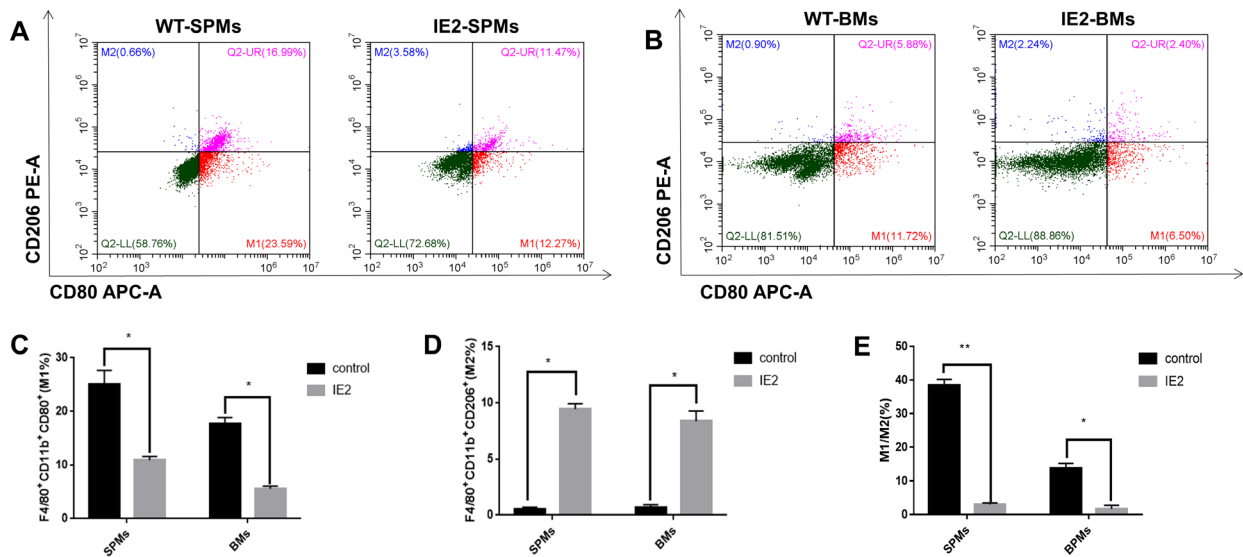


**Figure 3. HCMV IE2 leads to M2 polarization in both the spleen and bone marrow.** Representative FACS plots of M1 and M2 macrophages in the (A) spleen and (B) bone marrow. Bar graphs showing the number of (C) M1 macrophages and (D) M2 macrophages, and (E) M1/M2 ratios in the spleen and bone marrow. Data are expressed as the mean  $\pm$  SEM,  $n = 15$ . \* $p < 0.05$ , \*\* $p < 0.01$  vs. NC.

promoting viral transmission (39). In contrast, M2 macrophages allow long-term incubation of the virus and its reactivation in response to specific stimuli, and these macrophages are highly susceptible to HCMV infection (16,37).

Silencing of the IE2-encoding gene inhibits HCMV DNA replication and production of viral progeny, indicating that IE2 plays a major role in HCMV infection (40). Due to the high species specificity of

HCMV, studies of IE2 have been limited to *in vitro* models of infection. Use of ul122 overcomes species specificity and provides an effective way to study IE2 in macrophage-mediated immune changes. ul122 mice exhibited M2 polarization in their spleen and bone marrow, which is significant since the HCMV is known to evade the host immune response by promoting M2 polarization that enables long-term viral replication, survival, and transmission (20). In addition, HCMV also

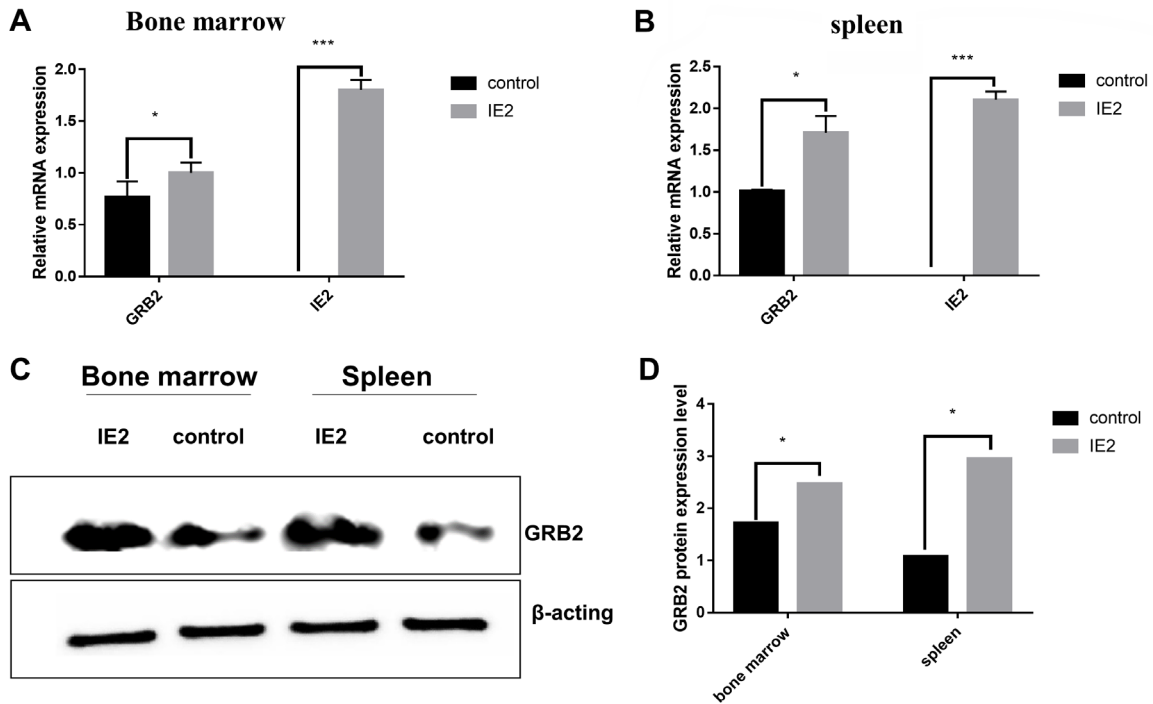


**Figure 4. GRB2 is upregulated in IE2-expressing mice.** Bar graph showing relative level of *grb2* mRNA in the (A) spleen and (B) bone marrow. (C). Immunoblots showing relative levels of GRB2 protein in IE2 mice. (D). Quantitative analysis of GRB2 protein levels in the IE2 group and control group. Data are expressed as the mean  $\pm$  SEM,  $n = 15$  mice per group, \* $p < 0.05$ ; \*\* $p < 0.01$ ; \*\*\* $p < 0.001$  vs. control group.

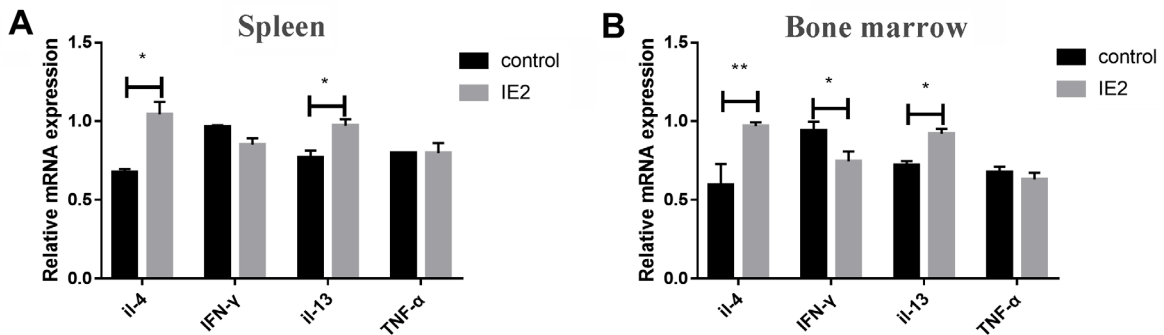


**Figure 5. IE2 modulates cytokines associated with macrophage polarization.** Bar graphs showing relative levels of IL-4, IFN- $\gamma$ , IL-13, and TNF- $\alpha$  mRNA in the (A) spleen and (B) bone marrow of the control group and IE2 mice. The qPCR data are normalized to GAPDH. Data are expressed as the mean  $\pm$  SEM,  $n = 15$  mice per group, \* $p < 0.05$ ; \*\* $p < 0.01$ ; \*\*\* $p < 0.001$  vs. control group.

interferes with the phagocytic function of macrophages *via* different mechanisms (41), and consistent with this increased phagocytic function of macrophages was noted in ul122 mice (Figures 2D and 2E). Taken together, these findings indicate that IE2 facilitates viral transmission and persistence in M2 macrophages, where they can be reactivated under specific conditions.

Previous studies have shown that GRB2 plays an important role in regulating macrophage differentiation, proliferation, phagocytosis, migration, adhesion, and invasion (21,24,42,43) and that silencing of *Grb2* disrupts phagocytosis (23). High levels of GRB2

expression and increased phagocytic activity were noted in the macrophages of IE2 mice, along with increased production of M2 cytokines such as IL-4 and IL-13. The binding of IL-4 to the IL-4 receptor recruits the p85 regulatory subunit of PI3K and GRB2, resulting in M2 polarization (44,45). Taken together, these findings indicate that IE2 significantly up-regulates GRB2 *via* increased production of M2-promoting IL-4, although the exact mechanism by which IE2-GRB2 mediates immune escape requires further investigation. The first step in viral infection is contact with the host cell and engulfment, which can enable long-term survival of

the virus in the host. Therefore, IE2 likely participates in long-term HCMV survival and latent infection by promoting GRB2-mediated macrophage polarization.

### Acknowledgements

The authors wish to thank the individuals who helped to make this study possible. This work was supported by the National Natural Science Foundation of China (81471958).

### References

- Nehme Z, Pasquereau S, Herbein G. Control of viral infections by epigenetic-targeted therapy. *Clin Epigenetics*. 2019; 11:55.
- Suarez NM, Musonda KG, Escriba E, Njenga M, Agbueze A, Camiolo S, Davison AJ, Gompels UA. Multiple-strain infections of human cytomegalovirus with high genomic diversity are common in breast milk from HIV-positive women in Zambia. *J Infect Dis*. 2019; 220:792-801.
- Buxmann H, Hamprecht K, Meyer-Wittkopf M, Friese K. Primary human cytomegalovirus (HCMV) infection in pregnancy. *Dtsch Arztebl Int*. 2017; 114:45-52.
- Becker T, Le-Trilling VTK, Trilling M. Cellular cullin RING ubiquitin ligases: Druggable host dependency factors of cytomegaloviruses. *Int J Mol Sci*. 2019; 20. DOI: 10.3390/ijms20071636
- Choi HJ, Park A, Kang S, Lee E, Lee TA, Ra EA, Lee J, Lee S, Park B. Human cytomegalovirus-encoded US9 targets MAVS and STING signaling to evade type I interferon immune responses. *Nat Commun*. 2018; 9:125.
- Luganini A, Terlizzi ME, Griboaud G. Bioactive molecules released from cells infected with the human cytomegalovirus. *Front Microbiol*. 2016; 7:715.
- Harkins LE, Matlaf LA, Soroceanu L, Klemm K, Britt WJ, Wang W, Bland KI, Cobbs CS. Detection of human cytomegalovirus in normal and neoplastic breast epithelium. *Herpesviridae*. 2010; 1:8.
- Chen HP, Jiang JK, Chen CY, Chou TY, Chen YC, Chang YT, Lin SF, Chan CH, Yang CY, Lin CH, Lin JK, Cho WL, Chan YJ. Human cytomegalovirus preferentially infects the neoplastic epithelium of colorectal cancer: A quantitative and histological analysis. *J Clin Virol*. 2012; 54:240-244.
- Samanta M, Harkins L, Klemm K, Britt WJ, Cobbs CS. High prevalence of human cytomegalovirus in prostatic intraepithelial neoplasia and prostatic carcinoma. *J Urol*. 2003; 170:998-1002.
- Melnick M, Sedghizadeh PP, Allen CM, Jaskoll T. Human cytomegalovirus and mucoepidermoid carcinoma of salivary glands: Cell-specific localization of active viral and oncogenic signaling proteins is confirmatory of a causal relationship. *Exp Mol Pathol*. 2012; 92:118-125.
- Rahbar A, Orrego A, Peredo I, Dzabic M, Wolmer-Solberg N, Straat K, Stragliotto G, Soderberg-Naucler C. Human cytomegalovirus infection levels in glioblastoma multiforme are of prognostic value for survival. *J Clin Virol*. 2013; 57:36-42.
- Krishna BA, Humby MS, Miller WE, O'Connor CM. Human cytomegalovirus G protein-coupled receptor US28 promotes latency by attenuating c-fos. *Proc Natl Acad Sci U S A*. 2019; 116:1755-1764.
- Nogalski MT, Collins-McMillen D, Yurochko AD. Overview of human cytomegalovirus pathogenesis. *Methods Mol Biol*. 2014; 1119:15-28.
- Hume DA, Ross IL, Himes SR, Sasmono RT, Wells CA, Ravasi T. The mononuclear phagocyte system revisited. *J Leukoc Biol*. 2002; 72:621-627.
- Barber GN. Host defense, viruses and apoptosis. *Cell Death Differ*. 2001; 8:113-126.
- Nikitina E, Larionova I, Choinzonov E, Kzhyshkowska J. Monocytes and macrophages as viral targets and reservoirs. *Int J Mol Sci*. 2018; 19. DOI: 10.3390/ijms19092821
- Xue N, Zhou Q, Ji M, Jin J, Lai F, Chen J, Zhang M, Jia J, Yang H, Zhang J, Li W, Jiang J, Chen X. Chlorogenic acid inhibits glioblastoma growth through repolarizing macrophage from M2 to M1 phenotype. *Sci Rep*. 2017; 7:39011.
- Herbein G, Varin A. The macrophage in HIV-1 infection: From activation to deactivation? *Retrovirology*. 2010; 7:33.
- Kerr MC, Teasdale RD. Defining macropinocytosis. *Traffic*. 2009; 10:364-371.
- Stevenson EV, Collins-McMillen D, Kim JH, Cieply SJ, Bentz GL, Yurochko AD. HCMV reprogramming of infected monocyte survival and differentiation: A Goldilocks phenomenon. *Viruses*. 2014; 6:782-807.
- Haidar M, Whitworth J, Noe G, Liu WQ, Vidal M, Langley G. TGF-beta2 induces Grb2 to recruit PI3-K to TGF-RII that activates JNK/AP-1-signaling and augments invasiveness of Theileria-transformed macrophages. *Sci Rep*. 2015; 5:15688.
- Cavignac Y, Lieber D, Laib Sampaio K, Madlung J, Lamkemeyer T, Jahn G, Nordheim A, Sinzger C. The cellular proteins Grb2 and DDX3 are increased upon human cytomegalovirus infection and act in a proviral fashion. *PLoS One*. 2015; 10:e0131614.
- Kantonen S, Hatton N, Mahankali M, Henkels KM, Park H, Cox D, Gomez-Cambronero J. A novel phospholipase D2-Grb2-WASp heterotrimer regulates leukocyte phagocytosis in a two-step mechanism. *Mol Cell Biol*. 2011; 31:4524-4537.
- Rajaram MVS, Arnett E, Azad AK, Guirado E, Ni B, Gerberick AD, He LZ, Keler T, Thomas LJ, Lafuse WP, Schlesinger LS. M. tuberculosis-initiated human mannose receptor signaling regulates macrophage recognition and vesicle trafficking by FcRgamma-chain, Grb2, and SHP-1. *Cell Rep*. 2017; 21:126-140.
- Knapek K, Frondorf K, Post J, Short S, Cox D, Gomez-Cambronero J. The molecular basis of phospholipase D2-induced chemotaxis: Elucidation of differential pathways in macrophages and fibroblasts. *Mol Cell Biol*. 2010; 30:4492-4506.
- Heilingloh CS, Grosche L, Kummer M, Muhl-Zurbes P, Kamm L, Scherer M, Latzko M, Stamminger T, Steinkasserer A. The major immediate-early protein IE2 of human cytomegalovirus is sufficient to induce proteasomal degradation of CD83 on mature dendritic cells. *Front Microbiol*. 2017; 8:119.
- Arend KC, Lenarcic EM, Moorman NJ. The 5' untranslated region of the major immediate early mRNA is necessary for efficient human cytomegalovirus replication. *J Virol*. 2018; 92. DOI: 10.1128/JVI.02128-17
- Paulus C, Nevels M. The human cytomegalovirus major

- immediate-early proteins as antagonists of intrinsic and innate antiviral host responses. *Viruses*. 2009; 1:760-779.
29. Liang Q, Liu Z, Zhu C, Wang B, Liu X, Yang Y, Lv X, Mu H, Wang K. Intrahepatic T-cell receptor beta immune repertoire is essential for liver regeneration. *Hepatology*. 2018; 68:1977-1990.
  30. Anzinger JJ, Chang J, Xu Q, Barthwal MK, Bohnacker T, Wymann MP, Kruth HS. Murine bone marrow-derived macrophages differentiated with GM-CSF become foam cells by PI3Kgamma-dependent fluid-phase pinocytosis of native LDL. *J Lipid Res*. 2012; 53:34-42.
  31. Long F, Wang YX, Liu L, Zhou J, Cui RY, Jiang CL. Rapid nongenomic inhibitory effects of glucocorticoids on phagocytosis and superoxide anion production by macrophages. *Steroids*. 2005; 70:55-61.
  32. Hance MA, Blackhart G, Dew M. Free to be me: The relationship between the true self, rejection sensitivity, and use of online dating sites. *J Soc Psychol*. 2018; 158:421-429.
  33. Koh YC, Yang G, Lai CS, Weerawatanakorn M, Pan MH. Chemopreventive effects of phytochemicals and medicines on M1/M2 polarized macrophage role in inflammation-related diseases. *Int J Mol Sci*. 2018; 19. DOI: 10.3390/ijms19082208
  34. Davis-Poynter NJ, Farrell HE. Masters of deception: A review of herpesvirus immune evasion strategies. *Immunol Cell Biol*. 1996; 74:513-522.
  35. Moore PS, Boshoff C, Weiss RA, Chang Y. Molecular mimicry of human cytokine and cytokine response pathway genes by KSHV. *Science*. 1996; 274:1739-1744.
  36. Smith GL. Virus proteins that bind cytokines, chemokines or interferons. *Curr Opin Immunol*. 1996; 8:467-471.
  37. Bayer C, Varani S, Wang L, Walther P, Zhou S, Straschewski S, Bachem M, Soderberg-Naucler C, Mertens T, Frascaroli G. Human cytomegalovirus infection of M1 and M2 macrophages triggers inflammation and autologous T-cell proliferation. *J Virol*. 2013; 87:67-79.
  38. Mosser DM, Edwards JP. Exploring the full spectrum of macrophage activation. *Nat Rev Immunol*. 2008; 8:958-969.
  39. Chan G, Bivins-Smith ER, Smith MS, Smith PM, Yurochko AD. Transcriptome analysis reveals human cytomegalovirus reprograms monocyte differentiation toward an M1 macrophage. *J Immunol*. 2008; 181:698-711.
  40. Bai Z, Li L, Wang B, Liu Z, Liu H, Jiang G, Wang H, Yan Z, Qian D, Ding S, Song X. Inhibition of human cytomegalovirus infection by IE86-specific short hairpin RNA-mediated RNA interference. *Biosci Biotechnol Biochem*. 2010; 74:1368-1372.
  41. Lin YL, Li M. Human cytomegalovirus and Epstein-Barr virus inhibit oral bacteria-induced macrophage activation and phagocytosis. *Oral Microbiol Immunol*. 2009; 24:243-248.
  42. Avila-Campos MJ, de Carvalho MA, Veiga-Damasceno CA, Osorio-Cisalpio E. In vitro activity of two beta-lactam antibiotics against strains of the *Bacteroides fragilis* group isolated from humans and from *Callithrix penicillata* marmosets. *Rev Latinoam Microbiol*. 1994; 36:159-162.
  43. Proctor BM, Ren J, Chen Z, Schneider JG, Coleman T, Lupu TS, Semenkovich CF, Muslin AJ. Grb2 is required for atherosclerotic lesion formation. *Arterioscler Thromb Vasc Biol*. 2007; 27:1361-1367.
  44. McCormick SM, Gowda N, Fang JX, Heller NM. Suppressor of cytokine signaling (SOCS) 1 regulates interleukin-4 (IL-4)-activated insulin receptor substrate (IRS)-2 tyrosine phosphorylation in monocytes and macrophages *via* the proteasome. *J Biol Chem*. 2016; 291:20574-20587.
  45. Heller NM, Qi X, Junttila IS, Shirey KA, Vogel SN, Paul WE, Keegan AD. Type I IL-4Rs selectively activate IRS-2 to induce target gene expression in macrophages. *Sci Signal*. 2008; 1:ra17.

(Received July 27, 2019; Revised September 29, 2019; Accepted October 28, 2019)

# A multiplex loop-mediated isothermal amplification assay for rapid detection of *Bacillus cereus* and *Staphylococcus aureus*

Yanglong Deng<sup>1</sup>, Yanquan Liu<sup>2</sup>, Zubin Jiang<sup>3</sup>, Jingxin Wang<sup>4</sup>, Qing Zhang<sup>1</sup>, Yeqian Qian<sup>1</sup>, Yuan Yuan<sup>1</sup>, Xiangyu Zhou<sup>1</sup>, Guiling Fan<sup>1</sup>, Yufeng Li<sup>1,\*</sup>

<sup>1</sup> School of Food and Bioengineering, Xihua University, Chengdu, Sichuan, China;

<sup>2</sup> College of Life and Geographic Sciences, Kashi University, Kashi, Xinjiang, China;

<sup>3</sup> Culinary school, Sichuan Tourism University, Chengdu, Sichuan, China;

<sup>4</sup> School of Materials and Environmental Protection, Chengdu Textile College, Chengdu, Sichuan, China.

## Summary

*Bacillus cereus* (*B. cereus*) and *Staphylococcus aureus* (*S. aureus*) are major human food-borne pathogens that may produce a variety of toxins and cause diarrhea, food poisoning, and even death. In order to monitor and prevent the spread of these pathogens, a multiplex loop-mediated isothermal amplification (multi-LAMP) assay was developed to simultaneously and rapidly detect *B. cereus* and *S. aureus*. The sensitivity and specificity of the loop-mediated isothermal amplification (LAMP) reactions were determined via electrophoresis. The multi-LAMP showed 100% inclusivity and exclusivity, the sensitivity was 10 fg/ $\mu$ L and was 10 times more sensitive than that of polymerase chain reaction (PCR), the results were consistent with those of conventional PCR assay, and the entire assay should be finished within 40 min. This multi-LAMP assay was confirmed as a rapid and reliable diagnostic technique upon application for clinical samples and food samples. To our knowledge, this is the first study to report the application of multi-LAMP to detect *B. cereus* and *S. aureus*.

**Keywords:** Multi-LAMP, *Bacillus cereus*, *Staphylococcus aureus*, pathogen, rapid detection

## 1. Introduction

*Bacillus cereus* (*B. cereus*) and *Staphylococcus aureus* (*S. aureus*) are the most common causes of foodborne pathogens in developed and developing countries. In the United States, during 2009-2015, Foodborne Disease Outbreak Surveillance System (FDOSS) received reports of 5,760 outbreaks that resulted in 100,939 illnesses, 5,699 hospitalizations, and 145 deaths (1). 1,229 food-borne outbreaks caused by *B. cereus* and *S. aureus* were reported; 39% were reported with a confirmed etiology. Vomiting was commonly reported in *B. cereus* (median, 75% of cases) and *S. aureus* outbreaks (median, 87%) (2). At the same time, China, Japan, South Korea and other

countries had also reported the outbreak of foodborne epidemics (3,4). Rice or soy dishes were commonly implicated in *B. cereus* (50%) outbreaks, and meat or poultry dishes were commonly implicated in *S. aureus* (55%) outbreaks (5). These pathogens cause illness through preformed toxin production in improperly handled foods or in vivo toxin production within the gastrointestinal tract after consumption of a contaminated food (6,7). Therefore, the development of a rapid and ready-to-use method for simultaneous detection of these pathogens is of great importance to improve food safety and protect human health.

Many methods have been developed to detect *B. cereus* and *S. aureus*, including convention culture-based, immunology-based, and molecular methods (8,9). Conventional culture-based methods are safe and simple and Cost efficiency, but time-consuming. Immunology-based assay, including enzyme-linked immunosorbent and immunofluorescence, are fast but not very effective in terms of sensitivity (10). Molecular methods such as PCR and nucleic acid probe technology, Which are rapidity, sensitivity and

Released online in J-STAGE as advance publication December 17, 2019.

\*Address correspondence to:

Dr. Yufeng Li, School of Food and Bioengineering, Xihua University, Road Jinzou, No.999, Chengdu, Sichuan Province, China.

E-mail: griffinyang123@yahoo.com

specificity, however, the instruments used in these methods are expensive and profession (11,12).

The LAMP technique is a novel constant-temperature nucleic acid amplification technique invented by Japanese scholars in 2000 with high sensitivity, specificity, and rapidity for the low-cost detection of pathogens (13-17). Song found that a loop-mediated isothermal amplification (LAMP) method for detecting *Shigella* and enteroinvasive *Escherichia coli*, the LAMP method efficiently detected the gene within 2 h at a minimal amount of bacteria (8 CFU) per reaction (18). Wan selected the heat-labile enterotoxin gene to design LAMP primers, optimized the reaction conditions of LAMP, and examined the specificity and sensitivity of the method (19). All the related reports did not study the *B. cereus* and *S. aureus*, and the LAMP assay can only detect a gene in a single reaction. In the present study, a multi-LAMP assay was developed to simultaneously detect *B. cereus* and *S. aureus*. The aim of this study is to establish a rapid and low-cost method for detecting *B. cereus* and *S. aureus*, and getting a better understanding of the distinguishing epidemiologic and clinical characteristics of outbreaks caused by these pathogens, it will help investigators determine which one pathogen was the likely cause.

## 2. Materials and Methods

### 2.1. Bacterial strains

11 bacterial strains were used in the present study (Table 1). They were cultured for 24-48 h at 37°C in nutrient broth. *B. cereus* and *S. aureus* were used as standard strains to develop the multi-LAMP assay.

### 2.2. DNA extraction

DNA from 11 compared strains used in this study was extracted according to DNA purification Kit (Shanghai Weijie Biological Engineering Co., Ltd., Shanghai, China). The DNA extracted was used as template in the later assay determining the optimum reaction conditions and analyzing the specificity of multi-LAMP in detecting two goal strains.

Use the bacterial genomic DNA extraction kit, follow the instructions in the instructions: 1.5 mL of the bacterial solution, centrifuge (Tabletop refrigerated centrifuge, Thermo Fisher Scientific, Chengdu, Sichuan Province, China), add buffer GA suspension, 37°C for 30 min, add 20 µL of proteinase K and mix well into 220 µL buffer GB, mix well, Warm bath at 70°C for 30 min. 220 µg of absolute ethanol was added, mix well, transfer to the adsorption column CB3, centrifuge, add 500 µL buffer GD and centrifuged at 10,000g for 2 min. 600 µL of the rinse solution PW was added to the adsorption column, centrifuged, and finally 75 µL of the elution buffer TE was added to the collection tube to extract

**Table 1. Bacterial strains used in the present study and their sources**

No	Bacterial species	Source
1	<i>Listeria monocytogenes</i> :1.4255	CDCP
2	<i>Escherichia coli</i> :1.2574	CDCP
3	<i>Salmonella enteritidis</i> :50040	CGMCC
4	<i>Listeria ivanovii</i> :1527	CDCP
5	<i>Lactobacillus delbrueckii subsp</i> :50040	CDCP
6	<i>Saccharomyces cerevisiae</i> :1.10599	CDCP
7	Enteroinvasive <i>E.coli</i> :ATCC44338	CGMCC
8	<i>Shigella flexneri</i> :1.1059	CDCP
9	Enterotoxingenic <i>E.coli</i> :44274	CGMCC
10	<i>Bacillus cereus</i> :NC7401	CGMCC
11	<i>Staphylococcus aureus</i> : 1.6739	CDCP

CDCP, Sichuan Center for Disease Control and Prevention, CGMCC, China General Microbiological Culture Collection Center.

the genomic DNA of the bacteria. The DNA of the extracted strain was detected by electrophoresis on a 0.7% agarosegel (DYY-8B type steady current electrophoresis instrument, Liuyi Instrument Factory, Beijing, China).

### 2.3. LAMP primer design

The result of comparison of similar strain sequences in the Gene Bank database showed that the *nhe* and *nuc* genes are well conserved. Then the LAMP primers (Shanghai Shenggong Company, Shanghai, China) were designed on the website (<http://primerexplorer.jp/e/>). According to the characteristics of LAMP primer design, two groups of LAMP primers were selected, including external primers F3 and B3, internal primers FIP and BIP, as shown in Table 2.

### 2.4. Optimization of LAMP reaction system

The reaction system of LAMP was optimized. First determine the composition of the 25 µL reaction system: 10 × Thermopol Buffer 2.5 µL Betaine (4 mol/L) 5 µL; four primers each (F3:B3:FIP:BIP = 5:5:40:40, µmol/L) 2 µL; Bst DNA polymerase large fragment (8 U) 1 µL; dNTPs (10 mmol/L) 4 µL; MgSO<sub>4</sub> (100 mmol/L) 1.5 µL; template 1 µL; sterile deionization 2 µL of water.

The following changes were attempted in the reaction to optimize the clearness of strips. (i) Optimization of amount of Mg<sup>2+</sup> addition amounts were increased progressively from 1.3 µL to 1.7 µL *i.e.*, 1.3, 1.5, 1.6, 1.7 µL; (ii) the temperatures were increased from 58°C to 64°C, *i.e.* 58, 60, 62, 64°C, (iii) the concentrations of primer were increased from 1.8 µL to 2.4 µL, *i.e.*, 1.8, 2.0, 2.2, 2.4 µL. According to the principle of the same amplification efficiency of the two LAMP systems, the 25 µL multiple LAMP reaction conditions were finally determined.

### 2.5. Specificity of multi-LAMP assay

All 9 bacterial strains in Table 1 were used as templates

**Table 2. LAMP primers used in this study to detect *B. cereus* and *S. aureus***

Target genes	Primer name	Sequence(5'-3')
<i>B. cereus</i>	CES-F3	AACAGTATATAGTGCAACTTCAA
	CES-B3	CTTTGTCAAACCTCGACTTCAA
	CES-FIP	TGTCATTGGTTGACCTTTGTACATT-AAAATTACATAAAGAACCTGCGA
	CES-BIP	GTTGATACACCTGAAACAAGCATC-ATTTTTTCGTAAATGCACTTGC
<i>S. aureus</i>	SEA-F3	CGATTGATGGTGCGGTTA
	SEA-B3	CAGTTCTTTGACCTTTGTCA
	SEA-FIP	TGCTTTGTTTCAGGTGTATCAACCA
		TTAATGTACAAAGGTCAACC
	SEA-BIP	AAGGTGTAGAGAAATATGGTACTGAT CGACTTCAATTTCTTTGCA

**Table 3. PCR primer for detecting *B. cereus* and *S. aureus***

Primer name	Sequence(5'-3')	Ref.
CES-F	CGCCGAAAGTGATTATACCAA	(23)
CES-R	TATGCCCGTTCTCAAACCTG	(23)
CES-P	GGGAAAATAACGAGAAATGCA	(23)
SEA-F	AAAATACAGTACCTTTGGAAACGGTT	(23)
SEA-R	TTTCCTGTAAATAACGTCTTGCTTGA	(23)
SEA-P	AACGAATAAGAAAAATGTAACCTG TTCAGGAGTTGGATC	(23)

to determine the specificity of multiplex LAMP reaction. Two sets of primers were added to the optimized reaction system (25 µL), and the LAMP detection was carried out by using the genomic DNAs of the two strains and the non-target strains as templates. The results were detected by agarose gel electrophoresis, to verify the accuracy and specificity of the method for detecting *B. cereus* and *S. aureus*.

**2.6. Sensitivity of multi-LAMP assay**

The DNA template (100 ng/µL) of the pathogenic bacteria *B. cereus* and *S. aureus* was diluted 10-fold to 100-10<sup>-7</sup> times to 1 fg/µL, and multiplex LAMP amplification was performed to detect the reaction. The multiple LAMP experiment was repeated 2 times, LAMP products were subjected to electrophoresis on 2.0% agarose gel.

**2.7. PCR assay**

A PCR assay was performed to compare its sensitivity and the clinical detection rates with those of the LAMP assay. Each plasmid sample was amplified in 20 µL reaction mixtures containing 10 µL PCR Master Mix (Tiangen Biotech Co., Ltd., Beijing, People's Republic of China), 400 pM primers (Table 3), and 1 µL DNA template. The cycling conditions were as follows: 3 mins at 95°C; 30 cycles of 30 s at 95°C, 30 s at 55°C, and 30 s at 72°C; 5mins at 72°C. The PCR products were analyzed electro-phonetically on a 2% agarose gel (13).

**3. Results**

**3.1. Optimization of LAMP reaction system**

The three reaction conditions of Mg<sup>2+</sup> concentration, temperature and primer concentration were optimized. The results of LAMP reaction of *B. cereus* were detected by 0.5% agarose gel electrophoresis (Figure 1). It can be known from the specific ladder strips in the group diagram of Figure 1 that the LAMP reaction was ideal, and the designed primer for the *nhe* gene can specifically and accurately identify the *B. cereus*. From Figure 1A, 25 µL of LAMP reaction system can be obtained, and the optimum amount of MgSO<sub>4</sub> is 1.5 µL. From Figure 1B, the optimum temperature was 60°C, and the optimal concentration of primers is 2.0 µL from Figure 1C. The LAMP reaction system was optimized based on the LAMP amplification assay of *B. cereus*, and the determination of amplification conditions laid the foundation for further identification of two pathogenic bacteria by multi-LAMP.

**3.2. Specificity of multi-LAMP**

The two pathogenic bacteria *B. cereus* and *S. aureus* were specifically detected by multiple LAMP, and the results are shown in Figure 2. It can be seen from Figure 2 that the pathogenic bacteria *B. cereus* and *S. aureus* bands in the LAMP amplification result was positive. The other 9 strains (1 to 9 in Figure 2) was negative. Comparing the blanks in 0, the positive results were accurate. It was indicated that the *B. cereus* and *S. aureus*, which were detected by multi-LAMP, were successful, and the reaction was rapid, simple and specific, which provided a basis for rapid detection of food pathogenic bacteria.

**3.3. Sensitivity of multiple LAMP and PCR assays**

The template concentration of the pathogens were 10-fold gradient dilution from 10 ng/µL DNA to 10<sup>-7</sup> times (1 fg/µL), and the electrophoresis results were shown in Figure 3. It can be seen from Figure 3 that the multiple

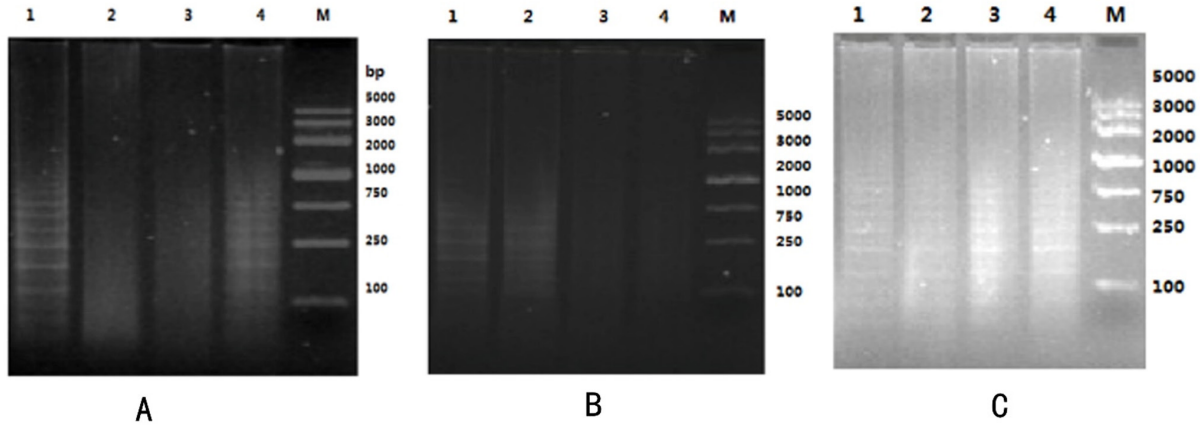


**Figure 1. Electrophoresis of LAMP products.** M indicates DL 2000 DNA Marker, 1~4 in A indicates 1.3, 1.5, 1.6, 1.7  $\mu\text{L}$  of  $\text{MgSO}_4$ , 1~4 amplification temperature in B is 58°C, 60°C, 62°C, 64°C, 1~4 primer in C Concentrations 1.8, 2.0, 2.2, 2.4  $\mu\text{L}$ .

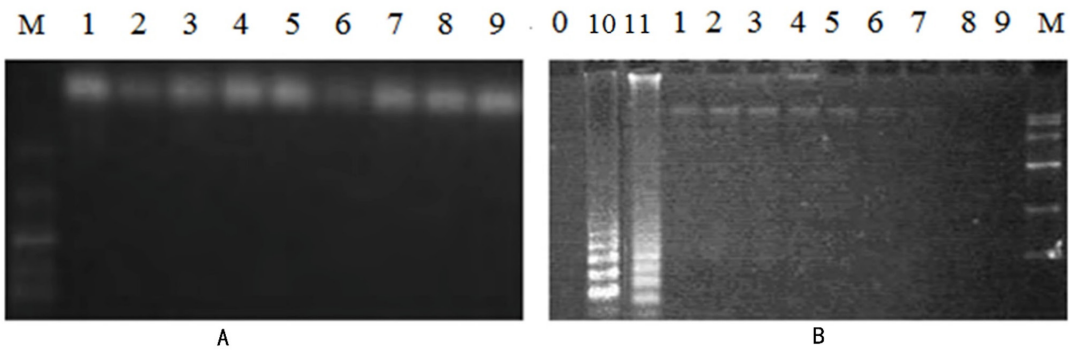


**Figure 2. Detection specificity of LAMP reaction for strain.** M in A indicates DL 2000 DNA Marker, 1~9 corresponds to the positive plasmid of 9 strains in sequence; 0 in B is blank control, 10 indicates *B. cereus*, 11 indicates *S. aureus*, 1~9 indicates 9 strains, M indicates DL 2000 DNA Marker.

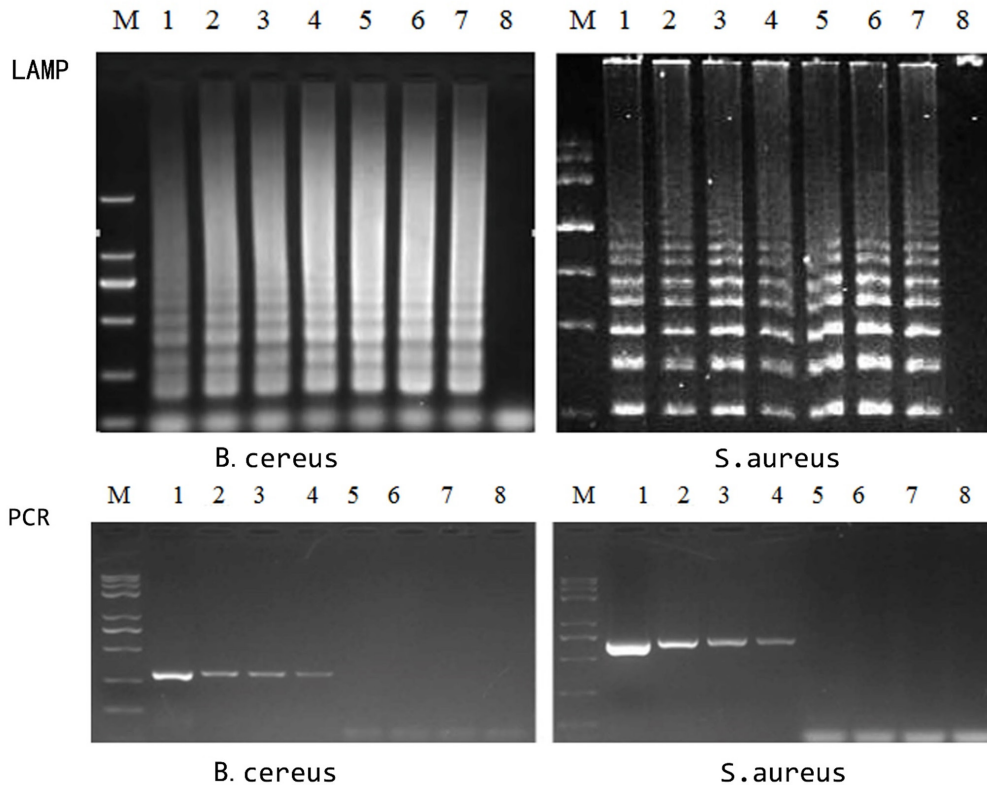


**Figure 3. The sensitivity of LAMP and PCR assays.** M indicates DNA Marker, 1~8 is the DNA template mass concentration 10, 1  $\text{ng}/\mu\text{L}$ ; 100, 10, 1  $\text{fg}/\mu\text{L}$ .

LAMP sensitivity detection is ideal, and the 10-fold gradient dilution of the two bacterial DNA templates to  $10^{-6}$  times (10 fg/ $\mu$ L) can still enlarge the clear ladder-like strips, while the dilution is not detected at a low concentration of  $10^{-7}$  times (1 fg/ $\mu$ L). Simultaneously, the bacterial samples were also subjected to traditional PCR. It was found that the sensitivity of the multiple LAMP amplification detection of pathogens in the experiment was 10 times higher than that of PCR.

#### 4. Discussion

The multiple LAMP reaction was used to detect the two pathogenic bacteria. In the experiment, two sets of primers were able to specifically amplify, indicated that the primers were specific. The sensitivity of the multiple LAMP reaction to identify pathogenic bacteria was also high, (reaching 10 fg/ $\mu$ L), which is higher than the sensitivity of 0.2 ng/L in the pistachio DNA detected by Liu and Huang (20). Simultaneously, we compared the sensitivity of LAMP with that of traditional PCR analysis, reporting that the detection limit of the LAMP assay was 10-fold that of conventional PCR analysis, and the results of LAMP being consistent with those of conventional PCR analyses (21). It shows that this method can identify food samples contaminating pathogens quickly, conveniently and accurately. Compared with traditional PCR, the present method exhibited the following advantages: 1) high specificity and sensitivity and ease of operation; 2) multiplex detections of genes using the same detection system, thus reducing manual operation; 3) a total operating time of < 40 min, as opposed to 90 min to detect via conventional PCR analysis; 4) greater user-friendliness than conventional PCR analysis, with no requirement of specialized instruments and complicated operations.

This experiment only uses a simple agarose gel electrophoresis test to obtain an ideal positive test result. However, the LAMP reaction only has negative and positive results. It is prone to false positives during the experiment, and the detection sensitivity is too high and it is easy to cause pollution, which has a great impact on the results. Therefore, it is necessary to pay attention to the addition of multiple LAMP reagents of different species in different rooms and places, personnel exchange to avoid contamination and false positives, and the length of the reaction target sequence is controlled below 300 bp, once non-specific amplification occurs, not easy to identify (22). If these deficiencies of LAMP are further improved and improved, the potential of multiple LAMP in food and sanitation identification of pathogenic bacteria can be made even greater.

#### Acknowledgements

This work was supported by a grant (Innovation project

of science and technology, Sichuan Province, China. No. 12205484) We thank Dr.Yongxin Li of The Sichuan University for her useful suggestions and ideas.

#### References

- Dewey-Mattia D, Manikonda K, Hall AJ, Wise ME, Crowe SJ. Surveillance for Foodborne Disease Outbreaks – United States, 2009-2015. MMWR Surveill Summ. 2018; 67:1-11.
- Bennett SD, Walsh KA, Gould LH. Foodborne disease outbreaks caused by *Bacillus cereus*, *Clostridium perfringens*, and *Staphylococcus aureus* – United States. 1998-2008. Clin Infect Dis. 2013; 57:425-433.
- Wu G, Yuan Q, Wang L, Zhao J, Chu Z, Zhuang M, Zhang Y, Wang K, Xiao P, Liu Y, Du Z. Epidemiology of foodborne disease outbreaks from 2011 to 2016 in Shandong Province, China. Medicine. Medicine (Baltimore). 2018; 97:e13142.
- Lee MJ, Song KY, Chang LW, Cheon JH, Sook KH, Jeong J, BAE D, Seo GH. Epidemiological aspects of pathogenic microbial foodborne disease outbreaks in Korea and Japan from 2011 to 2015. J Prev Vet Med. 2019; 43:62-67.
- Ke BX, He DM, Tan HL, Zeng HH, Yang T, Li BS, Liang Y H, Lu LL, Liang JH, Huang Q, Ke CW. Active etiological surveillance for foodborne diseases in Guangdong province, 2013-2014. Zhonghua Liu Xing Bing Xue Za Zhi. 2016; 37:1373-1378.
- Stefano Z, Marina B. Growth of *Staphylococcus aureus* and enterotoxin production in fresh egg pasta. J Food Process Preserv. 2018; 42:37-53.
- Pexara A, Govaris A. *Bacillus cereus*: an important foodborne pathogen. J Hellenic Vet Med Soc. 2018; 61:127-133.
- Law JW, Ab Mutalib NS, Chan KG, Lee LH. Rapid methods for the detection of foodborne bacterial pathogens: Principles, applications, advantages and limitations. Front Microbiol. 2014; 5:1-19.
- Zhao X, Lin CW, Wang J, Oh DH. Advances in rapid detection methods for foodborne pathogens. J Microbiol Biotechnol. 2014; 24:297-312.
- Kim HJ, Cho JC. Rapid and sensitive detection of *Listeria monocytogenes* using a PCR-Enzymelinked immunosorbent assay. J Microbiol Biotechnol. 2008; 18:1858-1861.
- Arunrut N, Kiatpathomchai W, Ananchaipattana C. Multiplex PCR assay and lyophilization for detection of *Salmonella* spp. *Staphylococcus aureus* and *Bacillus cereus* in pork products. Food Sci Biotechnol. 2018; 27:867-875.
- Chiang YC, Tsen HY, Chen HY, Chang YH, Lin CK, Chen CY, Pai WY. Multiplex PCR and a chromogenic DNA macroarray for the detection of *Listeria monocytogenes*, *Staphylococcus aureus*, *Streptococcus agalactiae*, *Enterobacter sakazakii*, *Escherichia coli* O157:H7, *Vibrio parahaemolyticus*, *Salmonella* spp. and *Pseudomonas fluoresc.* J Microbiol Methods. 2012; 88:110-116.
- Zhong LL, Zhou Q, Tan CY, Roberts AP, El-Sayed Ahmed MAE, Chen G, Dai M, Yang F, Xia Y, Liao K, Liang Y, Yang Y, Feng S, Zheng X, Tian GB. Multiplex loop-mediated isothermal amplification (multi-LAMP) assay for rapid detection of *mcr-1* to *mcr-5* in colistin-

- resistant bacteria. *Infect Drug Resist.* 2019; 12:1877-1887.
14. Niessen L, Luo J, Denschlag C, Vogel RF. The application of loop-mediated isothermal amplification (LAMP) in food testing for bacterial pathogens and fungal contaminants. *Food Microbiol.* 2013; 36:191-206.
  15. Sul SY, Kim MJ, Kim HY. Development of a direct loop-mediated isothermal amplification (LAMP) assay for rapid and simple on-site detection of chicken in processed meat products. *Food Control.* 2018; 98:194-199.
  16. Wachiralurpan S, Sriyapai T, Areekit S, Kaewphinit T, Sriyapai P, Santiwatanakul S, Chansiri K. Development of a rapid screening test for *Listeria monocytogenes* in raw chicken meat using loop-mediated isothermal amplification (LAMP) and lateral flow dipstick (LFD). *Food Anal Methods.* 2017; 10:3763-3772.
  17. Lim KT, Teh CSJ, Thong KL. Loop-mediated isothermal amplification assay for the rapid detection of *Staphylococcus aureus*. *BioMed Res Int.* 2013; 2013:895816.
  18. Song T, Toma C, Nakasone N, Iwanaga M. Sensitive and rapid detection of *Shigella* and enteroinvasive *Escherichia coli* by a loop-mediated isothermal amplification method. *FEMS Microbiol Lett.* 2010; 243:259-263.
  19. Wan HM, Li YF, Li S, Huang TR, Zheng CL. Optimization of reaction conditions for rapid detection of heat-labile enterotoxin *Escherichia coli* by loop-mediated isothermal gene amplification. *Mod Prev Med.* 2011; 38:321-323.
  20. Liu H, Huang WS, Deng TT, Fu K, Ju XR, Chen Y. Detection of pistachio allergens in food by LAMP method. *Food Sci.* 2013; 34:128-132.
  21. Wei S, Daliri EBM, Chelliah R, Park BJ, Lim JS, Baek MA, Nam YS, Seo KH, Jin YG, Oh DH. Development of a multiplex real – time PCR for simultaneous detection of *Bacillus cereus*, *Listeria monocytogenes*, and *Staphylococcus aureus* in food samples. *J Food Saf.* 2019; 39:1-7.
  22. Sowmya N, Thakur MS, Manonmani HK. Rapid and simple DNA extraction method for the detection of enterotoxigenic *Staphylococcus aureus* directly from food samples: comparison of PCR and LAMP methods. *J Appl Microbiol.* 2012; 113:106-113.
  23. Rebelo AR, Bortolaia V, Kjeldgaard JS, *et al.* Multiplex PCR for detection of plasmid-mediated colistin resistance determinants, *mcr-1*, *mcr-2*, *mcr-3*, *mcr-4* and *mcr-5* for surveillance purposes. *Euro Surveill.* 2018; 23:29-39.

(Received October 2, 2019; Revised November 23, 2019; Accepted December 5, 2019)

# IL16 deficiency enhances Th1 and cytotoxic T lymphocyte response against influenza A virus infection

Ran Jia<sup>1</sup>, Shuai Liu<sup>2</sup>, Jin Xu<sup>1,\*</sup>, Xiaozhen Liang<sup>2,\*</sup>

<sup>1</sup>Department of Clinical Laboratory, Children's Hospital of Fudan University, Shanghai, China;

<sup>2</sup>Key Laboratory of Molecular Virology & Immunology, Institut Pasteur of Shanghai, University of Chinese Academy of Sciences, Chinese Academy of Sciences, Shanghai, China.

## Summary

Influenza A virus (IAV) is the major cause of seasonal epidemics and flu outbreaks worldwide. Given that interleukin 16 (IL16) can regulate T cell function and is one of the signature markers for virus infection including IAV infection, the impact of IL16 on IAV-induced T cell immune response hasn't been elucidated yet. In this paper, we infected wild type and IL16 knockout (KO) mice with IAV and analyzed the immunity of mice by flow cytometry. We observed an increase in the percentage of T helper (Th) 1 cells in the spleens of IL16 KO mice and elevation of IFN- $\gamma$  and TNF- $\alpha$  secretion from CD8<sup>+</sup> T cells in the lungs and spleens of IL16 KO mice in response to IAV infection. Moreover, the expression of major histocompatibility complex II which represents the maturation of dendritic cells (DCs) was upregulated in the lungs of IL16 KO mice. Taken together, our study suggests that IL16 deficiency enhanced Th1 and cytotoxic T lymphocyte response as well as DC maturation upon IAV infection, which provides new insight into the host regulation of T cell immune responses during IAV infection.

**Keywords:** Interleukin 16, influenza A virus, T helper 1, cytotoxic T lymphocyte

## 1. Introduction

Influenza A virus (IAV), a member of the *Orthomyxoviridae* family, is the major cause of seasonal epidemics and flu outbreaks worldwide. It is estimated that 3 to 5 million severe cases and 250,000 to 500,000 deaths annually are attributed to IAV infection (1-3). IAV contains an eight-segmented genome of single-stranded negative sense RNA and can be divided into different subtypes according to the genetic and antigenic properties of hemagglutinin (HA) and neuraminidase (NA) (4,5). Two influenza

A virus subtypes currently common in general circulation among people are H1N1 and H3N2 (2,6-8). The emerging and reemerging threats caused by IAV highlight the necessity to understand more of the host factors limiting or supporting IAV infection.

Upon IAV infection, airway dendritic cells (DCs) recognize viral particles-termed pathogen-associated molecular patterns (PAMPs) through their pattern recognition receptors (PRRs). The recognition subsequently induces the production of interferon (IFN)- $\alpha/\beta$  and proinflammatory cytokines, which assist DCs to mature into professional antigen presenting cells (APCs) and migrate to peripheral lymphoid organs to initiate a T cell immune response (9,10). Noticeably, besides morphological changes, DC maturation triggers the upregulation of major histocompatibility complex (MHC) II on its surface to stimulate a helper T (Th) cell response (11,12).

CD4<sup>+</sup> T cells and CD8<sup>+</sup> T cells have distinct and critical roles in the control of virus infection. Upon activation by APCs, naïve CD4<sup>+</sup> T cells, also known as Th0, differentiate into specific subsets including Th1, Th2, Th17 and regulatory T cells (Treg). As was reported, CD4<sup>+</sup> T cells routinely exhibit a Th1-

Released online in J-STAGE as advance publication December 18, 2019.

\*Address correspondence to:

Dr. Jin Xu, Department of Clinical Laboratory, Children's Hospital of Fudan University, Shanghai 201102, China.  
E-mail: jinxu\_125@163.com

Dr. Xiaozhen Liang, Key Laboratory of Molecular Virology & Immunology, Institut Pasteur of Shanghai, University of Chinese Academy of Sciences, Chinese Academy of Sciences, Shanghai 200031, China.  
E-mail: xzliang@ips.ac.cn

biased immunity in response to IAV infection (13,14). Considered as an assistant of cellular immunity, Th1 not only assists APCs to exert more costimulatory molecules to promote CD8<sup>+</sup> T cells to differentiate into cytotoxic T lymphocytes (CTLs), but also restricts viral infection by secreting IFN- $\gamma$  and tumor necrosis factor (TNF)- $\alpha$  (15,16). Therefore, the percentage of Th1 can be regarded as an indicator to evaluate host immune response to IAV and adequate anti-IAV cellular immune response requires timely recognition of APCs, efficient Th1 assistance and robust CTL response.

Interleukin 16 (IL16) is a cytokine with multiple functions including T cell chemotaxis, IL-2R $\alpha$  upregulation, and T cell transient energy (23,24). An analysis of whole blood samples from patients infected with different viruses including influenza virus revealed that IL16 was a pan-viral biomarker (25). The relationship between IL16 and IAV infection hasn't been studied so far. In this paper, we studied the impact of IL16 on T cell response elicited by IAV and found that IL16 deficiency enhanced the Th1 and CTL response as well as DC maturation upon IAV infection.

## 2. Materials and Methods

### 2.1. Viruses, mice and infection

IAV infections in the study were performed using Influenza virus A/Puerto Rico/8/34 (H1N1) (PR8) strain. The original stock of PR8 virus was offered by Prof. Haikun Wang (Institut Pasteur of Shanghai). The PR8 virus was amplified in 10-day-old embryonated hen's eggs. Briefly, PR8 virus was injected into the allantoic cavity using a 1 ml syringe and incubated in a 37°C incubator with 82% humidity for 48hr. The infected eggs were then cooled overnight at 4°C and the clear allantoic fluid was harvested and stored at -80°C as the final virus stock.

IL16 KO C57BL/6 mice were generated by Shanghai Model Organisms Center. Mice were intranasally infected with PR8 virus at 8,000 PFU/mouse and were humanely euthanized when their weight loss met 25% of the initial weight. All experimental procedures on animals were performed in compliance with the guidelines of the Animal Ethics Committee of Institut Pasteur of Shanghai.

### 2.2. Preparation of splenocytes and lung cells

Lungs and spleens were isolated aseptically on day7 post-infection. Lungs were digested in DMEM supplemented with 20  $\mu$ g/mL Liberase (Roche, Switzerland) and 25  $\mu$ g/mL DNase I (Roche, Switzerland) for 30 min at 37°C. Then lungs were ground through a 70  $\mu$ m nylon mesh to yield single-cell suspensions. Red blood cells were removed using Ammonium-Chloride-Potassium (ACK) lysis buffer (final concentration: 150mM NH<sub>4</sub>CL, 10mM

KHCO<sub>3</sub>, 0.1mM Na<sub>2</sub>EDTA). Cells were counted and resuspended at 4 $\times$ 10<sup>6</sup> cells/mL in DMEM and stimulated with 50 ng/mL phorbol myristate acetate (PMA) (Sigma, Germany) and 1  $\mu$ g/mL Ionomycin (IM) (Sigma, Germany) for 4 hr. GolgiStop (BD Bioscience, America) was added in the last 2 hr of stimulation at 0.67  $\mu$ l/mL. Cells were washed twice with sterilized PBS to prepare for further analysis.

### 2.3. Flow cytometry analysis

Splenocytes and lung cells were incubated with anti-CD16/32 (BD Bioscience, USA) for 30min at 4°C in PBS supplemented with 2% FBS (FACS buffer) to block non-specific binding with Fc receptors. Cells were surface-stained with BV650-anti-CD8 (BD-563234, USA), BV711-anti-CD4 (BD-563050, USA), BV510-anti-CD3 (BD-563024, USA), PE-CY7-anti-CD25 (eBioscience-25-0251-82, USA), PE-anti-F4/80 (BD-565410, USA), BV510-anti-CD11b (BD-562950, USA), APC-anti-CD11c (eBioscience-17-0114-81, USA) for 20 min on ice and washed twice with PBS. For intracellular staining, cells were fixed and permeabilized using BD CytoFix/CytoPerm Kit (BD Bioscience, USA) and stained with APC-anti-IL-4 (eBioscience-17-7041-82, USA), PE-anti-IFN- $\gamma$  (eBioscience-12-7311-82, USA), PE-anti-IL-2 (eBioscience-12-7021-82, USA), BV421-anti-IL-17 (BD-563354, USA), PE-CY7-anti-TNF- $\alpha$  (BD-557644, USA), Pacific blue-anti-Foxp3 (eBioscience-48-5773-82, USA) for 20min. Cells were washed with 1 $\times$ BD Perm/Wash buffer and were finally resuspended in 4% paraformaldehyde (PFA) for flow cytometry analysis. Flow cytometry was performed using BD LSR Fortessa (BD Bioscience, USA) and raw data was analyzed using FlowJo software.

### 2.4. Statistical analysis

Statistical analysis was performed using Prism (Graph Pad Software). The data are presented as mean  $\pm$  SD. Differences between groups of research subjects were analyzed for statistical significance with two-tailed Student's *t* tests. A *p* value of 0.05 was considered significant.

## 3. Results

### 3.1. IL16 deficiency doesn't affect the function of T cells in resting state

T cell immunity is important in both viral clearance and host recovery (4,26). To detect the role of IL16 in T cell response during IAV infection, we first analyzed whether the function of T cells are affected by IL16 deficiency before infection. Flow cytometry analyses revealed that the population of T cells (Figure 1A), the CD4<sup>+</sup> T cell subsets (Th0/Th1/Th2/Th17/Treg) (Figure 1B), as well

as the IFN- $\gamma$ -secreting and TNF- $\alpha$ -secreting CD8<sup>+</sup> T cells (Figure 1C) were comparable in the spleens of uninfected wild type (WT) and IL16 KO mice, suggesting that IL16 deficiency doesn't change the populations and cytokine secretion of T cells in the resting state.

3.2. IL16 deficiency elevates Th1 response after IAV infection

Given that IL16 doesn't alter T cell functions in the resting state, we next assessed the T cell response in PR8-infected WT and IL16 KO mice. Flow cytometry

revealed that the percentage of CD4<sup>+</sup> T cells (Figure 2A) and CD4<sup>+</sup> T cell subsets (Figure 2B and C) in the lungs of WT mice were comparable to that of IL16 KO mice on day 7 post-infection. Splenocytes didn't show significant differences in the CD4<sup>+</sup> T cell population between WT and IL16 KO mice either (Figure 3A). But surprisingly, intracellular staining revealed that the percentage of Th1 in the spleens of IL16 KO mice markedly surpassed that of WT mice, albeit WT mice also displayed a Th1-biased response compared with PBS mock-infected mice (Figure 3B and C). These data suggest that IL16 deficiency enhances Th1 response in

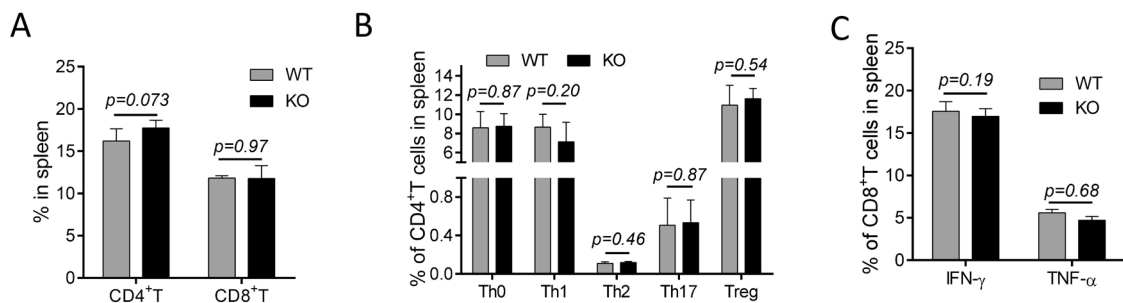


**Figure 1. IL16 deficiency doesn't affect T cell populations in spleens of uninfected mice.** Splenocytes were isolated from eight-week-old male WT and IL16-KO mice and analyzed by flow cytometry after 4 hr of phorbol myristate acetate (PMA) and Ionomycin (IM) stimulation. The percentage of CD4<sup>+</sup>T cells and CD8<sup>+</sup>T cells (A), the percentage of Th0/Th1/Th2/Th17/Treg (B), the secretion of IFN- $\gamma$  and TNF- $\alpha$  in CD8<sup>+</sup>T cells (C) were analyzed by flow cytometry. A p value of < 0.05 was considered significant. Data shown are representative of 3 independent experiments; n = 5 per group per experiment.

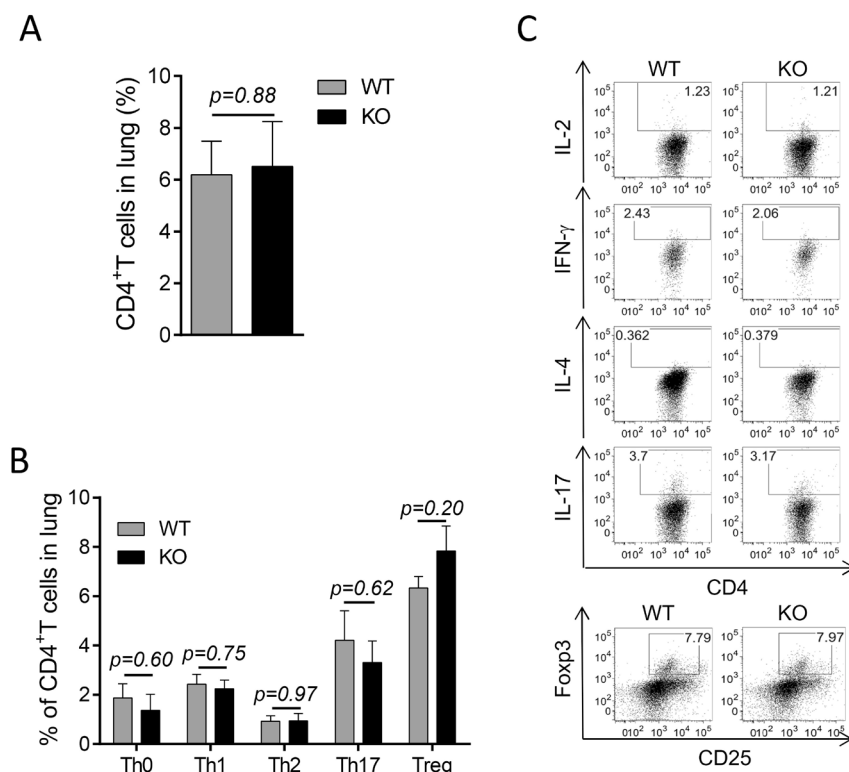


**Figure 2. CD4<sup>+</sup>T cell subsets in lungs of IAV-infected mice aren't significantly changed by absence of IL16.** PR8 virus was intranasally inoculated into WT and IL16 KO mice at 8,000 PFU/mouse. The percentage of CD4<sup>+</sup>T cells (A) and the percentage of Th0 (CD4<sup>+</sup>IL-2<sup>-</sup>), Th1 (CD4<sup>+</sup>IFN- $\gamma$ <sup>+</sup>), Th2 (CD4<sup>+</sup>IL-4<sup>+</sup>), Th17 (CD4<sup>+</sup>IL-17<sup>+</sup>) and Treg (CD4<sup>+</sup>CD25<sup>+</sup>Foxp3<sup>+</sup>) (B and C) in the lungs were detected by flow cytometry on day 7 post infection. A p value of < 0.05 was considered significant. Data shown are representative of 3 independent experiments; n = 5 per group per experiment.

the spleen after IAV infection.

### 3.3. IL16 deficiency enhances CTL response against IAV

Since Th1 assists CD8<sup>+</sup> T cell differentiation into CTLs, we next examined the CTL-secreted cytokines involved in anti-virus immune response. Flow cytometry revealed that CD8<sup>+</sup> T cells recruited in the lungs were reduced

(Figure 4A), while IFN- $\gamma$ -secreting CD8<sup>+</sup> T cells were increased in the lungs of IL16 KO mice (Figure 4B and C). Furthermore, CD8<sup>+</sup> T cells in the spleen were also decreased because of IL16 deficiency (Figure 5A), but the production of IFN- $\gamma$  and TNF- $\alpha$  in CD8<sup>+</sup> T cells in the spleen of IL16 KO mice were almost twice as many as that of WT mice (Figure 5B and C). Taken together, these data suggest that IL16 deficiency enhanced the

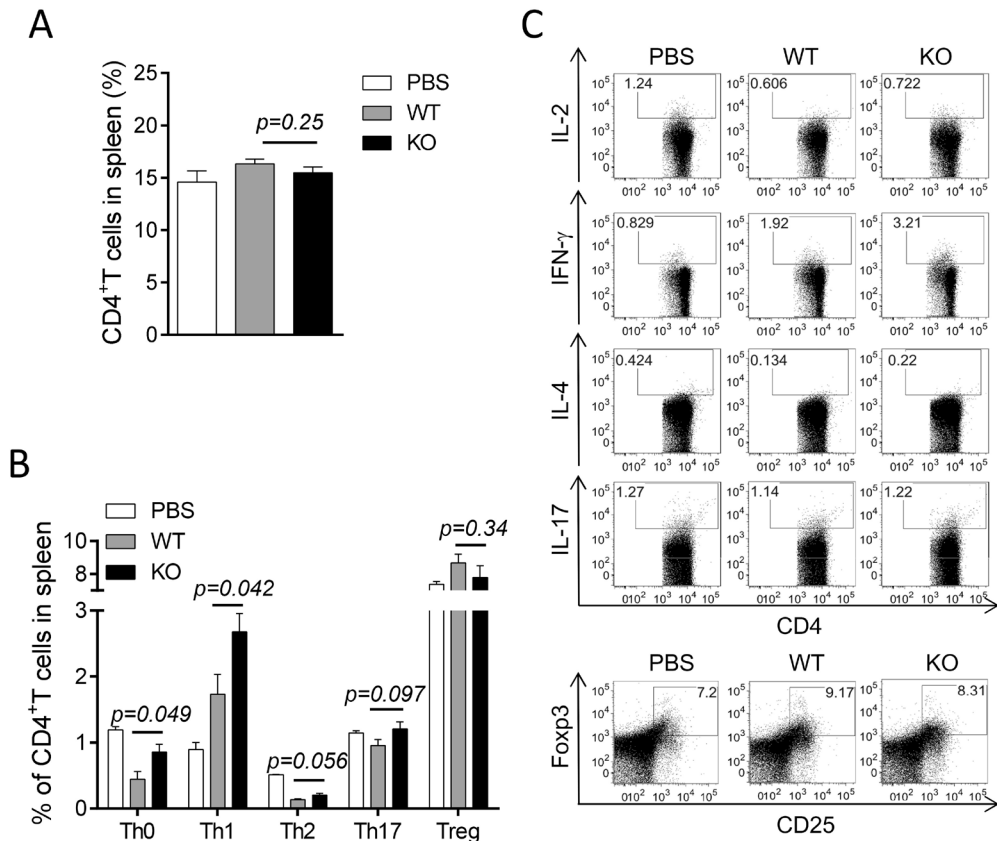


**Figure 3. IL16 deficiency promotes Th1 polarization in spleens of IAV-infected mice.** Seven-week-old male WT and IL16 KO mice were intranasally infected with PR8 virus, while control mice received mock inoculation with sterilized PBS. The percentage of CD4<sup>+</sup> T cells (A) and the Th0/Th1/Th2/Th17/Treg subsets (B and C) in the spleens were detected by flow cytometry on day 7 after infection. A *p* value of < 0.05 was considered significant. Data shown are representative of 3 independent experiments; *n* = 5 per group per experiment.

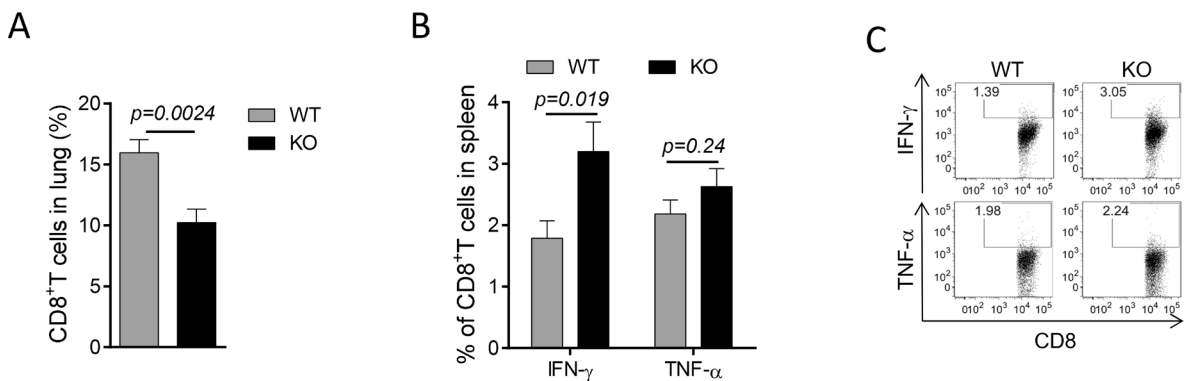


**Figure 4. IFN- $\gamma$ -secreting CD8<sup>+</sup> T cells are increased in lungs of IL16 KO mice after infection.** Mice were intranasally infected with PR8 virus. On day 7 after infection, the percentage of CD8<sup>+</sup> T cells (A), the IFN- $\gamma$ -secreting and TNF- $\alpha$ -secreting CD8<sup>+</sup> T cells (B and C) in the lungs were detected by flow cytometry respectively. A *p* value of < 0.05 was considered significant. Data shown are representative of 3 independent experiments; *n* = 4-5 per group per experiment.

CTL response after IAV infection.

3.4. Absence of IL16 elevates DC maturation in IAV-infected mouse

MHCII is mainly expressed on the surface of APCs and is upregulated as APCs become mature. With the involvement of the CD4 molecule and T cell receptor (TCR), MHCII on APCs was able to mediate CD4<sup>+</sup> T cell activation and differentiation (27). Since Th1 response in IL16 KO mice was increased after infection, we next detected the expression of MHCII on the surface of DCs.

Flow cytometry analyses revealed that the percentage of lung DCs from IL16 KO mice was decreased (Figure 6A and B), while the MHCII expression on lung DCs was increased in IL16 KO mice (Figure 6C and D). These results indicate that IL16 deficiency promotes DC maturation in response to IAV infection.

4. Discussion

Continuous antigen drift and antigen shift of IAV enable it to evolve fast, which makes it very common for newly-derived strains to escape from host immunity and

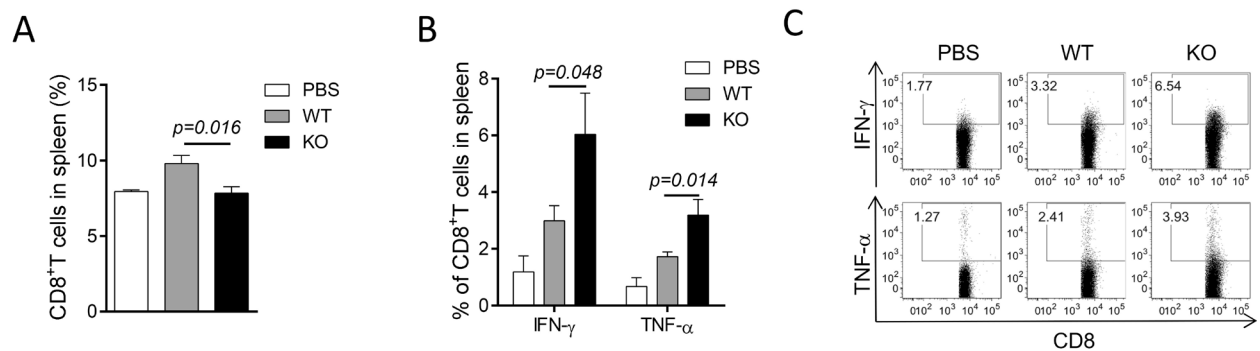


Figure 5. IL16 deficiency enhances both IFN- $\gamma$  and TNF- $\alpha$  secretion of CD8<sup>+</sup> T cells in spleens of IAV-infected mice. WT and IL16 KO mice were intranasally infected with PR8 virus and the percentage of CD8<sup>+</sup> T cells (A), the IFN- $\gamma$ -secreting and TNF- $\alpha$ -secreting CD8<sup>+</sup> T cells (B and C) in the spleens were detected by flow cytometry on day 7 after infection. A *p* value of < 0.05 was considered significant. Data shown are representative of 3 independent experiments; *n* = 4-5 per group per experiment.

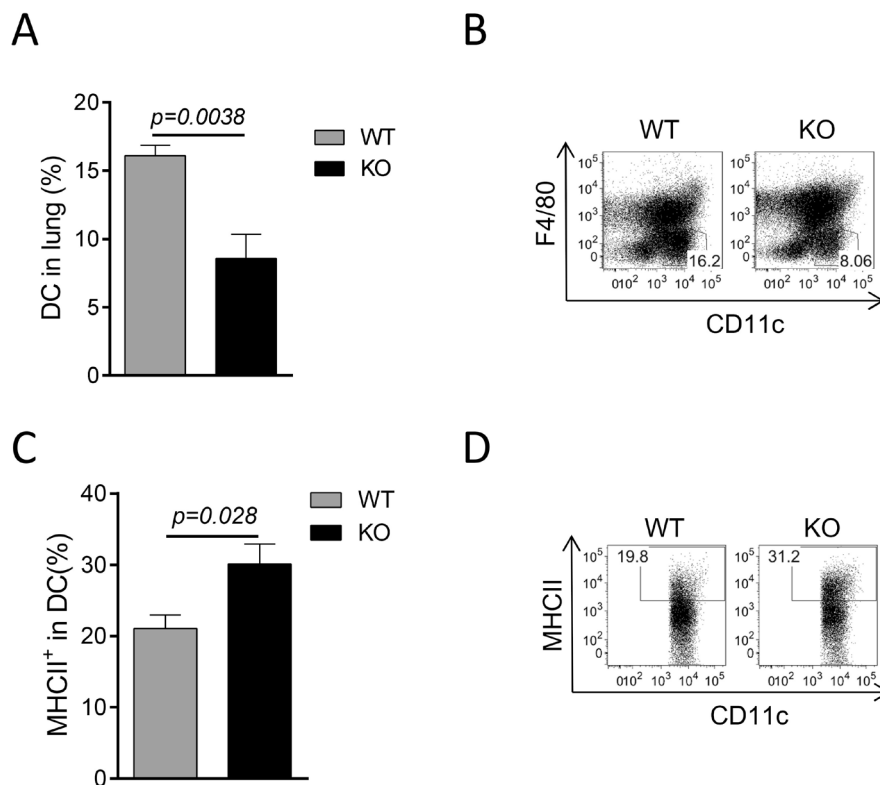


Figure 6. IL16 deficiency promotes DC maturation in lungs after IAV infection. WT and IL16 KO mice were infected with PR8 virus and the lungs were isolated on day 7 post infection. The percentage of DCs (F4/80<sup>+</sup>CD11c<sup>+</sup>) (A and B) and MHCII expression on the DCs (C and D) were detected by flow cytometry. A *p* value of < 0.05 was considered significant. Data shown are representative of 3 independent experiments; *n* = 4-5 per group per experiment.

result in flu pandemics and outbreaks (28). A thorough understanding of host factors involved in IAV infection might provide new treatment strategies or indicators for IAV-induced illness. In this study, we identified that IL16 deficiency promotes Th1 polarization and CTL response after IAV infection, in accordance with the relieved lung injury and decreased viral load we observed in IL16 KO mice in our unpublished data. Besides, we found that MHCII was elevated in lung DCs of IL16 KO mice, which might be associated with an elevated T cell response.

Th1 and CTL responses have vital roles in viral clearance and recovery of the host after influenza virus infection (21,22). As the two most important cytokines secreted by Th1 and CTLs, IFN- $\gamma$  and TNF- $\alpha$  have attracted lots of attention in host anti-viral immune response. IFN- $\gamma$  was first described in the year 1965 and has been tagged with an antiviral activity since then (29). Mounting evidence has revealed the link between IFN- $\gamma$  and viral clearance (26,30,31). In the terrible outbreak of H7N9 in 2013, the critical role of IFN- $\gamma$  was forcefully highlighted by the fact that the response of IFN- $\gamma$ -producing CD8<sup>+</sup> T cells was enhanced in recovery patients compared to dead ones (22). TNF- $\alpha$  is traditionally regarded as a pro-inflammatory cytokine given its role in inflammatory disorders (32,33). However, TNF- $\alpha$  deficiency was reported to result in severe inflammatory infiltration and lung injury, together with enhanced inflammatory cytokine secretions like IL-1 $\beta$ , suggesting that TNF- $\alpha$  was required to control immunopathology rather than viral clearance (34-36). Thus we assume that the alleviated pneumonia in IL16-deficient mice might be correlated with increased TNF- $\alpha$  secreted from Th1 and CTLs. The mechanism by which TNF- $\alpha$  balances different effects on immunopathology under specific circumstances needs to be studied more in the future.

Differentiation of Th1 is mainly mediated by a T-box transcription factor, T-bet, which was first isolated from a Th1 cDNA library and considered as a Th1-specific transcription factor (37). It has been demonstrated that T-bet-deficient mice displayed severely impaired ability for IFN- $\gamma$  secretion in CD4<sup>+</sup>T cells and a marked reversion of Th1/Th2 balance, indicating that T-bet plays critical roles in IFN- $\gamma$  secretion in Th1 (38,39). In the course of Th1 differentiation, IFN- $\gamma$ /STAT1 and IL12/STAT4 are considered as the two main upstream pathways of T-bet. Upon T cell activation, IFN- $\gamma$ /STAT1 signaling is supposed to initiate the first wave of T-bet expression, while IL12/STAT4 mainly participates in the second wave, which is critical in Th1 stabilization (40,41). Besides Th1, T-bet has also been reported to promote CTL activities by upregulating IFN- $\gamma$  expression in CD8<sup>+</sup>T cells, although the role of T-bet in CD8<sup>+</sup>T cells was less dominant and clear than that in Th1(40). Since we observed elevated IFN- $\gamma$  secretion both in Th1 and CTLs in IL16 KO mice, we

assume that there might be some correlation between IL16 and T-bet signaling. Whether IL16 enhances Th1 polarization and CTL activity by directly interacting with T-bet signaling or by other unknown mechanisms requires further study.

To conclude, our data suggest a potential link between IL16 and IAV-specific cellular immunity, which might implicate IL16 as a supporting factor for IAV-related illness and propose new insight into the network of virus-related host factors. Moreover, understanding the mechanisms by which IL16 exerts an immunoregulatory effect on cellular immunity might bring new clues for possible therapeutic strategies against IAV-associated illness.

### Acknowledgements

This work was supported by the National Key R & D Program of China (2016YFA0502100). We thank Prof. Haikun Wang from Institut Pasteur of Shanghai (IPS) for providing Influenza virus A/Puerto Rico/8/34 (H1N1) (PR8) virus strain, Prof. Bing Sun from IPS for providing IAV NP antibody, and Prof. Dimitri Lavillette from IPS for providing IAV NS antibody. We also thank Prof. Bing Sun's lab members for technical assistance for measuring the virus titer of IAV.

### References

1. Bender BS, Croghan T, Zhang L, Small PA, Jr. Transgenic mice lacking class I major histocompatibility complex-restricted T cells have delayed viral clearance and increased mortality after influenza virus challenge. *J Exp Med.* 1992; 175:1143-1145.
2. Peteranderl C, Herold S, Schmoltd C. Human Influenza Virus Infections. *Semin Respir Crit Care Med.* 2016; 37:487-500.
3. Krammer F. The human antibody response to influenza A virus infection and vaccination. *Nat Rev Immunol.* 2019; 19:383-397.
4. Grant EJ, Quinones-Parra SM, Clemens EB, Kedzierska K. Human influenza viruses and CD8<sup>+</sup> T cell responses. *Curr Opin Virol.* 2016; 16:132-142.
5. Meineke R, Rimmelzwaan GF, Elbaresh H. Influenza Virus Infections and Cellular Kinases. *Viruses.* 2019; 11:E171.
6. Yamayoshi S, Kawaoka Y. Current and future influenza vaccines. *Nat Med.* 2019; 25:212-220.
7. Lyu Y, Song S, Zhou L, Bing G, Wang Q, Sun H, Chen M, Hu J, Wang M, Sun H, Pu J, Xia Z, Liu J, Sun Y. Canine Influenza Virus A(H3N2) Clade with Antigenic Variation, China, 2016-2017. *Emerg Infect Dis.* 2019; 25:161-165.
8. Petrova VN, Russell CA. The evolution of seasonal influenza viruses. *Nat Rev Microbiol.* 2018; 16:47-60.
9. Hartmann BM, Albrecht RA, Zaslavsky E, Nudelmann G, Pincas H, Marjanovic N, Schotsaert M, Martínez-Romero C, Fenutria R, Ingram JP, Ramos I, Fernández-Sesma A, Balachandran S, García-Sastre A, Sealfon SC. Pandemic H1N1 influenza A viruses suppress immunogenic RIPK3-driven dendritic cell death. *Nat*

- Commun. 2017; 8:1931.
10. Iwasaki A, Pillai PS. Innate immunity to influenza virus infection. *Nat Rev Immunol.* 2014; 14:315-328.
  11. Kreijtz JH, Fouchier RA, Rimmelzwaan GF. Immune responses to influenza virus infection. *Virus Res.* 2011; 162:19-30.
  12. Vander Lugt B, Khan AA, Hackney JA, Agrawal S, Lesch J, Zhou M, Lee WP, Park S, Xu M, DeVoss J, Spooner CJ, Chalouni C, Delamarre L, Mellman I, Singh H. Transcriptional programming of dendritic cells for enhanced MHC class II antigen presentation. *Nat Immunol.* 2014; 15:161-167.
  13. Miyauchi K. Helper T cell responses to respiratory viruses in the lung: Development, virus suppression, and pathogenesis. *Viral Immunol.* 2017; 30:421-430.
  14. Whitmire JK. Induction and function of virus-specific CD4+ T cell responses. *Virology.* 2011; 411:216-228.
  15. Kidd P. Th1/Th2 balance: The hypothesis, its limitations, and implications for health and disease. *Altern Med Rev.* 2003; 8:223-246.
  16. Yoon SW, Wong SS, Zhu H, Chen R, Li L, Zhang Y, Guan Y, Webby RJ. Dysregulated T-Helper Type 1 (Th1):Th2 Cytokine Profile and Poor Immune Response in Pregnant Ferrets Infected With 2009 Pandemic Influenza A(H1N1) Virus. *J Infect Dis.* 2018; 217:438-442.
  17. Cox MA, Kahan SM, Zajac AJ. Anti-viral CD8 T cells and the cytokines that they love. *Virology.* 2013; 435:157-169.
  18. McMichael AJ, Gotch FM, Noble GR, Beare PA. Cytotoxic T-cell immunity to influenza. *N Engl J Med.* 1983; 309:13-17.
  19. Topham DJ, Tripp RA, Doherty PC. CD8+ T cells clear influenza virus by perforin or Fas-dependent processes. *J Immunol.* 1997; 159:5197-5200.
  20. Cerwenka A, Morgan TM, Dutton RW. Naive, effector, and memory CD8 T cells in protection against pulmonary influenza virus infection: homing properties rather than initial frequencies are crucial. *J Immunol.* 1999; 163:5535-5543.
  21. Mackenzie CD, Taylor PM, Askonas BA. Rapid recovery of lung histology correlates with clearance of influenza virus by specific CD8+ cytotoxic T cells. *Immunology.* 1989; 67:375-381.
  22. Wang Z, Wan Y, Qiu C, Quiñones-Parra S, Zhu Z, Loh L, Tian D, Ren Y, Hu Y, Zhang X, Thomas PG, Inouye M, Doherty PC, Kedzierska K, Xu J. Recovery from severe H7N9 disease is associated with diverse response mechanisms dominated by CD8(+) T cells. *Nat Commun.* 2015; 6:6833.
  23. Center DM, Kornfeld H, Cruikshank WW. Interleukin-16. *Int J Biochem Cell B.* 1997; 29:1231-1234.
  24. Cruikshank W, Little F. Interleukin-16: The ins and outs of regulating T-cell activation. *Crit Rev Immunol.* 2008; 28:467-483.
  25. Sampson DL, Fox BA, Yager TD, Bhide S, Cermelli S, McHugh LC, Seldon TA, Brandon RA, Sullivan E, Zimmerman JJ, Noursadeghi M, Brandon RB. A Four-Biomarker Blood Signature Discriminates Systemic Inflammation Due to Viral Infection Versus Other Etiologies. *Sci Rep.* 2017; 7:2914.
  26. Grant EJ, Chen L, Quinones-Parra S, Pang K, Kedzierska K, Chen W. T-cell immunity to influenza A viruses. *Crit Rev Immunol.* 2014; 34:15-39.
  27. Kambayashi T, Laufer TM. Atypical MHC class II-expressing antigen-presenting cells: Can anything replace a dendritic cell? *Nat Rev Immunol.* 2014; 14:719-730.
  28. Zhao M, Wang L, Li S. Influenza A virus-host protein interactions control viral pathogenesis. *Int J Mol Sci.* 2017; 18:E1673.
  29. Wheelock EF. Interferon-like virus-inhibitor induced in human leukocytes by phytohemagglutinin. *Science.* 1965; 149:310-311.
  30. Seo SH, Peiris M, Webster RG. Protective cross-reactive cellular immunity to lethal A/Goose/Guangdong/1/96-like H5N1 influenza virus is correlated with the proportion of pulmonary CD8(+) T cells expressing gamma interferon. *J Virol.* 2002; 76:4886-4890.
  31. Hillaire ML, van Trierum SE, Kreijtz JH, Bodewes R, Geelhoed-Mieras MM, Nieuwkoop NJ, Fouchier RA, Kuiken T, Osterhaus AD, Rimmelzwaan GF. Cross-protective immunity against influenza pH1N1 2009 viruses induced by seasonal influenza A (H3N2) virus is mediated by virus-specific T-cells. *J Gen Virol.* 2011; 92:2339-2349.
  32. Peper RL, Van Campen H. Tumor necrosis factor as a mediator of inflammation in influenza A viral pneumonia. *Microb Pathog.* 1995; 19:175-183.
  33. Semenzato G. Tumour necrosis factor: A cytokine with multiple biological activities. *Br J Cancer.* 1990; 61:354-361.
  34. Damjanovic D, Divangahi M, Kugathasan K, Small CL, Zganiacz A, Brown EG, Hogaboam CM, Gaudie J, Xing Z. Negative regulation of lung inflammation and immunopathology by TNF-alpha during acute influenza infection. *Am J Pathol.* 2011; 179:2963-2976.
  35. DeBerge MP, Ely KH, Enelow RI. Soluble, but not transmembrane, TNF-alpha is required during influenza infection to limit the magnitude of immune responses and the extent of immunopathology. *J Immunol.* 2014; 192:5839-5851.
  36. Xu L, Yoon H, Zhao MQ, Liu J, Ramana CV, Enelow RI. Cutting edge: pulmonary immunopathology mediated by antigen-specific expression of TNF-alpha by antiviral CD8+ T cells. *J Immunol.* 2004; 173:721-725.
  37. Zhang WX, Yang SY. Cloning and characterization of a new member of the T-box gene family. *Genomics.* 2000; 70:41-48.
  38. Finotto S, Neurath MF, Glickman JN, Qin S, Lehr HA, Green FH, Ackerman K, Haley K, Galle PR, Szabo SJ, Drazen JM, De Sanctis GT, Glimcher LH. Development of spontaneous airway changes consistent with human asthma in mice lacking T-bet. *Science.* 2002; 295:336-338.
  39. Chornoguz O, Hagan RS, Haile A, Arwood ML, Gamper CJ, Banerjee A, Powell JD. mTORC1 promotes T-bet phosphorylation to regulate Th1 differentiation. *J Immunol.* 2017; 198:3939-3948.
  40. Yang Y, Ochando JC, Bromberg JS, Ding Y. Identification of a distant T-bet enhancer responsive to IL-12/Stat4 and IFN-gamma/Stat1 signals. *Blood.* 2007; 110:2494-2500.
  41. Mullen AC, High FA, Hutchins AS, Lee HW, Villarino AV, Livingston DM, Kung AL, Cereb N, Yao TP, Yang SY, Reiner SL. Role of T-bet in commitment of TH1 cells before IL-12-dependent selection. *Science.* 2001; 292:1907-1910.

(Received October 20, 2019; Revised November 18, 2019; Accepted November 22, 2019)

# IFITM3 upregulates c-myc expression to promote hepatocellular carcinoma proliferation *via* the ERK1/2 signalling pathway

Jiaqi Min<sup>1,2,§</sup>, Junwen Hu<sup>1,3,§</sup>, Chen Luo<sup>1,§</sup>, Jinfeng Zhu<sup>1</sup>, Jiefeng Zhao<sup>1</sup>, Zhengming Zhu<sup>1</sup>, Linqun Wu<sup>1</sup>, Rongfa Yuan<sup>1,\*</sup>

<sup>1</sup>Department of General Surgery, Second Affiliated Hospital of Nanchang University, Nanchang, China;

<sup>2</sup>Department of General Surgery, Aviation General Hospital, Beijing, China;

<sup>3</sup>Department of Hepatobiliary Surgery, Guangxi Medical University Cancer Hospital, Nanning, China.

## Summary

Interferon-induced transmembrane protein 3 (IFITM3) is associated with cancer development. Proto-oncogene c-myc can promote tumor proliferation. However, collections of IFITM3 and c-myc in hepatocellular carcinoma (HCC) and the potential role and mechanisms of IFITM3 in c-myc-mediated tumor proliferation remain unclear. In this study, we investigated a positive correlation between the expression of IFITM3 and c-myc in HCC. The down-regulation of IFITM3 significantly reduced c-myc expression and inhibited the proliferation of HCC *in vitro* and *in vivo*. In addition, upregulated c-myc expression restored the decrease in cell proliferation caused by the downregulation of IFITM3, while downregulation of c-myc reduced the proliferation of HCC enhanced by IFITM3. Mechanistically, IFITM3 regulates c-myc expression *via* the ERK1/2 signalling pathway. In conclusion, a novel path of IFITM3–ERK1/2–c-myc regulatory circuitry was identified, and its dysfunction may lead to HCC tumorigenesis.

**Keywords:** IFITM3, c-myc, hepatocellular carcinoma, ERK1/2 signalling pathway, proliferation

## 1. Introduction

Hepatocellular carcinoma (HCC) is one of the most common primary malignancies of the liver and a leading cause of cancer-related mortality worldwide (1,2). Surgical resection is regarded as the primary treatment for HCC, but less than 20% of patients undergo timely radical surgical resection mainly due to high degree of malignancy and the rapid infiltrative growth of tumor cells (3,4). Thus, elucidating the mechanisms underlying HCC proliferation is critical to its treatment.

Interferon-induced transmembrane protein 3 (IFITM3) is a protein that is encoded by the IFITM3

gene in humans and that belongs to the interferon-inducible transmembrane protein family (5). Studies have shown that IFITM3 is involved in the processes of cellular differentiation, apoptosis, cell adhesion, and immune cell regulation (6-9). Recently, an increasing number of studies have focused on the role of IFITM3 in tumorigenesis and development. IFITM3 is reported to be significantly overexpressed in many tumors including colon cancer, astrocytoma, human glioma, myeloid leukemia, and prostate cancer, as well as HCC (10-14). In addition, the IFITM family seems to play an important role in the regulation of tumor cell proliferation (15,16). Moreover, the current authors previously reported that IFITM3 can promote HCC invasion and metastasis and that miR-29a can directly bind to IFITM3 to promote the growth of HCC cells (17,18). However, the downstream regulatory role played by IFITM3 in the proliferation of HCC is still unclear.

Proto-oncogene c-myc is one of the important members of the MYC gene family, and it participates in cellular metabolism, proliferation, and differentiation (19,20). c-myc is reported to play an important role in

Released online in J-STAGE as advance publication December 18, 2019.

<sup>§</sup>These authors contributed equally to this work.

\*Address correspondence to:

Dr. Rongfa Yuan, Department of General Surgery, The Second Affiliated Hospital of Nanchang University, No. 1 Minde Road, Nanchang 330006, China.

E-mail: yuanrf7788@163.com

the oncogenic transformation of normal cells and in tumor proliferation. For example, c-myc overexpression promotes oral cancer cell proliferation (21). Down-regulated c-myc can inhibit bladder cancer, prostate cancer, and gastric cancer cell proliferation (22-24). Many studies of HCC have also verified that down-regulated c-myc significantly inhibits tumor cell growth (25,26). However, the upstream regulatory role of c-myc in HCC has yet to be fully elucidated.

The current study confirmed that expression of the IFITM3 and c-myc genes is aberrantly overexpressed and positively correlated in HCC tissues. In addition, knockdown of IFITM3 inhibits HCC proliferation by downregulating c-myc expression *in vitro* and *in vivo*. Further investigations indicate that IFITM3 regulates c-myc *via* the ERK1/2 signalling pathway. Together, these findings have indicated a novel role for IFITM3 in activating the ERK1/2 signalling to promote the cell proliferation and growth of HCC.

## 2. Materials and Methods

### 2.1. Human tissue specimens

Subjects were 160 patients who underwent resection of HCC at the Second Affiliated Hospital of Nanchang University from January 2010 to December 2018. Tumor and adjacent tissue specimens were collected according to the protocol approved by the Ethics Committee of the Second Affiliated Hospital of Nanchang University. All patients provided informed consent.

### 2.2. Cell culture, plasmids, and reagents

The human HCC cell lines MHCC97H, HCCLM3, Hep3B, Huh-7, and SMCC7721 were purchased from the Shanghai Institute of Cell Biology, China. They were cultured in DMEM (Thermo Fisher Scientific, Shanghai, China) with 10% FBS (Thermo Fisher Scientific) and 1% penicillin-streptomycin at 37°C and in a 5% CO<sub>2</sub> atmosphere. Four short hairpin RNAs (shRNAs) were designed with siRNA Target Finder (InvivoGen, Hong Kong, China). The target sites of shRNA are shown in Table S1 (<http://www.biosciencetrends.com/action/getSupplementalData.php?ID=49>). Real-time quantitative PCR (qRT-PCR) and Western blotting (Figure S1, <http://www.biosciencetrends.com/action/getSupplementalData.php?ID=49>) confirmed the effects of interference. The most effective interference was used in experiments. Expression plasmids for pcDNA3.1(+)-IFITM3 and pcDNA3.1(+)-c-myc are been described in refs. 17, 18, 27, and 28.

The following antibodies and reagents were used: IFITM3, c-myc, c-Jun, c-Fos, ERK1/2, p-ERK1/2 (T202/Y204), tubulin antibody (Abcam, Cambridge, MA, USA); Lipofectamine3000 (Invitrogen); Total

Protein Extraction Kit (Applygen, Beijing, China); and U0126 (Sigma Chemical Co., St. Louis, MO, USA).

### 2.3. qRT-PCR, western blotting, and immunohistochemical staining (IHC)

qRT-PCR, Western blotting, and IHC were performed as described previously (17,29,30). The following primer pairs were used for qRT-PCR: IFITM3 (forward, 5'-ACTGTCCAAACCTTCTTCTCTCC-3', reverse, 5'-TCGCCAACCATCTTCCTGTC-3'), c-myc (forward, 5'- AATGAAAAGGCCCAAGGTAGTT ATCC-3', reverse, 5'- GTCGTTTCCGCAACAAGTCC TCTTC-3'); GAPDH (forward, 5'-CAGGGCTGCTTTT AACTCTGGT-3', reverse, 5'-GATTTTGGAGGGATC TCGCT-3') was used as an internal control.

### 2.4. Cell proliferation and colony formation assays

Cell proliferation and viability were assessed using an MTT assay. The differently transfected HCC cells were seeded on 96-well plates (1 × 10<sup>3</sup> cells/well). After culturing for 24, 48, 72, and 96 h, 10 µl of an MTT stock solution (5 mg/ml; Sigma) was added to each well with 100 µl of medium for 4 h at 37°C. The medium was replaced with 100 µl of dimethyl sulfoxide and the mixture was incubated at room temperature for 5 minutes. The absorbance was then measured at a wavelength of 570 nm.

To perform colony formation assay, 800 cells were seeded on 6-well plates. After 14 d, 4% paraformaldehyde was used to fix the cells, and cells were stained with 0.1% crystal violet. The number of colonies and their areas were counted.

### 2.5. Animal experiments

Animal protocols in accordance with the guidelines of the U.K. Animals (Scientific Procedures) Act, 1986, and EU Directive 2010/63/EU were approved by the Ethics Committee for Animal Experiments of the Second Affiliated Hospital of Nanchang University. The flanks of 6-week-old male BALB/c-nu/nu mice (SLAC Laboratory Animal Co., Ltd., Shanghai, China) were subcutaneously injected with 1 × 10<sup>7</sup> cells in 100 µl of PBS. After 14 d, the tumor tissues were resected, weighed, and imaged. The following formula was used to calculate tumor volume: (short diameter) × (longest diameter) × high × π/3.

### 2.6. Statistical analysis

All statistical analysis was performed with SPSS 17.0 (SPSS, Inc.). Results are expressed as the mean ± SD. The Student's *t*-test was used to analyze the differences between two groups, and one-way ANOVA was used to analyze differences when comparing more than two

groups. A  $P$  value of less than 0.05 was considered statistically significant.

### 3. Results

#### 3.1. *IFITM3* and *c-myc* expression are both upregulated and positively correlated in HCC tissues

To explore the correlation between the levels of *IFITM3* and *c-myc* expression in HCC, *IFITM3* and *c-myc* expression was first detected in 160 HCC specimens and adjacent tissue specimens using qRT-PCR, IHC, and Western blotting. The results of qRT-PCR indicated that average levels of expression of *IFITM3* and *c-myc* mRNA in cancer tissues were markedly higher than those in adjacent non-tumor tissues (Figure 1A). IHC confirmed that the *IFITM3* protein was highly expressed in 61.25% (98 of 160) of the HCC specimens and that the *c-myc* protein was highly expressed in 54.38% (87 of 160) of the HCC specimens (Figure

1B). Western blotting further indicated that levels of *IFITM3* and *c-myc* protein expression were markedly upregulated in HCC specimens ( $p < 0.001$  for both, Figure 1C and D). Moreover, scatter plots confirmed that levels of *IFITM3* and *c-myc* mRNA and protein were positively correlated in HCC specimens ( $p < 0.001$  for both, Figure 1E).

#### 3.2. Downregulation of *IFITM3* suppresses *c-myc* expression and inhibits HCC proliferation *in vitro* and *in vivo*

In order to determine whether *IFITM3* regulates the expression of *c-myc* in HCC cells, the levels of *IFITM3* and *c-myc* expression were first detected in various HCC cells using qRT-PCR and Western blotting. Results indicated that the level of *IFITM3* expression was positively correlated with the level of *c-myc* expression (Figure 2A). Subsequently, *IFITM3*-specific short hairpin RNA (sh*IFITM3*-c and sh*IFITM3*-d) was

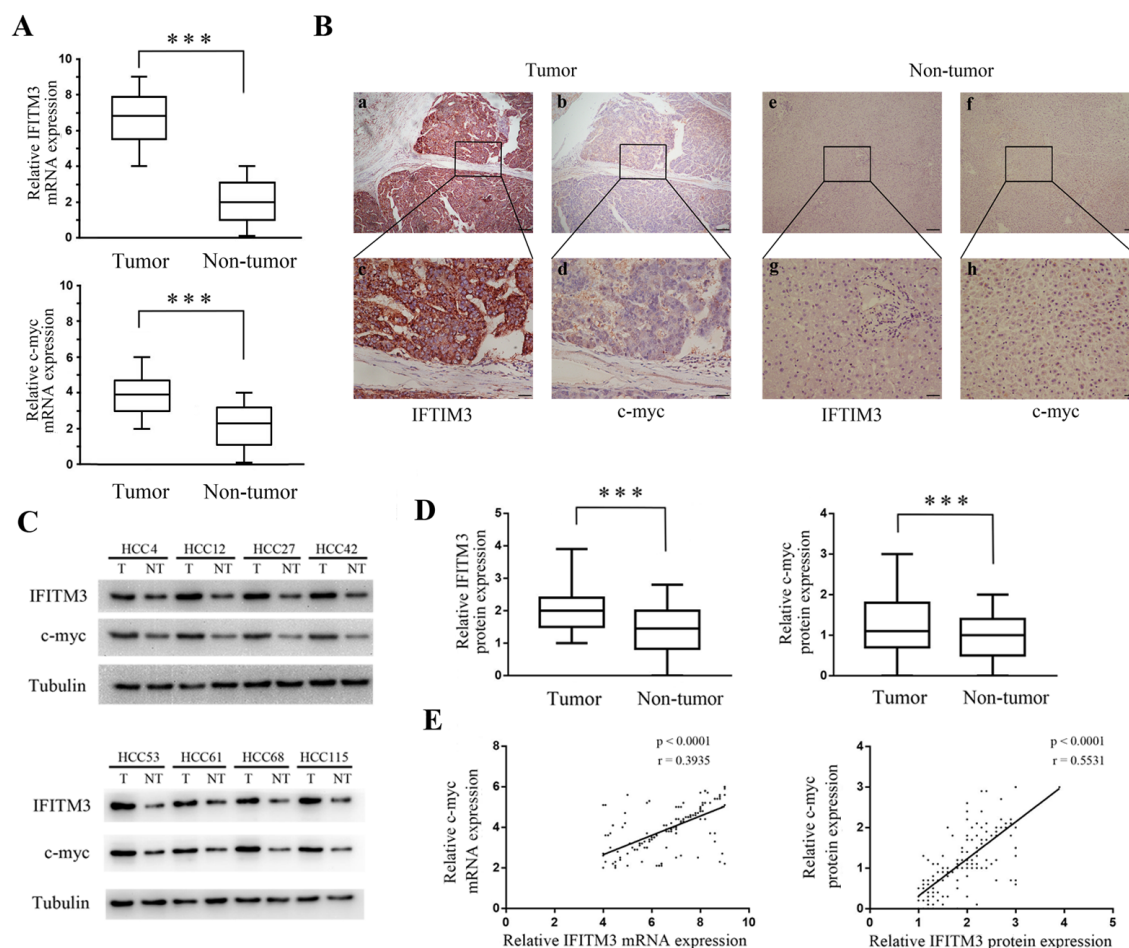


**Figure 1. Levels of *IFITM3* and *c-myc* expression are positively correlated in HCC.** (A) qRT-PCR analysis of *IFITM3* and *c-myc* mRNA expression in 160 HCC tumor specimens and adjacent normal tissue specimens ( $***p < 0.001$ , paired Student's  $t$ -test); (B) Representative IHC staining of *IFITM3* and *c-myc* in HCC tissues. Magnification: a, b, e, and f: 100 $\times$ ; c, d, g, and h: 400 $\times$ ; (C) Representative Western blot analysis of *IFITM3* and *c-myc* protein expression (T: tumor, NT: non-tumor tissues); (D) Quantification of *IFITM3* and *c-myc* protein expression using Western blot analyses in 160 paired HCC specimens and adjacent normal tissue specimens ( $***p < 0.001$ , paired Student's  $t$ -test); (E) Scatter plots show a positive correlation between *IFITM3* and *c-myc* in terms of levels of mRNA and protein (left,  $r = 0.3935$ ,  $p < 0.0001$ ; right,  $r = 0.5531$ ,  $p < 0.0001$ ).

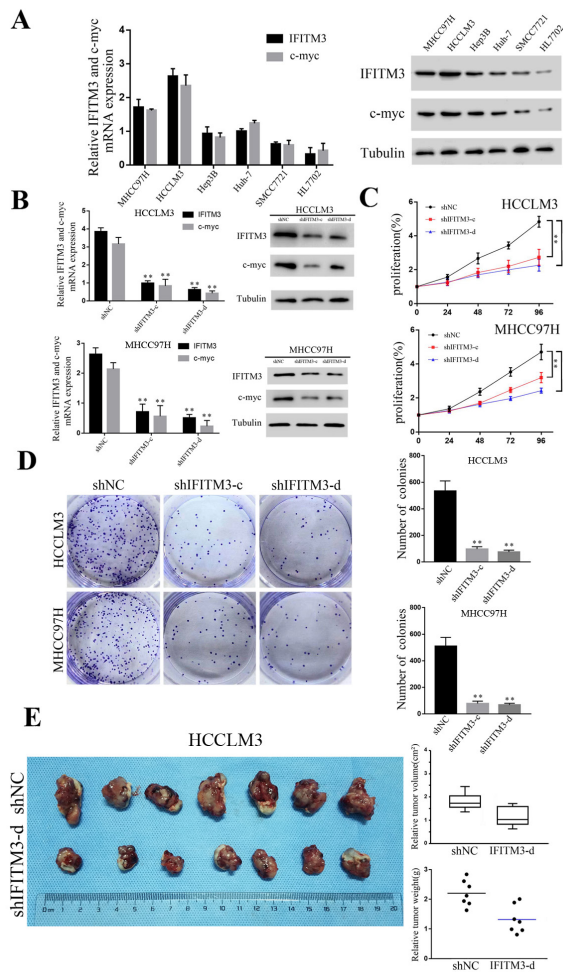


**Figure 2. Downregulation of IFITM3 reduces c-myc expression and represses HCC proliferation.** (A) qRT-PCR and Western blot analyses of IFITM3 and c-myc mRNA and protein expression in HL-7702 cells and HCC cell lines; (B) qRT-PCR and Western blot analyses were used to analyze IFITM3 and c-myc mRNA and protein expression in HCCLM3 and MHCC97H cells transfected with shIFITM3 (\*\**p* < 0.01); (C) An MTT proliferation assay indicated that IFITM3 knockdown significantly decreased cell proliferation in the HCCLM3 and MHCC97H cell lines (\*\**p* < 0.01); (D) Downregulation of IFITM3 suppressed colony formation in the HCCLM3 and MHCC97H cell lines (\*\**p* < 0.01); (E) A tumorigenicity assay indicated that knockdown of IFITM3 significantly suppressed tumor growth (*n* = 7 per group, *p* < 0.05, The formula for calculating the tumor volume was: (short diameter) × (longest diameter) × high ×  $\pi/3$ ).

stably transfected into HCCLM3 and MHCC97H cells to inhibit the expression of IFITM3. qRT-PCR and Western blot analysis confirmed that the knockdown of IFITM3 significantly decreased the expression of c-myc mRNA and protein in HCCLM3 and MHCC97H cells (Figure 2B). In addition, the proliferation capacity of cells was significantly inhibited in shIFITM3-c and shIFITM3-d cells (*p* < 0.01, Figure 2C). The number of colonies was significantly reduced in IFITM3-suppressed cells (*p* < 0.01, Figure 2D). In addition, a tumorigenicity assay similarly indicated that the downregulation of IFITM3 significantly suppressed tumor growth (*p* < 0.01, Figure 2E).

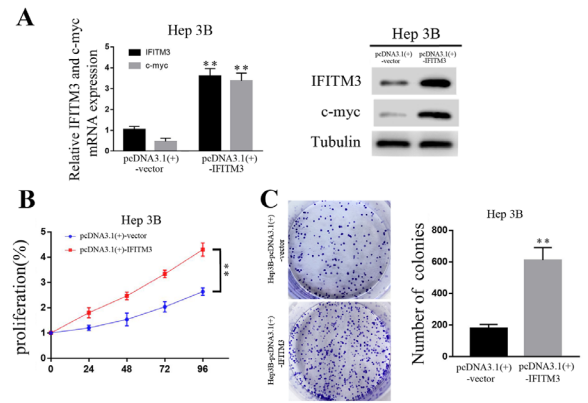


**Figure 3. Overexpression of IFITM3 increases c-myc expression and promotes HCC proliferation.** (A) qRT-PCR and Western blot analyses were used to analyze IFITM3 and c-myc mRNA and protein expression in Hep3B cells transfected with the pcDNA3.1(+)-IFITM3 plasmid (\*\**p* < 0.01); (B) An MTT proliferation assay indicated that IFITM3 overexpression significantly increased cell proliferation in the Hep3B cell line (\*\**p* < 0.01); (C) Upregulation of IFITM3 promoted colony formation in the Hep3B cell line (\*\**p* < 0.01).

To confirm the specificity of tumorigenicity, the plasmid pcDNA3.1(+)-IFITM3 was transfected into Hep3B cells to increase IFITM3 expression. Results indicated that overexpression of IFITM3 significantly increased the expression of c-myc (Figure 3A). The upregulation of IFITM3 markedly promoted the proliferation of HCC cells *in vitro* (Figure 3B and C). Taken together, these results confirmed that downregulation of IFITM3 reduced the expression of c-myc and inhibited the proliferation of HCC cells *in vitro* and *in vivo*.

### 3.3. c-myc is the key for IFITM3-mediated HCC cell proliferation

In order to further confirm that IFITM3 promotes the proliferation of HCC cells by regulating c-myc. We first increased the c-myc expression in IFITM3-knockdown HCC cells, and then observed the expression of IFITM3 and c-myc and cell-proliferation abilities. Western blotting indicated that the downregulation of IFITM3 reduced the expression of c-myc, while the upregulation of c-myc attenuated the loss of c-myc expression in IFITM3-knockdown HCCLM3 and MHCC97H cells (Figure 4A). The proliferation experiment also indicated that the down-regulation of IFITM3 significantly reduced the proliferation of HCCLM3 and MHCC97H cells, while the up-regulation of c-myc rescued the decreased proliferation ability caused by the knockdown of IFITM3 (Figure 4B).

Secondly, we decreased the expression of c-myc in IFITM3-overexpressing Hep3B cells, and then measured the levels of IFITM3 and c-myc proteins as well as cell proliferation. Western blotting indicated that overexpression of IFITM3 significantly upregulated

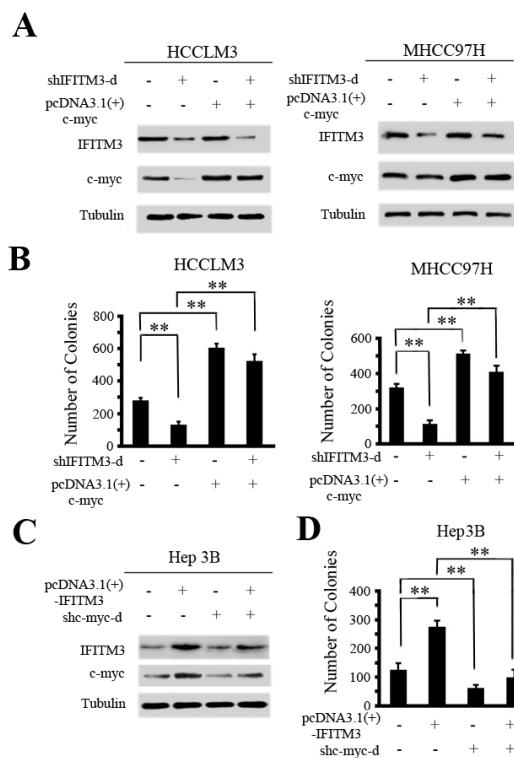


**Figure 4. c-myc is essential for IFITM3-mediated HCC proliferation.** (A) Levels of IFITM3 and c-myc protein were detected with Western blot analysis. The overexpression of c-myc attenuated the loss of c-myc expression in HCCLM3- and MHCC97H-shIFITM3-d cells; (B) Overexpression of c-myc rescued colony formation in HCCLM3- and MHCC97H-shIFITM3-d cells (\*\* $p < 0.01$ ); (C) The downregulation of c-myc expression significantly inhibited the increase in c-myc expression in Hep3B-IFITM3 cells; (D) Inhibition of c-myc reduced colony formation in IFITM3-overexpressing Hep3B cells (\*\* $p < 0.01$ ).

c-myc expression, while downregulation of c-myc dramatically inhibited the increase in c-myc expression induced by IFITM3 in Hep3B cells (Figure 4C). Moreover, the knockdown of c-myc reduced IFITM3-enhanced cell proliferation (Figure 4D). These results demonstrate that c-myc is necessary for IFITM3-mediated HCC cell proliferation.

#### 3.4. IFITM3 regulates c-myc expression via ERK1/2 signalling in HCC cells

c-myc is reported to be a target of ERK1/2 signalling (19,31,32). Therefore, the hypothesis was that IFITM3 regulates c-myc via the ERK1/2 signalling pathway in HCC cells. To verify this hypothesis, changes in the expression of phosphorylated ERK1/2 (p-ERK1/2) and total ERK1/2 were first detected in IFITM3-knockdown HCCLM3 and MHCC97H cells. Western blotting indicated that the down-regulation of IFITM3 significantly decreased the level of p-ERK1/2 but did not have a significant effect on the expression of total ERK1/2 protein in HCCLM3 and MHCC97H cells (Figure 5A). In contrast, up-regulation of IFITM3

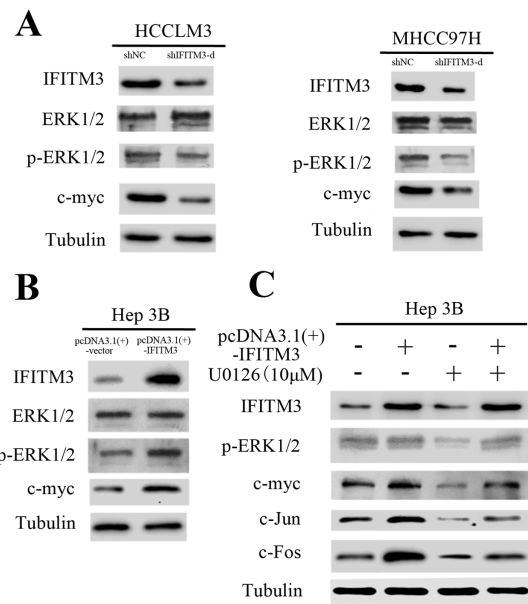


**Figure 5. IFITM3 regulates c-myc expression via the ERK1/2 signalling pathway.** (A and B) Levels of IFITM3, ERK1/2, p-ERK1/2, and c-myc protein expression were assessed with Western blotting in IFITM3-knockdown and IFITM3-overexpressing HCC cells; (C) Western blot analysis indicated levels of IFITM3 overexpression and ERK1/2 signalling inhibition (U0126, 10μM) and their effects on p-ERK1/2, c-myc, c-Jun, and c-Fos in Hep3B cells.

expression significantly increased the level of p-ERK1/2 but had not effect on total ERK1/2 protein expression in Hep3B cells (Figure 5B). In addition, up-regulation of IFITM3 expression increase the expression of other downstream genes in the ERK1/2 signalling pathway, *i.e.* c-Jun and c-Fos, in Hep3B cells. However, blockade of ERK1/2 signalling dramatically inhibited the increase in c-myc, c-Jun, and c-Fos expression in Hep3B-pcDNA3.1(+)-IFITM3 cells (Figure 5C). These findings confirmed that IFITM3 regulates c-myc via the ERK1/2 signalling pathway.

#### 4. Discussion

IFITM3 is a member of the IFITM family, which plays an important in regulating cellular differentiation, apoptosis, inflammation, and immune cell regulation (6,7,9,14). Recently, mounting evidence has indicated that IFITM3 plays a crucial role in oncogenesis and development. For example, Gan *et al.* found that knockdown of IFITM3 suppressed the growth of oral squamous cell carcinoma cells via the CCND1-CDK4/6-pRB axis (33). Another study found that knockdown of IFITM3 expression inhibited gastric cancer cell migration, invasion, and proliferation (34). A previous study by the current authors confirmed that IFITM3 is significantly overexpressed in HCC tissues and is associated with a poor prognosis (17). The current authors previously also reported that overexpression of IFITM3 enhances HCC invasion and

proliferation (17,18). These results indicate that IFITM3 can promote HCC tumorigenesis and development.

The current study investigated the downstream gene by which IFITM3 promotes HCC proliferation. Previous studies have confirmed that c-myc is overexpressed in many tumors and that it promotes tumor proliferation. For example, Tang *et al.* reported that LncRNA GLCC1 promotes colorectal carcinogenesis and tumor proliferation by stabilizing c-myc (35). Another study found that silencing of HMGA1 significantly inhibited gastric cancer cell proliferation by regulating c-myc expression (36). In addition, Yang *et al.* reported that the mistletoe extract fraxini inhibits the proliferation of HCC by down-regulating c-myc expression (37). These studies indicated that c-myc is a master regulator of tumor proliferation. The current study identified a novel regulatory mechanism in which IFITM3 promotes HCC cell proliferation by increasing c-myc expression. First, our results showed that IFITM3 and c-myc expression were significantly upregulated and were positively correlated in HCC tissues. In addition, downregulation of IFITM3 was found to reduce the expression of c-myc and to decrease HCC proliferation *in vitro* and *in vivo*. In addition, overexpression of c-myc rescued the decreased proliferation caused by the knockdown of IFITM3, while the inhibition of c-myc significantly reduced proliferation that increased by IFITM3 overexpression. These results suggest that one of the mechanisms by which IFITM3 promotes HCC proliferation is the upregulation of c-myc expression.

Next, the mechanism by which IFITM3 regulates c-myc was further investigated. c-myc is reported to be a target of ERK1/2 signalling, which is involved in the oncogenesis and development of many cancers (19,31,32). The relationship between IFITM3 and the ERK1/2 signalling pathway was first investigated. Interestingly, downregulation of IFITM3 was confirmed to decrease the level of p-ERK1/2, whereas overexpression of IFITM3 increased p-ERK1/2 expression. Moreover, upregulation of IFITM3 was found to also increase the other downstream genes in the ERK1/2 pathway, including c-Jun and c-Fos, whereas the blockade of ERK1/2 signalling dramatically inhibited the increase in c-myc, c-Jun, and c-Fos expression in Hep3B-pcDNA3.1(+)-IFITM3 cells. In conclusion, these findings have shown that IFITM3 regulates c-myc expression *via* the ERK1/2 signalling pathway.

In summary, the current study demonstrated that IFITM3 and c-myc expression are positively correlated in HCC tissues. Silencing IFITM3 decreases the expression of c-myc, inhibiting HCC cell proliferation *in vitro* and *in vivo*. In addition, we confirmed that IFITM3 regulates c-myc expression *via* the ERK1/2 pathway. The newly identified IFITM3-ERK1/2-c-myc axis facilitates the proliferation of HCC and represents a valuable target for treatment of HCC.

## Acknowledgments

This study was supported by grants from the National Natural Science Foundation of China (Nos. 81960436 and 81560396), the Key R & D projects of Jiangxi Province (No. 20181BBG70011), the Outstanding Young Talent Project of Jiangxi Province (No. 20192BCB23023), the Project of the Jiangxi Provincial Department of Education (No. GJJ150142), and the Project of the Jiangxi Provincial Health Commission (No. 20195223).

## References

1. Bray F, Ferlay J, Soerjomataram I, Siegel RL, Torre LA, Jemal A. Global cancer statistics 2018: GLOBOCAN estimates of incidence and mortality worldwide for 36 cancers in 185 countries. *CA Cancer J Clin.* 2018; 68:394-424.
2. Song P, Cai Y, Tang H, Li C, Huang J. The clinical management of hepatocellular carcinoma worldwide: A concise review and comparison of current guidelines from 2001 to 2017. *Biosci Trends.* 2017; 11:389-398.
3. Forner A, Reig M, Bruix J. Hepatocellular carcinoma. *Lancet.* 2018; 391:1301-1314.
4. Maluccio M, Covey A. Recent progress in understanding, diagnosing, and treating hepatocellular carcinoma. *CA Cancer J Clin.* 2012; 62:394-399.
5. Bailey CC, Kondur HR, Huang IC, Farzan M. Interferon-induced transmembrane protein 3 is a type II transmembrane protein. *J Biol Chem.* 2013; 288:32184-32193.
6. Hou Y, Zhang Y, Qin L, Zhang C, Wang S, Chen D, Li A, Lou J, Yu Y, Dong T, Li N, Zhao Y. Interferon-induced transmembrane protein-3 rs12252-CC is associated with low differentiation and progression of hepatocellular carcinoma. *Medicine (Baltimore).* 2019; 98:e13996.
7. Yamada S, Itoh N, Nagai T, Nakai T, Ibi D, Nakajima A, Nabeshima T, Yamada K. Innate immune activation of astrocytes impairs neurodevelopment *via* upregulation of follistatin-like 1 and interferon-induced transmembrane protein 3. *J Neuroinflammation.* 2018; 15:295.
8. Zhang D, Wang H, He H, Niu H, Li Y. Interferon induced transmembrane protein 3 regulates the growth and invasion of human lung adenocarcinoma. *Thorac Cancer.* 2017; 8:337-343.
9. Smith RA, Young J, Weis JJ, Weis JH. Expression of the mouse fragilis gene products in immune cells and association with receptor signaling complexes. *Genes Immun.* 2006; 7:113-121.
10. Li D, Peng Z, Tang H, Wei P, Kong X, Yan D, Huang F, Li Q, Le X, Li Q, Xie K. KLF4-mediated negative regulation of IFITM3 expression plays a critical role in colon cancer pathogenesis. *Clin Cancer Res.* 2011; 17:3558-3568.
11. Seyfried NT, Huysentruyt LC, Atwood JA, 3rd, Xia Q, Seyfried TN, Orlando R. Up-regulation of NG2 proteoglycan and interferon-induced transmembrane proteins 1 and 3 in mouse astrocytoma: a membrane proteomics approach. *Cancer Lett.* 2008; 263:243-252.
12. Zhao B, Wang H, Zong G, Li P. The role of IFITM3 in the growth and migration of human glioma cells. *BMC Neurol.* 2013; 13:210.

13. Liu Y, Lu R, Cui W, Pang Y, Liu C, Cui L, Qian T, Quan L, Dai Y, Jiao Y, Pan Y, Ye X, Shi J, Cheng Z, Fu L. High IFITM3 expression predicts adverse prognosis in acute myeloid leukemia. *Cancer Gene Ther.* 2019.
14. Liu X, Chen L, Fan Y, Hong Y, Yang X, Li Y, Lu J, Lv J, Pan X, Qu F, Cui X, Gao Y, Xu D. IFITM3 promotes bone metastasis of prostate cancer cells by mediating activation of the TGF-beta signaling pathway. *Cell Death Dis.* 2019; 10:517.
15. Yan J, Jiang Y, Lu J, Wu J, Zhang M. Inhibiting of Proliferation, Migration, and Invasion in Lung Cancer Induced by Silencing Interferon-Induced Transmembrane Protein 1 (IFITM1). *Biomed Res Int.* 2019; 2019:9085435.
16. Jin B, Jin H, Wang J. WITHDRAWN: Silencing of Interferon-Induced Transmembrane Protein 1 (IFITM1) Inhibits Proliferation, Migration, and Invasion in Lung Cancer Cells. *Oncol Res.* 2017.
17. Min J, Feng Q, Liao W, Liang Y, Gong C, Li E, He W, Yuan R, Wu L. IFITM3 promotes hepatocellular carcinoma invasion and metastasis by regulating MMP9 through p38/MAPK signaling. *FEBS Open Bio.* 2018; 8:1299-1311.
18. Liang Y, Li E, Min J, Gong C, Gao J, Ai J, Liao W, Wu L. miR29a suppresses the growth and metastasis of hepatocellular carcinoma through IFITM3. *Oncol Rep.* 2018; 40:3261-3272.
19. Cole MD. The myc oncogene: its role in transformation and differentiation. *Annu Rev Genet.* 1986; 20:361-384.
20. Zhu P, Li Y, Li P, Zhang Y, Wang X. c-Myc induced the regulation of long non-coding RNA RHPN1-AS1 on breast cancer cell proliferation *via* inhibiting P53. *Mol Genet Genomics.* 2019.
21. Wang T, Cai B, Ding M, Su Z, Liu Y, Shen L. c-Myc Overexpression Promotes Oral Cancer Cell Proliferation and Migration by Enhancing Glutaminase and Glutamine Synthetase Activity. *Am J Med Sci.* 2019; 358:235-242.
22. Sun J, Zhang H, Tao D, Xie F, Liu F, Gu C, Wang M, Wang L, Jiang G, Wang Z, Xiao X. CircCDYL inhibits the expression of C-MYC to suppress cell growth and migration in bladder cancer. *Artif Cells Nanomed Biotechnol.* 2019; 47:1349-1356.
23. Chuu CP, Kokontis JM, Hiipakka RA, Fukuchi J, Lin HP, Lin CY, Huo C, Su LC, Liao S. Androgen suppresses proliferation of castration-resistant LNCaP 104-R2 prostate cancer cells through androgen receptor, Skp2, and c-Myc. *Cancer Sci.* 2011; 102:2022-2028.
24. Hu Y, Yu K, Wang G, Zhang D, Shi C, Ding Y, Hong D, Zhang D, He H, Sun L, Zheng JN, Sun S, Qian F. Lanatoside C inhibits cell proliferation and induces apoptosis through attenuating Wnt/beta-catenin/c-Myc signaling pathway in human gastric cancer cell. *Biochem Pharmacol.* 2018; 150:280-292.
25. Zhao Y, Jian W, Gao W, Zheng YX, Wang YK, Zhou ZQ, Zhang H, Wang CJ. RNAi silencing of c-Myc inhibits cell migration, invasion, and proliferation in HepG2 human hepatocellular carcinoma cell line: c-Myc silencing in hepatocellular carcinoma cell. *Cancer Cell Int.* 2013; 13:23.
26. Lin CP, Liu JD, Chow JM, Liu CR, Liu HE. Small-molecule c-Myc inhibitor, 10058-F4, inhibits proliferation, downregulates human telomerase reverse transcriptase and enhances chemosensitivity in human hepatocellular carcinoma cells. *Anticancer Drugs.* 2007; 18:161-170.
27. Tang Y, Ji F. lncRNA HOTTIP facilitates osteosarcoma cell migration, invasion and epithelial-mesenchymal transition by forming a positive feedback loop with c-Myc. *Oncol Lett.* 2019; 18:1649-1656.
28. Ifandi V, Al-Rubeai M. Stable transfection of CHO cells with the c-myc gene results in increased proliferation rates, reduces serum dependency, and induces anchorage independence. *Cytotechnology.* 2003; 41:1-10.
29. Yuan R, Wang K, Hu J, Yan C, Li M, Yu X, Liu X, Lei J, Guo W, Wu L, Hong K, Shao J. Ubiquitin-like protein FAT10 promotes the invasion and metastasis of hepatocellular carcinoma by modifying beta-catenin degradation. *Cancer Res.* 2014; 74:5287-5300.
30. Qiu Y, Yuan R, Zhang S, Chen L, Huang D, Hao H, Shao J. Rock2 stabilizes beta-catenin to promote tumor invasion and metastasis in colorectal cancer. *Biochem Biophys Res Commun.* 2015; 467:629-637.
31. Xu W, Gu J, Ren Q, Shi Y, Xia Q, Wang J, Wang S, Wang Y, Wang J. NFATC1 promotes cell growth and tumorigenesis in ovarian cancer up-regulating c-Myc through ERK1/2/p38 MAPK signal pathway. *Tumour Biol.* 2016; 37:4493-4500.
32. Shen Z, Zhang C, Qu L, Lu C, Xiao M, Ni R, Liu J. MKP-4 suppresses hepatocarcinogenesis by targeting ERK1/2 pathway. *Cancer Cell Int.* 2019; 19:61.
33. Gan CP, Sam KK, Yee PS, Zainal NS, Lee BKB, Abdul Rahman ZA, Patel V, Tan AC, Zain RB, Cheong SC. IFITM3 knockdown reduces the expression of CCND1 and CDK4 and suppresses the growth of oral squamous cell carcinoma cells. *Cell Oncol (Dordr).* 2019; 42:477-490.
34. Hu J, Wang S, Zhao Y, Guo Q, Zhang D, Chen J, Li J, Fei Q, Sun Y. Mechanism and biological significance of the overexpression of IFITM3 in gastric cancer. *Oncol Rep.* 2014; 32:2648-2656.
35. Tang J, Yan T, Bao Y, *et al.* lncRNA GLCC1 promotes colorectal carcinogenesis and glucose metabolism by stabilizing c-Myc. *Nat Commun.* 2019; 10:3499.
36. Cao XP, Cao Y, Zhao H, Yin J, Hou P. HMGA1 promoting gastric cancer oncogenic and glycolytic phenotypes by regulating c-myc expression. *Biochem Biophys Res Commun.* 2019; 516:457-465.
37. Yang P, Jiang Y, Pan Y, Ding X, Rhea P, Ding J, Hawke DH, Felsher D, Narla G, Lu Z, Lee RT. Mistletoe extract Fraxini inhibits the proliferation of liver cancer by down-regulating c-Myc expression. *Sci Rep.* 2019; 9:6428.

(Received October 23, 2019; Revised November 23, 2019; Accepted November 28, 2019)

# Shufengjiedu capsules protect against neuronal loss in olfactory epithelium and lung injury by enhancing autophagy in rats with allergic rhinitis

Jinyu Mei<sup>1,§,\*</sup>, Hua Kong<sup>2,§</sup>, Zhentao Zhao<sup>1</sup>, Ziyu Chen<sup>3</sup>, Yatang Wang<sup>1</sup>, Jianming Yang<sup>1</sup>

<sup>1</sup> Department of Otorhinolaryngology Head and Neck Surgery, the Second Affiliated Hospital of Anhui Medical University, Hefei, Anhui, China;

<sup>2</sup> Department of Pharmacology, School of Basic Medical Sciences, Anhui Medical University, Hefei, Anhui, China;

<sup>3</sup> The Second Clinical College of Medicine, Anhui Medical University, Hefei, Anhui, China.

## Summary

Shufengjiedu capsules (SFJDCs), a traditional Chinese medicine, have been widely used as an antiviral, antibacterial, antitumor, and anti-inflammatory drug. However, the roles of SFJDCs in allergic rhinitis remain unclear. The purpose of this study was to investigate the effects of SFJDCs in olfaction and lung injury in rats with allergic rhinitis. An animal model of allergic rhinitis was created by intraperitoneal injection and intranasal administration of ovalbumin to rats. All rats were divided into seven groups: a model group, a low-dose SFJDC group, a medium-dose SFJDC group, a high-dose SFJDC group, a cetirizine group, and a control group. Hematoxylin and eosin (HE) staining was used to observe pathological changes in rat lung and olfactory epithelium (OE) tissue, and peripheral blood was collected and subjected to an enzyme-linked immunosorbent assay (ELISA) to detect IgE, tumor necrosis factor alpha (TNF- $\alpha$ ), and IL-1 $\beta$  levels. Western blotting, immunohistochemistry staining, and immunofluorescence staining were performed to detect inflammatory cytokines and levels of the autophagy biomarker beclin1 and the apoptosis biomarker cleaved-caspase3 in lung and OE tissue. ELISA indicated that SFJDCs significantly decreased IgE, TNF- $\alpha$ , and IL-1 $\beta$  levels in peripheral blood, the lungs, and OE tissue. In addition, Western blotting and staining indicated that SFJDCs repair lung injury, protect against neuronal apoptosis in OE, and rescue impaired autophagy in the lungs and OE tissue. In conclusion, results indicated that SFJDCs might protect against neuronal loss in the OE and lung injury by enhancing autophagy and decreasing apoptosis in rats with allergic rhinitis. Therefore, SFJDCs might serve as an alternative treatment for allergic rhinitis.

**Keywords:** Shufengjiedu capsules, allergic rhinitis, inflammation, autophagy, apoptosis

## 1. Introduction

Allergic rhinitis (AR) is the most common otorhinolaryngological disease (1). It is also one of

the main causes of olfactory dysfunction (2). The primary clinical manifestations of AR include nasal blockage, a runny and itching nose, sneezing, and olfactory dysfunction (1). AR is an IgE-mediated type I hypersensitivity inflammatory disease of the nasal mucosa (3). IgE bound to Fc $\epsilon$ RI on mast cells and eosinophils is cross-linked by allergens, resulting in the release of diverse preformed and newly synthesized mediators to promote the local recruitment and activation of leukocytes and the production of inflammatory cytokines and T helper 2 (T<sub>2</sub>) cytokines, which contribute to the development of late-phase reactions (3). Current treatments for AR include

Released online in J-STAGE as advance publication December 21, 2019.

<sup>§</sup>These authors contributed equally to this work.

\*Address correspondence to:

Dr. Jinyu Mei, Department of Otorhinolaryngology Head and Neck Surgery, the Second Affiliated Hospital of Anhui Medical University, 678 Furong Road, Hefei, Anhui 230601, China.

E-mail: meijinyu@ahmu.edu.cn

antihistamines and hormones, but these drugs often have many untoward effects.

In China, traditional Chinese medicine (TCM) formulations, such as Radix isatidis and Radix bupleuri, have been extensively used to treat various respiratory infectious diseases. Shufengjiedu capsules (SFJDCs) are a TCM formulation consisting of eight medicinal herbs, *Polygonum cuspidatum* Sieb. et Zucc., *Forsythia suspense* (Thunb) Vahl, *Isatis indigotica* Fort., *Bupleurum chinense* DC., *Thlaspi arvense* L., *Verbena officinalis* (Officinalis) L., *Phragmites communistrin* Trin, and *Glycyrrhiza uralensis* Fisch., that are clinically effective at treating upper respiratory tract infections and ALI/ARDS (4). Since SFJDCs have antiviral action, the China Food and Drug Administration (CFDA) has recommended SFJDCs as a treatment for H1N1- and H5N9-induced acute lung injury (5). In China, SFJDCs have been listed as a drug to combat avian influenza (4,6-8). Studies have reported that active constituents of SFJDCs such as resveratrol and quercetin may alleviate inflammation by suppressing the expression of inflammatory factors *via* the mitogen-activated protein kinase (MAPK)/nuclear factor- $\kappa$ B (NF- $\kappa$ B) signaling pathway (9-11).

Autophagy is an intracellular self-degradative process that is responsible for the systematic degradation and recycling of cellular components such as misfolded or accumulated proteins and damaged organelles (12). One of the pivotal contributions of autophagy to immunity is the cell autonomous control of inflammation. This property leads to systemic consequences and thereby influences the development of innate and adaptive immunity, which promotes or suppresses pathology in various disease contexts. Autophagy can prevent excessive inflammasome activation and reduce the release of inflammatory factors such as TNF- $\alpha$  and IL-1 $\beta$  (13).

Olfactory dysfunction is one of the most common symptoms of AR (14-16). Proinflammatory cytokines (IL-1 $\beta$ , TNF- $\alpha$ , IL-18, IL-22, and IL-33) and OVA-specific IgE levels in peripheral blood are reported to be significantly increased in guinea pigs with ovalbumin (OVA)-induced AR (17). OVA can induce lung injury, which is characterized by acute hypoxemic respiratory failure with several potential causes that include trauma, shock, viruses, and bacterial endotoxins (18). Cells are increasingly exposed to intracellular oxidative stress and the downstream inflammatory pathway is triggered, leading to lung injury (19,20). When clinically used to treat influenza, SFJDCs can effectively improve symptoms such as nasal congestion, a runny nose, and headaches. Bupleurum, licorice, and other traditional Chinese medicines are important components of SFJDCs (4) and could be used to treat AR. However, few studies have examined the effect of SFJDCs on AR, especially in olfaction. The mechanism of SFJDCs on olfaction and lung injury remain unclear. Thus, the current study

sought to explore the effects of treatment with SFJDCs in olfactory epithelium (OE) and the lungs of rats with AR.

The aim of the current study was determine if SFJDCs significantly decrease TNF- $\alpha$  and IL-1 $\beta$  levels and apoptosis, rescue impaired autophagy, and protect against neuronal loss in OE. If SFJDCs repair lung injury and improve olfactory function by enhancing autophagy in rats with AR, then SFJDCs might serve as an alternative treatment for AR.

## 2. Materials and Methods

### 2.1. Animals and Materials

SFJDCs were donated by Jiren Pharmaceutical (Anhui, China). Sixty specific-pathogen-free male Sprague-Dawley rats weighing  $250 \pm 20$  g were purchased from Anhui Medical University's Animal Research Center (Anhui, China). These animals were fed in cages with a 12-hour light/dark cycle, constant temperature, and constant humidity in which mice were given food and water *ad libitum*. All animals involved in experiments were sacrificed in accordance with international standards. Animal care procedures were approved by the Institutional Animal Care and Use Committee (IACUC) of Anhui Medical University in accordance with the guidelines of the National Institutes of Health (Approval number: LLSC20190513).

### 2.2. An animal model of OVA-induced AR and drug administration

A previously reported protocol was followed to create an animal model of AR (21). The experiment timeline is shown in Figure 1A. The rats were randomly divided into six groups (6 mice per group per cage): a control group (Control), a model group (Model), a cetirizine (Yiling Pharmaceutical Company, Shijiazhuang, China) group (Lev, 0.75 g/kg), a high-dose SFJDC (Jiren pharmaceutical Company, Anhui, China) group (SFJDC-H, 0.18 g/kg), a medium-dose group (SFJDC-M, 0.09 g/kg), and a low-dose group (SFJDC-L, 0.045 g/kg) by gradient dilution. Rats were sensitized (every other day for 14 days) by intraperitoneal injection of 0.3 mg of OVA (Sigma A8040, USA) as an antigen and 30 mg of aluminum hydroxide as an adjuvant dissolved in 1 mL of saline. When *i.p.* immunization concluded, rats were administered 0.25% OVA dissolved in saline *via* aerosol (days 14-18). A nasal antigen challenge (days 21-27) was performed with intranasal dripping of 50  $\mu$ l of 5% OVA daily for 7 consecutive days. Animals in the control group were administered the same volume of saline. After OVA administration, animals in the cetirizine group and SFJDC groups were administered cetirizine or different doses of SFJDCs (twice/day for 14 consecutive days). The dosages of cetirizine and SFJDCs are the clinical recommended doses according to the

Chinese Pharmacopoeia. Moreover, combined symptom and behavior scoring was used to evaluate the model (21). Serum levels of cytokines were measured using ELISA performed with commercially available kits. Blood samples and nasal mucosa were collected for various assays.

### 2.3. Hematoxylin and eosin (H&E) Staining

Turbinate bone and lungs embedded in paraffin were sliced at a thickness of 4  $\mu$ m. Paraffin sections were de-paraffinized in xylene, rehydrated in serial dilutions of alcohol, and immersed in distilled water for 30 sec. Sections were dipped in a hematoxylin solution and agitated for 10 min and then rinsed with distilled water for 1 min. Sections were subsequently stained with a 1% eosin solution for 10 sec with agitation. Stained sections were dehydrated with increasing concentrations of alcohol (70% and 90% alcohol) for 10 min at a time and then immersed in eosin for 3 min. The sections were dehydrated with alcohol and immersed in xylene. Stained sections were observed using an electron microscope (Olympus, Japan).

### 2.4. Toluidine blue staining

Turbinate bone embedded in paraffin was sliced at a thickness of 4  $\mu$ m. Paraffin sections were de-paraffinized in xylene, rehydrated in serial dilutions of alcohol, and immersed in a toluidine blue solution for 30 min. Then sections were dipped in a glacial acetic acid solution and rinsed with distilled water for 1 min. The sections were dehydrated with alcohol and immersed in xylene. Stained sections were observed using an electron microscope (Olympus, Japan) (22).

### 2.5. Immunohistochemistry

For olfactory epithelium staining, animals were first sacrificed and decapitated. Skin and brain tissue were removed, and then the turbinate was removed and immersed in a 0.5 M EDTA (pH 8.0) solution at room temperature (RT) for 2 weeks. Paraffin-embedded OE tissue was sectioned into 4- $\mu$ m-thick slices. All tissue sections were mounted on glass slides. The slides were incubated for 12 hours at 4°C temperature with TNF- $\alpha$  (Abcam, ab62609) primary antibody in a humidified chamber, washed, and incubated for 50 min with goat anti-rabbit (074-1505, KPL) secondary antibody. Sections were analyzed with a microscope using a 20 and 40-fold magnification. Cell counting was performed with Image J whereby the cell number was normalized to the neuronal layer area (23).

### 2.6. Immunofluorescent staining

The OE and lung sections were incubated with beclin-1

(Affinity, AF5128), cleaved-caspase3 (Affinity, AF7022) and IL-1 $\beta$  (Affinity, AF5103) primary antibodies overnight at 4°C, washed with PBS, and then incubated in second antibodies at 37°C for 50 min. After the sections were washing with PBS, they were incubated in DAPI Staining Solution (Beyotime, C1005) for 10 min. The sections were washed with PBS. Afterwards, the slides were mounted with Antifade Mounting Medium (Beyotime, P0126-5ml), viewed, and photographed under a fluorescence microscope (Leica, Germany), and the images were evaluated using the software ImageJ (NIH, Bethesda, MD, USA).

### 2.7. Western blotting

Rats were dissected on ice, and tissue was homogenized in lysis buffer containing 50 mM Tris, pH 7.5, 150 mM NaCl, 1% SDS P40, 5 mM EDTA, and protease inhibitors (Complete Mini; Roche). Cellular debris was removed by centrifugation at 14,000 rpm for 20 min at 4°C, and the supernatant was collected for analysis. Sodium dodecylsulphate polyacrylamide gel electrophoresis (SDS-PAGE) was performed using a 5% stacking gel and a 10% separation gel to separate 20 L of protein in running buffer. The stacking gel was run at 80 V for 0.5 h, and the separation gel was run at 100 V for 1.5 h. The separated proteins were then electrotransferred onto a nitrocellulose filter membrane in transfer buffer at 180 mA for 1.5 h. Protein blots were blocked with 5% defatted milk for 30 min and probed with specific antibodies against TNF- $\alpha$  (Abcam, ab62609), IL-1 $\beta$  (Affinity, AF5103), Beclin-1 (Affinity, AF5128), and cleaved-caspase3 (Affinity, AF7022). Anti- $\alpha$ -tubulin antibody (Sigma, T6557) was used as a loading control. After three washes with TBST, secondary antibody (CWS) was added at room temperature for 1 h using 5% milk in TBST followed by three additional washes with TBST. Bands were visualized using the Immobilon Western ECL system and were analyzed with the software Gel Pro Analysis (24).

### 2.8. Statistical analysis

Data were analyzed using one-way ANOVA or a two-sample *t*-test, where  $p < 0.05$  was considered statistically significant. All data are expressed as the mean  $\pm$  SEM.

## 3. Results

### 3.1. SFJDCs decreased increased serum IgE and mast cells in OE tissue

Nasal rubbing and watery rhinorrhea are two common symptoms of AR in rats (1). In order to detect the effects of SFJDCs on these symptoms, an experiment was performed along the timeline shown in Figure

1A. The frequency of sneezing and nasal rubbing was observed and recorded. All animals were closely observed for development of any nasal symptoms such as sneezing or watery rhinorrhea. In comparison to the control group, mice in the AR model group had clear nasal secretions and an increased frequency of nasal rubbing (data not shown). Figure 1B shows that rats with OVA-induced AR had more watery rhinorrhea. As shown in Figure 1C, IgE levels were lower in the SFJDC-M group than those in the model group but did not differ significantly from those in the SFJDC-L and SFJDC-H groups. As shown in Figure 1D, treatment with SFJDCs significantly reduced the number of mast cells in OE tissue. These findings indicate that SFJDCs alleviated allergic symptoms in rats with AR.

### 3.2. Morphological changes in lungs and OE tissue

As shown in Figure 2A, the model group displayed capillary congestion, obstruction of small airways by lymphocytic infiltrates, and widened alveolar septa in comparison to the control group. Treatment with medium-dose SFJDCs (0.09 g/kg) significantly reduced histological injury, such as decreasing obstruction of

small airways, to different degrees. As shown in Figure 2B and C, OE appeared thinner and had fewer neurons than that in the control group. The number of neurons in OE increased in the SFJDC-M and cetirizine groups.

### 3.3. Levels of $TNF-\alpha$ and $IL-1\beta$ in serum, the lungs, and OE tissues

As shown in Figure 3A, ELISA was used to determine levels of  $TNF-\alpha$  and  $IL-1\beta$  in serum in each group. Results indicated that  $TNF-\alpha$  and  $IL-1\beta$  levels increased significantly in the model group compared to those in the control group. Rats treated with SFJDCs had a marked decrease in levels of  $TNF-\alpha$  and  $IL-1\beta$ . As shown in Figure 3B, Western blotting was used to detect levels of  $TNF-\alpha$  and  $IL-1\beta$  expression in lung tissue. Results indicated that levels of  $TNF-\alpha$  and  $IL-1\beta$  protein increased in the model group in comparison to those in the control group. SFJDCs caused a marked decrease in the levels of  $TNF-\alpha$  and  $IL-1\beta$  expression in each group. As shown in Figure 3C, immunohistochemistry staining was used to quantify the  $TNF-\alpha$  expression in OE tissue in different groups. Results indicated that  $TNF-\alpha$  levels decreased significantly in the SFJDC-H and

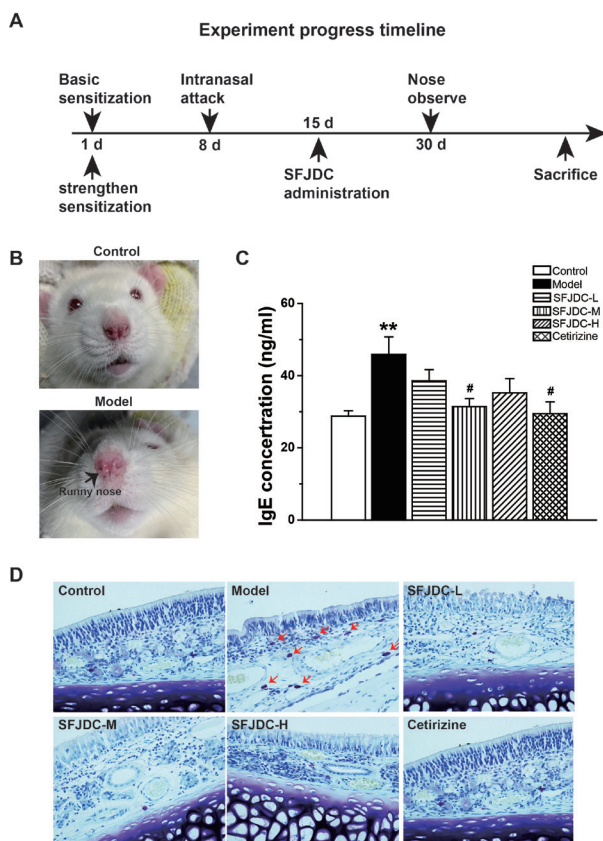


**Figure 1.** SFJDCs reduced levels of IgE and the number of mast cells in rats with AR. (A): Schematic overview of the study design. (B): Watery rhinorrhea in the model group. (C): Bar graph of the IgE level in serum according to ELISA. (D): Toluidine blue staining of OE from different groups. Arrows indicate mast cells. Data are representative of at least three separate experiments. (\*\* $p < 0.01$  vs. control group; # $p < 0.05$  vs. model group).

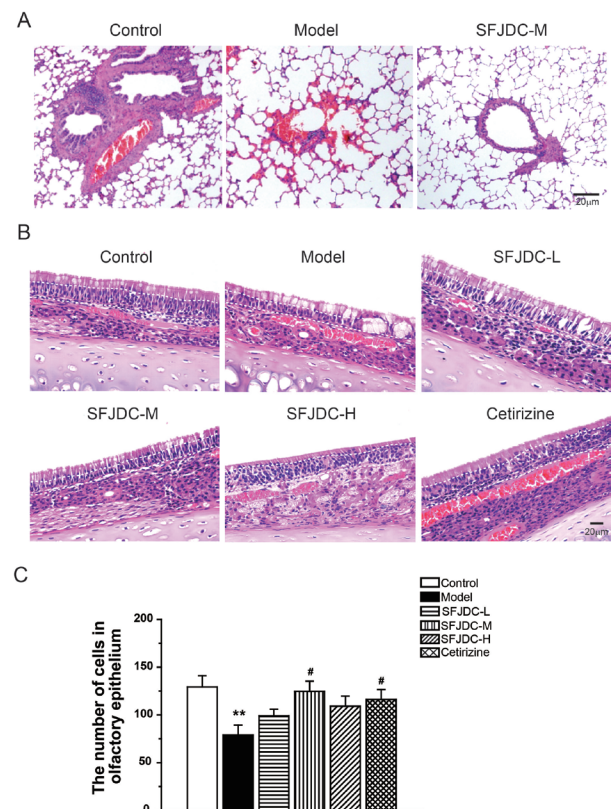


**Figure 2.** SFJDCs protect against lung injury and OE neuronal loss in rats with AR. (A): HE staining of lung tissue from the control, model, and SFJDC-M groups. (B): HE staining of OE from the control, model, SFJDC-L, SFJDC-M, SFJDC-H, and cetirizine groups. (C): Bar graph of cell numbers in OE. Data are representative of at least three separate experiments. (\*\* $p < 0.01$  vs. control group; # $p < 0.05$  vs. model group).

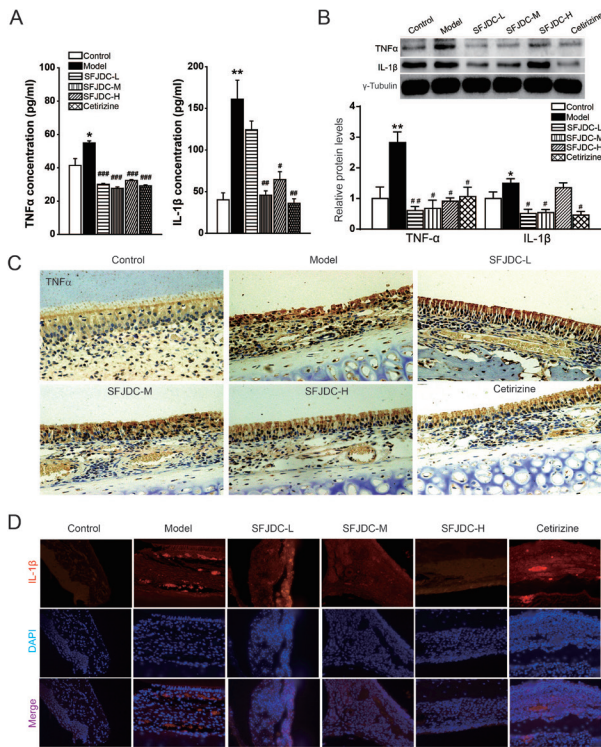


**Figure 3. SFJDCs reduced increased TNF- $\alpha$  and IL-1 $\beta$  levels in serum, the lungs, and OE. (A):** Bar graph of TNF- $\alpha$  and IL-1 $\beta$  concentrations in serum detecting with ELISA. **(B):** Western blot bands of TNF- $\alpha$  and IL-1 $\beta$  protein in lung tissue. Bar graph of levels of TNF- $\alpha$  and IL-1 $\beta$  protein in lung tissue. **(C):** Immunohistochemistry staining of TNF- $\alpha$  in OE tissue. **(D):** Immunofluorescent staining of IL-1 $\beta$  in OE tissue. Data are representative of at least three separate experiments. (\* $p < 0.05$ , \*\* $p < 0.01$  vs. control group; # $p < 0.05$ , ## $p < 0.01$ , ### $p < 0.001$  vs. model group).

cetirizine groups. There were no significant differences in those levels in the SFJDC-L and SFJDC-M groups. As shown in Figure 3D, immunofluorescent staining was performed to detect the level of IL-1 $\beta$  in OE tissue. Red fluorescence for IL-1 $\beta$  increased in the model group in comparison to that the control group, and red fluorescence decreased in the SFJDC-M and SFJDC-H groups. The results shown in Figure 3 indicate that SFJDCs decreased inflammation levels in rats with AR.

**3.4. Levels of autophagy and apoptosis in the lungs and OE tissue**

As shown in Figure 4, red fluorescence for beclin1 was not evident in the model group, indicating a very low level of autophagy. Green fluorescence for caspase3 increased in the model group in comparison to that in the control group, indicating that the level of apoptosis increased in the model group. When rats were treated with SFJDCs, the beclin1 level significantly increased in the SFJDC-M and SFJDC-H groups. A lower level of caspase3 was observed only in the SFJDC-L group. When Western blotting was used to detect levels of beclin1 and caspase3 protein expression, the same trend was observed, indicating that SFJDCs increased the level

of autophagy and decreased apoptosis. Since OE lesions also appeared, as shown in Figure 5, immunofluorescent staining was used to detect beclin1 and caspase3 levels in OE tissue. Results indicated that the beclin1 level decreased and the caspase3 level increased in the model group in comparison to levels in the control group. SFJDCs resulted in a marked increase in the level of beclin1 and a marked decrease in the level of caspase3 in the SFJDC-M and SFLDC-H groups.

**4. Discussion**

The current study found that SFJDCs reduce neuronal loss in OE and protect against lung injury induced by AR by increasing the level of autophagy and reducing apoptosis and inflammation factors in rats with AR. These findings are corroborated by several lines of evidence: (i) SFJDCs ameliorate the symptoms of AR, such as a runny or itching nose, sneezing, a decrease in the number of mast cells, and a lower level of IgE (which are markers of an allergy); (ii) TNF $\alpha$  and IL-1 $\beta$  levels in serum, OE, and lung tissues are downregulated by treatment with SFJDCs; (iii) SFJDCs rescue the levels of beclin1 and cleaved-caspase3 protein, which are respective biomarkers of autophagy and apoptosis. Together, these findings indicate that SFJDCs may play a critical role in AR.

In order to study the effects of SFJDCs on AR, the first step in the current study was to create a reliable animal model of AR. OVA is mainly used as an allergen to create animal models of AR (25-27). The primary clinical manifestations of AR include nasal blockage, a runny and itching nose, sneezing, and olfactory dysfunction (1). In the current study, rats had a runny and itching nose and sneezing after OVA treatment (Figure 1B). A high level of IgE and an increase in mast cells are common hallmarks of AR. Mast cells release molecules that can lead to an allergic reaction. Treatment with SFJDCs decreased nasal rubbing and watery rhinorrhea in rats with AR. Together, these findings indicate that an animal model of AR was successfully created and that SFJDCs ameliorated some symptoms of AR.

OVA is mainly used as an allergen to create animal models of AR (21). In the current study, however, OVA-induced AR produced pathological changes in rats not only in olfactory tissue but also in the lungs (Figure 2A-C). Although several studies have found that asthma and rhinitis are characterized by a similar inflammatory process (28-30), pathophysiologic interactions between the upper and lower airways are not entirely understood. The condition of the upper airway definitely influences the lower airway. The current study considered whether lung injury was caused by AR. AR triggers a systemic increase in inflammation (31). Numerous studies have indicated that the active constituents of SFJDCs, such as resveratrol and other flavonoids, inhibit acute lung injury (ALI). In addition, the MAPK and NF-kB signaling

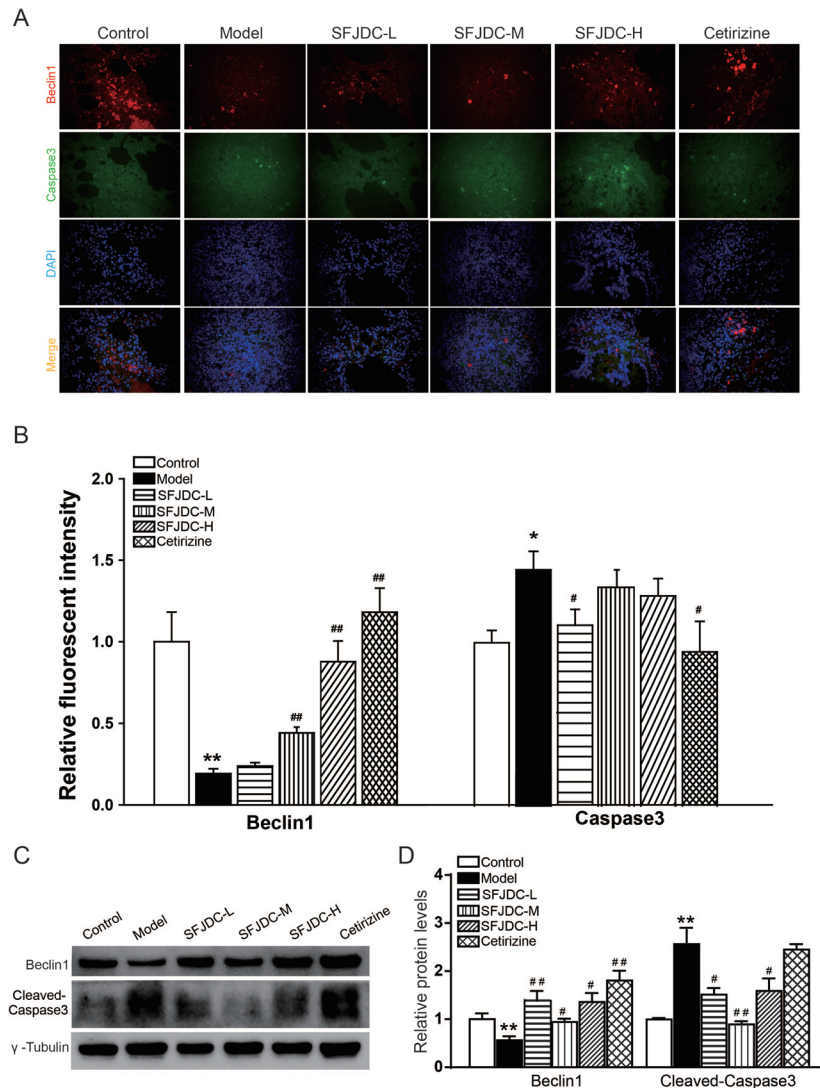


**Figure 4. SFJDCs rescued impaired autophagy and levels of apoptosis in lung tissue. (A):** Immunofluorescent staining of beclin1 and cleaved-caspase3 in lung tissue. **(B):** Bar graph of levels of beclin1 and cleaved-caspase3 expression in lung tissue. **(C):** Western blot bands of beclin1 and cleaved-caspase3 protein in lung tissue. **(D):** Bar graph of Western blot bands in Figure 5 (C). Data are representative of at least three separate experiments. (\* $p < 0.05$ , \*\* $p < 0.01$  vs. control group; # $p < 0.05$ , ## $p < 0.01$  vs. model group).

pathways may be involved in ALI (32-38). NF- $\kappa$ B is a key factor in the inflammatory response and is involved in the release of inflammatory factors and development of ALI (39,40). IL-1 $\beta$  and TNF- $\alpha$  may serve as biomarkers of the NF- $\kappa$ B inflammatory pathway. SFJDCs are reported to alleviate inflammation by inhibiting IL-1 $\beta$  in the NF- $\kappa$ B signaling pathway. The current study found that IL-1 $\beta$  and TNF- $\alpha$  levels decreased significantly when rats were treated with SFJDCs, indicating that SFJDCs ameliorate AR by regulating inflammation levels. Autophagy can prevent excessive inflammasome activation and reduce the release of inflammatory factors such as TNF- $\alpha$  and IL-1 $\beta$  (13). In a physiological state, autophagy can promote apoptosis. Examination of nasal lavage fluid from rats with AR has revealed apoptosis of eosinophils. However, the role of autophagy in AR still remain unknown. Measurement of beclin1 and caspase3 protein levels revealed that SFJDCs improved levels of

autophagy and inhibited apoptosis in OE and lung tissue. These findings indicate that SFJDCs may alleviate lung injury by mediating autophagy and apoptosis and by reducing the release of inflammatory factors in lung tissue.

Olfactory function is reported to be impaired in rats with AR (14). The current study used HE staining to observe the pathology of OE tissue in rats. Rats treated with SFJDCs had more neurons in OE tissue. The immunofluorescent staining of caspase3 indicated that SFJDCs markedly decreased apoptosis in OE tissue. Inflammatory factors such as TNF- $\alpha$  and IL-1 $\beta$  can induce an increase in apoptosis. Like rats treated with cetirizine, rats treated with SFJDCs had a marked decrease in inflammatory factors and levels of apoptosis in OE tissue. The level of autophagy increased when rats were treated with SFJDCs. These findings indicate that SFJDCs may protect against neuronal loss in OE

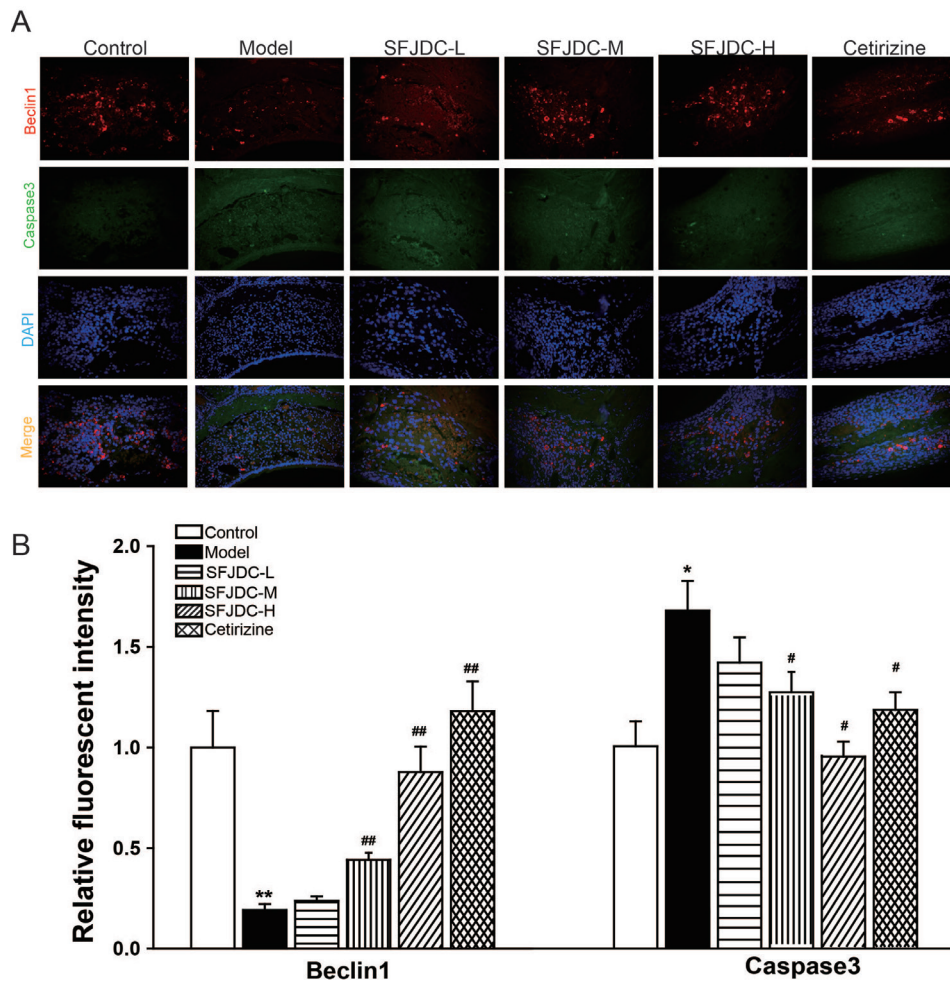


**Figure 5. SFJDCs rescued impaired autophagy and levels of apoptosis in OE tissue. (A):** Immunofluorescent staining of beclin1 and cleaved-caspase3 in OE tissue. **(B):** Bar graph of levels of beclin1 and cleaved-caspase3 expression in OE tissue. Data are representative of at least three separate experiments. (\* $p < 0.05$ , \*\* $p < 0.01$  vs. control group; # $p < 0.05$ , ## $p < 0.01$  vs. model group).

by mediating autophagy, apoptosis, and the release of inflammatory factors.

In conclusion, this study revealed that SFJDCs alleviate OVA-induced AR in a rat model by mediating levels of autophagy and apoptosis and by suppressing the release of inflammatory factors. Thus, SFJDCs might serve as an alternative medication to inhibit inflammation in OE and lung tissue, and SFJDCs have great potential for widespread clinical use.

**Acknowledgements**

This work was financially supported by grants from the Major Basic Research Program in Universities of Anhui (No. KJ2018ZD021). The authors wish to thank Wanpeng Lu and Xiangming Tao for providing technical support.

*Statement of Ethics*

Animal care procedures were approved by the Institutional Animal Care and Use Committee (IACUC)

at Anhui Medical University in accordance with the guidelines of the National Institutes of Health.

**References**

1. Bousquet J, Khaltaev N, Cruz AA, *e al.* Allergic Rhinitis and its Impact on Asthma (ARIA) 2008 update (in collaboration with the World Health Organization, GA(2) LEN and AllerGen). *Allergy*. 2008; 63 Suppl 86:8-160.
2. Guilemany JM, García-Piñero A, Alobid I, Cardelús S, Centellas S, Bartra J, Valero A, Picado C, Mullol J. Persistent allergic rhinitis has a moderate impact on the sense of smell, depending on both nasal congestion and inflammation. *Laryngoscope*. 2009; 119:233-238
3. Wei-Xu H, Wen-Yun Z, Xi-Ling Z, Zhu W, Li-Hua W, Xiao-Mu W, Hui-Ping W, Wen-Ding W, Dan H, Qin X, Guo-Zhu H. Anti-Interleukin-1 beta/tumor necrosis ractor-alpha IgY antibodies reduce pathological allergic responses in Guinea pigs with allergic rhinitis. *Mediators Inflamm*. 2016; 2016:3128182.
4. Tao Z, Gao J, Zhang G, Xue M, Yang W, Tong C, Yuan Y. Shufeng Jiedu Capsule protect against acute lung injury by suppressing the MAPK/NF-kappaB pathway. *Biosci Trends*. 2014; 8:45-51.

5. Tao Z, Yang Y, Shi W, Xue M, Yang W, Song Z, Yao C, Yin J, Shi D, Zhang Y, Cai Y, Tong C, Yuan Y. Complementary and alternative medicine is expected to make greater contribution in controlling the prevalence of influenza. *Biosci Trends*. 2013;7:253-256.
6. Bao Y, Gao Y, Cui X. Effect of Shufeng Jiedu capsules as a broad-spectrum antibacterial. *Biosci Trends*. 2016; 10:74-78.
7. Cheng L, Li F, Ma R, Hu X. Forsythiaside inhibits cigarette smoke-induced lung inflammation by activation of Nrf2 and inhibition of NF- $\kappa$ B. *Int Immunopharmacol*. 2015; 28:494-499.
8. Li Y, Chang N, Han Y, Zhou M, Gao J, Hou Y, Jiang M, Zhang T, Bai G. Anti-inflammatory effects of Shufengjiedu capsule for upper respiratory infection *via* the ERK pathway. *Biomed Pharmacother*. 2017; 94:758-766.
9. Busch F1, Mobasheri A, Shayan P, Lueders C, Stahlmann R, Shakibaei M. Resveratrol modulates interleukin-1 $\beta$ -induced phosphatidylinositol 3-kinase and nuclear factor  $\kappa$ B signaling pathways in human tenocytes. *J Biol Chem*. 2012; 287:38050-380563.
10. Gao J, Inagaki Y, Li X, Kokudo N, Tang W. Research progress on natural products from traditional Chinese medicine in treatment of Alzheimer's disease. *Drug Discov Ther*. 2013; 7:46-57.
11. Song Y, Liu J, Zhang F, Zhang J, Shi T, Zeng Z. Antioxidant effect of quercetin against acute spinal cord injury in rats and its correlation with the p38MAPK/iNOS signaling pathway. *Life Sci*. 2013; 92:1215-1221.
12. Glick D, Barth S, Macleod KF. Autophagy: Cellular and molecular mechanisms. *J Pathol*. 2010; 221:3-12.
13. Deretic V, Levine B. Autophagy balances inflammation in innate immunity. *Autophagy*. 2018; 14:243-251.
14. Ozaki S, Toida K, Suzuki M, Nakamura Y, Ohno N, Ohashi T, Nakayama M, Hamajima Y, Inagaki A, Kitaoka K, Sei H, Murakami S. Impaired olfactory function in mice with allergic rhinitis. *Auris Nasus Larynx*. 2010; 37:575-583.
15. Mott AE, Cain WS, Lafreniere D, Leonard G, Gent JF, Frank ME. Topical corticosteroid treatment of anosmia associated with nasal and sinus disease. *Arch Otolaryngol Head Neck Surg*. 1997; 123: 367-372.
16. Simola M, Malmberg H. Sense of smell in allergic and nonallergic rhinitis. *Allergy*. 1998; 53:190-194.
17. Guo-Zhu H, Xi-Ling Z, Zhu W, Li-Hua W, Dan H, Xiao-Mu W, Wen-Yun Z, Wei-Xu H. Therapeutic potential of combined anti-IL-1 $\beta$  IgY and anti-TNF- $\alpha$  IgY in guinea pigs with allergic rhinitis induced by ovalbumin. *Int Immunopharmacol*. 2015; 25:155-161.
18. Vlaar AP, Juffermans NP. Transfusion-related acute lung injury: A clinical review. *Lancet*. 2013; 382:984-994.
19. Ellison MA, Ambruso DR, Silliman CC. Therapeutic options for transfusion related acute lung injury: The potential of the G2A receptor. *Curr Pharm Des*. 2012; 18:3255-3259.
20. Ward PA. Oxidative stress: Acute and progressive lung injury. *Ann N Y Acad Sci*. 2010 Aug;1203:53-59.
21. Wang X, Zhu Y, Ni D, Lv W, Gao Z, Qi F. Intranasal application of glucocorticoid alleviates olfactory dysfunction in mice with allergic rhinitis. *Exp Ther Med*. 2017; 14:3971-3978.
22. Ratna Kumari TVN, Ahmed Mujib BR. Toluidine blue with a synergistic effect in morphological assessment of oral cytosmeas. *J Cytol*. 2018; 35:8-14.
23. Zhang J, Hao C, Jiang J, Feng Y, Chen X, Zheng Y, Liu J, Zhang Z, Long C, Yang L. The mechanisms underlying olfactory deficits in apolipoprotein E-deficient mice: Focus on olfactory epithelium and olfactory bulb. *Neurobiol Aging*. 2018; 62:20-33.
24. Chen M, Wang J, Jiang J, *et al*. APP modulates KCC2 expression and function in hippocampal GABAergic inhibition. *Elife*. 2017; 6. pii: e20142.
25. Takahashi N, Aramaki Y, Tsuchiya S. Allergic rhinitis model with Brown Norway rat and evaluation of antiallergic drugs. *J Pharmacobiodyn*. 1990; 13:414-420.
26. Nakaya M, Dohi M, Okunishi K, Nakagome K, Tanaka R, Imamura M, Baba S, Takeuchi N, Yamamoto K, Kaga K. Noninvasive system for evaluating allergen-induced nasal hypersensitivity in murine allergic rhinitis. *Lab Invest*. 2006; 86:917-26.
27. Tanaka K, Okamoto Y, Nagaya Y, Nishimura F, Takeoka A, Hanada S, Kohno S, Kawai M. A nasal allergy model developed in the guinea pig by intranasal application of 2,4-toluene diisocyanate. *Int Arch Allergy Appl Immunol*. 1988; 85:392-397.
28. Bousquet J, Chanez P, Lacoste JY, Barnéon G, Ghavanian N, Enander I, Venge P, Ahlstedt S, Simony-Lafontaine J, Godard P, Michel F. Eosinophilic inflammation in asthma. *N Engl J Med*. 1990; 323:1033-1039.
29. Bentley AM, Jacobson MR, Cumberworth V, Barkans JR, Moqbel R, Schwartz LB, Irani AM, Kay AB, Durham SR. Immunohistology of the nasal mucosa in seasonal allergic rhinitis: Increases in activated eosinophils and epithelial mast cells. *J Allergy Clin Immunol*. 1992; 89:877-883.
30. Bradley BL, Azzawi M, Jacobson M, Assoufi B, Collins JV, Irani AM, Schwartz LB, Durham SR, Jeffery PK, Kay AB. Eosinophils, T-lymphocytes, mast cells, neutrophils, and macrophages in bronchial biopsy specimens from atopic subjects with asthma: Comparison with biopsy specimens from atopic subjects without asthma and normal control subjects and relationship to bronchial hyperresponsiveness. *J Allergy Clin Immunol*. 1991; 88:661-674.
31. Borish L. Allergic rhinitis: systemic inflammation and implications for management. *J Allergy Clin Immunol*. 2003; 112:1021-1031.
32. Meng G, Liu Y, Lou C, Yang H. Emodin suppresses lipopolysaccharide-induced pro-inflammatory responses and NF- $\kappa$ B activation by disrupting lipid rafts in CD14-negative endothelial cells. *Br J Pharmacol*. 2010; 161:1628-1644.
33. Nepal M, Li L, Cho HK, Park JK, Soh Y. Kaempferol induces chondrogenesis in ATDC5 cells through activation of ERK/BMP-2 signaling pathway. *Food Chem Toxicol*. 2013; 62:238-245.
34. Chien YC, Sheu MJ, Wu CH, Lin WH, Chen YY, Cheng PL, Cheng HC. A Chinese herbal formula "Gan-Lu-Yin" suppresses vascular smooth muscle cell migration by inhibiting matrix metalloproteinase-2/9 through the PI3K/AKT and ERK signaling pathways. *BMC Complement Altern Med*. 2012; 12:137.
35. Kim A, Yim NH, Im M, Jung YP, Liang C, Cho WK, Ma JY. Ssanghwa-tang, an oriental herbal cocktail, exerts anti-melanogenic activity by suppression of the p38 MAPK and PKA signaling pathways in B16F10 cells. *BMC Complement Altern Med*. 2013; 13:214.
36. Wu JS, Shi R, Zhong J, Lu X, Ma BL, Wang TM, Zan B, Ma YM, Cheng NN, Qiu FR. Renal Protective

- Role of Xiexin Decoction with Multiple Active Ingredients Involves Inhibition of Inflammation through Downregulation of the Nuclear Factor- $\kappa$ B Pathway in Diabetic Rats. *Evid Based Complement Alternat Med.* 2013; 2013:715671.
37. Yoo H, Ku SK, Baek YD, Bae JS. Anti-inflammatory effects of rutin on HMGB1-induced inflammatory responses *in vitro* and *in vivo*. *Inflamm Res.* 2014; 63:197-206.
38. Xia JF, Gao JJ, Inagaki Y, Kokudo N, Nakata M, Tang W. Flavonoids as potential anti-hepatocellular carcinoma agents: Recent approaches using HepG2 cell line. *Drug Discov Ther.* 2013; 7:1-8.
39. Chi G, Wei M, Xie X, Soromou LW, Liu F, Zhao S. Suppression of MAPK and NF- $\kappa$ B pathways by limonene contributes to attenuation of lipopolysaccharide-induced inflammatory responses in acute lung injury. *Inflammation.* 2013; 36:501-511.
40. Zhu T, Wang DX, Zhang W, Liao XQ, Guan X, Bo H, Sun JY, Huang NW, He J, Zhang YK, Tong J, Li CY. Andrographolide protects against LPS-induced acute lung injury by inactivation of NF- $\kappa$ B. *PLoS One.* 2013; 8:e56407

(Received May 17, 2019; Revised September 2, 2019; Re-revised December 4, 2019; Accepted December 15, 2019)

# The impact of apurinic-apyrimidinic endonuclease I on hepatocyte immuno-inflammatory factors and cell apoptosis

Tatsuo Sawakami<sup>1,§</sup>, Zhipeng Sun<sup>2,§,\*</sup>, Yoshinori Inagaki<sup>1</sup>, Kiyoshi Hasegawa<sup>1</sup>, Wei Tang<sup>1,3</sup>, Guangzhong Xu<sup>2</sup>, Nengwei Zhang<sup>2,\*</sup>

<sup>1</sup> Division of Hepato-Biliary-Pancreatic Surgery, Department of Surgery, Graduate School of Medicine, The University of Tokyo, Tokyo, Japan;

<sup>2</sup> Oncology Surgery Department, Beijing Shijitan Hospital, Capital Medical University (Peking University Ninth School of Clinical Medicine), Beijing, China;

<sup>3</sup> National Center for Global Health and Medicine, Tokyo, Japan.

## Summary

To explore the effect of apurinic-apyrimidinic endonuclease I (APE-1) on hepatocyte immune inflammatory factors and cell apoptosis. The gene expression profiles of peripheral blood of patients with or without immune tolerance after liver transplantation were obtained from the Gene Expression Omnibus (GEO). Differentially expressed genes were analyzed with a program in the R language, and the APE-1 gene was identified as a gene related to immune tolerance of liver transplantation. Four APE-1 shRNA vectors were constructed in parallel and verified as correct using plasmid sequencing, real-time PCR, and Western blotting. An APE-1 overexpression vector was similarly constructed and verified as correct. The STRING website predicted the protein-protein interaction network of APE-1. ELISA was used to detect the effects of APE-1 silencing and overexpression on inflammatory cytokines IL-1 $\beta$ , IL-10, TNF $\alpha$ , and INF- $\gamma$  in the control group, APE-1-silenced group, and APE-1 overexpression group. Flow cytometry was used to detect apoptosis in each group. Forty differentially expressed genes related to immune tolerance after liver transplantation were screened, and the highly expressed gene APE-1 was selected. The best APE-1 shRNA\_1 vector and APE-1 overexpression vector were obtained. APE-1 is predicted to interact with ANP32A, FEN1, HMGB2, LIG1, MUTYH, NTHL1, OGG1, PCNA, POLB, SET, and other proteins. APE-1 silencing resulted in a significant increase in the expression of the inflammatory factors IL-1 $\beta$ , IL-10, TNF $\alpha$ , and INF- $\gamma$  in L-02 cells. In contrast, the expression of APE-1 led to a significant decrease in the expression of inflammatory factors. APE-1 silencing significantly increased the rate of apoptosis of L-02 cells, and APE-1 overexpression resulted in a significant decrease in the rate of apoptosis of L-02 cells. In conclusion APE-1 affects the expression of inflammatory factors and apoptosis in L-02 cells, so it may be a key gene in immune tolerance of liver transplantation.

**Keywords:** Liver transplantation; immune tolerance; apurinic-apyrimidinic endonuclease I (APE-1); small hairpin RNA (shRNA); cell apoptosis

## 1. Introduction

Liver transplantation has become an effective method for the treatment of end-stage liver disease. Patients

have a 1-year and 5-year survival rate of 85% and 70%, respectively. However, the incidence of primary graft non-function is still as high as 15%. Liver transplantation faces the challenge of immune rejection (I). Over the past few years, an increasing number of studies have shown that peripheral blood microarray detection can provide biomarkers of transcriptions that help to identify immune tolerance after liver transplantation. The current study was based on transcriptome data from patients with immune tolerance after liver transplantation. Once apurinic-apyrimidinic endonuclease I (apurinic-

<sup>§</sup>These authors contributed equally to this work.

\*Address correspondence to:

Drs. Zhipeng Sun & Nengwei Zhang, Oncology Surgery Department, Beijing Shijitan Hospital, Capital Medical University (Peking University Ninth School of Clinical Medicine), Beijing 100038, China.

E-mail: sunzhipeng56084@163.com, zhangnw1@sohu.com

aprimidinic endonuclease I, or APE-1) was identified as a gene related to immune tolerance after liver transplantation, APE-1 shRNA and an overexpression vector were constructed to further explore its impact on the expression of immunoinflammatory factors and apoptosis in the L-02 human normal liver cell line.

**2. Materials and Methods**

*2.1. Data acquisition and main reagents*

*2.1.1. Data acquisition and cell sources*

GSE11881 raw data were downloaded from the Gene Expression Omnibus (GEO) (<https://www.ncbi.nlm.nih.gov/geo/query/acc.cgi?acc=GSE11881>). The L-02 human normal liver cell line was purchased from the Peking Union Basic Research Institute.

*2.1.2. Main reagents*

The total RNA extraction reagent TRIzol, the SYBR<sup>®</sup> PrimeScript<sup>™</sup> RT-PCR Kit, and mRNA SYBR Green fluorescent PCR reagents were purchased from Takara, Japan. A RIPA lysate for protein extraction, a BCA protein concentration test kit, and SDS-PAGE gel reagents were purchased from Jiangsu Beyotime. IL-1 $\beta$ , IL-10, TNF $\alpha$ , and INF- $\gamma$  ELISA kits were purchased from Beijing Berui Technology. The cell transfection reagent Lipo 2000 was purchased from Invitrogen, USA. APE1 antibody and GAPDH antibody were purchased from Abcam, UK. An Annexin V-FITC/PI double-stain apoptosis detection kit was purchased from Jiangsu Keygen Biotech. The pLKO.1-puro vector was purchased from Sigma Aldrich China.

*2.2. Procedure*

*2.2.1. Screening for differentially expressed genes related to immune tolerance after liver transplantation*

After gene expression values for each sample were homogenized using a program in the R language, the statistical significance of the differences was set at < 0.05, and patients with or without immune tolerance after liver transplantation were screened for

differentially expressed genes.

*2.2.2. Construction of an APE-1 shRNA vector*

Four pairs of APE-1 shRNA sequences were designed and synthesized, as shown in Table 1. Annealing of shRNA primers. The primers were diluted with ultrapure water to 10  $\mu$ M. After the upstream primer was mixed with the downstream primer at a ratio of 1:1, the mixture was denatured at 100 $^{\circ}$ C for 10 min in a water bath and then cooled down naturally to room temperature. Selection of the pLKO.1 plasmid vector (<https://www.sigmaaldrich.com/content/dam/sigma-aldrich/docs/Sigma/Bulletin/shc001bul.pdf>) and linearized pLKO.1 plasmid vector: 30  $\mu$ l and 150 ng/ $\mu$ L of pLKO.1 were prepared for digestion. A pLKO.1 vector double-digestion system was constructed. After digestion at 37 $^{\circ}$ C for 3 h, the plasmid was recovered, purified, and dissolved in 30  $\mu$ L of TE buffer. The pLKO.1 plasmid was ligated into the vector and verified with sequencing.

*2.2.3. Cell transfection / Seeding cells*

L-02 cells were seeded onto 6-well plates (1x10<sup>6</sup> cells/well) 1 day prior to transfection. Transfection started when cell confluence reached 90%, and the media were changed 2 h before transfection. Seven-point-five  $\mu$ g of plasmid DNA was added to 250  $\mu$ L of OPTI-MEM media and mixed thoroughly. Then, 10  $\mu$ l of Lipo 2000 was added to another 250  $\mu$ L of OPTI-MEM and mixed gently. The mixture was allowed to stand at room temperature for 5 min. The DNA suspension was mixed with the Lipo 2000 suspension, reaching a total volume of 500  $\mu$ L. After gentle mixing, the mixture was allowed to stand at room temperature for 20 min. After thorough mixing by shaking, the DNA and Lipo 2000 mixture was added to each well of the 6-well plates. The plates were placed in an incubator. After transfection for 6 h, the media were changed (2 mL in each well). After transfection for 48 h, the cells were harvested for detection of expression.

*2.2.4. Real-time PCR detection of APE-1 mRNA expression in L-02 cells*

Total cellular RNA was extracted using the Trizol

**Table 1. Four pairs of APE-1 shRNA sequences in parallel**

shRNA name	Sequence information
shRNA_1-F	CCGGCAGAGAAATCTGCATTCTATTCTCGAGAATAGAATGCAGATTCTCTGTTTT
shRNA_1-R	AATTCAAAAACAGAGAAATCTGCATTCTATTCTCGAGAATAGAATGCAGATTCTCTG
shRNA_2-F	CCGGCCTGGACTCTCTCATCAATACTCGAGTATTGATGAGAGAGTCCAGGCTTTTT
shRNA_2-R	AATTCAAAAAGCTGGACTCTCTCATCAATACTCGAGTATTGATGAGAGAGTCCAGGC
shRNA_3-F	CCGGCCACTCTCTGTTACCTGCATTCTCGAGAATGCAGGTAACAGAGAGTGGTTTTT
shRNA_3-R	AATTCAAAAACCACTCTCTGTTACCTGCATTCTCGAGAATGCAGGTAACAGAGAGTGG
shRNA_4-F	CCGGCCTGGATTAAGAAGAAAGGATCTCGAGATCCTTTCTTCTTAATCCAGTTTTT
shRNA_4-R	AATTCAAAAACCTGGATTAAGAAGAAAGGATCTCGAGATCCTTTCTTCTTAATCCAGG

technique. Ten  $\mu\text{L}$  of RNA was used for reverse transcription. GAPDH was used as internal reference for relative quantitative analysis. The quantitative reaction system included 12.5  $\mu\text{L}$  of SYBR Premix Ex Taq, 1  $\mu\text{L}$  of PCR Forward Primer, 1  $\mu\text{L}$  of PCR Reverse Primer, 2  $\mu\text{L}$  of cDNA template and 8.5  $\mu\text{L}$  of ddH<sub>2</sub>O, with a total volume of 25  $\mu\text{L}$ . Three parallel wells were prepared for each sample. The amplification procedures were as follows: pre-denaturation at 95°C for 30 s; 95°C for 5 s and 60°C for 20 s, for a total of 40 cycles. The relative expression of APE-1 mRNA was calculated using the  $2^{-\Delta\Delta\text{Ct}}$  method.

### 2.2.5. Determination of APE-1 protein expression in L-02 cells using Western blotting

Cells were collected to extract total proteins for quantification using the BCA method. *SDS-PAGE gel electrophoresis*: After the transfer, the membrane was placed in a blocking solution containing 5% skim milk powder-TBST for blocking at room temperature for 1 h. Diluted APE-1 and GAPDH primary antibodies (1:800 dilution) were added and gently shaken at 4°C overnight; then, the corresponding secondary antibody (1:5,000 dilution) was added, and the mixture was incubated at 37°C for 1 h on a constant-temperature shaker. *Color development for calculation of the relative expression of protein*: The software ImageJ was used to calculate the gray value and APE1/GAPDH of APE1 expression.

### 2.2.6. Detection of inflammatory factor expression using ELISA

Concentrations of IL-1 $\beta$ , IL-6, IL-10, TNF $\alpha$ , INF- $\gamma$ , and other inflammatory factors in the cell culture supernatant were determined in accordance with the ELISA kit instructions. The standard curves were plotted according to concentrations and OD values of the standards. Then, the concentration in a sample was calculated on the standard curve according to the OD values. The result was the relative level of expression.

### 2.2.7. Detection of apoptosis using Annexin V-FITC/PI double labeling technique

Cells in each group were collected, placed on a 100-mesh copper screen, and rubbed gently. After rinsing with normal saline, the samples were centrifuged at 2,500 r/min. The supernatant and cell debris were discarded, and then the cell suspension was collected. Flow cytometry was used for analysis based on the method described in instructions in the Annexin V-FITC/PI double-staining apoptosis detection kit.

### 2.3. Statistical processing

SPSS 17.0 was used for statistical analysis. Measurement

data were expressed as mean  $\pm$  SD, and inter-group differences were compared using one-way analysis of variance. If the inter-group difference was statistically significant, a *t*-test was used to further compare the difference between 2 groups. When  $P < 0.05$ , the difference was statistically significant.

## 3. Results

### 3.1. Screening for genes related to immune tolerance after liver transplantation

Gene expression profiles of peripheral blood from 9 patients with immune tolerance after liver transplantation (GSM124753, GSM124834, GSM124836, GSM124845, GSM124851, GSM124853, GSM124646, GSM124850, GSM124648) and 8 patients without immune tolerance (GSM124863, GSM124833, GSM124575, GSM124748, GSM124838, GSM124840, GSM124842, GSM124675) in the GEO database were selected. As shown in Figure 1, screening yielded 40 significantly differentially expressed genes ( $P < 0.05$ ). Previous studies by the current authors indicated that APE-1 protein can reduce immunogenicity in addition to the dual functions of redox and DNA repair. Immune tolerance of the donor liver resulted (8). The results of this microarray screening suggested that the APE-1 gene is still highly expressed in patients with immune tolerance after liver transplantation, which is consistent with results of previous studies. Therefore, the APE-1 gene was selected for subsequent study.

### 3.2. Construction of an APE-1 shRNA vector and evaluation of silencing efficiency

Plasmid sequencing verified that the 4 APE-1 shRNAs

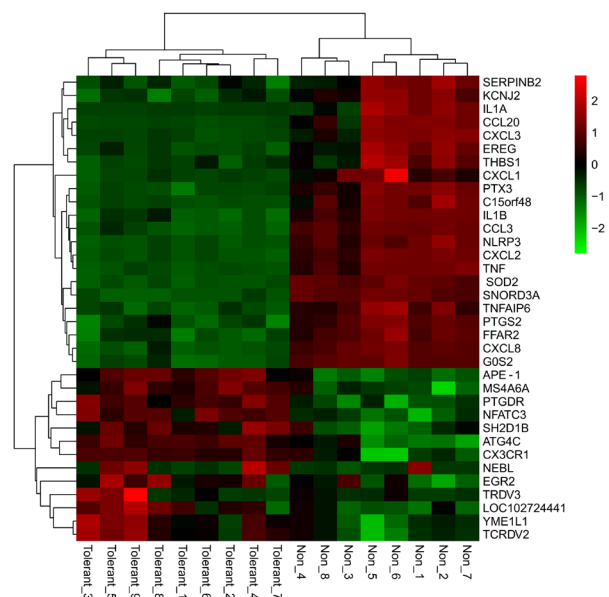


**Figure 1. Screening for differentially expressed genes related to immune tolerance after liver transplantation.**

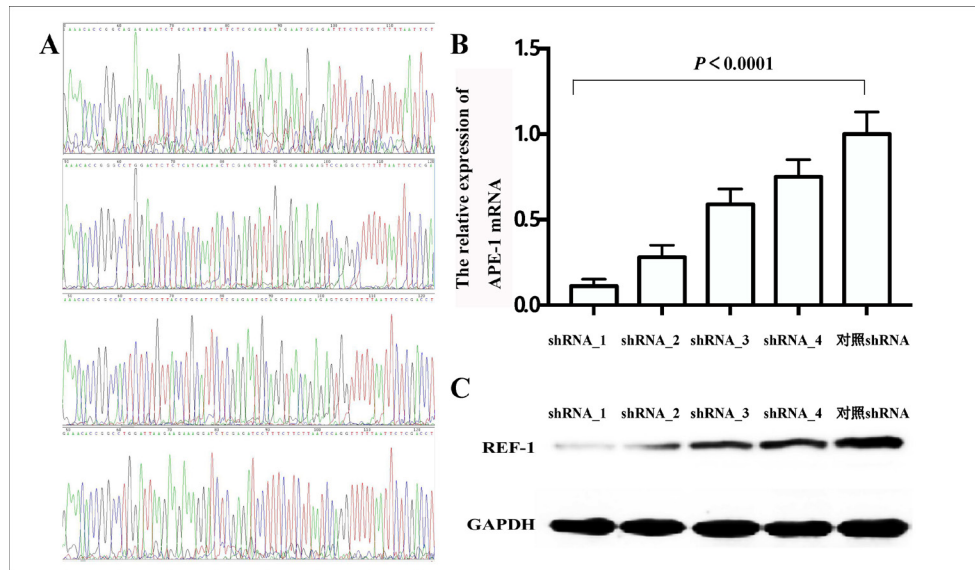


Figure 2. Construction of an APE-1 shRNA vector and evaluation of silencing efficiency.

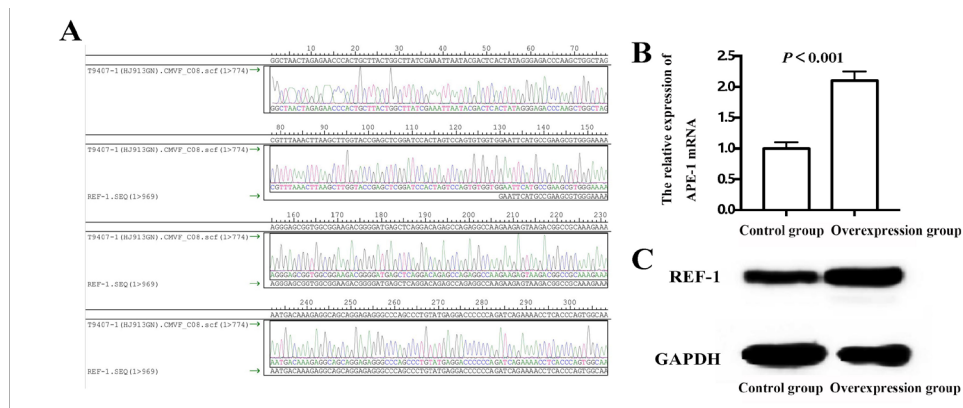


Figure 3. Construction of an APE-1 overexpression vector and evaluation of overexpression efficiency.

were successfully constructed in parallel, as shown in Figure 2A. After stable transfection of L-02 cells, real-time PCR was used to detect the expression of APE1 mRNA in hepatocytes. Results indicated that APE-1 mRNA expression was significantly lower in cells transfected with the 4 APE-1 shRNAs than in the control shRNA transfection group ( $P < 0.05$ ), as shown in Figure 2B. When protein expression in each group was detected using Western blotting, the results were consistent with those of mRNA detection. APE-1 protein expression was significantly lower in each APE-1 shRNA group than in the control shRNA group (Figure 2C), demonstrating the effectiveness of the designed shRNA interference sequence. Silencing was most apparent with APE-1 shRNA\_1, so it was used in subsequent experiments.

### 3.3. Construction of an APE-1 overexpression vector and evaluation of overexpression efficiency

Plasmid sequencing verified that the APE-1 overexpression vector was successfully constructed

(Figure 3A). After stable transfection of L-02 cells, real-time PCR was used to detect the expression of APE1 mRNA in hepatocytes. results indicated that mRNA expression was significantly higher in the APE-1 overexpression group than in the control group ( $P < 0.05$ , Figure 3B). The results of Western blotting were consistent with the level of mRNA detected. Protein expression was significantly higher in the APE1 overexpression group than in the control group (Figure 3C), demonstrating that the APE-1 overexpression vector was successfully constructed.

### 3.4. Prediction of the protein-protein interaction network of APE-1

The protein-protein interaction network of APE-1 was predicted using the STRING website (Version: 10.5). APE-1 was found to potentially interact with proteins such as ANP32A, FEN1, HMGB2, LIG1, MUTYH, NTHL1, OGG1, PCNA, POLB, and SET (Figure 4A). Correlation coefficients are shown in Figure 4B.

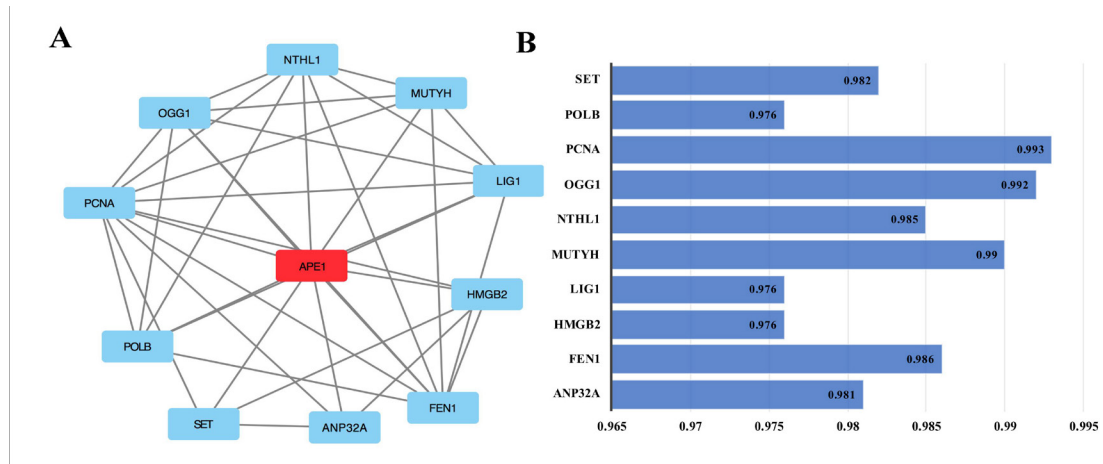


Figure 4. Prediction of the protein-protein interaction network of APE-1.

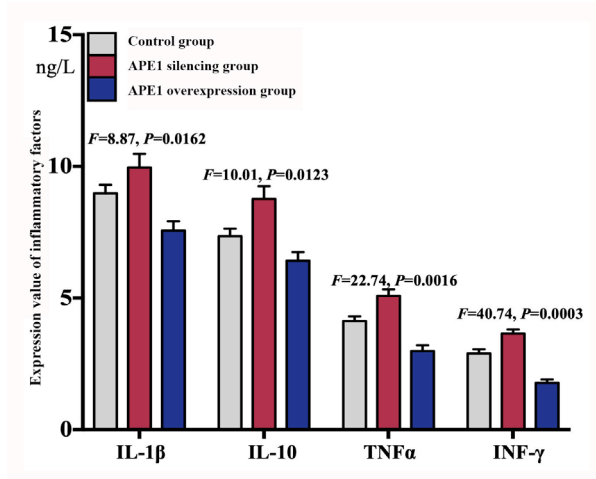


Figure 5. Impact of APE-1 silencing and overexpression on immune factors in L-02 cells.

### 3.5. Impact of APE-1 silencing and overexpression on the expression of immune factors in hepatocytes

ELISA was used to determine changes in expression of the inflammatory factors IL-1 $\beta$ , IL-10, TNF $\alpha$ , and INF- $\gamma$  in L-02 cells in the control group, the APE-1-silenced group, and the APE-1 overexpression group. Results indicated that the expression of inflammatory factors increased significantly in the APE-1-silenced group and decreased significantly in the APE-1 overexpression group (Figure 5).

### 3.6. Impact of APE-1 silencing and overexpression on hepatocyte apoptosis

The Annexin V-FITC/PI double-labeling technique was used to detect the apoptosis of L-02 cells in the control group, the APE-1-silenced group, and the APE-1 overexpression group. The total rate of apoptosis was  $13.24 \pm 0.234\%$ ,  $19.75 \pm 0.398\%$ , and  $10.61 \pm 0.366\%$ , respectively. One-way analysis of variance revealed

significant differences among the groups ( $F = 192.6$ ,  $P < 0.01$ ). APE-1 silencing significantly increased the rate of apoptosis of L-02 cells while overexpression of APE-1 significantly decreased the rate of apoptosis of L-02 cells ( $P < 0.01$ ) (Figure 6).

## 4. Discussion

Liver transplantation is the most effective means for the treatment of end-stage liver disease. Patients have a 1-year and 5-year postoperative survival rate of 85% and 70%, respectively. However, liver transplant recipients still have a lower long-term life expectancy than the normal population. Immune tolerance is a topic of interest in the field of organ transplantation. Due to low selectivity, the currently available immunosuppressants inevitably cause extensive suppression of the recipient's immune system, which can induce infections and tumors while reducing the acceptance of the organ transplant. The adverse effects of immunosuppressants, including renal impairment, diabetes, cardiovascular diseases, and metabolic syndrome, are also important causes of a diminished quality of life and even death of recipients (2-3). The use of genetic technologies to induce immune tolerance is an important part of the current research in the field of organ transplantation, where the search for effective target genes is crucial.

Various types of new detection technologies emerging over the past few years have made clinical high-throughput detection possible, greatly facilitating advances in the study of potential target genes involved in immune tolerance. Using an oligonucleotide microarray to examine PBMC specimens from patients with immune tolerance and patients lacking immune tolerance, studies have found that some genes are overexpressed in peripheral  $\gamma\delta$  T cells and NK cells. Further studies have identified 3 gene combinations from 13 genes, resulting in an amazing accuracy in distinguishing between patients with immune tolerance and patients lacking immune tolerance with an error rate

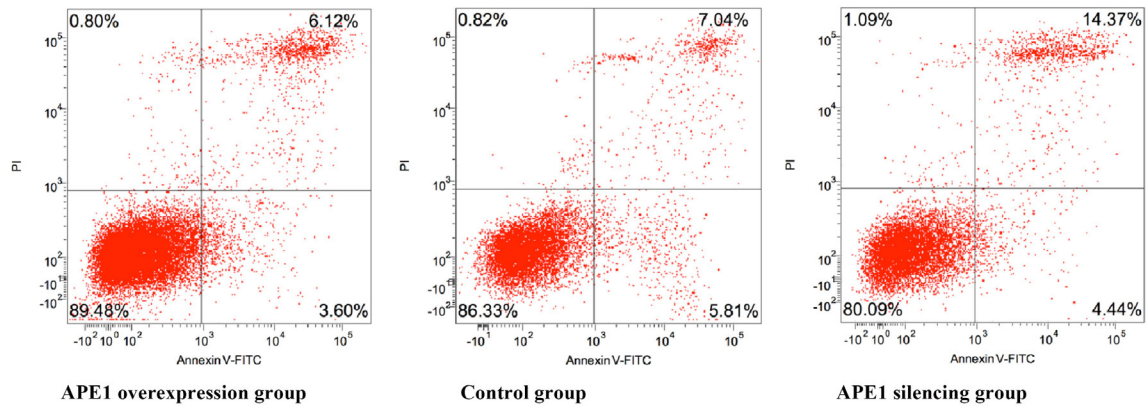


**Figure 6. Impact of APE-1 silencing and overexpression on the apoptosis of L-02 cells.**

of merely 13-17%. Pathological data from peripheral blood and liver transplants have been analyzed, revealing significant differences in gene transcription products between patients with immune tolerance and patients lacking immune tolerance (4). Some studies have found that the rate of immune tolerance was significantly higher in children than in adults, but the mechanisms differed in those sets of patients. In order to identify the target genes for immune tolerance in child and adult recipients of liver transplants, transcriptional profiles were obtained from 300 child and adult liver transplant recipients and normal tissues and blood samples. Results indicated that all 13 genes overexpressed in peripheral blood of patients with immune tolerance came from NK cells. The ERBB2, FEM1C, and SENP6 genes had a sensitivity of 1.00, a specificity of 0.83, and an area under the curve of 0.988 (5).

In the current study, gene expression profiles of peripheral blood of patients with or without immune tolerance after liver transplantation were downloaded from the GEO. A program in the R language was used to analyze differentially expressed genes, and the APE-1 gene was identified as a gene related to immune tolerance after liver transplantation. An APE-1shRNA\_1 silencing vector and an APE-1 overexpression vector were successfully constructed, revealing that APE-1 silencing resulted in significant up-regulation of the expression of the inflammatory factors IL-1 $\beta$ , IL-10, TNF $\alpha$ , and INF- $\gamma$  in L-02 cells. In contrast, overexpression of APE-1 resulted in significant down-regulation of inflammatory factor expression. Silencing of APE-1 expression significantly increased the apoptosis of L-02 cells while APE-1 overexpression resulted in significantly decreased apoptosis of L-02 cells, suggesting that changes in APE-1 immunoreactivity may be related to apoptosis. APE-1 is able to excise and repair bases. Diminished ability to repair damaged DNA due to reduced APE-1 may be an important cause of increased apoptosis.

In addition, the current authors' team previously explored the phenomenon whereby overexpression of APE-1 protein enhanced immune escape of the graft.

Creation of an orthotopic liver transplantation model in rats indicated that hepatocyte apoptosis gradually declined and liver function gradually improved with potentiated APE-1 gene expression and accumulation of intracellular APE-1 protein (6-7). Multiple organ failure after liver transplantation was treated as an adverse reaction to immunosuppressants. The current authors' team found that multiple organ failure after liver transplantation in the established rat model mainly occurred in the liver and kidneys. Liver transplantation causes little damage to the lungs and intestines. APE-1 protein plays a role in repairing renal injury after liver transplantation. When APE-1 protein expression is up-regulated, renal function improved according to indices such as CREA and BUN, and the apoptosis of renal cells gradually decreased (8-9). Those changes in apoptosis were consistent with the results of the current study.

Predictions indicated that APE-1 potentially interacted with ANP32A, FEN1, HMGB2, LIG1, MUTYH, NTHL1, OGG1, PCNA, POLB, SET, and other proteins. These functional proteins are all involved in the development and progression of liver cancer and immune tolerance (10-11). PCNA, for example, is related to histological differentiation, tumor size, and prognosis for patients with hepatocellular carcinoma, and it is also involved in immune signaling pathways in liver cancer cells. ANP32A participates in the development and progression of liver cancer and is closely related to tumor prognosis. FEN1 is overexpressed in hepatocellular carcinoma tissues, and FEN1 overexpression is indicative of low tumor differentiation, ready metastasis, and a poor prognosis.

In summary, APE-1 affects the expression of inflammatory factors in L-02 cells and apoptosis; it may be the key gene for immune tolerance after liver transplantation.

#### Acknowledgements

This study was supported by the Beijing Municipal Education Commission general scientific research

project (no. KM202010025008), Opening Foundation of Beijing Key Lab of Therapeutic Cancer Vaccines (no. 2019-JS04), the Foundation of Beijing Shijitan Hospital, Capital Medical University (no. 2019-C10), and grants-in-aid from the Ministry of Education, Science, Sports, and Culture of Japan.

## References

1. Chen GH, Jiang N. Research hotspots and considerations of immune tolerance in liver transplantation. *Organ Transplantation*, 2017; 8:1-4.
2. Geng L, Huang JJ, Lin BY, Chen TC, Shen T, Zheng SS. Characteristics of recipients with complete immunosuppressant withdrawal after adult liver transplantation. *Hepatobiliary Pancreat Dis Int*. 2017; 16:437-439.
3. Hussaini T, Turgeon RD, Partovi N, Erb SR, Scudamore CH, Yoshida EM. Immunosuppression practices in liver transplantation: A survey of North American centers. *Exp Clin Transplant*. 2018; 16:550-553.
4. Bohne F, Martínez-Llordella M, Lozano JJ, *et al*. Intra-graft expression of genes involved in iron homeostasis predicts the development of operational tolerance in human liver transplantation. *J Clin Invest*. 2012; 122:368-382.
5. Li L, Wozniak LJ, Rodder S, Heish S, Talisetti A, Wang Q, Esquivel C, Cox K, Chen R, McDiarmid SV, Sarwal MM. A common peripheral blood gene set for diagnosis of operational tolerance in pediatric and adult liver transplantation. *Am J Transplant*. 2012; 12:1218-1228.
6. Zhang P, Du X, Sun ZP, Xu L. Expression of redox factor-1 in early injury period after liver transplantation in rat model. *Cell Mol Immunol*. 2009; 6:309-313.
7. Guo L, Haga S, Enosawa S, Naruse K, Harihara Y, Sugawara, Y. Improved hepatic regeneration with reduced injury by redox factor-1 in a rat small-sized liver transplant model. *American journal of transplantation*. 2004; 4:879-887.
8. Sun ZP, Zhu YB, Am BH, Gong K, Zhang NW. Redox factor-1 may mediate the repair of multiple organ injuries after liver transplantation. *Chin Med J*. 2013; 126:2504-2509.
9. Sun ZP, Am BH, Zhu B, Gong K, Zhang NW. Anti-inducible costimulator immunotherapy inhibits accelerated and chronic cardiac allograft rejection in rats. *Journal of Clinical Rehabilitative Tissue Engineering Research*. 2010; 14:8347-8351. (in Chinese)
10. Yan W, Chen X. Research progress on the relationship between ANP32A and tumor. *Acta Medicinæ Sinica*, 2017; 30:141-144.
11. Yin R, Wu WX, Wang HH, Chen Y. Effects of FEN1 overexpression on the biological behaviors of hepatocellular carcinoma cells and the prognosis of patients. *Cancer Research on Prevention and Treatment*, 2016; 43:848-853.

(Received November 26, 2019; Revised December 14, 2019; Accepted December 16, 2019)

# Male rats exhibit higher pro-BDNF, c-Fos and dendritic tree changes after chronic acoustic stress

David Fernandez-Quezada, Alejandra García-Zamudio, Yaveth Ruvalcaba-Delgadillo, Sonia Luquín, Joaquín García-Estrada, Fernando Jáuregui Huerta\*

Department of Neurosciences, Health Sciences University Centre, Guadalajara, Jalisco, Mexico.

## Summary

Prolonged or intense exposure to environmental noise (EN) has been associated with a number of changes in auditory organs as well as other brain structures. Notably, males and females have shown different susceptibilities to acoustic damage as well as different responses to environmental stressors. Rodent models have evidence of sex-specific changes in brain structures involved in noise and sound processing. As a common effect, experimental models have demonstrated that dendrite arborizations reconfigure in response to aversive conditions in several brain regions. Here, we examined the effect of chronic noise on dendritic reorganization and c-Fos expression patterns of both sexes. During 21 days male and female rats were exposed to a rats' audiogram-fitted adaptation of a noisy environment. Golgi-Cox and c-Fos staining were performed at auditory cortices (AC) and hippocampal regions. Sholl analysis and c-Fos counts were conducted for evidence of intersex differences. In addition, pro-BDNF serum levels were also measured. We found different patterns of c-Fos expression in hippocampus and AC. While in AC expression levels showed rapid and intense increases starting at 2 h, hippocampal areas showed slower rises that reached the highest levels at 21 days. Sholl analysis also evidenced regional differences in response to noise. Dendritic trees were reduced after 21 days in hippocampus but not in AC. Meanwhile, pro-BDNF levels augmented after EN exposure. In all analyzed variables, exposed males were the most affected. These findings suggest that noise may exert differential effects on male and female brains and that males could be more vulnerable to the chronic effects of noise.

**Keywords:** Noise, hippocampus, auditory cortex, sex differences, Golgi-Cox

## 1. Introduction

Noise represents a growing health problem for industrialized and developing countries (1). Recreational, occupational or environmental noise (EN) has long been known to induce damage in classic auditory structures including cochlear hair cells, auditory nerve fiber terminals and superior cortical structures (2). At the central level, changes in spontaneous firing rates, neural synchrony, tonotopic map reorganization, cell death, abnormal neural coding and axonal sprouting have been reported affecting neurons in auditory cortices (AC) (3-6). Several organs and functions beyond the auditory

system, can also be affected by noise (7). EN may affect non-auditory brain regions such as the hippocampus, a limbic structure that receives direct and/or indirect neuronal projections from the auditory system (8). As an environmental stressor, EN may also affect hippocampal integrity by inducing dysregulation of the hypothalamic-pituitary-adrenal (HPA) axis since the hippocampus contains one of the higher distributions of the stress hormone receptors in the brain: the glucocorticoid (GR) and mineralocorticoid receptors (MR) (9).

Accumulated evidence previously demonstrated that noise might affect hippocampal-related cognition (10-12), cell proliferation, neurotransmitter function and neurogenesis (13-16). The most consistent data depicting the effect of environmental stressors over the brain has been reported as structural changes affecting the plastic properties of neurons in the hippocampus and other stress-related structures. The protein product

\*Address correspondence to:

Dr. Fernando Jáuregui Huerta, Departamento de Neurociencias. Centro Universitario de Ciencias de la Salud. C.p. 44340. Col. Independencia. Guadalajara, Mexico.  
E-mail: fernando.jhuerta@academicos.udg.mx

of the Fos proto-oncogene, has been frequently used to evidence changes in neuronal activity associated to environmental threats (17). Studies assessing effects of stress have evidenced changes on c-Fos levels after acute and chronic exposures (18-20). Also, it has also been consistently reported a causal relationship between stress and atrophy of dendrite arbors in specific subregions of the hippocampus (21-24). Yet, expansion of dendrites and reversible dendritic remodeling over a time frame of days or weeks has also been described inside and outside the hippocampus (25,26). Since the patterning of dendrites and the overall shape of the dendritic arbor depends on synaptic input, it follows that changes in the structure of the dendritic tree may instead reflect changes in the plastic/adaptive properties of neurons (27). So, conditions challenging the adaptive capability of the brain should affect and reshape dendritic complexity at specific regions of the brain.

Mechanisms underlying stress-induced dendritic remodeling have also been investigated. It has been suggested that glucocorticoids, excitatory amino acid release, serotonin and some neurotrophic factors could be critical mediators of this effect (28). Accounting for neurotrophins, it has been documented that stress effects on structural plasticity of neurons are related to changes in brain-derived neurotrophic factor (BDNF) signaling (29). While BDNF promotes plasticity by enhancing survival, differentiation or dendrite growing, its precursor pro-BDNF has been associated with debranching of dendritic arbors (30-32). Then, changes on BDNF or its precursor pro-BDNF could be associated with structural changes induced by environmental stressors.

In the last years, sex has also been recognized as an important determinant of brain susceptibility to environmental threats (33-35). Since the susceptibility to noise may differ among individuals, investigators in this area have begun to suspect that gender may indeed be a main condition determining the neurobiological effects of noise. Concerning other stressors, a growing number of investigations have established that males and females present different amounts of susceptibility to threatening conditions (34). Moreover, it has been established that most of the stress-related disorders that affect the hippocampus integrity show sex differences in severity of symptoms. While depression or Alzheimer disease shows greater severity in females, schizophrenia and other diseases are more severe in males (36-38). Therefore, it could be expected that changes induced by environmental stressors on the integrity of hippocampus and/or AC, deeply vary from one sex to another.

To analyze these differences, we designed an experiment to compare Golgi-stained dendrites and c-Fos activity patterns in AC and hippocampal neurons from male and female rats exposed to environmental noise. Fluctuations of serum pro-BDNF levels were

also investigated in order to support the expected morphological changes.

## 2. Materials and Methods

### 2.1. Experimental animals

In order to compare differences, we used 40 adult Wistar male and female rats (age 90 days old) obtained from the in-house breeding facility at the West Center for Biomedical Research, Guadalajara, México. These animals were randomly divided to evaluate the effects of noise on c-Fos expression levels ( $n = 12$  for each sex) and dendritic arborizations ( $n = 8$  for each sex). All groups were maintained in a 12:12 light-darkness cycle with lights on at 07:00. Temperature in the experimental room was maintained at  $22 \pm 2^\circ\text{C}$  and humidity at 70%. We guaranteed free access to tap water and balanced food. All animal experiments complied with National Institutes of Health guide (NIH Publications No. 8023, revised 1978) for the care and use of Laboratory animals.

### 2.2. Noise exposure

To produce a noisy environment, we disposed a rats' audiogram-fitted adaptation provided with representative sounds of urban environments (*i.e.*, turbines, hooters, horns, *etc*) as described by Rabat (39). The administered sounds considered the rats' lower capacity to detect low frequencies (under 500 Hz) and its greater capacity to perceive high frequencies (over 8,000 Hz). We used metal grid cages to avoid sound refraction and housed the animals in groups of 4 in a soundproofed room. Professional tweeters (Yamaha, Inc. Japan) were placed 1 m above the cages and were powered by a Mackie amplifier (Mackie M1400; freq. 20 Hz to 70 kHz; 300 W at 8  $\Omega$ ). The speaker and tweeter characteristics allowed sound delivery between 20 and 50,000 Hz. Audio files containing unpredictable noise events were presented in random tracks that alternated noisy events (18-39 s of turbine, hooter or horn sounds) with silent intervals ranging from 20 to 165 s. Soundtracks were presented with mixer software that transmitted the signal at levels ranging from 70 dB(A) to 103 dB(A).

To avoid housing effects, both, control and experimental rats were transferred to the testing room 48 hours before the start of the stimuli. A few minutes before the speakers were activated, control rats were transferred to the surgical room for further sacrifice.

Prior to sacrifice, female rats were examined to determine estrous phase. Vaginal lavages were achieved and exfoliate cytology was observed under light microscopy. Estrous phase was determined based on the morphology of cells present and the day of sacrifice was chosen avoiding proestrus and estrus since these phases could generate confounding results.

### 2.3. pro-BDNF assays

To identify changes on circulating pro-BDNF levels, we collected a blood sample from each rat before sacrifice. pro-BDNF levels were measured using an enzyme immunoassay kit (Aviva Systems Biology OKAG00197). Blood samples were obtained immediately after the noise was ended in day 21 and from tail veins at day 7 (always between 07:00 and 08:00 hours, in order to avoid circadian variation).

### 2.4. c-Fos immunohistochemistry

The rats received an *i.p.* injection of sodium pentobarbital (60 mg/kg) and were perfused through the left cardiac ventricle with 150 ml of saline solution followed by 200 ml of 3.8% paraformaldehyde in 0.1 M phosphate buffer saline (PBS), pH 7.4. After perfusion, brains were removed and sectioned in coronal slices (40  $\mu$ m) using a vibratome Leica VT1000E.

To evaluate the neuronal activity on the exposed subjects, the protein product of the proto-oncogene c-Fos was immunohistochemically analyzed. We perfused the animals at the acute phase of 2h ( $n = 4/\text{sex}$ ), and, at chronic phase of 21d ( $n = 4/\text{sex}$ ). The 0h group ( $n = 4/\text{sex}$ ) was considered the control for all groups.

We selected one of every third section spanning from Bregma -2.1mm to Bregma -3.8mm to conduct immunohistochemistry (40). Sections were blocked with 10% normal goat serum (NGS) in Tris-buffered saline (0.05M, 0.9%, pH 7.4) plus 0.3% of Triton X-100 (TBST) for 1 h at room temperature. After blocking, tissues were incubated overnight with rabbit anti c-Fos primary antibody at a 1:1000 dilution (Santacruz Biotechnology, Santa Cruz, CA) in TBST + 1% NGS at 4°C with 50 rpm shaking. On the next day, sections were rinsed three times for 10 min with TBST and incubated for 2 h at room temperature with biotinylated goat anti-rabbit secondary antibody (1:500; Vector Labs, Burlingame, CA). Next, tissues were incubated in avidin-biotin-peroxidase complex (Elite ABC kit, Vector labs) for 1 h and revealed with diaminobenzidine 0.05% as chromogen. Once revealed, sections were rinsed and mounted in permount-mounting medium. c-Fos immunoreactive nuclei per 540  $\mu$ m (40x microscopic field) were counted using a Leica DMi8 microscope.

### 2.5. Golgi-Cox Staining

When the animals completed the 3 weeks in the noise room, both exposed ( $n = 4/\text{sex}$ ) and control ( $n = 4/\text{sex}$ ) rats were anesthetized and decapitated. The skulls were opened, the brains quickly removed, cut with a blade into 1 cm thick slabs and processed using a FD Rapid GolgiStain™ kit (FD Neuro Technologies, Ellicott city, MD, USA). On each procedure, blocks from 1 control and 1 exposed rat were put in the dark at

room temperature into a mixture of solutions (provided by the kit producer) for the next 2 weeks. The tissues were then transferred into a protectant solution C (0.1 M phosphate buffer, sucrose, polyvinylpyrrolidone and ethylene glycol) and stored for 48 hours in the dark at 4°C. The tissues were sectioned into 200 $\mu$ m slices using a vibratome (Leica, VT1000 S). Each section was mounted with protectant solution on gelatin-coated microscope slides. Sections were then dried at room temperature in the dark for a couple of weeks. For the next procedure the slides were collocated into the staining solution D and E (ammonia and sodium thiosulfate). Then the tissues were dehydrated in 50%, 75%, 95% and 100% ethanol and cleared in xylene. The tissues were coverslipped in Permount™ Mounting Medium. The slides were finally viewed under a Leica DMi8 microscope.

### 2.6. Morphological analysis

Sections containing the hippocampus and the auditory cortex (AC) were delineated according to anatomical atlases and with the help of c-Fos stained sections.

Sholl analysis was employed to assess dendritic trees as described by Kutzing (2010). We quantified the number of intersections in concentric rings at 3  $\mu$ m intervals. We also quantified the total number of dendrites and the total length of dendrites.

To conduct the Sholl analysis, photographs were obtained using bright-field microscopy (Leica DMi8 microscope) 20 $\times$  magnification connected to a DFC 7000T camera, which transmitted the microscopic image to a PC coupled with MATLAB (MathWorks), NeuroJ plugin for ImageJ and NeuroStudio. Spatial information related to the position of dendritic segments in relation to soma was acquired with ImageJ/NeuroJ, identification of branch and endpoints was realized with NeuroStudio, and writing of scripts to convert data was conducted in MATLAB. We analyzed 400 neurons on the hippocampus and 200 neurons in AC. To select neurons, we observed that Golgi impregnation was consistent, the neurons presented at least some tertiary branches, were visualized in isolation from other neurons, and the soma was visible and centrally located.

### 2.7. Statistical analysis

The particular measurements from selected neurons were averaged to get a single value of the number of intersections, the dendritic length and the number of segments for one animal and group means were obtained from 4 subjects. The significance of the differences between morphological or serological data from exposed and control groups of rats were tested by ANOVA. All statistical analysis was performed using GraphPad (GraphPad, version prism 8). Results were

expressed as mean  $\pm$  SEM. Post hoc test (Sidak analysis to correct multiple comparisons) was employed to explore differences in single time points between male and female exposed rats as well as in comparison with the control group. Differences were considered statistically significant at a value  $*p < 0.05$  ( $**p < 0.01$ ,  $***p < 0.001$ ); (\*) control vs. male noise; (°) control vs. female noise, (&) male vs. female.

### 3. Results

#### 3.1. Serum pro-BDNF concentrations

ANOVA analysis evidenced main differences for serum pro-BDNF levels [ $F(5,6) = 10.15$ ;  $p < 0.006$ ]. Post hoc comparisons showed that noise-exposed males increased their pro-BDNF levels after 7 ( $t = 5.994$ ;  $p < 0.001$ ) and 21 days ( $t = 5.691$ ;  $p < 0.010$ ) compared to their own control. Female differences did not reach significance when compared to controls. We found differences between exposed males and females when comparisons were made on day 21 ( $t = 5.994$ ;  $p < 0.001$ ). Figure 1 illustrates pro-BDNF differences.

#### 3.2. c-Fos immunohistochemistry

##### 3.2.1. Auditory Cortex

Exposed males increased their expression levels after 2h ( $t = 18.51$ ;  $p < 0.001$ ) and 21d ( $t = 9.432$ ;  $p < 0.001$ ) when compared to control. Females also showed significant increases at 2h ( $t = 11.67$ ;  $p < 0.001$ ) and 21d ( $t = 6.691$ ;  $p < 0.001$ ). Intersex comparisons showed that males outnumbered females at 2h ( $t = 6.855$ ;  $p < 0.001$ ) and 21 days ( $t = 5.766$ ;  $p < 0.001$ ). Figure 2 illustrates AC differences in c-Fos counting.

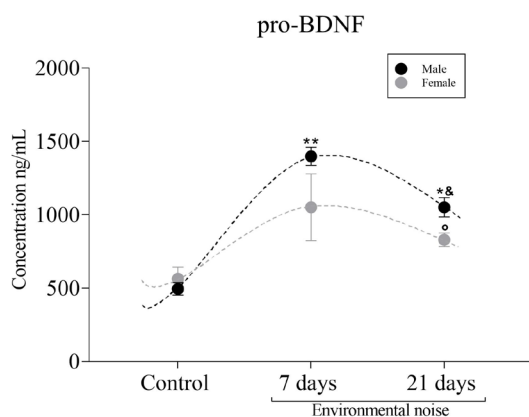


**Figure 1. Serum pro-BDNF levels in male and female rats exposed to acoustic stress.** Shows results of samples collected on 7 seven and 21 days of exposure. Data represent the mean  $\pm$  SEM.  $*p < 0.05$  ( $**p < 0.01$ ,  $***p < 0.001$ ); (\*) control vs. exposed males; (°) control vs. exposed females, (&) exposed males vs. exposed females.

#### 3.2.2. Hippocampus

Male rats exposed to environmental noise showed higher amounts of c-Fos+ cells at 2h ( $t = 12.56$ ;  $p < 0.001$ ) and 21d ( $t = 15.03$ ;  $p < 0.001$ ) when compared with control. Also, females displayed higher expression levels at 2h ( $t = 9.897$ ;  $p < 0.001$ ), and 21d ( $t = 14.90$ ;  $p < 0.001$ ). Analysis of differences between sexes, showed that male increases were higher than females at 2h ( $t = 6.635$ ;  $p < 0.001$ ), and 21d ( $t = 9.985$ ;  $p < 0.001$ ). Figure 3 illustrates these differences.

#### 3.3. Dendritic complexity in auditory cortex (AC)

Sholl analysis was employed to assess the dendritic branching tree, the number of segments and the total length of dendrites as shown in Figure 4.

No differences in the number of intersections (Figure 5), branches (Figure 6) and dendrite lengths (Figure 7) were found when comparing exposed groups with their respective control or in intersex comparisons. However, we noted that basal numbers of branches were higher in females ( $t = 13.19$ ;  $p < 0.001$ ), and that basal dendrite lengths were higher in males ( $t = 4.761$ ;  $p < 0.001$ ). Such patterns changed under EN since males decreased

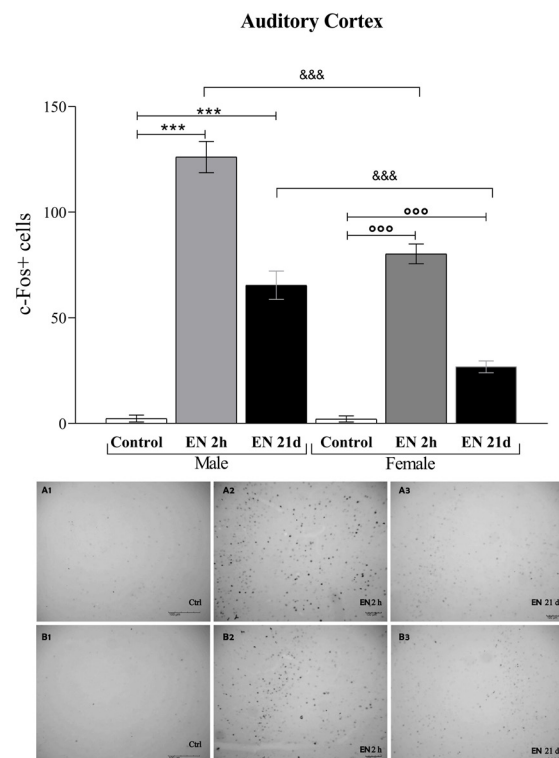


**Figure 2. c-Fos expression levels in AC of male and female rats exposed acoustic stress.** Shows results of c-Fos counts after 2 hour and 21 days of environmental noise. Data represent the mean  $\pm$  SEM.  $*p < 0.05$  ( $**p < 0.01$ ,  $***p < 0.001$ ) (\*) control vs. exposed males; (°) control vs. exposed females, (&&&) exposed males vs. exposed females. Representative sections of c-Fos expression in Auditory cortex (AC). Figures A1-A3 represent male groups. Figures B1-B3 female groups. Magnification 10X, scale bars indicate 100  $\mu$ m.

their numbers of branches ( $t = 10.89$ ;  $p < 0.001$ ) but increased their dendrite lengths ( $t = 3.878$ ;  $p < 0.001$ ).

### 3.4. Dendritic complexity in hippocampus

ANOVA analysis revealed significant differences in Sholl analyses [ $F(3, 342) = 10.84$ ;  $p < 0.001$ ]. Figure

8 illustrates this. Compared to control, exposed males reduced the total number of intersections ( $t = 3.951$ ;  $p < 0.001$ ). Those reductions were significant for branches ( $t = 4.366$ ;  $p < 0.001$ ) (Figure 9) but not for dendrite lengths (Figure 10). Females in the other hand showed no differences in the number of intersections but exhibited reductions in branches ( $t = 4.694$ ;  $p < 0.001$ ) that were compensated with increases in lengths ( $t = 9.338$ ;  $p < 0.001$ ). Intersex comparisons exhibited that male reductions were significant for the number of branches ( $t = 2.915$ ;  $p < 0.001$ ).

### 4. Discussion

Our data demonstrated that EN differentially increased c-Fos expression levels, induced structural changes in dendritic trees, and elevated serum levels of pro-BDNF. While c-Fos quantification showed strong 2h-increases that diminished at 21 days in auditory cortex, the hippocampus showed the opposite effect by registering bigger increases after 21 days. In contrast, the analysis of dendritic trees showed no main differences in the complexity of the dendrite arbors of AC, but intense reductions in the dendritic trees of hippocampal neurons. The differences were significantly higher in the hippocampus and markedly affected the group of exposed males. Those changes were also accompanied by differential increases in the serum levels of pro-BDNF.

Given the probed utility of c-Fos to evidence neural responses to environmental threats, it was expected that auditory cortices reacted to environmental noise with regional increases of c-Fos expression (41). As expected, our results demonstrated that the protein product c-Fos quickly increased its expression patterns after acute exposures. Beyond this, we noted that patterns of c-Fos activation include not only peaks in the range of the first 2 hours affecting auditory structures, but also retarded increased expressions

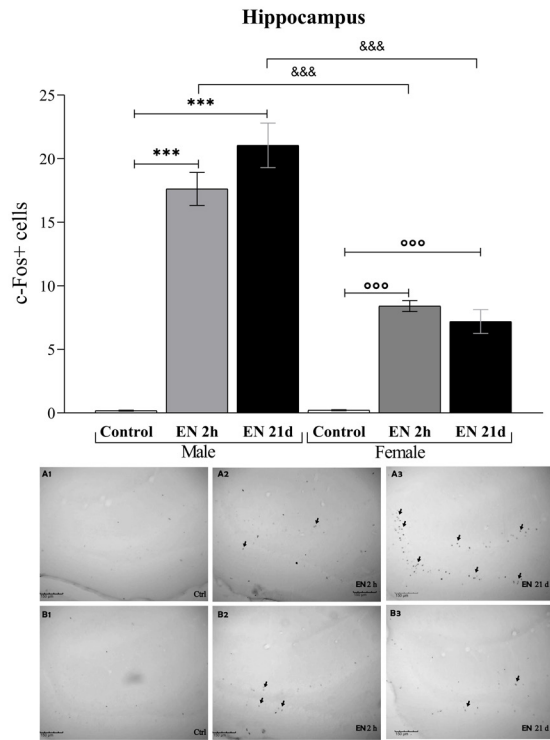


**Figure 3. c-Fos expression levels in hippocampus of male and female rats exposed to acoustic stress.** Shows results of c-Fos counts after 2 hour and 21 days of environmental noise. Data represent the mean  $\pm$  SEM. \* $p < 0.05$  (\*\* $p < 0.01$ , \*\*\* $p < 0.001$ ) (\*) control vs. exposed males; (°) control vs. exposed females, (&) exposed males vs. exposed females. Representative sections of c-Fos expression in hippocampus. Figures A1-A3 represent male groups. Figures B1-B3 female groups. Magnification 10X, scale bars indicate 100  $\mu$ m.

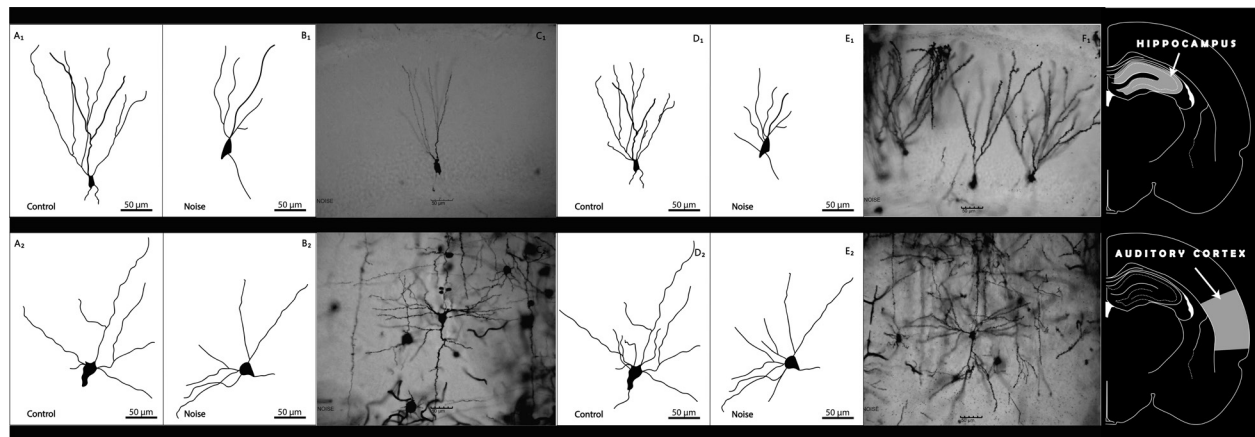


**Figure 4. Morphometric analysis in AC and hippocampus of male and female rats exposed to acoustic stress.** Figure above shows hippocampal representative neurons. Panel below shows auditory cortex representative neurons. Male groups are displayed with letters A, B and C, females with D, E and F. C<sub>1</sub>, C<sub>3</sub>, F<sub>1</sub>, F<sub>2</sub> illustrates 21 days of EN exposure. Magnification 20 $\times$ , scale bars indicate 50  $\mu$ m.

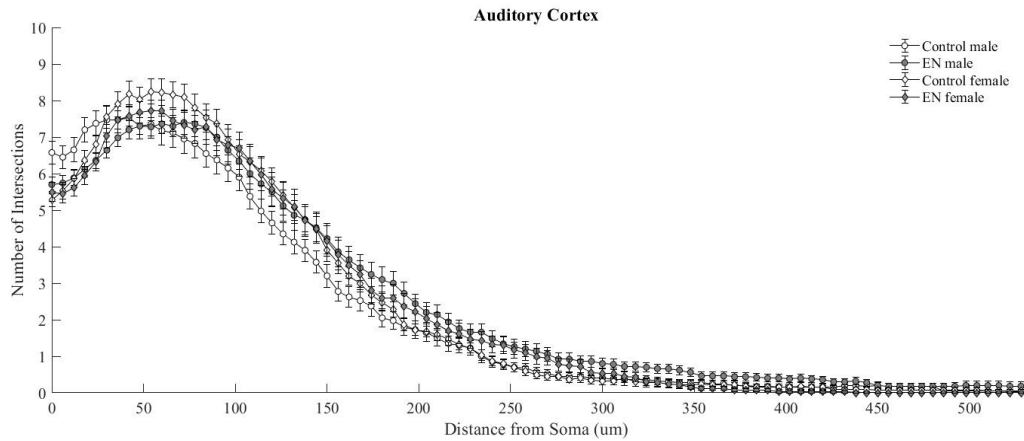


**Figure 5. Sholl analysis in AC of male and female rats exposed to acoustic stress.** Illustrates the number of intersections found in 200 neurons of auditory cortex. Data represent the mean  $\pm$  SEM. \* $p < 0.05$  (\*\* $p < 0.01$ , \*\*\* $p < 0.001$ ); (\*) control vs. exposed males; (°) control vs. exposed females, (&) exposed males vs. exposed females.

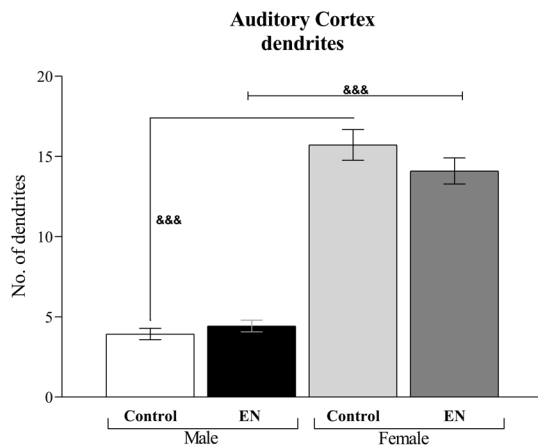


**Figure 6. Total number of dendrites in neurons of AC from male and female rats exposed to acoustic stress.** Illustrates the number of dendrites counted per neuron in auditory cortex of male and female rats exposed to 21 days of environmental noise. Data represent the mean  $\pm$  SEM. \* $p < 0.05$  (\*\* $p < 0.01$ , \*\*\* $p < 0.001$ ); (\*) control vs. exposed males; (°) control vs. exposed females, (&) exposed males vs. exposed females.

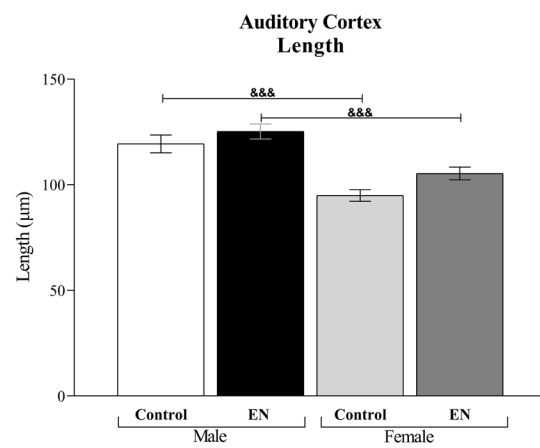


**Figure 7. Length of dendrites in neurons of AC from male and female rats exposed to acoustic stress.** Illustrates the length of dendrites registered in neurons of auditory cortex of male and female rats exposed to 21 days of environmental noise. Data represent the mean  $\pm$  SEM. \* $p < 0.05$  (\*\* $p < 0.01$ , \*\*\* $p < 0.001$ ); (\*) control vs. exposed males; (°) control vs. exposed females, (&) exposed males vs. exposed females.

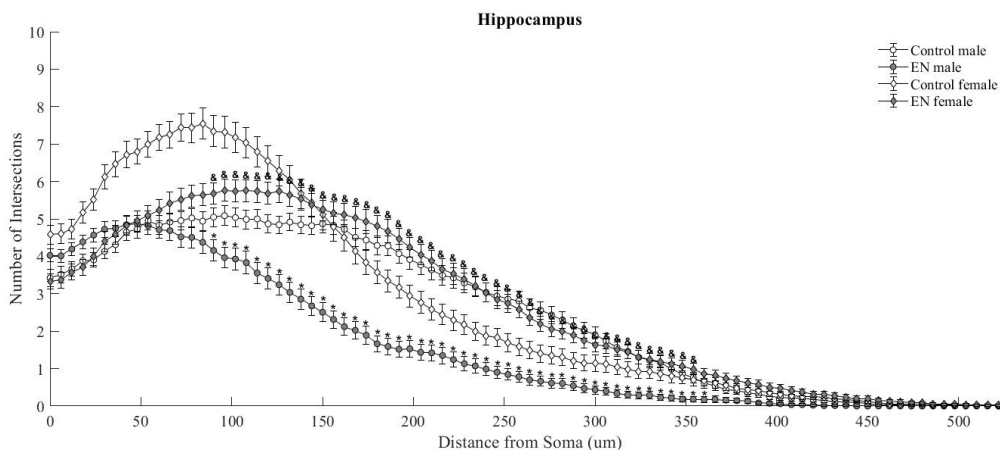


**Figure 8. Sholl analysis in hippocampus of male and female rats exposed to acoustic stress.** Illustrates the number of intersections found in 400 neurons of hippocampal area. Data represent the mean  $\pm$  SEM. \* $p < 0.05$  (\*\* $p < 0.01$ , \*\*\* $p < 0.001$ ); (\*) control vs. exposed males; (°) control vs. exposed females, (&) exposed males vs. exposed females.

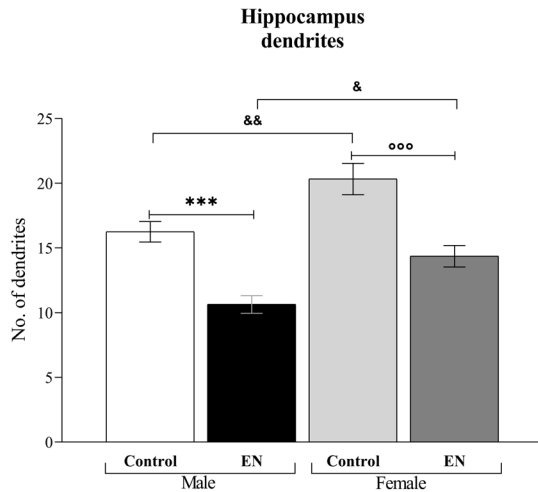


**Figure 9. Total number of dendrites in neurons of the hippocampus from male and female rats exposed to acoustic stress.** Illustrates the number of dendrites counted per neuron in the hippocampus of male and female rats exposed to 21 days of environmental noise. Data represent the mean  $\pm$  SEM. \* $p < 0.05$  (\*\* $p < 0.01$ , \*\*\* $p < 0.001$ ); (\*) control vs. exposed males; (°) control vs. exposed females, (&) exposed males vs. exposed females.

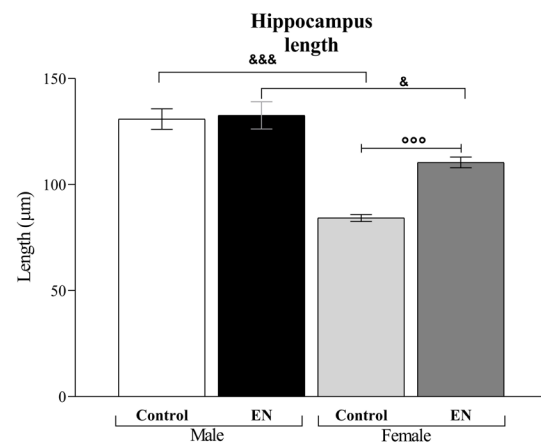


**Figure 10. Length of dendrites in neurons of the hippocampus from male and female rats exposed to acoustic stress.** Illustrates the length of dendrites registered in neurons of hippocampal areas of male and female rats exposed to 21 days of environmental noise. Data represent the mean  $\pm$  SEM. \* $p < 0.05$  (\*\* $p < 0.01$ , \*\*\* $p < 0.001$ ); (\*) control vs. exposed males; (°) control vs. exposed females, (&) exposed males vs. exposed females.

affecting the hippocampus (42). Then, our experiment demonstrated regional differences with expression patterns differing as a function of time and structure. In support of this, time and region differences in expression patterns of *c-Fos* have been previously described. Reported patterns include fast general rises after a few hours affecting large regions of the brain, and retarded or sustained elevations affecting restricted areas of the limbic system (*i.e.* prefrontal cortex or other limbic structures) (20,42,43). Since this seems to be the case in our results (the hippocampus became lately activated), we may suppose in agreement with these authors that while some structures may be critical for the rapid processing of noise, other areas may be more dedicated to the chronic adaptation to the stimuli. Then, beyond the confirmation that neural activation varies in a time and region-dependent manner, our data also support the hypothesis that hippocampal regions and perhaps other limbic structures could be critical to respond to persistent noisy environments.

Sholl analysis confirmed that EN, is capable of inducing enduring structural changes affecting limbic extra-auditory structures. Recent evidence supports our results by showing that when exposing rats to other models of noise, the dendritic trees of hippocampal neurons became diminished (44,45). Since changes affecting dendritic arborizations may correspond to changes in firing properties of the hippocampal neurons (27), it could be supposed that noise-induced debranchings should reduce the subjects ability to process hippocampus-dependent information and to adapt to challenging conditions. Studies in the stress area support this assumption by showing that dendritic retractions have indirect functional consequences on

spatial memory and the regulatory capacity of the HPA axis (28). According to this idea, some studies have demonstrated that noise-induced structural changes affecting the hippocampus are accompanied by deficits in learning and memory abilities (14,15,46-48). Given this coincidence, the chronic effects of noise over the hippocampal dendrites, could in great part be attributed to the stressing properties of noise. In this respect, it was previously demonstrated that the model of noise employed here is capable of exacerbating the activity of the HPA axis hormones (46). Therefore, besides the well documented effects on hearing structures (*i.e.* noise induced hearing loss -NIHL-), our study provides evidence linking noise exposure to activational and morphological effects outside the classical auditory structures. In view of this, it should be now considered that noise induced damage may also include brain structures and mechanisms different from that previously described for NIHL. Given the similarity with results in experimental stress, mechanisms of stress response could be responsible for some of the noise-induced damage outside the auditory system. Unlike common stressors that transiently affect the subject's life, it must be considered that environmental noise is an omnipresent stimuli affecting almost every part of human life.

In line with this, our results showed that hippocampal neurons could be more affected than AC neurons when noisy environments persist over longer periods. Recent evidence offers support for this idea. The main group of data has been provided by Cheng and colleagues (49,50) in a series of experiments designed to assess peroxidation levels and tau phosphorylation in time lapses of 1, 3 and 6

weeks. After exposing rodents to moderate levels of noise, investigators suggested that hippocampal cells could be more vulnerable since oxidative damage and tau hyperphosphorylation appeared faster and stronger than appreciated in AC. Otherwise, results obtained in a parallel experiment conducted in our lab, showed that dendritic trees belonging to AC neurons were increased after 7 days of noise, but turned-back to basal values after 21 days. On the contrary, neurons in hippocampal regions showed no alterations after 7 days but exhibited strong reductions after 21 days (51). Then, in addition to the hypothesis sustaining that chronic effects of noise could be largely explained by its stressing properties, it could be added now the fact that the hippocampus may also exhibit more vulnerability than AC under chronic mild-level circumstances.

Apart from the above discussed, our results showed that males and females were differently affected by EN since males exhibited higher c-Fos expression, larger dendritic tree reductions and higher pro-BDNF increases. About c-Fos, reports exist demonstrating different patterns of expression in male and female rats. According to available evidence, females should be more sensitive to the effects of both, acute and chronic stress (35). However, our results found the opposite effect since males exhibited higher expression levels. In line with our results, greater increases in males were also reported in a recent experiment that evaluated the acute effect of restraint stress over c-Fos expression levels (35). Accordingly, chronically stressed females also showed less c-Fos expressions after a novel acute stressor (52). Contrasted with our own data, it seems that unlike other commonly used stressors *i.e.* foot and tail shock (53), neonatal handling (54), restraint (55) and immune challenge (56), environmental noise provokes a stressor-specific response that strongly affects males. Babb and colleagues supported this idea by demonstrating that contrary to males, females show less HPA-axis and c-Fos changes after noise than after restraint (57).

Similar patterns were observed in our Sholl analysis. Males exhibited lower number of intersections, shorter dendritic lengths, and a smaller number of segments. Then, the observed dendrite retractions confirmed the above suggested increased vulnerability from males to acoustic stress. Since other experiments have showed that females also exhibit less dendritic remodeling after chronic stress (58) it seems clear that plastic capabilities of females are more efficient dealing with some environmental stressors. To support this, previous studies have established that auditory organs of females are more resistant to deterioration over the years (59). Moreover, human observations have also suggested that men are more susceptible compared to women in hearing loss induced by long-term occupational exposure (60). Then, in order to optimize noise-induced treatment and prevention strategies, sex bias must be considered as well. In our experiment, resilience or

adaptive capability of females was illustrated by data showing that even when reductions occurred in the number of dendrites, compensatory increases in the length of arborizations were activated to ameliorate the impact of aversive stimulation. Results on serum pro-BDNF also support this idea. While females exhibited non-significant increases, males significantly augmented this parameter at both assessments. As previously mentioned, reduced dendritic trees may at least in part be due to exacerbated p75NTR signaling since elevated pro-BDNF levels has been associated with dendrite retraction (32). Results showing that blood BDNF measurements are reliable predictors of brain BDNF offers additional support for our results (61). Moreover, there is also the possibility that BDNF conducts differential signaling cascades in male and females under physiological or pathological settings, offering for this mechanism novel opportunities for BDNF-based therapeutic strategies.

Limitations of our study include the lack of assessments for molecular mechanisms linking BDNF to dendrite retractions and c-Fos expression. By including sex steroids in the analysis, future studies could obtain reliable explanations for sex differences. Such mechanisms must be explored in new studies. Increasing the size of the sample, future studies could produce stronger results.

In conclusion, we generated evidence supporting that chronic acoustic stress may affect adaptive capabilities of subjects by inducing regional morphological changes outside the auditory structures. Our results indicate that hippocampal neurons could be particularly sensitive to longer effects of noise, and markedly, these effects could be gender biased with higher probabilities of damage in males.

### Acknowledgements

This work was supported by the Consejo Nacional de Ciencia y Tecnología (CONACyT México) grant numbers 238313 to YRD, 221092 to FJH, and fondo fortalecimiento UdeG 2019-249876 to FJH.

### References

1. Ising H, Kruppa B. Health effects caused by noise: Evidence in the literature from the past 25 years. *Noise Health*. 2004; 6:5-13.
2. Salvi RJ, Wang J, Ding D. Auditory plasticity and hyperactivity following cochlear damage. *Hear Res*. 2000; 147:261-274.
3. Basta D, Tzschentke B, Ernst A. Noise-induced cell death in the mouse medial geniculate body and primary auditory cortex. *Neurosci Lett*. 2005; 381:199-204.
4. Frohlich F, Basta D, Strubing I, Ernst A, Groschel M. Time course of cell death due to acoustic overstimulation in the mouse medial geniculate body and primary auditory cortex. *Noise Health*. 2017; 19:133-139.
5. Pienkowski M, Eggermont JJ. Reversible long-term

- changes in auditory processing in mature auditory cortex in the absence of hearing loss induced by passive, moderate-level sound exposure. *Ear Hear.* 2012; 33:305-314.
6. Willott JF, Lu SM. Noise-induced hearing loss can alter neural coding and increase excitability in the central nervous system. *Science.* 1982; 216:1331-1334.
  7. DeJoy DM. The nonauditory effects of noise: review and perspectives for research. *J Aud Res.* 1984; 24:123-150.
  8. Kraus KS, Canlon B. Neuronal connectivity and interactions between the auditory and limbic systems. Effects of noise and tinnitus. *Hear Res.* 2012; 288:34-46.
  9. de Kloet ER. Hormones, brain and stress. *Endocr Regul.* 2003; 37:51-68.
  10. Jauregui-Huerta F, Ruvalcaba-Delgadillo Y, Garcia-Estrada J, Feria-Velasco A, Ramos-Zuniga R, Gonzalez-Perez O, Luquin S. Early exposure to noise followed by predator stress in adulthood impairs the rat's re-learning flexibility in Radial Arm Water Maze. *Neuro Endocrinol Lett.* 2010; 31:538-548.
  11. Kim H, Lee MH, Chang HK, Lee TH, Lee HH, Shin MC, Shin MS, Won R, Shin HS, Kim CJ. Influence of prenatal noise and music on the spatial memory and neurogenesis in the hippocampus of developing rats. *Brain Dev.* 2006; 28:109-114.
  12. Ruvalcaba-Delgadillo Y, Luquin S, Ramos-Zuniga R, Feria-Velasco A, Gonzalez-Castaneda RE, Perez-Vega MI, Jauregui-Huerta F, Garcia-Estrada J. Early-life exposure to noise reduces mPFC astrocyte numbers and T-maze alternation/discrimination task performance in adult male rats. *Noise Health.* 2015; 17:216-226.
  13. Cui B, Wu M, She X. Effects of chronic noise exposure on spatial learning and memory of rats in relation to neurotransmitters and NMDAR2B alteration in the hippocampus. *J Occup Health.* 2009; 51:152-158.
  14. Jauregui-Huerta F, Garcia-Estrada J, Ruvalcaba-Delgadillo Y, Trujillo X, Huerta M, Feria-Velasco A, Gonzalez-Perez O, Luquin S. Chronic exposure of juvenile rats to environmental noise impairs hippocampal cell proliferation in adulthood. *Noise Health.* 2011; 13:286-291.
  15. Jauregui-Huerta F, Zhang L, Yañez-Delgadillo G, Hernandez-Carrillo P, García-Estrada J, Luquín S. Hippocampal cytogenesis and spatial learning in senile rats exposed to chronic variable stress: effects of previous early life exposure to mild stress. *Front Aging Neurosci.* 2015; 7.
  16. Kraus KS, Mitra S, Jimenez Z, Hinduja S, Ding D, Jiang H, Gray L, Lobarinas E, Sun W, Salvi RJ. Noise trauma impairs neurogenesis in the rat hippocampus. *Neuroscience.* 2010; 167:1216-1226.
  17. Chaudhuri A, Zangenehpour S, Rahbar-Dehgan F, Ye F. Molecular maps of neural activity and quiescence. *Acta Neurobiol Exp (Wars).* 2000; 60:403-410.
  18. Martinez M, Phillips PJ, Herbert J. Adaptation in patterns of c-fos expression in the brain associated with exposure to either single or repeated social stress in male rats. *Eur J Neurosci.* 1998; 10:20-33.
  19. Stamp JA, Herbert J. Multiple immediate-early gene expression during physiological and endocrine adaptation to repeated stress. *Neuroscience.* 1999; 94:1313-1322.
  20. Watanabe Y, Stone E, McEwen BS. Induction and habituation of c-fos and zif/268 by acute and repeated stressors. *Neuroreport.* 1994; 5:1321-1324.
  21. Magarinos AM, McEwen BS. Stress-induced atrophy of apical dendrites of hippocampal CA3c neurons: comparison of stressors. *Neuroscience.* 1995; 69:83-88.
  22. McEwen BS, Magarinos AM. Stress effects on morphology and function of the hippocampus. *Ann N Y Acad Sci.* 1997; 821:271-284.
  23. McEwen BS, Magarinos AM. Stress and hippocampal plasticity: implications for the pathophysiology of affective disorders. *Hum Psychopharmacol.* 2001; 16:S7-s19.
  24. McKittrick CR, Magarinos AM, Blanchard DC, Blanchard RJ, McEwen BS, Sakai RR. Chronic social stress reduces dendritic arbors in CA3 of hippocampus and decreases binding to serotonin transporter sites. *Synapse.* 2000; 36:85-94.
  25. Magarinos AM, McEwen BS, Saboureau M, Pevet P. Rapid and reversible changes in intrahippocampal connectivity during the course of hibernation in European hamsters. *Proc Natl Acad Sci U S A.* 2006; 103:18775-18780.
  26. Vyas A, Mitra R, Shankaranarayana Rao BS, Chattarji S. Chronic stress induces contrasting patterns of dendritic remodeling in hippocampal and amygdaloid neurons. *J Neurosci.* 2002; 22:6810-6818.
  27. Mainen ZF, Sejnowski TJ. Influence of dendritic structure on firing pattern in model neocortical neurons. *Nature.* 1996; 382:363-366.
  28. Conrad CD. What is the functional significance of chronic stress-induced CA3 dendritic retraction within the hippocampus? *Behav Cogn Neurosci Rev.* 2006; 5:41-60.
  29. Duman RS, Monteggia LM. A neurotrophic model for stress-related mood disorders. *Biol Psychiatry.* 2006; 59:1116-1127.
  30. Fayard B, Loeffler S, Weis J, Vogelin E, Kruttgen A. The secreted brain-derived neurotrophic factor precursor pro-BDNF binds to TrkB and p75NTR but not to TrkA or TrkC. *J Neurosci Res.* 2005; 80:18-28.
  31. Je HS, Yang F, Ji Y, Nagappan G, Hempstead BL, Lu B. Role of pro-brain-derived neurotrophic factor (proBDNF) to mature BDNF conversion in activity-dependent competition at developing neuromuscular synapses. *Proc Natl Acad Sci U S A.* 2012; 109:15924-15929.
  32. Yang F, Je HS, Ji Y, Nagappan G, Hempstead B, Lu B. Pro-BDNF-induced synaptic depression and retraction at developing neuromuscular synapses. *J Cell Biol.* 2009; 185:727-741.
  33. Luine V, Gomez J, Beck K, Bowman R. Sex differences in chronic stress effects on cognition in rodents. *Pharmacol Biochem Behav.* 2017; 152:13-19.
  34. Verma R, Balhara YPS, Gupta CS. Gender differences in stress response: Role of developmental and biological determinants. In: *Ind Psychiatry J.* 2011; pp. 4-10.
  35. Zavala JK, Fernandez AA, Gosselink KL. Female responses to acute and repeated restraint stress differ from those in males. *Physiol Behav.* 2011; 104:215-221.
  36. Irvine K, Laws KR, Gale TM, Kondel TK. Greater cognitive deterioration in women than men with Alzheimer's disease: a meta analysis. *J Clin Exp Neuropsychol.* 2012; 34:989-998.
  37. Keers R, Aitchison KJ. Gender differences in antidepressant drug response. *Int Rev Psychiatry.* 2010; 22:485-500.
  38. Mendrek A, Mancini-Marie A. Sex/gender differences in the brain and cognition in schizophrenia. *Neurosci Biobehav Rev.* 2016; 67:57-78.
  39. Rabat A. Extra-auditory effects of noise in laboratory

- animals: the relationship between noise and sleep. *J Am Assoc Lab Anim Sci.* 2007; 46:35-41.
40. Paxinos G, Watson C. *The Rat Brain in Stereotaxic Coordinates*, 6th Edn. Vol. 70. San Diego, CA: Academic Press, 2006.
  41. Palkovits M, Dobolyi A, Helfferich F, Usdin TB. Localization and chemical characterization of the audiogenic stress pathway. *Ann N Y Acad Sci.* 2004; 1018:16-24.
  42. Campeau S, Dolan D, Akil H, Watson SJ. c-fos mRNA induction in acute and chronic audiogenic stress: possible role of the orbitofrontal cortex in habituation. *Stress.* 2002; 5:121-130.
  43. Campeau S, Watson SJ. Neuroendocrine and behavioral responses and brain pattern of c-fos induction associated with audiogenic stress. *J Neuroendocrinol.* 1997; 9:577-588.
  44. Bose M, Munoz-Llanca P, Roychowdhury S, Nichols JA, Jakkamsetti V, Porter B, Byrapureddy R, Salgado H, Kilgard MP, Aboitiz F, Dagnino-Subiabre A, Atzori M. Effect of the environment on the dendritic morphology of the rat auditory cortex. *Synapse.* 2010; 64:97-110.
  45. Ouda L, Burianova J, Balogova Z, Lu HP, Syka J. Structural changes in the adult rat auditory system induced by brief postnatal noise exposure. *Brain Struct Funct.* 2016; 221:617-629.
  46. Gonzalez-Perez O, Chavez-Casillas O, Jauregui-Huerta F, Lopez-Virgen V, Guzman-Muniz J, Moy-Lopez N, Gonzalez-Castaneda RE, Luquin S. Stress by noise produces differential effects on the proliferation rate of radial astrocytes and survival of neuroblasts in the adult subgranular zone. *Neurosci Res.* 2011; 70:243-250.
  47. Huet-Bello O, Ruvalcaba-Delgadillo Y, Feria-Velasco A, Gonzalez-Castaneda RE, Garcia-Estrada J, Macias-Islas MA, Jauregui-Huerta F, Luquin S. Environmental noise exposure modifies astrocyte morphology in hippocampus of young male rats. *Noise Health.* 2017; 19:239-244.
  48. Manikandan S, Padma MK, Srikumar R, Jeya Parthasarathy N, Muthuvel A, Sheela Devi R. Effects of chronic noise stress on spatial memory of rats in relation to neuronal dendritic alteration and free radical-imbalance in hippocampus and medial prefrontal cortex. *Neurosci Lett.* 2006; 399:17-22.
  49. Cheng L, Wang SH, Chen QC, Liao XM. Moderate noise induced cognition impairment of mice and its underlying mechanisms. *Physiol Behav.* 2011; 104:981-988.
  50. Cheng L, Wang SH, Huang Y, Liao XM. The hippocampus may be more susceptible to environmental noise than the auditory cortex. *Hear Res.* 2016; 333:93-97.
  51. Fernandez-Quezada D LS, García-Samudio A, Ruvalcaba-Delgadillo Y, Jauregui-Huerta F. Chronic exposure to environmental noise promotes changes in dendritic arborization of male rat cortex and limbic system. *Society for Neuroscience, Chicago, Ill.* 2019.
  52. Moench KM, Breach MR, Wellman CL. Chronic stress produces enduring sex- and region-specific alterations in novel stress-induced c-Fos expression. *Neurobiol Stress.* 2019; 10:100147.
  53. Heinsbroek RP, Van Haaren F, Feenstra MG, Enderit E, Van de Poll NE. Sex- and time-dependent changes in neurochemical and hormonal variables induced by predictable and unpredictable footshock. *Physiol Behav.* 1991; 49:1251-1256.
  54. Panagiotaropoulos T, Papaioannou A, Pondiki S, Prokopiou A, Stylianopoulou F, Gerozissis K. Effect of neonatal handling and sex on basal and chronic stress-induced corticosterone and leptin secretion. *Neuroendocrinology.* 2004; 79:109-118.
  55. Le Mevel JC, Abitbol S, Beraud G, Maniey J. Temporal changes in plasma adrenocorticotropin concentration after repeated neurotropic stress in male and female rats. *Endocrinology.* 1979; 105:812-817.
  56. Seale JV, Wood SA, Atkinson HC, Harbuz MS, Lightman SL. Gonadal steroid replacement reverses gonadectomy-induced changes in the corticosterone pulse profile and stress-induced hypothalamic-pituitary-adrenal axis activity of male and female rats. *J Neuroendocrinol.* 2004; 16:989-998.
  57. Babb JA, Masini CV, Day HE, Campeau S. Stressor-specific effects of sex on HPA axis hormones and activation of stress-related neurocircuitry. *Stress.* 2013; 16:664-677.
  58. Galea LA, McEwen BS, Tanapat P, Deak T, Spencer RL, Dhabhar FS. Sex differences in dendritic atrophy of CA3 pyramidal neurons in response to chronic restraint stress. *Neuroscience.* 1997; 81:689-697.
  59. Balogová Z, Popelář J, Chiumenti F, Chumak T, Burianová JS, Rybalko N, Syka J. Age-Related Differences in Hearing Function and Cochlear Morphology between Male and Female Fischer 344 Rats. *Front Aging Neurosci.* 2017; 9:428.
  60. Szanto C, Ionescu M. Influence of age and sex on hearing threshold levels in workers exposed to different intensity levels of occupational noise. *Audiology.* 1983; 22:339-356.
  61. Klein AB, Williamson R, Santini MA, Clemmensen C, Ettrup A, Rios M, Knudsen GM, Aznar S. Blood BDNF concentrations reflect brain-tissue BDNF levels across species. *Int J Neuropsychopharmacol.* 2011; 14:347-353.

(Received October 22, 2019; Revised November 25, 2019; Accepted December 14, 2019)

# PRKCH polymorphism is associated with rheumatoid arthritis in a Chinese population

Yue Zhuang<sup>1</sup>, Yanan Di<sup>2</sup>, Lulin Huang<sup>2</sup>, Jing Zhu<sup>1,\*</sup>

<sup>1</sup>Department of Rheumatology and Immunology, Sichuan Academy of Medical Sciences & Sichuan Provincial People's Hospital, Affiliated Hospital of University of Electronic Science and Technology of China, Chengdu, China;

<sup>2</sup>Sichuan Provincial Key Laboratory for Human Disease Gene Study, Sichuan Academy of Medical Sciences & Sichuan Provincial People's Hospital, Affiliated Hospital of University of Electronic Science and Technology of China, Chengdu, China.

## Summary

Genetic factors have been widely considered to have a substantial effect on the susceptibility to rheumatoid arthritis (RA). The purpose of this study was to determine whether the four newly discovered polymorphisms in a genome-wide association study (GWAS) meta-analysis confer susceptibility to RA in a Chinese Han population. We conducted a case-control study involving 359 RA cases and 873 age- and gender-matched controls and performed genotyping of four single nucleotide polymorphisms (SNPs), rs227163, rs726288, rs3783782 and rs2469434, using the dye terminator-based SNaPshot method. Consequently, we detected significant differences of genotype distribution of rs3783782 in *PRKCH* between RA and controls. The minor allele frequencies (MAFs) of rs3783782 were significantly higher in RA patients compared to control subjects. Moreover, the rs227163 in *TNFRSF9* had higher MAFs in male RA compared with male controls. In addition, the polymorphism of rs3783782 in *PRKCH* was significantly associated with RA susceptibility (OR = 1.67, 95% CI = 1.32-2.11,  $p = 1.32 \times 10^{-5}$ ). After stratification by gender, the minor (A) allele was strongly associated with increased risk for RA in males (OR = 1.87, 95% CI = 1.34-2.60;  $p = 1.62 \times 10^{-4}$ ) and in females (OR = 1.51, 95% CI = 1.08-2.10;  $p = 0.014$ ). For rs227163, the minor (C) allele was found to be associated with RA risk only in males (OR = 1.34, 95% CI = 1.02-1.75;  $p = 0.036$ ). These findings for the first time confirmed that rs3783782 in *PRKCH* was associated with RA susceptibility in a Chinese population, and rs227163 in *TNFRSF9* was associated with RA risk in Chinese males; these SNPs may serve as genetic markers for RA.

**Keywords:** Rheumatoid arthritis, single nucleotide polymorphisms, *PRKCH*

## 1. Introduction

Rheumatoid arthritis (RA) is one of the most common autoimmune diseases, characterized by progressive joint destruction, autoantibody formation, and synovitis, eventually leading to functional disability. Epidemiological data has estimated that RA affects approximately 0.5-1.0% of the world's population and

0.2-0.37% of the Chinese population (1,2). Particularly, the prevalence of RA is estimated to be 2-4% in siblings, 5-10% in same-sex dizygotic twins, and even 12-30% in monozygotic twins, supporting the critical role of genetic factors in RA susceptibility (3,4). Human leukocyte antigen (HLA) class II molecules are well-studied genetic factors closely associated with RA development (5). However, the contribution of the HLA is considered to only account for 30% of the total genetic factors of susceptibility (6). Thus, it is critical to identify novel biomarkers responsible for RA susceptibility.

A genome-wide association study (GWAS) meta-analysis discovered 42 novel non-HLA RA risk loci at a genome-wide level of significance. Interestingly, four risk single nucleotide polymorphisms (SNPs) were found to be significantly different between the European and Asian populations, including rs3783782

Released online in J-STAGE as advance publication Accepted December 26, 2019.

\*Address correspondence to:

Dr. Zhu Jing, Department of Rheumatology and Immunology, Sichuan Academy of Medical Sciences & Sichuan Provincial People's Hospital, Affiliated Hospital of University of Electronic Science and Technology of China, No.32 The First Ring Road West 2, Chengdu 610072, China.  
E-mail: zhujingys@sina.com

in *PRKCH*, rs227163 in *TNFRSF9*, rs726288 in *SFTPD*, and rs2469434 in *CD226* (7). The *PRKCH* gene encodes protein kinase C  $\eta$ , a member of protein kinase C (PKC). Although *PRKCH* was identified in 1990, its specific functions in the pathogenesis of RA have not been elucidated. It has been reported that *PRKCH* may be a susceptibility gene for RA in the Japanese population, but not in the French Caucasian population, suggesting the genetic diversity of patients with RA (8,9).

Tumor Necrosis Factor  $\alpha$  (TNF- $\alpha$ ) is a prototypical pro-inflammatory cytokine, which is highly expressed in the synovitis of RA patients and targeting TNF- $\alpha$  by monoclonal antibodies proves to be an effective therapeutic approach for this disease. TNF receptor superfamily member 9 (*TNFRSF9*) is a key factor for communication signals between many cell types during development of multiple organs (10). Surfactant protein D gene (*SFTPD*) is mainly synthesized in alveolar type II cells of the lung. Studies have shown that *SFTPD* plays a diverse role in the innate immune system, and suppression of T-lymphocyte proliferation and cytokine production (11). The Cluster of Differentiation-226 (*CD226*) is expressed on immune cells such as T lymphocytes, monocytes and natural killer (NK) cells. There is some evidence regarding the potential role of *CD226* gene polymorphisms in autoimmune diseases (12).

Currently, few studies have explored the potential association between these SNPs (rs3783782 in *PRKCH*, rs227163 in *TNFRSF9*, rs726288 in *SFTPD*, and rs2469434 in *CD226*) and RA susceptibility in the Chinese population. In this study, we selected these four SNPs for RA association in a Chinese Han population.

## 2. Materials and Methods

### 2.1. Ethical approval

This study was approved by the Ethics Committee of Sichuan Academy of Medical Sciences & Sichuan Provincial People's Hospital. Informed consent was obtained from all individual participants included in the study. All procedures performed in this study involving human participants were in accordance with the ethical standards of the institutional and/or national research committee and with the 1964 Helsinki declaration and its later amendments or comparable ethical standards.

### 2.2. Subjects

A total of 1,232 Chinese subjects, including 359 patients with RA (201 men and 158 women; mean age  $51.3 \pm 13.07$  years) were recruited from the Sichuan Provincial People's Hospital. 873 age-and-gender-matched healthy controls (481 men and 392 women; mean age  $51.2 \pm 15.81$  years) were recruited from

the physical examination center. All patients were diagnosed with RA according to the American College of Rheumatology criteria (2). Demographic data and laboratory testing were obtained by reviewing hospital records of the hospital.

### 2.3. Genomic DNA extraction

Genomic DNA from all participants was isolated from peripheral blood leukocytes using a Gentra Puregene Blood DNA kit (Minneapolis, MN, USA) according to the manufacturer's protocol. The concentration of DNA samples was measured by NanoDrop 2000 (Thermo Scientific, USA).

### 2.4. Genotyping

The DNA sequences containing the target SNPs were amplified by polymerase chain reaction (PCR) with designed primers (Table 1). PCR amplification was performed on each sample in a 20- $\mu$ L reaction volume containing 50 ng of genomic DNA and 2 $\times$ Taq Master Mix. After PCR amplification, the concentration of each primer was defined. Then, the products of the four SNPs were added together in the same concentration for multiplex reaction. SNP genotyping was performed using the dye terminator-based SNaPshot method according to the protocol (Applied Biosystems, USA). The SNaPshot primers included the 20-60bp upstream sequence or reverse complement of the downstream sequence of each SNP position (Table 1). All probe Primers were synthesized by Sangon Biotech (Shanghai, China). The SNPs analysis was performed on the ABI 3130XL genetic analyzer (Applied Biosystems, USA). The genotypes of the SNPs were determined using Genemapper software 5.0 (Applied Biosystems, USA).

### 2.5. Statistical analysis

All of the statistical analyses were performed using the software Statistical Product and Service Solutions (SPSS) version 17.0 (Prentice Hall International, Chicago, USA). The *p* values of the SNPs were calculated using an additive model. Hardy-Weinberg equilibrium was tested for each allele using the  $\chi^2$  test. The unadjusted odds ratios of the alleles and genotypes were estimated by the  $\chi^2$  test. Odds ratios (ORs) and 95 % confidence intervals (95 % CIs) were calculated. *P* < 0.05 was considered statistically significant.

## 3. Results and Discussion

### 3.1. Clinical characteristics in RA patients and controls

Between 10 February 2017 and 30 May 2018, 359 patients with RA and 873 sex-and-age-matched controls were enrolled. All subjects were Han Chinese. In RA

**Table 1. Primers used in this study**

Primer Name	Sequence	T <sub>m</sub> (°C)
rs726288-F	GGTTCCTCTGGGACTTTTC	54
rs726288-R	AGAGCAGCAGGAATCCAAAA	50
rs726288-SNapSHOT-primer	AGGCAAATGTGCACCACACTCCCAGCCTGC	
rs3783782-F	CCAAGAACCTCATGCCGTAT	52
rs3783782-R	CCTGAGGTCAGGAGTTCGAG	56
rs3783782-SNapSHOT-primer	TTTAAAGACAGAGTCTCGCTCTGTTGCCAGGCTGGAGTG	
rs2469434-F	GGCTCCACCAGATTAACCAA	52
rs2469434-R	ACCACAGCAATCGTCAACAG	52
rs2469434-SNapSHOT-primer	AAAAAGTTCTAGAGGCCTGGACTTGCAATTGGTGTCTGAAGGGCAGGGTT	
rs227163-F	CCTGGAAAGTCATCCAGGTC	54
rs227163-R	CCTCTCTTACCACCCACA	54
rs227163-SNapSHOT-primer	ACGTTTTTCTAGGGAATTGGTCATTTTGTCTGAGTTTTCAAATGTATTGGCAAAAACC	

T<sub>m</sub>, DNA melting temperature.

**Table 2. Characteristics of the RA cases and controls**

Characteristics	Total RA cohort (n = 359)	Healthy Controls (n = 873)	p value
Male, n (%)	201 (56)	481 (55)	0.08
Age (years), mean (SD)	51.3 (13.07)	51.2 (15.81)	0.97
BMI (kg/m <sup>2</sup> ), mean (SD)	21.6 (3.16)	20.4 (4.32)	0.53
Age of onset (years), mean (SD)	45.2 (13.84)	-	
Disease duration (years), median (p25-p75)	3.0 (1.0-9.0)	-	

RA, rheumatoid arthritis; BMI, Body Mass Index; p25-p75, 25<sup>th</sup> to 75<sup>th</sup> percentile.

group, the mean age of all the RA patients was 51.3 years old. In healthy controls, the mean age was 51.2 years old. The characteristics of the study participants are shown in Table 2. The sex ratio, mean age and body mass index (BMI) of the RA patients were not statistically different from those of controls. Not all SNPs were successfully genotyped in every individual. The results of the genotyping experiments are given in Table 3.

### 3.2. Hardy-Weinberg equilibrium test

There were no significant deviations from Hardy-Weinberg equilibrium test (HWE) at any of the four SNPs. The p values for the tests of HWE were 0.106 vs. 0.906 for rs3783782, 0.769 vs. 0.689 for rs726288, 0.689 vs. 0.188 for rs2469434, and 0.425 vs. 0.704 for rs227163, in cases and controls, respectively.

### 3.3. Genotype and allele frequencies of the four SNPs in RA patients and controls

The genotypes distribution and allele frequencies of the four SNPs are shown in Table 3 and Table 4, respectively. RA is a chronic inflammatory disease manifested by joint synovial tissue inflammation, and activation of T cells is involved in the synovial inflammatory response, tissue damage and bone invasion (13-15). Previous studies have shown that the protein

kinase C (PKC) family plays an important role in T lymphocyte activation and autoimmune disorders (16). Therefore, *PRKCH*, as a member of the PCK family, is speculated to be associated with the pathophysiologic mechanism of RA (17). Indeed, Takata *et al.* reported *PRKCH* as a susceptibility gene for RA in a Japanese population. They found that multiple SNPs of *PRKCH* may influence susceptibility to this disease (8). Nevertheless, another study by Teixeira *et al.* confirmed that these susceptibility alleles of *PRKCH* were not associated with RA in a French Caucasian population (9). These contrary findings suggest the variation of *PRKCH* across different ethnic populations and identification of these variants in other populations is necessary. In our study, we observed a significant difference of genotype distribution of *PRKCH* rs3783782 between RA patients and control subjects ( $p = 3.09 \times 10^{-5}$ ). The minor allele frequencies (MAFs) of rs3783782 were significantly higher in RA patients compared to control subjects both in males (18.1% in RA vs. 10.6% in control,  $p = 1.62 \times 10^{-4}$ ) and females (22.1% in RA vs. 15.8% in control,  $p = 0.014$ ).

Controlling the excessive production of pro-inflammatory cytokines such as tumor necrosis factor (TNF) represents a remarkable therapeutic approach for RA treatment (18). TNFRSF9 is a 30 kDa membrane glycoprotein which belongs to the tumor necrosis factor receptor (TNFR) family. TNFRSF9 is widely expressed

**Table 3. Genotype frequencies of the four SNPs in RA patients and controls**

SNPs	Gene	Gender	RA, n (%)	Control, n (%)	p value	
rs726288	<i>SFTPD</i>	Male	200	475	0.056	
		TT	7 (3.50)	19 (4.0)		
		CT	29 (14.50)	155 (32.63)		
		Female	CC	164 (82.00)	301 (63.37)	0.54
			TT	157	387	
			CT	10 (6.37)	20 (5.17)	
			CT	64 (40.76)	143 (36.95)	
			CC	83 (52.87)	224 (57.88)	
			All			
rs3783782	<i>PRKCH</i>	Male	196	478	$3.99 \times 10^{-4}$	
		AA	5 (2.55)	8 (1.67)		
		AG	61 (31.12)	85 (17.78)		
		Female	GG	130 (66.33)	385 (80.54)	0.035
			AA	154	386	
			AG	4 (2.60)	6 (1.55)	
			AG	60 (38.96)	110 (28.50)	
			GG	90 (58.44)	270 (69.95)	
			All			
rs2469434	<i>CD226</i>	Male	199	455	0.34	
		CC	28 (14.07)	46 (10.11)		
		CT	93 (46.73)	222 (48.79)		
		Female	TT	78 (39.20)	187 (41.10)	0.85
			CC	157	384	
			CT	17 (10.83)	48 (12.50)	
			CT	75 (47.77)	177 (46.09)	
			TT	65 (41.40)	159 (41.41)	
			All			
rs227163	<i>TNFRSF9</i>	Male	199	454	0.09	
		CC	14 (7.04)	25 (5.50)		
		CT	80 (40.20)	148 (32.60)		
		Female	TT	105 (52.76)	281 (61.89)	0.98
			CC	150	366	
			CT	9 (6.0)	20 (5.46)	
			CT	55 (36.67)	128 (34.97)	
			TT	91 (60.67)	218 (59.56)	
			All			

RA, Rheumatoid Arthritis; MAF, minor allele frequency; SNPs, single nucleotide polymorphisms; OR, odds ratio.

**Table 4. MAFs of the four SNPs in RA patients and controls**

SNPs (MAF)	Gene	Gender	RA, n (%)	Control, n (%)	OR (95% CI)	p value
rs726288 (T)	<i>SFTPD</i>	Male	43 (10.8)	193 (20.3)	1.129 (0.85-1.50)	0.399
		Female	84 (26.8)	183 (23.6)	1.179 (0.87-1.59)	0.28
		All	127 (17.9)	376 (21.8)	1.15 (0.94-1.42)	0.181
rs3783782 (A)	<i>PRKCH</i>	Male	71 (18.1)	101 (10.6)	1.87 (1.34-2.60)	$1.62 \times 10^{-4}$
		Female	68 (22.1)	122 (15.8)	1.51 (1.08-2.10)	0.014
		All	139 (19.9)	223 (12.9)	1.67 (1.32-2.11)	$1.32 \times 10^{-5}$
rs2469434 (C)	<i>CD226</i>	Male	149 (37.4)	314 (34.5)	1.135 (0.89-1.45)	0.308
		Female	109 (34.7)	273 (35.5)	0.964 (0.73-1.27)	0.79
		All	258 (36.2)	587 (35.0)	1.056 (0.88-1.27)	0.558
rs227163 (C)	<i>TNFRSF9</i>	Male	108 (27.1)	198 (21.8)	1.34 (1.02-1.75)	0.036
		Female	73 (24.3)	168 (23.0)	1.03 (0.76-1.42)	0.83
		All	181 (25.9)	366 (22.3)	1.20 (0.97-1.47)	0.087

SNPs, single nucleotide polymorphisms; MAF, minor allele frequency; RA, rheumatoid arthritis; OR, odds ratio.

in a variety of immune cells, including activated T/B, NK, and NKT cells (10). Previous studies have found that SNPs of *TNFRSF9* are associated with autoimmune disorders, such as psoriatic arthritis in Europeans by GWAS, and RA in African Americans (19,20). In our study, we did not find a significant difference in genotype distribution of *TNFRSF9* rs227163 between

RA patients and controls ( $p = 0.21$ ), but we found that rs227163 appeared to have higher MAFs in male RA compared male controls (27.1% in male RA vs. 21.8% in male controls,  $p = 0.036$ ). However, we failed to detect any differences between RA and control subjects with respect to rs726288 and rs2469434 genotype distribution and allele frequencies.

### 3.4. Polymorphisms of the four SNPs and risk of RA

Furthermore, we evaluated the effects of rs3783782 in *PRKCH* and rs227163 in *TNFRSF9* for RA risk, as shown in Table 4. As a result, we found rs3783782 polymorphism was significantly associated with RA susceptibility (OR = 1.67, 95% CI = 1.32-2.11,  $p = 1.32 \times 10^{-5}$ ). After stratification by gender, the minor (A) allele was strongly associated with increased risk for RA in males (OR = 1.87, 95% CI = 1.34-2.60;  $p = 1.62 \times 10^{-4}$ ) and in females (OR = 1.51, 95% CI = 1.08-2.10;  $p = 0.014$ ). For rs227163, the minor (C) allele was found to be associated with RA risk only in males (OR = 1.34, 95% CI = 1.02-1.75;  $p = 0.036$ ). Unfortunately, we failed to find any obvious association of rs227163 polymorphism with female RA (OR = 1.03, 95% CI = 0.76-1.42;  $p = 0.83$ ).

Previous studies have shown that *SFTPD* and *CD226* is critically involved in the innate immune system by suppressing T cell proliferation and cytokine production (11,12). Accumulating evidence also supports the role of *SFTPD* polymorphisms in a diversity of human diseases, such as chronic obstructive pulmonary disease, obesity, and RA (21-23). However, we found no association of *SFTPD* (rs726288) and *CD226* (rs2469434) with RA in a Chinese Han population, probably due to the SNP loci and genetic differences in different populations.

There are some limitations in this study. First, the study sample size is relatively small, and more participants need to be involved to confirm our findings. Second, the physiological and pathophysiological functions of SNPs of *PRKCH* and *TNFRSF9* in RA have not yet been investigated.

In conclusion, these findings for the first time confirmed that rs3783782 in *PRKCH* was associated with RA susceptibility in a Chinese population, and rs227163 in *TNFRSF9* was associated with RA risk in Chinese males. These SNPs may serve as genetic markers for RA. Further functional investigations are needed to elucidate the precise role of *PRKCH* and *TNFRSF9* in RA pathogenesis.

### Acknowledgements

This study was supported by Applied Basic Research Programs of Science and Technology Commission Foundation of Sichuan Province and Health Department of Sichuan Province. We are grateful to all patients and volunteers for participation in this study. We greatly appreciate Hongtao Xiao (Sichuan Provincial People's Hospital) and Deying Kang (Sichuan University) for revision of this manuscript.

### References

- McInnes IB, Schett G. The pathogenesis of rheumatoid arthritis. *N Engl J Med*. 2011; 365:2205-2219.
- Gibofsky A. Overview of epidemiology, pathophysiology, and diagnosis of rheumatoid arthritis. *Am J Manag Care*. 2012; 18:S295-S302.
- Karami J, Aslani S, Jamshidi A, Garshasbi M, Mahmoudi M. Genetic implications in the pathogenesis of rheumatoid arthritis; An updated review. *Gene*. 2019; 702:8-16.
- Deane KD, Demoruelle MK, Kelmenson LB, Kuhn KA, Norris JM, Holers VM. Genetic and environmental risk factors for rheumatoid arthritis. *Best Pract Res Clin Rheumatol*. 2017; 31:3-18.
- van Drongelen V, Holoshitz J. Human leukocyte antigen-disease associations in rheumatoid arthritis. *Rheum Dis Clin North Am*. 2017; 43:363-376.
- Pratt AG, Isaacs JD. Genotyping in rheumatoid arthritis: A game changer in clinical management? *Expert Rev Clin Immunol*. 2015; 11:303-305.
- Okada Y, Wu D, Trynka G, et al. Genetics of rheumatoid arthritis contributes to biology and drug discovery. *Nature*. 2014; 506:376-381.
- Takata Y, Hamada D, Miyatake K, Nakano S, Shinomiya F, Scafe CR, Reeve VM, Osabe D, Moritani M, Kunika K, Kamatani N, Inoue H, Yasui N, Itakura M. Genetic association between the *PRKCH* gene encoding protein kinase ceta isozyme and rheumatoid arthritis in the Japanese population. *Arthritis Rheum*. 2007; 56:30-42.
- Teixeira VH, Jacq L, Moore J, Lasbleiz S, Hilliquin P, Resende Oliveira C, Cornelis F, Petit-Teixeira E. Association and expression study of *PRKCH* gene in a French Caucasian population with rheumatoid arthritis. *J Clin Immunol*. 2008; 28:115-121.
- El Kramani N, Elsherbiny NM, El-Gayar AM, Ebrahim MA, Al-Gayyar MMH. Clinical significance of the TNF- $\alpha$  receptors, *TNFRSF2* and *TNFRSF9*, on cell migration molecules Fascin-1 and Versican in acute leukemia. *Cytokine*, 2018; 111:523-529.
- Sarashina-Kida H, Negishi H, Nishio J, Suda W, Nakajima Y, Yasui-Kato M, Iwaisako K, Kang S, Endo N, Yanai H, Asagiri M, Kida H, Hattori M, Kumanogoh A, Taniguchi T. Gallbladder-derived surfactant protein d regulates gut commensal bacteria for maintaining intestinal homeostasis. *Proc Natl Acad Sci U S A*. 2017; 114:10178-10183.
- Gaud G, Roncagalli R, Chaoui K, Bernard I, Familiades J, Colacios C, Kassem S, Monsarrat B, Burlet-Schiltz O, de Peredo AG, Malissen B, Saoudi A. The costimulatory molecule CD226 signals through VAV1 to amplify TCR signals and promote IL-17 production by CD4+ T cells. *Sci Signal*. 2018; 11. pii:eaar3083.
- Yang X, Chang Y, Wei W. Endothelial dysfunction and inflammation: immunity in rheumatoid arthritis. *Mediators Inflamm*, 2016; 2016:6813016.
- Lv M, Miao J, Zhao P, Luo X, Han Q, Wu Z, Zhang K, Zhu P. CD147-mediated chemotaxis of CD4<sup>+</sup>CD161<sup>+</sup> T cells may contribute to local inflammation in rheumatoid arthritis. *Clin Rheumatol*. 2018; 37:59-66.
- Byng-Maddick R, Ehrenstein MR. The impact of biological therapy on regulatory T cells in rheumatoid arthritis. *Rheumatology (Oxford)*. 2015; 54:768-775.
- Baier G. The PKC gene module: molecular biosystematics to resolve its T cell functions. *Immunol Rev*. 2003; 192:64-79.
- Wang L, Wu LF, Lu X, Mo XB, Tang ZX, Lei SF, Deng FY. Integrated analyses of gene expression profiles digs out common markers for rheumatic diseases. *Plos One*.

- 2015; 10:e137522.
18. McInnes IB, Buckley CD, Isaacs JD. Cytokines in rheumatoid arthritis - shaping the immunological landscape. *Nat Rev Rheumatol*. 2016; 12:63-68.
  19. Stuart PE, Nair RP, Tsoi LC, *et al*. Genome-wide association analysis of psoriatic arthritis and cutaneous psoriasis reveals differences in their genetic architecture. *Am J Hum Genet*. 2015; 97:816-836.
  20. Danila MI, Laufer VA, Reynolds RJ, Yan Q, Liu N, Gregersen PK, Lee A, Kern M, Langefeld CD, Arnett DK, Bridges SL Jr. Dense genotyping of immune-related regions identifies loci for rheumatoid arthritis risk and damage in African Americans. *Mol Med*. 2017; 23:177-187.
  21. Issac MS, Ashur W, Mousa H. Genetic polymorphisms of surfactant protein D rs2243639, Interleukin (IL)-1 $\beta$  rs16944 and IL-1RN rs2234663 in chronic obstructive pulmonary disease, healthy smokers, and non-smokers. *Mol Diagn Ther*. 2014; 18:343-354.
  22. Lin Z, Thorenoor N, Wu R, DiAngelo SL, Ye M, Thomas NJ, Liao X, Lin TR, Warren S, Floros J. Genetic association of pulmonary surfactant protein genes, SFTPA1, SFTPA2, SFTPB, SFTPC, and SFTPD with cystic fibrosis. *Front Immunol*. 2018; 9:2256.
  23. Mosaad YM, El-Toraby EE, Tawhid ZM, Abdelsalam AI, Enin AF, Hasson AM, Shafeek GM. Association between CD226 polymorphism and soluble levels in rheumatoid arthritis: relationship with clinical activity. *Immunol Invest*. 2018; 47:264-278.

(Received September 12, 2019; Revised November 13, 2019; Accepted December 13, 2019)

### Guide for Authors

#### 1. Scope of Articles

BioScience Trends is an international peer-reviewed journal. BioScience Trends devotes to publishing the latest and most exciting advances in scientific research. Articles cover fields of life science such as biochemistry, molecular biology, clinical research, public health, medical care system, and social science in order to encourage cooperation and exchange among scientists and clinical researchers.

#### 2. Submission Types

**Original Articles** should be well-documented, novel, and significant to the field as a whole. An Original Article should be arranged into the following sections: Title page, Abstract, Introduction, Materials and Methods, Results, Discussion, Acknowledgments, and References. Original articles should not exceed 5,000 words in length (excluding references) and should be limited to a maximum of 50 references. Articles may contain a maximum of 10 figures and/or tables.

**Brief Reports** definitively documenting either experimental results or informative clinical observations will be considered for publication in this category. Brief Reports are not intended for publication of incomplete or preliminary findings. Brief Reports should not exceed 3,000 words in length (excluding references) and should be limited to a maximum of 4 figures and/or tables and 30 references. A Brief Report contains the same sections as an Original Article, but the Results and Discussion sections should be combined.

**Reviews** should present a full and up-to-date account of recent developments within an area of research. Normally, reviews should not exceed 8,000 words in length (excluding references) and should be limited to a maximum of 100 references. Mini reviews are also accepted.

**Policy Forum** articles discuss research and policy issues in areas related to life science such as public health, the medical care system, and social science and may address governmental issues at district, national, and international levels of discourse. Policy Forum articles should not exceed 2,000 words in length (excluding references).

**Case Reports** should be detailed reports of the symptoms, signs, diagnosis, treatment, and follow-up of an individual patient. Case reports may contain a demographic profile of the patient but usually describe an unusual or novel occurrence. Unreported or unusual

side effects or adverse interactions involving medications will also be considered. Case Reports should not exceed 3,000 words in length (excluding references).

**News** articles should report the latest events in health sciences and medical research from around the world. News should not exceed 500 words in length.

**Letters** should present considered opinions in response to articles published in BioScience Trends in the last 6 months or issues of general interest. Letters should not exceed 800 words in length and may contain a maximum of 10 references.

#### 3. Editorial Policies

**Ethics:** BioScience Trends requires that authors of reports of investigations in humans or animals indicate that those studies were formally approved by a relevant ethics committee or review board.

**Conflict of Interest:** All authors are required to disclose any actual or potential conflict of interest including financial interests or relationships with other people or organizations that might raise questions of bias in the work reported. If no conflict of interest exists for each author, please state "There is no conflict of interest to disclose".

**Submission Declaration:** When a manuscript is considered for submission to BioScience Trends, the authors should confirm that 1) no part of this manuscript is currently under consideration for publication elsewhere; 2) this manuscript does not contain the same information in whole or in part as manuscripts that have been published, accepted, or are under review elsewhere, except in the form of an abstract, a letter to the editor, or part of a published lecture or academic thesis; 3) authorization for publication has been obtained from the authors' employer or institution; and 4) all contributing authors have agreed to submit this manuscript.

**Cover Letter:** The manuscript must be accompanied by a cover letter signed by the corresponding author on behalf of all authors. The letter should indicate the basic findings of the work and their significance. The letter should also include a statement affirming that all authors concur with the submission and that the material submitted for publication has not been published previously or is not under consideration for publication elsewhere. The cover letter should be submitted in PDF format. For example of Cover Letter, please visit <http://www.biosciencetrends.com/downcentre.php> (Download Centre).

**Copyright:** A signed JOURNAL PUBLISHING AGREEMENT (JPA) form must be provided by post, fax, or as a scanned file before acceptance of the article. Only forms with a hand-written signature are accepted. This copyright will ensure the widest possible dissemination of information. A form facilitating transfer of copyright can be downloaded by clicking the

appropriate link and can be returned to the e-mail address or fax number noted on the form (Please visit [Download Centre](#)). Please note that your manuscript will not proceed to the next step in publication until the JPA Form is received. In addition, if excerpts from other copyrighted works are included, the author(s) must obtain written permission from the copyright owners and credit the source(s) in the article.

**Suggested Reviewers:** A list of up to 3 reviewers who are qualified to assess the scientific merit of the study is welcomed. Reviewer information including names, affiliations, addresses, and e-mail should be provided at the same time the manuscript is submitted online. Please do not suggest reviewers with known conflicts of interest, including participants or anyone with a stake in the proposed research; anyone from the same institution; former students, advisors, or research collaborators (within the last three years); or close personal contacts. Please note that the Editor-in-Chief may accept one or more of the proposed reviewers or may request a review by other qualified persons.

**Language Editing:** Manuscripts prepared by authors whose native language is not English should have their work proofread by a native English speaker before submission. If not, this might delay the publication of your manuscript in BioScience Trends.

The Editing Support Organization can provide English proofreading, Japanese-English translation, and Chinese-English translation services to authors who want to publish in BioScience Trends and need assistance before submitting a manuscript. Authors can visit this organization directly at <http://www.iacmhr.com/iac-eso/support.php?lang=en>. IAC-ESO was established to facilitate manuscript preparation by researchers whose native language is not English and to help edit works intended for international academic journals.

#### 4. Manuscript Preparation

Manuscripts should be written in clear, grammatically correct English and submitted as a Microsoft Word file in a single-column format. Manuscripts must be paginated and typed in 12-point Times New Roman font with 24-point line spacing. Please do not embed figures in the text. Abbreviations should be used as little as possible and should be explained at first mention unless the term is a well-known abbreviation (e.g. DNA). Single words should not be abbreviated.

**Title Page:** The title page must include 1) the title of the paper (Please note the title should be short, informative, and contain the major key words); 2) full name(s) and affiliation(s) of the author(s), 3) abbreviated names of the author(s), 4) full name, mailing address, telephone/fax numbers, and e-mail address of the corresponding author; and 5) conflicts of interest (if you have an actual or potential conflict of interest to disclose, it must be included as a footnote on the title page of the manuscript; if no conflict of

interest exists for each author, please state "There is no conflict of interest to disclose"). Please visit [Download Centre](#) and refer to the title page of the manuscript sample.

**Abstract:** The abstract should briefly state the purpose of the study, methods, main findings, and conclusions. For article types including Original Article, Brief Report, Review, Policy Forum, and Case Report, a one-paragraph abstract consisting of no more than 250 words must be included in the manuscript. For News and Letters, a brief summary of main content in 150 words or fewer should be included in the manuscript. Abbreviations must be kept to a minimum and non-standard abbreviations explained in brackets at first mention. References should be avoided in the abstract. Key words or phrases that do not occur in the title should be included in the Abstract page.

**Introduction:** The introduction should be a concise statement of the basis for the study and its scientific context.

**Materials and Methods:** The description should be brief but with sufficient detail to enable others to reproduce the experiments. Procedures that have been published previously should not be described in detail but appropriate references should simply be cited. Only new and significant modifications of previously published procedures require complete description. Names of products and manufacturers with their locations (city and state/country) should be given and sources of animals and cell lines should always be indicated. All clinical investigations must have been conducted in accordance with Declaration of Helsinki principles. All human and animal studies must have been approved by the appropriate institutional review board(s) and a specific declaration of approval must be made within this section.

**Results:** The description of the experimental results should be succinct but in sufficient detail to allow the experiments to be analyzed and interpreted by an independent reader. If necessary, subheadings may be used for an orderly presentation. All figures and tables must be referred to in the text.

**Discussion:** The data should be interpreted concisely without repeating material already presented in the Results section. Speculation is permissible, but it must be well-founded, and discussion of the wider implications of the findings is encouraged. Conclusions derived from the study should be included in this section.

**Acknowledgments:** All funding sources should be credited in the Acknowledgments section. In addition, people who contributed to the work but who do not meet the criteria for authors should be listed along with their contributions.

**References:** References should be numbered in the order in which they appear in the text. Citing of unpublished results, personal communications, conference abstracts, and theses in the reference list is not recommended but these sources may be mentioned in the text. In the reference list,

cite the names of all authors when there are fifteen or fewer authors; if there are sixteen or more authors, list the first three followed by *et al.* Names of journals should be abbreviated in the style used in PubMed. Authors are responsible for the accuracy of the references. Examples are given below:

*Example 1* (Sample journal reference): Inagaki Y, Tang W, Zhang L, Du GH, Xu WF, Kokudo N. Novel aminopeptidase N (APN/CD13) inhibitor 24F can suppress invasion of hepatocellular carcinoma cells as well as angiogenesis. *Biosci Trends*. 2010; 4:56-60.

*Example 2* (Sample journal reference with more than 15 authors): Darby S, Hill D, Auvinen A, *et al.* Radon in homes and risk of lung cancer: Collaborative analysis of individual data from 13 European case-control studies. *BMJ*. 2005; 330:223.

*Example 3* (Sample book reference): Shalev AY. Post-traumatic stress disorder: diagnosis, history and life course. In: Post-traumatic Stress Disorder, Diagnosis, Management and Treatment (Nutt DJ, Davidson JR, Zohar J, eds.). Martin Dunitz, London, UK, 2000; pp. 1-15.

*Example 4* (Sample web page reference): Ministry of Health, Labour and Welfare of Japan. Dietary reference intakes for Japanese. <http://www.mhlw.go.jp/houdou/2004/11/h1122-2a.html> (accessed June 14, 2010).

**Tables:** All tables should be prepared in Microsoft Word or Excel and should be arranged at the end of the manuscript after the References section. Please note that tables should not be image format. All tables should have a concise title and should be numbered consecutively with Arabic numerals. If necessary, additional information should be given below the table.

**Figure Legend:** The figure legend should be typed on a separate page of the main manuscript and should include a short title and explanation. The legend should be concise but comprehensive and should be understood without referring to the text. Symbols used in figures must be explained.

**Figure Preparation:** All figures should be clear and cited in numerical order in the text. Figures must fit a one- or two-column format on the journal page: 8.3 cm (3.3 in.) wide for a single column, 17.3 cm (6.8 in.) wide for a double column; maximum height: 24.0 cm (9.5 in.). Please make sure that the symbols and numbers appeared in the figures should be clear. Please make sure that artwork files are in an acceptable format (TIFF or JPEG) at minimum resolution (600 dpi for illustrations, graphs, and annotated artwork, and 300 dpi for micrographs and photographs). Please provide all figures as separate files. Please note that low-resolution images are one of the leading causes of article resubmission and schedule delays. All color figures will be reproduced in full color in the online edition of the journal at no cost to authors.

**Units and Symbols:** Units and symbols

conforming to the International System of Units (SI) should be used for physicochemical quantities. Solidus notation (*e.g.* mg/kg, mg/mL, mol/mm<sup>2</sup>/min) should be used. Please refer to the SI Guide [www.bipm.org/en/si/](http://www.bipm.org/en/si/) for standard units.

**Supplemental data:** Supplemental data might be useful for supporting and enhancing your scientific research and BioScience Trends accepts the submission of these materials which will be only published online alongside the electronic version of your article. Supplemental files (figures, tables, and other text materials) should be prepared according to the above guidelines, numbered in Arabic numerals (*e.g.*, Figure S1, Figure S2, and Table S1, Table S2) and referred to in the text. All figures and tables should have titles and legends. All figure legends, tables and supplemental text materials should be placed at the end of the paper. Please note all of these supplemental data should be provided at the time of initial submission and note that the editors reserve the right to limit the size and length of Supplemental Data.

## 5. Submission Checklist

The Submission Checklist will be useful during the final checking of a manuscript prior to sending it to BioScience Trends for review. Please visit [Download Centre](#) and download the Submission Checklist file.

## 6. Online Submission

Manuscripts should be submitted to BioScience Trends online at <http://www.biosciencetrends.com>. The manuscript file should be smaller than 5 MB in size. If for any reason you are unable to submit a file online, please contact the Editorial Office by e-mail at [office@biosciencetrends.com](mailto:office@biosciencetrends.com).

## 7. Accepted Manuscripts

**Proofs:** Galley proofs in PDF format will be sent to the corresponding author via e-mail. Corrections must be returned to the editor ([proof-editing@biosciencetrends.com](mailto:proof-editing@biosciencetrends.com)) within 3 working days.

**Offprints:** Authors will be provided with electronic offprints of their article. Paper offprints can be ordered at prices quoted on the order form that accompanies the proofs.

**Page Charge:** Page charges will be levied on all manuscripts accepted for publication in BioScience Trends (\$140 per page for black white pages; \$340 per page for color pages). Under exceptional circumstances, the author(s) may apply to the editorial office for a waiver of the publication charges at the time of submission.

(Revised February 2013)

## Editorial and Head Office:

Pearl City Koishikawa 603  
2-4-5 Kasuga, Bunkyo-ku  
Tokyo 112-0003 Japan  
Tel: +81-3-5840-8764  
Fax: +81-3-5840-8765  
E-mail: [office@biosciencetrends.com](mailto:office@biosciencetrends.com)

---

### JOURNAL PUBLISHING AGREEMENT (JPA)

---

**Manuscript No.:**

**Title:**

**Corresponding Author:**

---

The International Advancement Center for Medicine & Health Research Co., Ltd. (IACMHR Co., Ltd.) is pleased to accept the above article for publication in BioScience Trends. The International Research and Cooperation Association for Bio & Socio-Sciences Advancement (IRCA-BSSA) reserves all rights to the published article. Your written acceptance of this JOURNAL PUBLISHING AGREEMENT is required before the article can be published. Please read this form carefully and sign it if you agree to its terms. The signed JOURNAL PUBLISHING AGREEMENT should be sent to the BioScience Trends office (Pearl City Koishikawa 603, 2-4-5 Kasuga, Bunkyo-ku, Tokyo 112-0003, Japan; E-mail: [office@biosciencetrends.com](mailto:office@biosciencetrends.com); Tel: +81-3-5840-8764; Fax: +81-3-5840-8765).

#### 1. Authorship Criteria

As the corresponding author, I certify on behalf of all of the authors that:

- 1) The article is an original work and does not involve fraud, fabrication, or plagiarism.
- 2) The article has not been published previously and is not currently under consideration for publication elsewhere. If accepted by BioScience Trends, the article will not be submitted for publication to any other journal.
- 3) The article contains no libelous or other unlawful statements and does not contain any materials that infringes upon individual privacy or proprietary rights or any statutory copyright.
- 4) I have obtained written permission from copyright owners for any excerpts from copyrighted works that are included and have credited the sources in my article.
- 5) All authors have made significant contributions to the study including the conception and design of this work, the analysis of the data, and the writing of the manuscript.
- 6) All authors have reviewed this manuscript and take responsibility for its content and approve its publication.
- 7) I have informed all of the authors of the terms of this publishing agreement and I am signing on their behalf as their agent.

#### 2. Copyright Transfer Agreement

I hereby assign and transfer to IACMHR Co., Ltd. all exclusive rights of copyright ownership to the above work in the journal BioScience Trends, including but not limited to the right 1) to publish, republish, derivate, distribute, transmit, sell, and otherwise use the work and other related material worldwide, in whole or in part, in all languages, in electronic, printed, or any other forms of media now known or hereafter developed and the right 2) to authorize or license third parties to do any of the above.

I understand that these exclusive rights will become the property of IACMHR Co., Ltd., from the date the article is accepted for publication in the journal BioScience Trends. I also understand that IACMHR Co., Ltd. as a copyright owner has sole authority to license and permit reproductions of the article.

I understand that except for copyright, other proprietary rights related to the Work (e.g. patent or other rights to any process or procedure) shall be retained by the authors. To reproduce any text, figures, tables, or illustrations from this Work in future works of their own, the authors must obtain written permission from IACMHR Co., Ltd.; such permission cannot be unreasonably withheld by IACMHR Co., Ltd.

#### 3. Conflict of Interest Disclosure

I confirm that all funding sources supporting the work and all institutions or people who contributed to the work but who do not meet the criteria for authors are acknowledged. I also confirm that all commercial affiliations, stock ownership, equity interests, or patent-licensing arrangements that could be considered to pose a financial conflict of interest in connection with the article have been disclosed.

---

**Corresponding Author's Name (Signature):**

**Date:**



